KU Leuven
Biomedical Sciences Group
Faculty of Medicine
Department of Neurosciences

MULTIMODAL IMAGE-GUIDED TRANSCRANIAL MAGNETIC STIMULATION IN THE DELINEATION OF ELOQUENT CEREBRAL CORTEX IN THE NEUROSURGICAL PATIENT AND THE TREATMENT OF REFRACTORY FOCAL EPILEPSY

Laura SEYNAEVE

Jury:

Promoter:	Prof. Dr. Wim Van Paesschen
Co-promoter:	Prof. Dr. Steven De Vleeschouwer
	Prof. Dr. Stefan Sunaert
Chair:	Prof. Dr. Steven Dymarkowski
Jury members:	Prof. Dr. Sandro Krieg
	Prof. Dr. Alain Maertens de Noordhout
	Prof. Dr. Vasilios K. Kimiskidis
	Prof. Dr. Johan van Loon
	Prof. Dr. Stephan Claes

Dissertation presented in partial fulfilment of the requirements for the degree of Doctor in Medical Sciences

June 2019

KU Leuven
Groep Biomedische Wetenschappen
Faculteit Geneeskunde
Departement Neurowetenschappen

MULTIMODALE BEELDVORMING-GESTUURDE TRANSCRANIELE MAGNETISCHE STIMULATIE VOOR HET AFBAKENEN VAN DE ELOQUENTE CEREBRALE CORTEX BIJ DE NEUROCHIRURGISCHE PATIENT EN DE BEHANDELING VAN REFRACTAIRE FOCALE EPILEPSIE

Laura SEYNAEVE

Promotor:	Prof. Dr. Wim Van Paesschen
Co-promotor:	Prof. Dr. Steven De Vleeschouwer
	Prof. Dr. Stefan Sunaert
Voorzitter:	Prof. Dr. Steven Dymarkowski
Jury:	Prof. Dr. Sandro Krieg
	Prof. Dr. Alain Maertens de Noordhout
	Prof. Dr. Vasilios K. Kimiskidis
	Prof. Dr. Johan van Loon
	Prof. Dr. Stephan Claes

Proefschrift voorgedragen tot het behalen van de graad van Doctor in de Medische wetenschappen

Juni 2019

The title of my PhD thesis is multimodal image-guided transcranial magnetic stimulation (TMS) in the delineation of (brain regions in) the neurosurgical patient and the treatment of refractory focal epilepsy. In this thesis, you will read about several techniques, mostly TMS. All investigations in this thesis were performed on humans, mostly patients, but also healthy volunteers who were so kind to participate in this translational research. The general idea was that advances in technology often do not enter into the clinical arena in an early stage, even though in clinical practice we are often confronted with the limitations of the currently available armamentarium. Each chapter will focus on a clinical problem. The questions concern how to predict what part of the cortex to spare in order to prevent that the patient becomes paralyzed or unable to speak after surgery, and if we can really cure epilepsy by just putting a magnet on the head. For each problem, the pitfalls and some recent technological advances that might be useful to tackle this problem are sketched. The ultimate question to answer in each chapter is if we can help a specific patient with a particular clinical problem by implementing advanced technology. Each chapter ends with some remarks, insights and possibilities for future improvements. I hope you enjoy reading this thesis as much as I liked working on it.

Table of contents

Abbreviations

3D: three-dimensional
AED: anti-epileptic drugs
APB: abductor pollicis brevis muscle
ATL: anterior temporal lobe
AUC: area under the curve
BOLD: Brain Oxygen Level Dependent imaging technique (principle of fMRI)
CI: confidence interval
CoG: center of gravity
CSSR: Columbia suicide severity rating scale
CST: corticospinal tract
DBS: deep brain stimulation
DCS/ECS: direct cortical stimulation/ electrical cortical stimulation
DTI: diffusion tensor imaging
EEG: electro-encephalography
EMG: electromyography
EPs: evoked potentials
FDG-PET: 2-deoxy-2-[^{18}F]-fluoro-D-glucose (FDG)-PET
fMRI: functional Magnetic Resonance Imaging
FN: false negative
FP: false positive
FWHM: full width at half maximum
IFNC: international federation of clinical neurophysiology
LTD: long-term depression
LTP: long-term potentiation magnetic resonance
MEP: motor evoked potential
MLEM: maximum likelihood expectation maximization
MR/MRI: magnetic resonance/ magnetic resonance imaging
MT/ %MT: motor threshold/ percentage of motor threshold
PET: positron emission tomography
Phonemes: VOW: vowels; VSTP: voiced stops e.g. /b/, /d/; USTP: unvoiced stops e.g. /k/,/p/,/t/; NAS: nasals e.g. /n/,/m/; SIB: sibilant fricatives e.g. /s/,/z/; NSIB: non-sibilant fricatives e.g. /h/,/f/; LIQ: liquids e.g. /y/,/l/
PT: phosphene threshold
QOLIE-31: quality of life in epilepsy questionnaire
ROC: receiver operating characteristic
ROI: region of interest
rMT: resting motor threshold
RNS: responsive brain neurostimulation
RT/ RTs: reaction time/ reactions times
rTMS: repetitive transcranial magnetic stimulation
SD: standard deviation
SISCOM: subtraction ictal SPECT co-registered with MRI
SPECT: single photon emission computed tomography
SPM: statistical parametric mapping
SSEP: somatosensory evoked potential
T: tesla
TA: tibialis anterior muscle

TMS: transcranial magnetic stimulation
TMS-pulse: a single discharge of current in the TMS coil
TN: true negative
TP: true positive
VNS: vagal nerve stimulation

1. Introduction: Brain tumors, epilepsy and their treatment

This PhD project has its roots in the clinical care of patients with intracranial lesions or refractory focal epilepsy. Brain lesions causing refractory epilepsy and brain tumors are often resected, but only if the patient will not suffer motor or language deficits after surgery. In these patients, we focus on three aspects that need improvement: delineation of the motor cortex, delineation of the language cortex and treatment of patients with refractory epilepsy who cannot be helped with a resection.

When a lesion arises in the brain, the trouble is double. On the one hand, there are the problems associated with the lesion itself. All types of brain lesions - benign and tumorous, congenital and acquired - can cause seizures. For a tumor there are the added problems of growth and invasion by the tumor, destruction of healthy tissue, mass-effect and in finality dying from the disease. On the other hand, the lesion is embedded in a brain: an intricate system in which each neuron has its unique role. This entails that removing a lesion always poses a risk of inducing functional deficits by destruction of neurons indispensable for a certain function. Luckily, there is a certain amount of flexibility in the brain so that not all neurosurgical procedures are likely to induce lasting deficits. The ability for functional changes in the brain and the resulting functional changes in the brain are referred to as brain plasticity. The term plasticity is used independent of whether the process is induced by brain lesions, after surgery, by natural processes like learning, or by experimental procedures (see also part 1.3 on the mechanism of repetitive transcranial magnetic stimulation (rTMS) for some examples of experimentally inducing plasticity). However, the functional possibilities of a neuron depends on its characteristics, the characteristics of its neighbors, the network it is in, its connections to other neurons, its integration in other brain networks and its output onto effector cells. For example, the neurons that can undergo changes that underpin this brain plasticity for motor functioning are limited to those that have a connection to the anterior horn of the spinal cord. In the anterior horn of the spinal cord, the neurons reside that directly activate muscles. The corticospinal tract (CST) is the direct pathway from the brain to the anterior horn of the spinal cord and responsible for voluntary, skilled movements. This bundle of axons if highly organized so that each part of the spinal cord receives its innervation from a specific part of the cerebral cortex. Traditionally, it was said that the axons innervating the anterior horn neurons and thus (solely) responsible for movement were those of the large pyramidal neurons of Betz in the fifth layer of the precentral gyrus. The reality is certainly more complex than this, with neurons of other parts of the frontal lobe and neurons of the postcentral gyrus also contributing. As a general principle however, when the neurons forming the CST are damaged, permanent deficits in skilled movements ensue. To prevent this, it is necessary to spare the neurons giving rise to the CST and extra caution is needed with surgeries in the peri-Rolandic area - called after the Rolandic sulcus, the divide between the frontal and the parietal lobe. A similar principle governs decisions on resection in other brain areas. Resections should not be performed if the chances of inducing permanent deficits are deemed large, especially not if the function you want to spare is considered crucial for the quality of life. In this respect, sparing language function is critical.

Although neurosurgery for brain tumors can induce permanent functional deficit, there are also obvious benefits. In short, increased survival is observed when all pathological tissue is macroscopically removed and no permanent deficits are induced. This has been demonstrated for both high- and low-grade intrinsic brain tumors, single brain metastasis and non-tumorous lesions causing epilepsy. The most prevalent group of intrinsic brain tumors are the gliomas and those are subdivided into four grades based on histological criteria. They are further subdivided based on histological characteristics and molecular markers. From a prognostic standpoint, the division in low- and high (class III and IV) gliomas is most relevant. Low-grade gliomas are however also not benign, since in 5-10 years' time more than half of low-grade gliomas will have transformed into high-grade gliomas[1]. For diagnostic and therapeutic reasons, it is necessary to perform a resection of the tumor.

In glioma surgery, the term gross total resection is used to describe the fact that all macroscopically visible abnormal tissue has been removed. Evaluation of the resection is preferentially based on a post-operative MR image. Since gliomas are infiltrative tumors, the classically used definition of a full resection, which includes negative section margins on pathological examination of the resection specimen, cannot be used. In low grade glioma early gross total resection leads to statistically significant increase in 5-year survival rates[2,3]. Survival is also increased in high grade glioma if a gross total resection is performed, both in adults and children[4,5]. However, this survival benefit seems to be negated if post-operative motor or language deficits arise[6]. In isolated brain metastasis, resection of this lesion in combination with radiotherapy increases survival from 4 to 10 months[7]. Also in these instances, it is primordial to preserve neurological functioning and quality of life, the more so because survival in cancer patients is linked to overall functioning (e.g. Karnofsky score)[8]. In patients with epilepsy who continue to have seizures despite adequate treatment with anti-epileptic drugs (AEDs), many will have circumscribed abnormalities in the brain, amenable to surgery. While those patients often have benign underlying lesions, abolishing seizures or reducing the number of tonic-clonic seizures by surgery leads to a clear survival benefit over the best available medical therapy[9]. Mortality rates were two- to threefold lower in the surgical group compared to the medically treated group. This is in line with the two- to threefold increase in risk of premature death in patients with uncontrolled epilepsy compared to age-matched controls[10,11]. Increased mortality is primarily due to sudden unexplained death in epilepsy (SUDEP, overall risk 1/1000 patient years), followed by accidents, suicide, cardiovascular events and progression of the underlying disease. Seizure control is dependent on a complete resection of the epileptogenic zone[12]. In patients with epilepsy, survival is directly linked with the completeness of the resection, just as it is in tumor surgery. The absolute number of the survival benefit in these cases is of course in a different order of magnitude than in patients with brain tumors. Therefore, even more care is taken to prevent permanent post-operative deficits, including deficits that would be considered less critical in patients in whom short-term survival is at stake. The most frequent type of refractory epilepsy in adult patients is mesial temporal lobe epilepsy. The studies on post-operative outcome of epilepsy surgery thus often include those patients. Homogeneous groups can be defined so the outcome parameters of these studies can be very reliable. There is class I evidence that anterior temporal lobe resection is the preferred treatment in this group, with a 60-80% success rate[13]. However, it is underutilized partly due to fear for post-operative cognitive deficits. Even in selected patients, a decline in verbal memory has been observed in 40-50% of patients after left-sided anterior temporal lobe (ATL) resection and 30% of patients after right ATL resection. Decline in naming occurred in 25% after left ATL resection[14]. This decline was present even though epilepsy centers exclude those patients thought to be at high risk for post-operative cognitive or language decline. Independent of the type of epilepsy, uncontrolled epilepsy in itself also leads to cognitive decline. Compared to continued medical therapy, cognitive functioning after surgery can be worse but it might have also declined without the surgery. The worst outcome is seen after failed epilepsy surgery[12]. On the other hand, successful surgery - including the possibility to stop medical treatment - leads to an improvement in all aspects of quality of life. The unifying force driving survival, quality of life and cognitive functioning is the fact that a patient can be rendered seizure free. If medication and surgery cannot deliver, alternative treatments are needed. This is where our study using rTMS in patients with refractory focal epilepsy (see chapter 3) is to be positioned.

The pathologies just described, are frequently encountered. One out of every one to two hundred persons has epilepsy. People with epilepsy have a 70% chance to become seizure free with medication. Unfortunately, this leaves 30% that are not seizure free. Of those, 60% have seizures originating in one specific part of the brain. This type of epilepsy is called focal epilepsy. It is thought to be caused by a circumscribed abnormality in the brain and therefore possibly amenable to surgery. It is good clinical practice to send all those patients for a presurgical evaluation[15–17]. If only half of those patients would be referred, this would still translate into 750 new patients each year in Belgium.

Each year, more than 65,000 people are diagnosed with cancer in Belgium. Of those, 10-25% will experience brain metastasis at some point in the disease course. In about half of the cases, a solitary brain lesion is seen[18]. This translates into a huge number of patients with brain metastasis possibly amenable to surgery each year. In comparison, primary brain tumors are much rarer, with an age-adjusted incidence rate of 21.42 per 100,000 (including more benign tumors like meningioma). However, morbidity rates are very high and survival rates very poor[19].

The necessity to spare eloquent cortex in patients with tumors or epilepsy, the frequency with which we encounter patients with tumors and/or epilepsy and the current methods being felt to be insufficient, led us to design the studies presented in this thesis, focusing in large part on the role of transcranial magnetic stimulation (TMS) in the management of those patients.

2. Modalities used in this thesis

The aim of this PhD was to improve clinical care by using a combination of different modalities to study the brain, to obtain a complementary and detailed picture of the brain functioning. In this chapter, the different modalities are described. For each technique, the advantages and pitfalls as well as the practical setup are described.

2.1. General setup of a TMS experiment

TMS is based on the principle of electromagnetic induction. To generate a magnetic field a brief, high-current pulse is introduced in a coil of wire, called the magnetic coil, which is placed on the scalp. The magnetic field is produced with lines of flux passing perpendicularly to the plane of the coil. An electric field is induced perpendicularly to the magnetic field. The electric field can cause a current to flow in loops parallel to the plane of the coil (Fig 2.1).

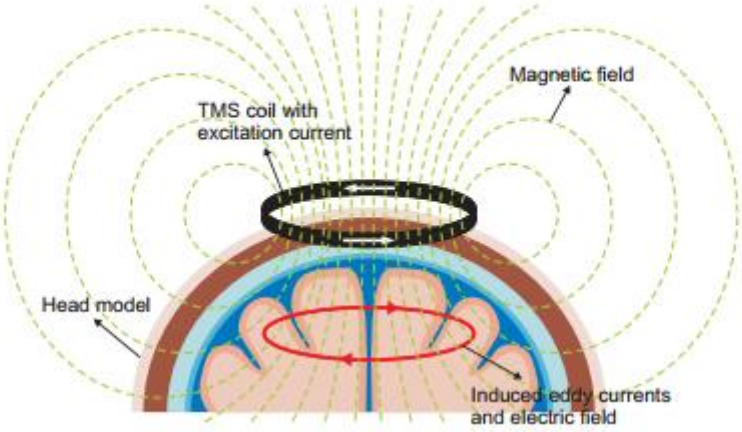

Figure 2.1
Basic principles of TMS. Electrical currents and electric field are induced in the brain through magnetic pulses applied by means of the current-carrying coil positioned above the head.
Reproduced with permission from:
A diffusion tensor-based computational model for TMS: from macroscopic fields to neuronal membrane potentials (doctoral dissertation). De Geeter N.

Magnetic coils can have different shapes (Fig 2.2). Round coils stimulate over a relatively large area of the brain. Figure-eight-shaped coils are designed to give a focal induced field, producing maximal current at the intersection of the two round components. The system used in our experiments was a Magstim Rapid2 (Magstim, Whitland, UK) coupled with the neuronavigation system BrainSight (Rogue Research, Montreal, Canada). The focal coil used was the D70 70mm figure-8 coil (product number 9925-00), the round and thus less focal coil used was the HP 90mm coil (product number 9784-00), and if sham stimulation was needed, the matched placebo coil was used. The maximal voltage that can be generated in the system is 1.67kV, resulting in a magnetic field with a strength up to 1 tesla (T).

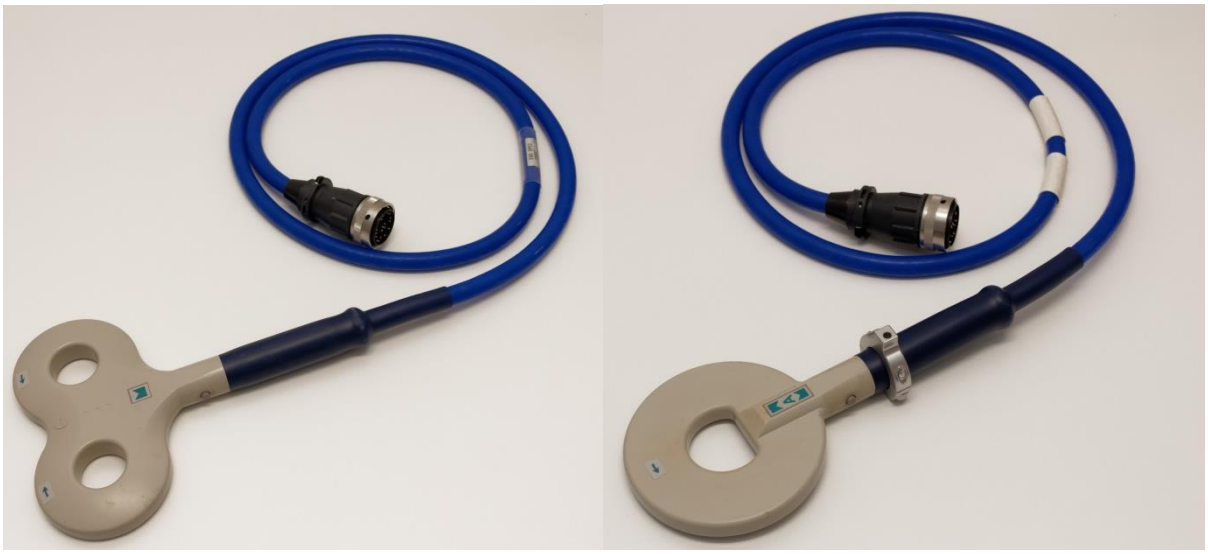

Figure 2.2
The two types of coils used in this thesis: on the left the figure-8 coil and on the right the round coil

The intensity used during the experiments, will be expressed as a percentage. The intensity of the current affects in turn the magnitude of the induced field. Two ways of expressing the intensity of the current flowing through the coil are used. The first is expressing the intensity as a percentage of the maximum output that can be generated by the system. The advantage of using this notation is that it converts rather easily to an absolute magnitude of the intensity used - but only if the full characteristics of the system are known. The disadvantages are that it can only be interpreted in the light of a full description of the system parameters and that it is not related to the physiological responses of interest. Therefore, the second way of expression of the intensity based on a percentage needed to generate a physiological response in the subject under study is often used. The most frequently used method for this second way of expressing the intensity, is as a percentage of the intensity needed to generate a response when stimulating over the motor cortex. This intensity is called the motor threshold (MT) and thus an intensity used in an experiment will be expressed as a percentage of the motor threshold (%MT). The practical setup of a TMS experiment, including the measurements to obtain this MT-intensity and some variation in the definition of the MT, will be discussed further in the introduction.
The induced field is dependent on the properties of the system that is stimulated, i.e. on the individual properties of a subject's brain. The effect we are aiming for using TMS, can also vary, depending on the research question. Since the TMS coil is placed on the scalp, it will always stimulate more superficial structures easier then deeper structures. It will also have higher intensities of the induced field closer to the coil than at a distance, since the field strength decreases quadratic with the distance. However, the intensity of the induced electric field depends on the conductive properties of the tissue. No or only small currents are induced in pain-sensitive structures like skin and scalp, making TMS a painless technique in most instances - unlike when a current of similar intensity would be induced in the brain by applying the current on the scalp - a technique called transcranial electrical stimulation of the brain. Transcranial electrical stimulation at an intensity high enough to induce depolarization in brain neurons has been largely abandoned in awake subjects, because it is too painful.

The first part of most TMS experiments, is to determine the optimal stimulation intensity. The trade-off would be between too low and thus not effective and too high leading to discomfort for the subjects, overheating of the system and exposing the brain to currents higher than the physiological range. In the description of the experiments, an intensity defined relative to the MT will be used,

similar to what is most often done in the literature. The aim is to induce an electric field of sufficient intensity and in the correct location, to cause depolarization of neurons and thus actions potentials in the neurons (and their axons) being part of the motor cortex. Those neurons will, when activated, send signals (via the CST) to the motor neurons in the anterior horn of the spinal cord, which in turn activate muscles. This elicited muscle potential is called a motor evoked potential (MEP). The muscle contractions can be observed by looking for twitches in muscles, or measured using electromyography (EMG). The upside of using EMG is that even small potentials of the muscles can be measured. The downside is that only those muscles that have electrodes attached to them can be used. In order to know the exact location on the scalp where the coil was located at the time a discharge of current in the TMS coil (called a TMS-pulse in the remainder of this text) is applied, the TMS-coil is coupled to a neuronavigation system. This system matches the position of the TMS coil with the patient's brain imaging. This is done by attaching infrared trackers to the patient, the coil (Fig 2.4) and other attributes used during the sessions and matching unique points of the subjects head with the location of those points on the brain imaging of the subject. Points that can be used are the nasion, points around the ear like the tragus and the intertragic notch or other uniquely definable points around nose, ear and eyes. The result of this matching procedure is checked by going over the surface of the head to make sure that the error between the real surface of the head as delineated during this validation procedure and the surface of the head on the brain imaging does not exceed 3mm.
The position of the tracker relative to coil also needs to be measured and loaded into the system, to determine its exact center prior to an experiment. This needs to be done since the orientation of the tracker relative to the coil can be adapted to optimize visibility of the coil tracker depending on the area of the brain to be stimulated and the position of the infrared camera. The inbuilt system of BrainSight is based on positioning the coil on three pins. Since this allowed for inaccuracies, a frame was developed in house by the people of *Medische Instrumentatie, fijnmechanische werkplaats* (Fig 2.5). The idea of the frame was based on a design by Dustin Martin and Bryan Wilcox (http://evelinatapia.com/research/research-tools/coil-calibration/) but further optimized in house. Our frame can also be used to calibrate the round coil. I am not aware of any other study that used a calibrated round coil but it is possible to track any type of coil with the neuronavigation system, as long as a tracker is attached and the coil calibrated.

The navigation system is routinely used during neurosurgery and its' accuracy has been guaranteed. However, just to be sure the whole setup was streamlined and flawless, the trajectory from MRI scanning, over the performance of the neuronavigation during TMS and intra-operative neuronavigation was tested on a phantom.

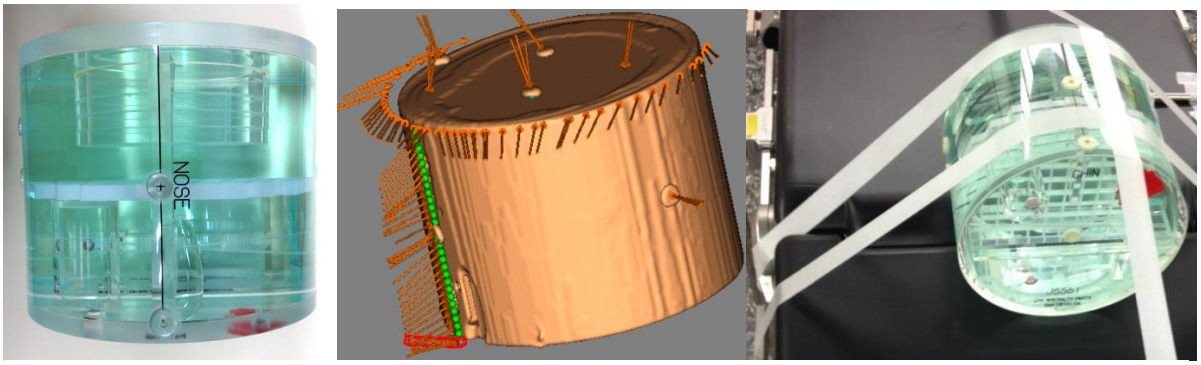

Phantom | TMS-based mapping of phantom | surgical preparation of the phantom

Figure 2.3
Illustration of test run on phantom: the phantom was equipped with fiducials (adhesive circular marker), scanned in the MRI as it were a real patient, taken to the TMS suite and to the operating theater to test the different neuronavigation systems.

Figure 2.4

Setup of an experiment: in order to be able to use neuronavigation, the subject and the coil must be tracked: this is done by attaching infrared trackers

and referencing the subjects head to anatomical MRI of the subject, by matching points on the head with the same points on the MRI - *referencing of the coil is illustrated in Figure 2.5*

The setup also consists of a computer, an infrared camera, the TMS-machine to generate the pulse through the coil and an EMG-measuring device

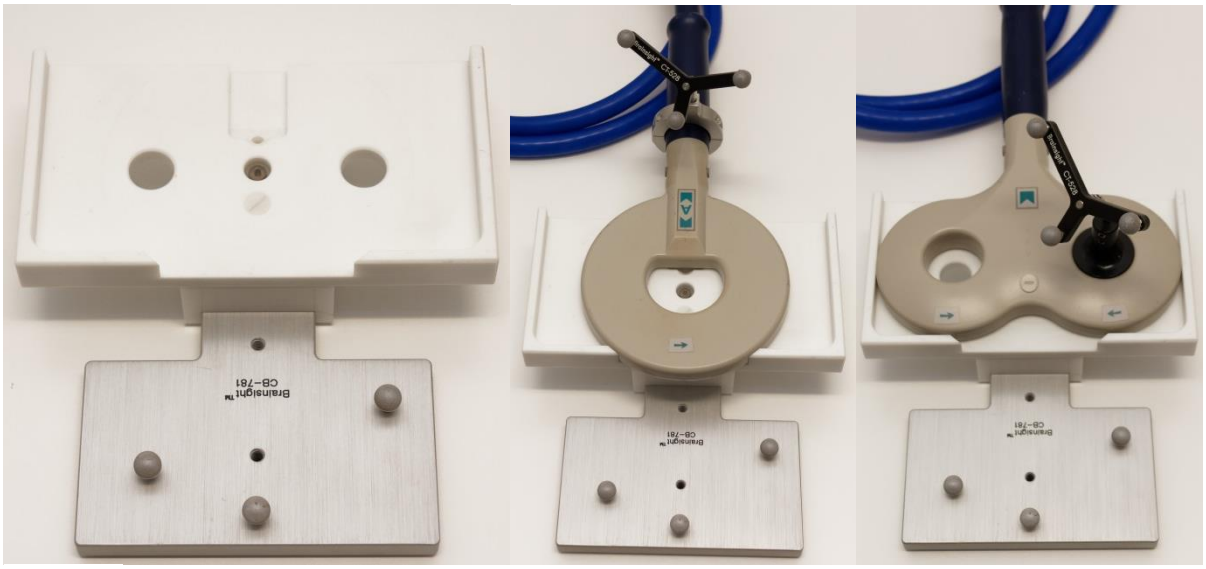

Figure 2.5
Coil referencing frame, loaded with the round coil and the figure-8 coil

Afterwards, the navigation system can be used to target the area of the brain most likely to be the primary motor cortex of the hand, called the “hand knob”, anterior to the central sulcus, based on a 3D reconstruction of the brain surface, generated by the BrainSight navigation system. The location where large-amplitude MEPs are elicited most easily is called the “motor hotspot”. This hotspot is the target of subsequent TMS-pulses of varying intensity. By varying the intensity and observing the resulting motor responses, the MT is determined.

Although the method of determining the MT, as just described, seems quite straightforward, variations are paramount. Variability arises from three main sources: the experimental setup, the operational definition of the MT and the multitude of factors influencing the MT at a given time. Variability in setup entails factors like the use of neuronavigation and EMG. We have some idea about the magnitude of the effect of changes in setup, since those have been studied in a dozen of healthy volunteers. Determining the motor hotspot can be done based on measured distances between different points on the scalp, instead of neuronavigation. This even happens in experiments that use neuronavigation for the remainder of the experiment (personal observation). I used the 3D reconstruction since this has been described to have the highest accuracy in identifying the precentral gyrus, also in patients with brain tumors in this area[20]. In one study in healthy controls, adding neuronavigation however did not affect the MT[21]. In this study, using neuronavigation, the MT was only determined based on measurements on this anatomically defined spot, whereas using scalp-based landmarks, the coil was moved around first to determine the spot resulting in the highest MEP. The way one then searches for the scalp position generating the highest MEP in the neighborhood from this starting point, can also be tackled in multiple ways. The coil is often moved around the starting point in small increments, to find the spot that gives rise to the highest MEP and this spot is than named the motor “hotspot” for this muscle. Even when using neuronavigation, it seems useful to search for a hotspot, due to variability in the location of the motor cortex in relation to anatomical landmarks. Some studies describe using a 5x5 grid with 1 cm spacing[22] and that they sample first over each of those spots, and sometimes also vary the orientation of the coil slightly with each measurement[23], to determine the hotspot. However most studies do not detail the way the hotspot was determined (e.g. “free point-to-point stimulation”[24]) or just omit the procedure used to determine the motor hotspot. Using some free-hand searching for the hotspot in combination with neuronavigation, however did also not affect the MT in healthy volunteers compared to using no navigation[25]. In my opinion, this lack of proven benefit of searching the hotspot can be explained by

the variability in the MEP measurements when stimulating the same location (as discussed in the following section). MEP amplitudes are dependent on small alterations in position of the coil- otherwise it would contradict many of the observations of motor cortex mapping with TMS (see part about rationale of using advanced head models for mapping & chapter 5). This is why I felt compelled to find a strategy to determine the motor hotspot. A good way to find the hotspot, would be to determine the MT on several different (the more, the better) locations and take the point with the lowest MT as hotspot. However, the hotspot is used as the one point to target the coil in order to determine the MT. Determining the MT at several locations would greatly increase the number of pulses in a TMS experiment and would not be advisable. No systematic way of determining the hotspot was available in the literature, likely because it was not felt to influence the resulting MT. During all experiments described in this thesis, I used a neuronavigation system to guide coil positioning during the determination of the hotspot using a 5x5 grid guided sampling over the anatomical landmark and averaging of several MEPs in order to decrease variability. In practice, I position the coil over the anatomical target, increase the intensity in 5% increments until an MEP is seen, then move around over the 5x5 grid. Some variability in coil orientation is added. With 20-30 samples - or more if the anatomical target seemed inaccurate in patients with tumors in the Rolandic region - the spatial averaging function included in the BrainSight system was used to obtain a very simple averaged MEP color map. This is done by taking each coil position on the scalp as the center of a bell-shaped 3D spherical object with the diameter of this shape being adaptable but set at its standard value of 17mm full width at half maximum (FWHM). If only one coil position is taken into account, all voxels inside this spherical object get the value of the MEP, and all those outside are set at zero. When taking all coil positions into account, a weighted average MEP value is attributed to every voxel. This resulting image is color-coded and the hotspot of the map is chosen as target to position the coil, to determine the MT. The way this first map is constructed is very similar to the projection model we will discuss in chapter 5 but it is based on only a limited amount of samples and the spread is set at 17mm FWHM, whereas the closest point model uses an interpolation for each value of the grid, based on neighboring values of the MEP. Please note that the BrainSight model uses a sphere-like structure to build the model, which should not be confused with using a spherical head model that is inbuilt in TMS-systems of the Nexstim Company. In that device the electric field is modelled over a sphere, whereas here a spread of the MEP amplitude in a bell-shape curve is modelled and a weighted average of the MEPs is visualized.

Figure 2.6
Searching for the 'motor hotspot' used place the coil while determining the MT
Left: 3D reconstruction of the head (created in BrainSight) with a virtual 5x5mm grid over the anatomical hand knob
Right: illustration of the algorithm used to average the different MEP-responses
Bottom: resulting color-coded map created by running this algorithm, with miniature TMS coil visualized on the resulting motor hotspot

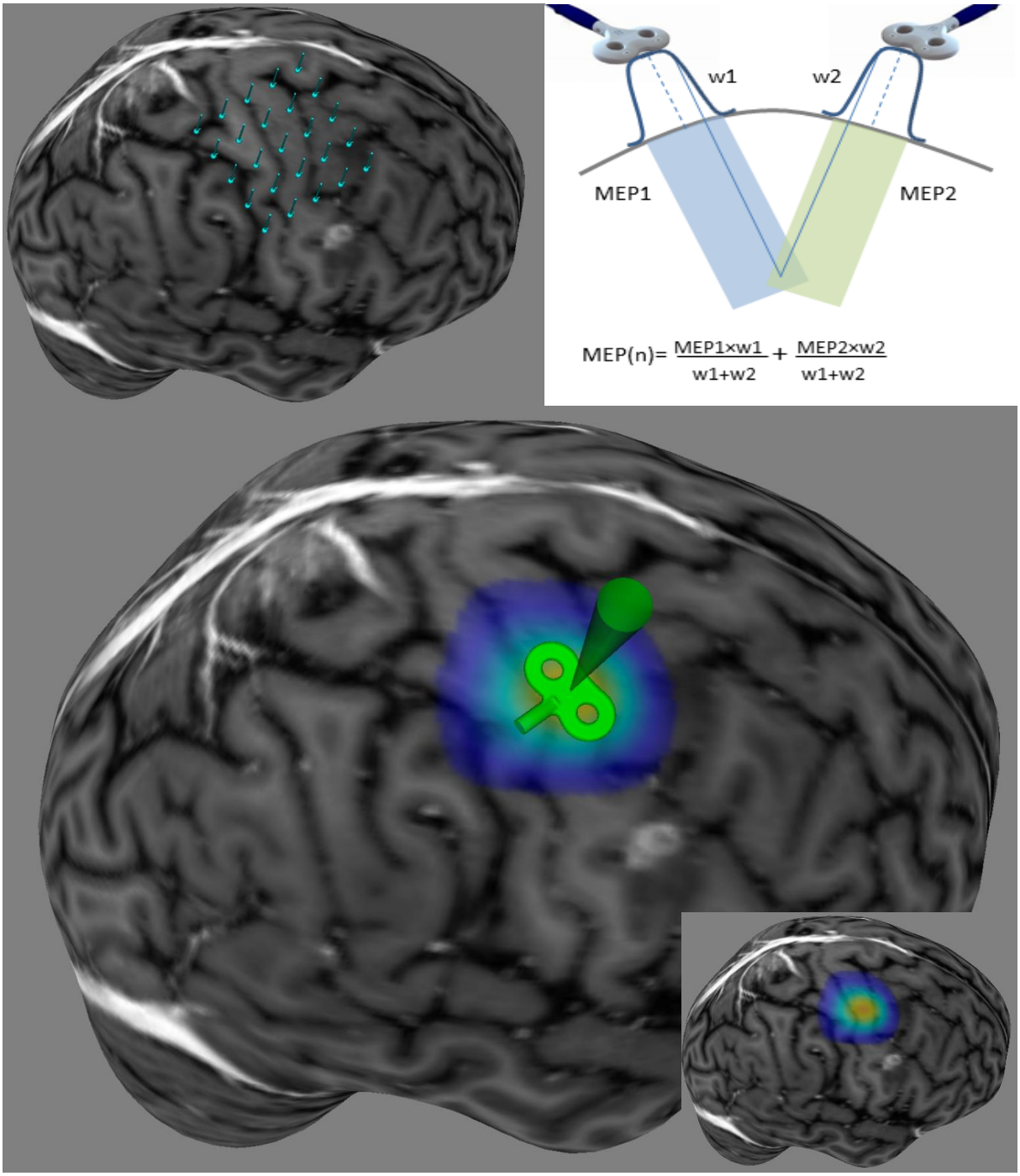

Determining the hotspot may be ill-defined, but the way to measure muscle contraction is quite clear. Using EMG instead of observing for visual twitches has been demonstrated to change the value of the resulting MT. Using EMG, the MT is on average more than 10% lower in healthy subjects[26]. It seems prudent to use EMG to determine the MT, in order not to use too high intensities. It is important to check the functionality of the EMG and if twitches are observed in muscles that are not targeted with the EMG-electrodes, it is best to change the setup. In all cases were only one hemisphere was of interest, the abductor pollicis brevis (APB) and the abductor digiti minimi in the hand were recorded - even though for most purposes only one muscle is needed. Although it is theoretically possible to be over a brain region with your coil that e.g. only activates muscles for the second finger, using aforementioned muscles (muscles moving the first or fifth fingers), makes the chances of not picking up a signal on EMG smaller.

Figure 2.7
Measurement setup for MEP of APB
(the abductor digiti minimi would also be covered but for clarity, the setup for a single muscle is demonstrated)

An interesting source of variability is the operational definition of the MT. The standard definition of the MT, as formulated in 1994 by the International Federation of Clinical Neurophysiology (IFCN) Committee, is the minimum intensity eliciting MEPs of >100μV[27] (or >50 μV in the subsequent paper[28]) in the resting muscle in at least 5 of 10 consecutive trials. The idea of using a cut-off of >100 μV was based on the signal-to-noise ratio of the EMG signal at that time. This paper has been cited over 2000 times since its publication (Google Scholar: 2638 times cited, checked 03/2019). How this is done in practice has been described in a follow-up paper from 2012[29]. Using a threshold based on a set number of positive trials relative to the total number of trials (at a certain intensity of stimulation) will be called "relative frequency" setup. It is important to use a fixed protocol to determine the MT, since a detail like whether you increase or decrease the intensity to determine the motor cortex in a “relative frequency” setup, affects the result[30]. In the following experiments, the setup was used as described below. After determining the hotspot, as detailed above, the stimulator intensity was increased with another 5%. This usually resulted in 10/10 trials with a large MEP response. From a suprathreshold intensity, the intensity was lowered in 1-2% steps to determine the intensity resulting in a 5/10 positive response. In order to decrease the number of stimuli needed just to determine the MT, it has been proposed to use only six trials per intensity, although this has not been validated. To increase the reliability, using a relative frequency cut-off from 10/20 has been proposed. In the guideline of the IFCNcommittee[29], the MT is determined as the highest intensity resulting in <5/10 positive trials and adding 1% to this intensity. Another way of determining the MT is determining both the lowest intensity resulting in 10/10 positive responses and the highest intensity resulting in 0/10 positive responses and taking the average of those two intensities as the MT[31]. A less-time consuming method with a more logical biological and mathematical basis, is an adaptive method that takes the probability to evoke a MEP at a given stimulus intensity into account[32]. The software supporting this “threshold-hunting” used to be freely available but seems now to be only incorporated in the software of the Nexstim Company. The following experiments used a classic “relative frequency” setup as opposed to a “threshold-hunting”

approach, and used an average of 100 trials (±50) to determine the MT, prior to start with the experiment proper.
One further remark is needed concerning the cut-off value of >50 µV to call a deflection a positive MEP response. Much smaller deflections can be reliably picked up with modern equipment. Proof of this is that it took several years before it became clear that there was a bug in the BrainSight software, which caused the deflections to be increased with a factor of 5.4. All MT maps that were determined before April 18 2015 - the day version 2.2.13 that fixed the bug was released - used the rule >9-10µV (thus a clearly discernible MEP, recorded with more advanced technology in comparison to the setup of the experiments in the IFCN guidelines[27,28]) instead of using a cut-off value of >50 µV as a - result. This would result in a few percent difference in the determination of the MT. According to the developers of BrainSight (Roch M. Comeau, personal communication) the bug would cause an underestimating the MT by 3-5% (mostly around 3%) of the Magstim 200 output. Comparing the effect of using the 50µV MEP cut-off with the "any clearly discernible MEP" in a few patients that were included after the bug was fixed did not or only minimally lower the MT. For consistency, the "any clearly discernible MEP" was thus used for future experiments. The small effect is due to the non-linear relation between intensity of stimulation and the resulting MEP output, a concept clarified in the so-called input-output curves that have been extensively studied for TMS.

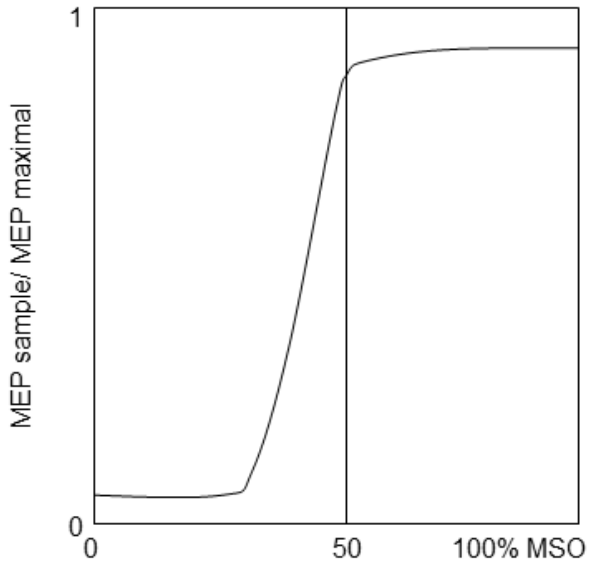

Figure 2.8
Illustrative representation of an input-output curve using TMS: stimulating with increasing intensities results in no muscle contraction until a certain threshold is reached, then a fast increase in MEP amplitude is seen with minimal increments in stimulation intensity until a maximal is reached and the resulting MEP amplitudes plateau.
MSO: maximal stimulator output, intensities expressed as % of MSO; MEP sample/ MEP max: MEP amplitude expressed as a fraction of the maximal measured MEP in the subject

The effect of the bug on the outcome of the results should be minimal in any case. For mapping studies over the motor cortex, it just scales all MEPs. Since the amplitude of the MEP in mapping is used relative to the amplitude of the MEPs of the other coil positions in the same patient, it would not affect the results. Moreover, the amplitudes were rescaled to the correct value before using the data in further calculations. For mapping studies over other parts of the cortex, the relation between the MT and the threshold needed for a biological effect on other brain regions is low in any case. For example, the correlation between the MT and the intensity needed to evoke a response over the visual cortex (this is the phosphene threshold PT) is low and not significantly correlated and the PT is higher than the MT[33]. MT is generally used because this is easier to obtain, since in half of healthy subjects, phosphenes cannot be elicited. In an effort to compensate for differences in intensity needed to activate different brain regions, stimulation in regions at a distance from the motor cortex, often use an intensity that is higher than the motor cortex and implicitly entail some margin in the hope to obtain suprathreshold intensity also in non-motor regions. In language-mapping, for example, an intensity of 120% of MT was used. A small change in the MT would thus be diluted in the much larger uncertainty of the intensity needed to stimulate other brain regions. Moreover, all

language-mapping studies described in this thesis were performed with a newer version of the software. In patients with epilepsy, this small change in intensity, is likely negligible compared to the disease-related fluctuations in motor cortex excitability[34]. In any case, a few percentage difference in the MT is within the expected range of the variability, when repeating the experiment in the same subject on another day[30]. It was not possible to repeat the experiments after this bug was solved - among others because the patient was already operated in the meantime- and the small difference in MT that would result theoretically, would dilute into the multitude of factors know to influence the MT, like time of day, hours of sleep, menstrual cycle, glucose level, ongoing brain activity…

Having gone through this setup, the following chapters will focus on the experiments themselves. Either the experiments consisted of repeated pulses of TMS over different positions of the head or a repeated application of TMS-pulses over the same spot - a technique called repetitive TMS (rTMS). The aim of rTMS is to induce lasting changes in the brain. The mechanisms by which rTMS works, are detailed in part three of this introduction.

2.2. Effect of a single TMS-pulse on the brain

The first question is what the effect is of applying a time-varying magnetic field and what characteristics of the magnetic field are needed to induce an effect in one neuron. To study these questions, experiments were performed with an isolated nerve suspended in spherical container, filled with a solution containing ions[35–37]. These studies have shown that the orientation of the field relative to the bend of the nerve, affects where the depolarization leading to an action potential takes place. Alternatively, the depolarization in a straight nerve takes place where the rate of change of the induced electric field is the greatest, that is at the negative-going first spatial derivative of the induced electric field (charge/surface, e.g. V/m²). Depolarization in these experiments was not induced at the point where the induced electric field had the greatest magnitude. However, every head model used - from the most simple to the most detailed encountered in the literature - calculates the induced electric field and not its spatial derivative. Coils are also studied based on the magnitude of their induced electric field, without taking the variation over time into account[38]. This fuels the ongoing debate about where the induced electric field affects the brain most (crowns of gyri or banks of gyri) and which feature of the electric field is most important for the stimulation (e.g. magnitude versus radial component)[39,40]. Based on mathematical modelling and those experiments on isolated nerves just described, the rate of change of the electric field would be a parameter worth studying and might shed light on the debate about what parameter of the electric field is most important. In addition, since any bend in a neuron affects how this neuron is influenced by the induced electric field, a real realistic head model would need to take every bend of every neuron into account. This is of course impossible.

Adding to the complexity of the effect of a magnetic field on the brain is that its conductivity is not homogenous. When inhomogeneity is induced in the experiment with the single nerve, this results in a lower threshold of excitation in specific locations. The overall effect in an inhomogeneous structure like a brain, full with curving neurons and interneurons, gets inextricable. Thus, using a head model based on individual anatomy and the magnitude of the induced electric field is the best achievable model with the current state of knowledge. More information on realistic head models and its performance in mapping studies can be found in chapter 5. However, most studies do not use any type of head modelling. In our study on rTMS in patients with epilepsy (chapter 3), the coil was placed on the scalp so that it was above the desired target and angulated to be perpendicular to the nearest sulcus. This was done using the neuronavigation system. Many previous studies however, used skull based reference points, which is a crude way of establishing the area of the brain that will be affected by the TMS-field. In a trial for depression, it was noted that using a measure based on distances over the head, the coil was positioned in an incorrect location in 9% of subjects, due to inter-individual variation in head and brain anatomy[41], not even taking functional variability into account. In a study on healthy subjects, it was shown that using neuronavigation, an rTMS experiment over the motor cortex resulted in significant changes in the outcome parameters

measured whereas the same experiment without neuronavigation, resulted in non-significant findings[42].
Since there is compelling evidence that neuronavigation is beneficial in experiments using TMS, it was used throughout every experiment. However, the neuronavigation reduces the TMS positioning to a positioning of one point. Together with this point, there is also a vector of its directionality. However, thinking of the TMS-field as being focused in a single point is very reductionist. The cross-section of a figure-8 coil- the so-called “focal coil”- along the long axis is 14cm. This means approximately one third of the whole head is directly underneath the coil.

Figure 2.9
the induced field from a single coil position modeled and visualized as an arrow representing the vector of the induced field in different voxels of the image, color-coded for the relative strength of the induced field

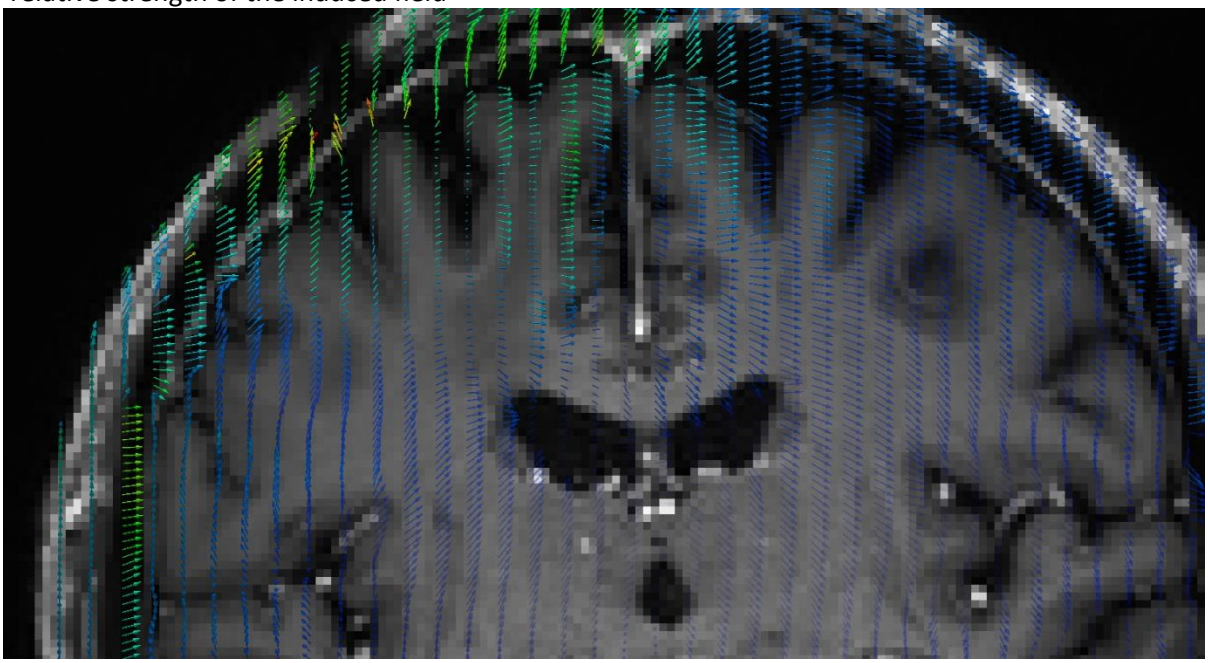

or visualized as a map of the relative strength of the induced field on the cortical surface

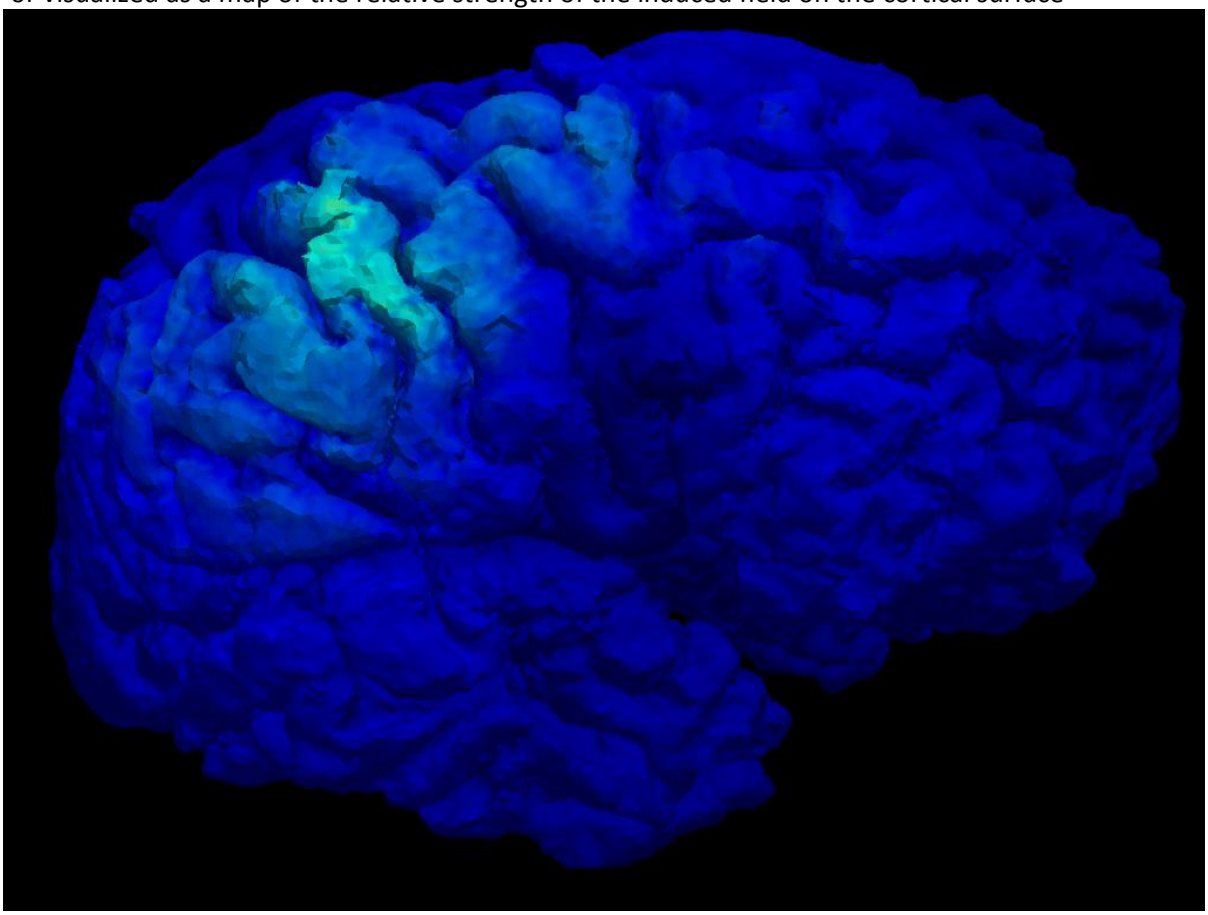

Add to this non-focal effect the known fact that effects of a TMS-pulse are not only seen in parts of the brain directly influenced by the field, but also at a distance and the resulting effect of a single TMS-pulse on the brain becomes very complex. An example of this effect of a single TMS-pulse in a brain network can be seen by using paired-pulse paradigms. This collection of paradigms is used to study the effect of one TMS-pulse (called the conditioning pulse) on the effect induced by the next pulse (called the test pulse). It can be used to test the characteristics and time-dependency of the excitability of a part of the brain locally like in short, intermediate and long term intra-cortical inhibition protocols[43] but also at a distance like in measuring interhemispheric facilitation/inhibition. In this thesis, no direct measures of the effect of a TMS-pulse on the network was included, but the knowledge that TMS affects a whole network in the brain, was part of the rationale to include whole-brain functional imaging in the study in patients with epilepsy (chapter 4).
Besides the field being non-focal and the effects at a distance, the state of the brain also influences the measured effect of a TMS pulse. Even when a coil is held in a fixed position and the characteristics of the TMS pulse are unchanged, there is an important trial-by-trial variability. Examples of this are the variability in MEPs and the variable effect of TMS-pulses on measures of the EEG. The trial-to-trial variability in MEP peak-to-peak amplitude has a standard deviation (SD) that can easily exceed 50% of the mean MEP amplitude and can even be higher than 100%[44]. Therefore, it is important to acquire several measures to average out the variability - in every step of an experiment. This information was taken into account in the way the MT was determined in the experiments described in this thesis, as detailed previously. This variability is paramount in the brain and can for example also be seen in patients with epilepsy, where TMS can both induce and stop ongoing epileptic discharges in a seemingly stochastic manner. This process is however far from random and is based the state of excitability of the brain at the moment the pulse is applied[45].

2.3. Effect of rTMS on the brain

Since a single pulse evokes measurable alteration in the brain in the time-period following the pulse (during at least 200ms post-stimulus), it should come as no surprise that the repetitive application of TMS-pulses can result in aftereffects. These aftereffects are the basis of using rTMS as a therapeutic tool. Repeated pulses are considered to have cumulative effects at a frequency higher than 0.33Hz or when using specific patterns of repeated pulses. The repeated use of pulses at a certain frequency is called “conventional rTMS” and the use of a specific pattern of pulses with interleaved blocks of stimulation is called “patterned rTMS”.
The exact interplay of different mechanisms involved in the long-term effect of rTMS remains elusive. Traditionally, the effect of rTMS has been described along the lines of long-term depression (LTD) or MA (LTP). The first descriptions of long term potentiation were made in the seventies when it was seen that in hippocampal slices, after applying high frequency electrical stimulation the amplitude of the post-synaptic potentials could increase[46]. This is the basis of considering high-frequency stimulation as an “activating” stimulation. In rTMS research, high-frequency conventional rTMS is considered being > 1Hz. Later, it was noted that the temporal pattern of stimulation was also critically important, especially the order in which the pre- and post-synaptic neuron were stimulated respectively. In order to induce plasticity (either LTP or LTD) the stimulus intensity, number of pulses and the pattern of stimulation must be of sufficient magnitude and applied to active synapses in order to have any effect. The mechanism by which this effect ensues starts with the influx of calcium in the post-synaptic cell. This leads to a cascade of Ca^{2+}-dependent processes. When the Ca^{2+} influx is swift, it leads to post-synaptic changes including the upregulation of AMPA-receptors and increasing its sensitivity for glutamate. On the other hand, LTD is induced by long and slow frequency stimulation, leading to a slow build-up of the post-synaptic Ca^{2+}, leading to activation of phosphates and internalization of the AMPA receptors. Long-term changes (>60 minutes post-procedure) are based on downstream alterations in gene expression. As already noted, plasticity occurs in active synapses. This means that the effect of the applied stimulation is dependent on the ongoing activity of the brain. Concepts that relate to this phenomenon are called metaplasticity and homeostatic

plasticity[47]. Metaplasticity refers to the fact that prior activation influences the result of the protocol aiming to induce plasticity. It is also sometimes referred to as "state-dependency" of the effect of rTMS. Homeostatic plasticity stabilizes neural activity within a physiological meaningful range, preventing a runaway process in inducing plasticity. This implies that a multitude of factors affect the result of an rTMS protocol. Factors that have been noted to relate to a variability in effect of a rTMS protocol are age, gender, time of day, previous physical and mental activity, genetic factors[48], brain states during stimulation[49,50], short breaks in sessions[51] and corticospinal excitability[52]. Whereas age and gender have probably more to do with anatomical differences, all the other factors relate directly to the mechanisms underlying plasticity as just described. This leads to the fact that the effect of rTMS is quite variable and hard to predict in individual subjects.
Considering its unpredictability, having a technique to induce plasticity non-invasively in humans, is really world-changing. It opens a new window on brain research and a whole field of new therapeutic avenues for brain diseases. There have been more than thousand clinical trials using this technique for a wide variety of brain disorders in the last ten years (PubMed: 1319 trials, last checked 03/2019).

2.4. Safety of TMS studies

Since TMS affects the brain, questions about safety hazards need to be addressed, especially since it is utilized so extensively. From a safety perspective, not only the intensity of the TMS pulse is important but also how often it is repeated, since cumulative effects ensue. Only to determine the MT, I used an average of 100 TMS-pulses. However, those repeated pulses are not considered to have a cumulative effect - although one paper reports an improvement of motor functioning after a mapping procedure with 1098 pulses over 62minutes[53]. However, when checking the supplementary material of this paper, their procedure was more than just a mapping session, using frequencies that approach rTMS frequencies, bilateral stimulation protocols, paired pulse paradigms and intensities up to 318%MT. To consider repeated pulses of TMS as independent, there should be sufficient time in-between two consecutive pulses, in the order of several seconds.
Generally, TMS is considered a very safe technique. Several reviews about the safety of TMS have been published, both from a more general perspective[29,54] and in specific diseases like in subjects with epilepsy[55–57] and guidelines have been issued about ranges of TMS parameters that are considered to be safe[58,59].

Real and potential safety hazards are heating, effects on implanted metal and devices, exposure to high intensity magnetic fields, induction of long-term changes in brain function, induction of seizures, syncope, pain and other acute side-effects.
Like every system with electric currents, heating ensues. First, the coil itself gets warm with repeated use. To prevent burning, a temperature sensor is built in the coils and the system shuts down when the coil gets too warm. Second, the underlying brain tissue can also heat. The magnitude of this effect is estimated to be small and due to brain perfusion, heat is dissipated easily. The heating of the brain is estimated to be almost an order of magnitude smaller than the tissue heating induced by deep brain stimulation[58]. Metal implants and surface electrodes pose a specific problem, since metal with high conductivity will heat excessively when applying TMS. Moreover, they can move in the magnetic field and high voltages can be induced in those systems. The safety using TMS in those instances has not been studied extensively. Due to uncertainties of its safety, it seems prudent not to use TMS on subjects with (ferromagnetic) metal implants in their head or implanted stimulators. Nevertheless interesting data have been recorded from patients with deep brain stimulators or epidural grids using single and paired pulse TMS protocol, without any side effects. In DBS systems, currents of sufficient intensity to activate neurons could however be induced with TMS - which could lead to undesired side effects and could entail a safety hazard. It is also important to keep in mind that even if a device is cleared for use under the MRI, its safety when using TMS still needs to be addressed. For example, gold EEG-electrodes attached to the skin are considered safe to use in the MRI but pose a risk of excessive heating with skin burns when applying TMS[60]. We were especially interested in the safety of TMS in patients with a vagal nerve stimulator. Vagal nerve stimulators are

implanted as a treatment in patients with refractory epilepsy - and are used in refractory depression. These diseases are also amendable to rTMS treatment and if patients are not cured with their vagal nerve stimulation, many researchers feel like offering them rTMS might be advantageous. Several studies addressed the safety of using TMS with an implanted vagal nerve stimulator. An ex vivo study showed that a single TMS-pulse did not affect the performance of the vagal nerve stimulator and the induced current in the stimulator remained well below those needed to activate the vagal nerve[61]. Studies demonstrated the safe use of single and paired pulse paradigms in patients with vagal nerve stimulators[62,63] A survey of rTMS clinics in the US learned that in twenty subjects with depression with a vagal nerve stimulator, rTMS had been performed without complications[64]. All checked the parameters of the implant after the stimulation and turned off the device during the rTMS session itself. For patients with epilepsy, one case of a patient with status epilepticus who had a vagal nerve stimulator in whom rTMS was used without complications, is published[65]. In this case, the VNS was also turned off during the rTMS session, similar to the instructions of preparation of the VNS prior to a head-MRI. Based on these data and the fact that the VNS is at a distance of the coil, patients with a VNS could participate in the experiments detailed in this PhD. All other metal implants and disconnected VNS-stimulators were an exclusion criterion.

Whereas the effect of heat and current can be directly measured and side effects of these are proportional to its magnitude, the effect of exposure to magnetic fields over short and long term is less clear. The long-term effects are especially relevant for the operator, who is exposed over longer periods. Several effects of magnetic fields on biological tissue have been described but the relevance of these effects for TMS-experiments is not clear. The magnetic field may influence electron pairs and induce magnetic spin effects. These effects may in turn have an influence on the rate of several chemical processes. It could also influence the structure of charged macromolecules[66]. Several bacteria, invertebrates and animal species have sensor for magnetic fields, including the “compass” of traveling birds. Whether humans are affected by the surrounding magnetic field, has not been clearly demonstrated.

The most important factor is likely the effect of the protocol itself. As detailed in the previous part, rTMS can induce long-term effects. However, since it is hard to predict the exact effect of the protocol, undesired long-term effects can ensue. This has not received much attention in the literature, but the long-term effects that are seen in animal models of rTMS do not only influence the synaptic strength of existing synapses, but also affects the structure of the synaptic network and even leads to changes in neurogenesis, differentiation, (inhibition of) apoptosis and astrocytic migration. These long-term structural changes are mostly induced by high-frequency, high-intensity stimulation but are also seen in some studies with low-frequency stimulation. Relevant examples of the effect of low-frequency stimulation in models of epilepsy are based on brain slices and mice models. Using 1Hz stimulation over hippocampal slices increased dendritic sprouting. In a mice model of chemically-induced epileptogenesis, low-frequency rTMS exhibited anti-epileptogenic and anti-apoptotic properties, with concurrent changes in gene expression[66]. Whereas low-frequency stimulation could be beneficial in epilepsy, repeated high-frequency stimulation could in theory lead to induction of epilepsy. This hypothesis is based on the observation that in animal experiments electrically-induced epileptogenesis does occur. This process is referred to as kindling. However, the possibility of kindling in humans using TMS has never been demonstrated[60]. It needs to be noted that results from small animal models cannot be directly applied to humans due to large difference in size of the brain and brain conductivity.

Whereas long-term safety has not received much attention, a wealth of literature is available describing acute side effects of TMS, the most dramatic of those being the induction of a seizure. The risk of seizure induction would be especially present in protocols using high-frequency, high-intensity stimulation without breaks in-between pulse-trains. The risk of seizure induction is however very small. In patients with epilepsy, the risk is estimated at a crude per subject seizure risk of 2.9% (95%

CI: 1.3–4.5), given that 12 subjects reported seizures out of 410 subjects described in the literature. This analysis excluded data of patients with epilepsia partialis continua or status epilepticus[67]. Other side effects are considered mild, including fainting, dizziness, nausea, headache, muscle aches, insomnia, sensory symptoms and cognitive slowing. From those symptoms, headache and nausea were most often reported. No clear difference in side effects was seen between active and sham stimulation, although stimulation with an active coil over the occipital area, was associated with nausea[68]. This list of possible side effects was adapted to use as a screening tool for side effects in our experiments. A more practical concern is the induction of hearing problems due to the noise generated with the discharge of each TMS-pulse. To mitigate this effect, all rTMS experiments and all studies including stimulation over the lateral areas of the head were performed with both patient and operator wearing foam earplugs.
The most troublesome side effect for subjects is pain. Pain is especially prevalent when stimulating over anterolateral parts of the head, probably due to activation of the trigeminal pathways (including toothache). In a large multicenter report of language mapping in patients with intracranial lesions, pain was reported by 70% of the subjects[69]. In the conclusion of this study, it was reported that the procedure was "well-tolerated". The fact that 70% of subjects report pain and many studies report the necessity to decrease stimulation intensity and/or frequency to make the procedure better tolerable for the subjects[69–72], does seem to contradict the idea that language mapping with TMS is a patient-friendly option for language mapping before surgery. Our ways of making language mapping better tolerable are detailed in a later part (chapter 6) of this thesis.

2.5. fMRI

In previous parts, we discussed the role of TMS in delineating the functional neuroanatomy. TMS is of course not the only technique that can give us insight into the functional organization of the brain. Functional magnetic resonance imaging (fMRI) has a long-standing record of giving us insight in the functioning of the brain. It has revolutionized the field of neuroscience. The last ten years there have been more than 9000 clinical trials using fMRI published.

The basic principle underlying fMRI is the difference in paramagnetic properties between oxygenated and deoxygenated hemoglobin. With neuronal activity, the expenditure of oxygen increases. More oxygen is extracted from the blood, which is rapidly (2-6s) compensated by an increase of blood supply and oxygen to this region. Thus neuronal activity leads to a net increase in oxygenated hemoglobin in the area, shortly after and time-locked with the activity. This is also seen in the signals originating from venous structures, due to the relative large amount of blood in these structures and the time-course of the blood flowing though these structures. Since deoxygenated hemoglobin is paramagnetic and oxygenated hemoglobin is not, in areas with more deoxygenated hemoglobin, there is more dephasing, thus a decrease in the transversal relaxation decay constant T2* and a darkening of the voxels containing blood vessels with deoxygenated hemoglobin on heavily T2* weighted images. This change in signal caused by differences in oxygenated/ deoxygenated hemoglobin is called the Blood Oxygen Level Dependent (BOLD) signal. The predicted changes in BOLD signal after neuronal activation are modelled as the hemodynamic response function. It models both the time course with a rising phase up to 6s after onset of neuronal activation and the expected magnitude of change, which is in the order of 2%. To determine what voxels of the brain have an increased neuronal activation, the timing onsets of the neuronal activation are convoluted with the hemodynamic response function and this predicted signal change is compared with the measured BOLD signal. To know the onset times of neuronal activation, special sequences of tasks are designed to be done by the subject during the fMRI scanning. Most commonly, these tasks contain epochs in which the subject does a task, interleaved with no-task or "rest" epochs. These types of tasks are referred to as block-designs. The duration of one epoch or "block" is chosen so it is at least as long as the hemodynamic response function, so a stable change ensues. The epochs are repeated several times so multiple measurements can be obtained. During the whole task, heavily T2* weighted images are acquired. This results in a time-series of images. For each voxel, the change in BOLD signal

over time can be followed. The image of interest in fMRI is the resulting image after statistical interference, in which each voxel has a value that expresses how similar the BOLD signal changes in this voxel was over time compared to the predicted BOLD signal changes based on the task that was designed. The design of the tasks to be performed during fMRI scanning needs to take into account the MRI environment. Since the MR-scan generates a lot of noise during operation, auditory presented tasks pose specific challenges, so most experiments use visually presented instructions and tasks. BOLD signals are also extremely sensitive to movement artifacts, so head movements need to be avoided. This makes using spoken responses also challenging. Limb movements, including button presses and silent word generation often do not generate head movements, so can be used more easily. In designing fMRI tasks, the idea is often not to see all areas involved in a task, from the reading of the instruction to processing the command and selecting the specific output program. Frequently, one specific subset of the task is of interest. Therefore, a control task is designed that is as similar to the task of interest as possible, except that it does not use the specific brain function of interest. The visual processing of the task instructions is often not a brain function one is interested in, so the instruction for the control task could be presented in the same way. Since the area for visual processing of the task instructions will in that way be similarly activated in both conditions, these areas will not show in a differential image. It can be hard to design a control task that uses all the same brain processes as the task of interest except one specific subset and is equally challenging. This is however a prerequisite so the amount of activation in all non-interest regions is of similar magnitude. Moreover, one is limited by the amount of time the subject can comfortably lay still. This is often shorter in patients than in controls - and in patients, several brain functions are often studied sequentially, making the time available for each fMRI task even shorter. This means it is often hard to add multiple control tasks in order to tease out the specific brain function of interest. fMRI scans were performed routinely in patients included in my studies prior to surgery. The abnormal brain tissue in itself however, affects the neurovascular coupling and thus the possibility to generate and the shape of the BOLD signal. Therefore, it is often desirable to add a positive control condition- for example contralateral activation. In motor mapping studies, bilateral movements are often used to serve both as a positive control and to use as a comparator to judge the amount and location of activation on the pathological site. For lateralized brain functions that activate a whole network of brain regions - like language tests - designing positive control and negative control tasks, is much more challenging. Beside these general concerns, studying the temporal lobes with fMRI poses the additional problem of suboptimal BOLD signals in this region. As detailed before, deoxygenated hemoglobin gives rise to a lower signal, due to local field inhomogeneity. However, much larger local field inhomogeneity is present at air-bone interfaces like close to the petrosal bone, nasal and oral cavities, affecting especially the temporal lobe. This means that there is no perfect technique to sample the temporal lobes, since TMS is also not good due to the deep location of the mesial temporal structures and the pain associated with stimulation in this region, as detailed in the part about safety of TMS.

2.6. Other functional imaging techniques: DTI, PET, SISCOM, EPs

As detailed in previous parts, the connections of a neuron within a network determines what functions this neuron can have. Neighboring neurons often have similar connections and their axons can run together in fiber bundles, called tracts. Visualizing these tracks can be done using a technique called tractography. A non-invasive method of tractography in individual subjects is using MRI. The MRI technique used for this purpose is diffusion tensor imaging (DTI). The underlying principle of DTI is that water molecules can diffuse more easily along the main direction of a fiber tract compared to other directions. For tractography, the amount of diffusion is measured in each voxel, for different directions. The resulting images contain information in each voxel on the magnitudes of the diffusion in each of the directions measured. From this information, it is possible to derive the preferential direction of diffusion starting in one place of the brain, and follow it to other brain regions. The connections generated in this way reflect closely the known anatomy of fiber tracts in the brain. The color-coded paths of connectivity as measured by MRI tractography are

therefore considered to measure and display existing fiber tracts and are named accordingly. In order to obtain usable tracts from the diffusion information, several assumptions and constraints need to be imposed. These have to do with what tracts one wants to visualize, often done by manually selecting regions of interest based on prior anatomical knowledge. Other choices have to do with how to draw tracts based on the diffusion information. One can decide that each voxel can only have one preferential direction and draw tracts along those directions- a technique called deterministic tractography. Alternatively, one can take into account that those values contain more information than just one main direction and use statistical interference methods to determine the most likely paths based on the diffusion information- a technique called probabilistic tractography. For both methods, constraints need to be imposed on many factors, e.g. the maximal bends in the tracts that are acceptable, or stopping rules on how small the diffusion values can become. There is also the inherent problem that for each voxel, only one measure is obtained and if this voxel contains axons running in different directions, it is very difficult to disentangle this solely on its value. With advanced modelling and information of other sources and information of neighboring voxels, it might be possible to overcome this drawback. This is an area of active research. However, for better tractography, more measurements are needed and again we are limited in clinical practice for time one can comfortably scan a patient. Therefore, the tractography used before surgery in clinical practice is a deterministic tractography, limited to the tracts of interest in a specific case. It uses regions of interest (ROIs) to be connected based on the location of the tumor and anatomical knowledge. The ROIs are manually delineated. The ROIs and constraints are manually and iteratively adapted from a set standard and visually checked by an experienced reader, to obtain the final tracts. This is done in inbuilt scanner software, the Philips FiberTacks software (Eindhoven, The Netherlands).

Besides imaging based on MRI, there exists an at least equally versatile functional imaging technique, namely positron emission tomography (PET). The basic principle of PET is to bring a radioactively labelled tracer into the body, and measure its distribution. Detectors around the subjects that pick up the gamma-photons that are created when the radioactive label of the tracer decays, obtain the measurements. Based on the pair of detectors that pick up a signal, the position in space of the (in theory) single tracer molecule at the time of its decay can be determined. Taken together, the measurements create a map of the distribution of the tracer in the body.
The versatility of the technique stems from the variety of tracers that can be used, spanning analogues of gasses like oxygen, metabolic substrates like glucose, analogues of endogenous substances like neurotransmitters, drugs… This means one could image most processes of interest. Examples that relate to this thesis are the use of PET for localization of eloquent cortex, determining the malignant nature of brain lesions, detecting metastasis, measuring functional alterations in epilepsy and after experimental procedures. Localization of neuronal activation in response to a task, used to be measured with PET. For this application, however it has been largely replaced by fMRI, which does not use ionizing radiation. PET is still used to determine the metabolic characteristics of brain lesions, helping to predict if a lesion represents a glioma and giving some insight in its grade. This information was often used in selecting patients for surgery. The main PET measurement used in this thesis is the metabolic activity of the brain by use of a glucose analogue injected intravenously. This analogue is taken up in the brain and used as would regular glucose, but then is trapped in the cell trying to burn the glucose, since the tracer is slightly different from regular glucose. The radioactively labelled tracer on the metabolite then decays and its position can be detected. In that way the metabolic activity of neurons in the brain can be imaged. It has many applications, including the work-up of neurodegenerative diseases or the detection of brain metastasis, and is also used in patients with epilepsy and can be used to measure the effect of experimental procedures on neuronal (metabolic) functioning. Chapter 4 details to our experiments using PET to measure metabolic alterations after rTMS in epilepsy patients.

Since PET measures metabolic changes, it can only detect the changes in metabolism caused by a seizure, if a seizure occurs between the time of injection and the time of imaging (timeframe of 1 hour). Since seizures are often unpredictable, a technique able to image changes in activity in the brain that is reliable if the tracer is injected at the onset of the seizure would be more suited. Single photon emission computed tomography (SPECT) can be used for this purpose. The principle is that at the onset of a seizure, a tracer is injected intravenously that gets trapped in the brain. Its distribution is proportional to the perfusion in the brain at the time of injection. As stated in the section on the principle of fMRI (part 2.5), neuronal activation is accompanied by a compensatory increase in perfusion to this area. So an increase is seen in the areas that are active during a seizure. In order to be able to detect an increase, a similar scan is performed at a time that no seizures are detected and both scans are proportionally scaled and then subtracted to obtain a differential image. For anatomical localization, this differential image is projected onto the MRI. This way of analyzing the SPECT image has been named SISCOM (subtraction ictal SPECT co-registered with MRI). This imaging technique has been used to determine - together with all other available information - the location of the onset of a seizure in patients undergoing rTMS (chapter 3).

Besides measuring brain activation indirectly based on changes in perfusion - like with SPECT obtained during a seizure - it is also possible to measure the electrical activation itself. An easy way to get this information is by placing electrodes on the head that measure voltage differences between each pair of electrodes. This is the principle of electro-encephalography (EEG). Specific discharges on the EEG are the hallmark of epilepsy and the localization of the discharges points to the area involved in generating the seizures. This information was evidently also used in determining the onset of a seizure in patients undergoing rTMS.
The electrical activation of brain areas can also be used to localize functional areas of the brain. This was not explored in detail in this thesis, but is included here for the sake of completeness. The way this is performed is similar to any experiment using evoked potentials (EPs). The underlying idea is that a trigger gives rise to an electrical signal in the brain, time locked to the trigger and in the specific brain regions involved in processing this specific type of trigger. An example is sensory information. Electrically stimulating a peripheral nerve, will generate a response in different brain areas, including the primary sensory cortex, classically located in the postcentral gyrus. This response will not be evident on the EEG. However, when repeating the same stimulus and averaging each stimulation epoch, this response will become clear since the other ongoing brain activity will have averaged out. In this way a somatosensory evoked potential (SSEP) is obtained. Classically, only two brain electrodes are used to measure the SSEP. For localizing the activity, many more distributed electrodes over the brain are needed. By measuring the same response from different locations, the source of the signal can be localized. Determining the source of the signal is based on the path and the conductive properties of the tissues it needs to cross before reaching the measuring electrodes. This gives rise to similar problems as those encountered when using advanced head models for mapping brain tumor patients with TMS, as described in chapter 5. The difference is that in a head model of TMS, the source of the electrical activity is known whereas in electrical source modelling of EEG data, it is what needs to be modelled. This inverse modelling is an area of active research outside the scope of this thesis.

2.7. Outcome parameters and gold standard

Having gone over all different modalities and alluding to the problems inherent to every technique, the question that pops to mind is, is it worth the effort? This is a question of defining what would be a good outcome and what it takes so more patients could have this good outcome.
In this PhD, the focus is always on helping the individual patient. Data will thus always be given for each individual in the study- not just as an average of all patients.

2.7.1. Electrical cortical stimulation

Direct electrical cortical stimulation (DCS/ECS) is considered the ground truth for mapping the eloquent cortex in neurosurgical patients[73,74]. A meta-analysis of case-series reporting the outcome of glioma surgery with or without peroperative ECS has been published, that it improves survival by increasing the number of patients that undergo a gross total resection without an increase in long-term neurological deficits[75]. However, short-term neurological deficits including transient worsening of motor and language functions, appears to be more frequent using ECS, likely due to a more aggressive resection. The principle of ECS is straightforward and is similar to the experiments of Penfield and Jasper in the 1930s. In an awake patient, the brain is exposed and probed with small electric currents and all observable and subjective experiences reported by the patient are noted. In this way, the function of the brain is mapped.

Even in the current era where high-quality 3D anatomical images and fMRI are routinely available and loaded into the intra-operative neuronavigation software, combined with the trained eye of an experienced neurosurgeon; ECS still plays an important role to determine the functional role of different parts of the brain. To demonstrate this, the data of all awake surgeries, performed after January 2008 and before the start of the experiments described in this PhD were reviwed. Data of 59 surgeries were available. Prior to any mapping, sterile number tags are placed on the cortex by the neurosurgeon, based on his interpretation of the tumor localization and functional organization of the brain. The neurosurgeon than assigns a functional label to each tag, based on his interpretation of brain anatomy and functional fMRI findings. These “pre-ECS functional labels” were prospectively recorded for all patients. These labels were compared to the findings of ECS.

motor function	pre-ECS +	pre-ECS -	sens/ spec
ECS +	45	14	0.76
ECS -	44	250	0.85
PPV/NPV	0.51	0.95	

language function	pre-ECS +	pre-ECS -	sens/ spec
ECS +	17	27	0.39
ECS -	67	186	0.74
PPV/NPV	0.20	0.87	

Table 2.1: Comparison of the predicted functional relevance of a brain area (around a sterile number tag placed during surgery) based on all non-invasive data routinely available to the surgeon during the operation to the findings of ECS.
NPV: negative predictive value, PPV: positive predictive value, sens: sensitivity, spec: specificity.

As can be seen from the positive predictive values, without ECS surgeries would often be to conservative, wrongly assuming a part of the brain to be eloquent in up to half of the surgeries

around the motor cortex and up to 80% of the surgeries in areas around the language network. Conversely, there would also be a small risk of inducing new deficits of around 5% for surgeries around the motor cortex and 13% of the surgeries in areas around the language network. These data are in alignment with the consensus in the literature that using ECS, larger but safer resections can be performed.

Although there is a consensus about the usefulness of the technique in selected cases, the practical setup of these experiments varies widely. In our center, almost all procedures are carried out using an asleep-awake procedure. This means the patient is anesthetized at the onset of the surgery and awoken after the craniotomy. Only in patients that have clear contra-indications for the asleep-awake procedure (young age, factors making intubation difficult and thus potentially compromising procedural safety…) an asleep mapping for peri-Rolandic tumors is performed. The peri-Rolandic area can be mapped during an asleep procedure, if specific care is taken during anesthesia, so MEPs and SSEPs are still obtainable. The added benefit of awake surgery for mapping of the motor cortex is that subjective sensory symptoms and interference with motor planning can also be monitored. In asleep subjects, only an estimate the intactness of the pathways is available. This is the reason why in our center awake surgery is also preferred for peri-Rolandic surgeries. Since behavioral parameters give a good feedback of functioning, no MEPs or SSEPs are recorded during awake procedures. For language mapping, it is a prerequisite that patients are awake during the procedure. Behavioral testing consists routinely of naming line drawings from the Snodgrass set[76] and using this word in a correct sentence. This is supplemented based on anatomical location of the tumor with repetition and counting. In-between mapping and resection, spontaneous speech is quasi-continuously monitored.
Information from ECS is inherently limited to the part of the brain that has been exposed during surgery. Large craniotomies have the advantage that larger parts of the brain can be sampled with ECS. Small craniotomies on the other hand are associated with faster healing and less complications. Thus tailored craniotomies are often preferred, including the tumor with 2-4 cm margin[77].

Routinely, stimulation is performed using a bipolar stimulator with 5mm spacing of the anode and the cathode, applying current for 3s at a frequency of 5.31 Hz, using biphasic pulses with a pulse width of 200µs and an inter-stimulus interval of 200µs. Current is increased in a stepwise fashion to 20mA (occasionally 24mA) and the voltage is limited to 80V. Monitoring for seizures is done by checking the patient- no grid is used to check for afterdischarges. In asleep mapping, the setup depends on the pathology and the preference of the surgeon. In surgeries that need a grid anyhow, like those for motor cortex stimulation in chronic pain, phase reversal of the SSEP is used to localize the central sulcus, and electrical stimulation between neighboring contacts of the grid is used afterwards to evoke MEPs to check for the correct localization of the grid. In young children, this is also the preferred setup, since SSEPs are easier to obtain compared to MEPs due to differences in myelination. For mapping tumor patients in asleep conditions, either monopolar or bipolar stimulation can be used. Bipolar stimulation is preferred for cortical mapping in our center, since limiting the path of current flow seems safer in order to prevent eliciting seizures. For this procedure, a train-of-five stimulation is used, applying current in five anodal pulses of 500µs pulse width and an inter-stimulus interval of 4ms. Current is increased in a stepwise fashion to 10mA. Repetition rate is limited to 2Hz. A similar stimulation protocol is used for monopolar subcortical stimulation. Occasionally, this setup was also used in awake patients in conjunction with the 5.31 Hz stimulation, since it sometimes seems to give a better activation. Infrequently, stimulation at 50Hz was used. Although this is the classic stimulation setup, its use was limited due to the higher risk of eliciting seizures, using this setup[78–81]. ECS data were obtained to guide the resection. The ECS protocol was the same in patients included in the studies, as it would have been without the study, with the difference that the points of stimulation were recorded in the intra-operative neuronavigation system, for offline analysis. The ECS points thus are a limited set of points probed during surgery, of the cortex that was exposed through the craniotomy.

In mapping the eloquent cortex, ECS is the established technique to compare a newer diagnostic technique with. This comparison can be done in multiple ways. Examples of possible research questions are: is the outcome using either technique similar based on functional outcome and/or gross total resection; how does the newer technique compare in surgical decision making; what is the performance of the newer technique compared to the results obtained by ECS. The approach taken in this PhD is that it would be useful to have a technique one could rely on if ECS was not available for whatever reason. The operational question linked to this is how another diagnostic technique compares to ECS in surgical decision-making. A related but different question would be if the newer technique were able to delineate essential cortical areas. This needs to be operationally defined, since it is impossible to determine experimentally in individual patients with brain lesions what the minimal cortical area is in each location that can be removed without permanent functional deficits or the maximal extent that is safe to resect. In that way delineating essential cortical areas resembles delineating the epileptogenic zone[82]. Another approach to link post-operative outcome with pre-operative findings, is relating pre-operative findings of the newer diagnostic technique with the resection zone. This poses two problems for research. The first is that due to brain shift after resection, it is harder to link pre- and post-op data. As of now, no satisfying method has been described to fully compensate for brain shifts after surgery. The second reason is that almost all patients had a favorable neurological functioning at follow-up- which is of course desirable but to associate our observations with outcome, negative outcomes are also needed. This approach was therefore not used.

2.7.2. Seizure diaries

A good outcome in patients with epilepsy is classically defined as a reduction –or even better, an abolition- of seizures. Outcome measures are expressed as the change in the number of seizures over certain period after a treatment has been initiated compared to the seizure frequency before (the so-called baseline seizure frequency). Examples of these outcome measures are the percentage seizure reduction or the proportion of patients experiencing at least a fifty percent reduction in seizure frequency, the latter is called the responder rate.
However, the seizure frequencies are based on the patients' report of seizures, or of those of a caregiver. This can be problematic in itself. Seizures are often accompanied by a clouding of consciousness or even by loss of consciousness and a post-ictal amnesia. Reports of caregivers can be unreliable since it is impossible to monitor a patient 24/7 and more subtle events can be missed.
In a study on seizure prediction using an implanted device to continuously record and analyze EEG signals, little correlation was seen between the seizure frequency reported by the patients and that measured on EEG. In only half of the included patients, there was a significant correlation between both measures (Spearman's rank correlation coefficient) and most patients underestimated the number of seizures they experienced. Moreover, the accuracy of reporting varied unpredictable over time in individual patients[83]. Wearable seizure detection devices are there for an active area of research, since adequate outcome measures are a prerequisite for adequate treatments. In our study on using rTMS for the treatment of epilepsy, we included one person with epilepsy, who was unable to record seizure frequencies. Since one of the symptoms of the seizures, was ictal tachycardia, an implantable heart-rhythm device (Medtronic Reveal XT 9529 implantable loop recorder) was read out to determine seizure frequency rates. Tachycardia as an ictal phenomenon is well-known[84] and has been used in wearable seizure detection devices[85,86] and is now also part of the algorithm of the heart-rate triggered vagal nerve stimulator[87]. Based on video-EEG recordings that included ECG-traces, it was concluded that in this patient, using ictal tachycardia as a telltale sign of seizures was reliable. It would seem prudent to assume that future studies on the treatment of epilepsy, will use objective measures to record seizure frequencies, and would lead to results that are more reliable. For now, however, seizure diaries will remain the norm. Moreover, using patient-reported outcome parameters is very useful, to grasp the effect of the disease on the patients' life. This is especially

true for quality of life measures, which are subjective measures. Validated questionnaires were used to record these outcome measures, in the study on rTMS for the treatment of epilepsy.

3. Repetitive transcranial magnetic stimulation for the treatment of refractory focal epilepsy

In this chapter, the clinical outcome data of the study using rTMS for the treatment of epilepsy are reported. This chapter has been published:
Randomized crossover sham-controlled clinical trial of targeted low-frequency transcranial magnetic stimulation comparing a figure-8 and a round coil to treat refractory neocortical epilepsy.
Laura Seynaeve, Annemie Devroye, Patrick Dupont, Wim Van Paesschen. Epilepsia. 2016 Jan;57(1):141-50. doi: 10.1111/epi.13247. PMID: 26642974[88]

3.1 Summary

Objective:
Determine the efficacy and side effects of low-frequency rTMS to treat refractory neocortical epilepsy and study differences in effect between a figure-8 and round coil type.

Methods:
This single-center randomized sham-controlled crossover trial (NCT01745952 on ClinicalTrials.gov) included 11 patients with well-defined focal epilepsy. rTMS (0.5 Hz) was targeted to the focus during three treatment conditions consisting of 1,500 stimulations/day for 10 weekdays at 90% of resting motor threshold (rMT) followed by a 10-week observation period. Patients were randomized for the order in which the figure-8, round, and sham coil were used. Outcome assessors and patients were blinded to the type of coil used. The primary outcome measure was the percentage of seizure reduction after active rTMS treatment. Other outcome measures were responder rate, quality of life, and side effects.

Results:
There was no difference between a figure-8 and round coil. None of the patients achieved an overall 50% seizure reduction. One patient responded during 1 month after treatment with either active coil, followed by a significant increase in seizure frequency. Another patient had a fourfold increase in seizure frequency during rTMS treatment.

Significance:
This study provides evidence that rTMS is on average not effective for reducing seizure frequency. No difference in effectiveness between the different coil types was observed. It can, however, exacerbate seizures during treatment and lead to a rebound in seizure frequency after an initial reduction.

Key points

- Low frequency rTMS is overall ineffective to reduce seizure frequency in a 2-month period following active treatment
- No difference was seen between treatments using a figure-8 or a round coil positioned over the focus
- rTMS can cause rebound seizures after an initial response
- rTMS can acutely exacerbate seizures

3.2 Introduction

rTMS is a non-invasive brain stimulation technique that can alter the excitability of cortical regions by patterned application of a time-varying electromagnetic field.[89] Inhibitory protocols such as low-frequency rTMS seem to hold promise for epilepsy treatment. Until now, 13 studies with a total of 196 patients undergoing active treatment showed mixed results.[90–102] This could be due in part to the variability in inclusion criteria and treatment protocols. Based on individual trials and the meta-

analysis of Hsu et al.,[103] it was demonstrated that low-frequency rTMS is especially promising for patients with cortical dysplasia or neocortical epilepsy, if the stimulation was targeted to the epileptic focus. rTMS aimed at the vertex was not effective,[102,103] probably because the epileptogenic zone was not targeted. rTMS of mesial temporal structures was not effective[103] because these structures are too deep to be affected directly by rTMS.
In most studies, the target of stimulation was the most active point in the 10-20 or 10-10 electroencephalography (EEG) system. However, in one patient,[92] the ictal EEG and single-photon emission computerized tomography coregistered to MRI (SISCOM) data were used to define the focus, and neuronavigation was used to position the TMS coil. This patient experienced a 90% seizure reduction. This was the only study[92] to date using neuronavigation. Treatment protocols also differed in their stimulation frequencies and intensities, but those differences were not clearly associated with outcome.[103] A wide range of coil types, both commercially available and custom-made, have been used. The number of rTMS pulses a day, days of treatment, and spread of treatment sessions over time were also diverse, ranging from 100[91] to 3,000[92] stimuli per day with treatments administered daily in most studies but biweekly in others.[91,97] Studies using higher numbers of stimuli obtained better results than those using lower numbers. To capture the full potential of rTMS to reduce seizure frequency, we decided to incorporate all factors that have been shown to be beneficial, namely low-frequency stimulation targeting the epileptic focus using neuronavigation, inclusion of patients with well-delineated neocortical epilepsy, and a high number of total stimuli during a treatment block.
A factor that has not been studied to date is whether the coil type used influences the effect of rTMS. All studies with stimulation over the epileptic focus used a figure-8 coil.[92–95,97,99,101] With use of the figure-8 coil, the maximal stimulation will occur near its center, whereas with the round coil, inhibition of brain tissue surrounding the center of the coil is expected. Both could be effective, since epilepsy is not only a problem of hyperexcitability of the focus but also of failure to prevent spread to neighboring brain regions. It has been shown that the round coil—when positioned over the focus—is more effective than the figure-8 coil for aborting epileptic discharges in patients with frontal lobe epilepsy.[104] No study to date, however, has evaluated the potential to reduce seizures when targeting the epileptic focus with a round coil. To investigate whether there are differences in effect between the figure-8 and the round coil in individual patients, we performed a double-blind randomized sham-controlled crossover clinical trial. The primary aim of our study was to validate rTMS as a clinical tool to treat selected patients with refractory neocortical epilepsy.

3.3 Methods

3.3.1 Participants

Eligible participants were 16–75 years old, with refractory focal epilepsy and a single epileptogenic zone, which was determined during a presurgical investigation. Resection was not an option due to the proximity of eloquent cortex or the patient declined surgery. The seizure frequency was at least four per month and was recorded reliably in a seizure diary by the patient or a caregiver. AEDs were kept unchanged throughout the study. Exclusion criteria were the exclusion criteria for TMS (intracranial metal devices, pacemakers, ICDs, and so on), non-epileptic seizures, rapidly progressive medical diseases, suicidal ideation, pregnancy, and alcohol or drug abuse. Patients were referred by epileptologists involved in multidisciplinary presurgical evaluation. No information about the details of the randomization protocol was given to referring physicians. Previous failed epilepsy surgery was not an exclusion criterion.

3.3.2 Study design

The trial utilized a prospective, randomized, double-blind crossover design using three different coils to compare a figure-8 and round coil versus sham in each patient. The order in which the three coils were used in each patient was randomized using a computerized random number generator and a permutation for each block of three patients. After 8 weeks of baseline evaluation on a stable drug dose, patients underwent 2 weeks of stimulation (10 sessions) with 1,500 stimuli a day at a frequency

of 0.5 Hz, followed by a 10-week observation period. Treatments were performed in an outpatient setting, and sessions lasted about an hour each day. This treatment was repeated twice, using the figure-8 coil, the round coil, or the sham coil during the treatment sessions. Patients were screened for inclusion by one epileptologist (WVP). The treatment was always administered by the same investigator (LS) who was blinded to seizure count. Seizures diaries were checked by the study nurse (AD) every 5 weeks and assessed by the epileptologist (WVP) at the end of each treatment period. Both assessors were blinded to the order of the treatments. The study nurse also systematically inquired about side effects after each session.[68] During baseline evaluation and at the end of each observation period Quality Of Life In Epilepsy-31 (QOLIE-31),[105] the Columbia Suicide Severity Rating Scale (CSSRS), and global impression of change-scales were rated. In order to assess if patients could be blinded in a satisfactory manner in a crossover trial, they were asked to write down after the first day of each treatment block if they thought a real or sham coil was used that day. These data remained in a sealed envelope until all statistical analyzes were performed. The center of the ictal onset zone, as determined by the multidisciplinary epilepsy surgery team based on magnetic resonance imaging (MRI), video-EEG, fluorodeoxyglucose–PET (FDG-PET), and SISCOM data (Table 3.1, Fig. 3.1) was chosen as the target to aim the center of the TMS coil. Neuronavigation using BrainSight (Rogue Research, Montreal, QC, Canada) was used for coil placement, and continued feedback was used during the whole stimulation session. A Magstim Rapid2 (Magstim, Whitland, United Kingdom) was used, with standard 70-mm figure-8 coil, a standard round 90-mm coil, and the commercially available sham coil. Intensity was set as 90% of the rMT, as determined at the onset of the study using the figure-8 coil. rMT was measured by first localizing the motor hotspot by mapping a 5 × 5 cm area around the hand knob, using neuronavigation, with electromyography (EMG) recordings from the APB. Intensity was first increased until motor evoked potentials (MEPs) could be provoked to determine the hotspot. Next, intensity was lowered in steps of 1% to determine the lowest intensity needed to provoke 5/10 MEPs on EMG. We preferred this protocol to using a different intensity when using the round coil or adapting the threshold each day, to minimize chances of inadvertent unblinding of the patients. The orientation of the coil was chosen so that it was perpendicular to the nearest important sulcus, as determined by a three-dimensional (3D) reconstruction of the patients anatomic brain MRI (Fig. 3.1). The choice between clockwise and counterclockwise current flow with the round coil depended on the hemisphere that was targeted and was based on the optimal orientation for eliciting motor responses.[106] The 1,500 stimuli a day were divided in three blocks, with short breaks in between to allow for coil cooling and to check if the neuronavigation system was still correctly calibrated. All patients used foam earplugs (3M EAR Classic). The trial was approved by the ethical committee of the University Hospitals Leuven and registered as NCT01745952 on ClinicalTrials.gov. Written informed consent was obtained from all patients.

3.3.3 Statistical analysis methods

Based on a coefficient of variation equal to 1 derived from data reported by Fregni and colleagues[10], 29 patients were needed to have at least 80% power to show a reduction of 50% between the active coil and the sham conditions based on a two-sided t-test for lognormal data (since two comparisons are performed, alpha is set at 0.025). For the main comparison of both coil conditions versus sham, 18 patients were needed. These calculations were performed under the worst case scenario of no correlation between the conditions (i.e. no patient effect). Since it is reasonable to expect a patient effect on the seizure rate, we aimed at including at least 20 patients in the study. Recruitment was slower than anticipated and, therefore, it was decided to terminate the study before the planned number of subjects was included. Note that the number of daily measurements per patient per condition was large enough to guarantee at least 80% power for the within-patient comparisons. First, for each patient separately, the number of seizures has been compared between conditions with a Quasi-Poisson regression model for count data followed by pairwise comparisons with Tukey adjustments for multiple testing. Data were also analyzed using negative binomial regression model as a sensitivity analysis since this model gives more weight to lower counts. Second, the aggregated

data over all analyzed patients were compared between conditions using a negative binomial model with extra correction for overdispersion by adding a multiplicative overdispersion parameter using Pearson chi-square statistics. The analysis on the aggregated data did not take into account the within-patient correlation between the different treatment conditions. The analyzes on patient level as well as on all patients combined did not model the evolution over time within each condition or the order of the treatment conditions within a patient. An analysis of carry-over effect was planned but could not be performed due to small numbers. A corrected p-value of 0.05 was considered significant. Analyzes have been performed using SAS software (version 9.2, Windows).

Table 3.1: Patient characteristics

Randomization number	Age (years)	Gender	Duration of epilepsy (years)	Previously failed AEDs (number)	Current AEDs	Average number of seizures/week during baseline ±95% CI	Lateralization	Stimulated lobe	Previous surgery	Clinical ictal semiology	MRI diagnosis	Interictal EEG	Ictal EEG	FDG-PET hypometabolism	SISCOM
1	61	F	5	12	CLZ, PGB, TPM	53.9 (49.3 - 58.9)	R	F	N	Painful clonic movements	several ischemic lesions	L T	artifacts	Corresponding to ischemic lesions	R F
2	27	M	27	15	CLB, LEV, PGB	5.6 (3.8 - 8.3)	L	F	Y	Bilateral tonic posturing, irresponsive	tuberous sclerosis	L FC	L F	several areas (tubers)	L F
3	41	F	40	9	CBZ, LCM, TPM	7,1 (5.8 - 8.7)	L	P	N	Version, tonic R, dystonic L	MCD	L T	L para-sagittal	NA	L P
4	30	F	28	10	LCM, LEV, TPM	18.8 (15.7 - 22.4)	L	P	N	Sensory aura R leg -> fencing	MRI negative	para-central	L FCP	LP	L P
5	29	M	23	9	CBZ, LEV, RTG	7.3 (5.3 - 9.9)	R	F	N	Arrest, dystonic posture L	poly-microgyria	R hemisphere	RF	NA	R F
6	43	M	36	6	CBZ, LCM, PGB,	16.7 (13.9-20.0)	R	F	N	Tonic -> clonic L arm	MCD	none	no changes	none	R

					PHT, TMP									
7	34	F	28	15	CBZ, LEV, RTG	2.9 (1.7 - 5.0)	L	T	N	Nightly, blinking, version R -> tonic posturing *	MCD	L OT	L O	OT	L T
8	36	F	18	13	PGB + VNS	124.6 (111.5 - 139.2)	L	O	N	"dizziness" sensation, hypomotor, frequently stimulus provoked	MCD	para-central & T, L > R	posterior, mostly left	none	R&LO
9	27	F	12	11	LEV	0.5 (0.2 - 1.1)	R	F	Y	Tonic -> clonic L arm	resected lesion, probably LGG	R FC	R FC	normal	NA
10	33	F	27	7	LTG, TMP	6.1 (5.2-7.1)	L	P	Y	Irresponsive, abnormal movements R arm, aphasia	MCD	L posterior	L PT	L PO	L PO
11	24	M	17	9	CLB, LEV, PGB, VPA	22.7 (16.6 - 31.0)	L	T	Y	Irresponsive, later: R paresis	MCD	T	midT	ictal study: hypermetabolism LT	L T

*Infrequent daytime seizures start with aphasia and visual hallucinations

C: central, CBZ: carbamazepine, CLB: clobazam, CLZ: clonazepam, F: frontal, ^{18}FDG-PET: ^{18}fluorodeoxyglucose-positron emission tomography, L: left, LCM: lacosamide, LEV: levetiracetam, LGG: low-grade glioma, LTG: lamotrigine, MCD: malformation of cortical development, N: no, NA: not applicable, P: parietal, PGB: pregabalin, O: occipital, PTH: phenytoin, R: right, RTG: retigabine, SISCOM: single-photon emission computerized tomography coregistered to MRI, T: temporal, TPM: topiramate, VPA: valproic acid; Y: yes

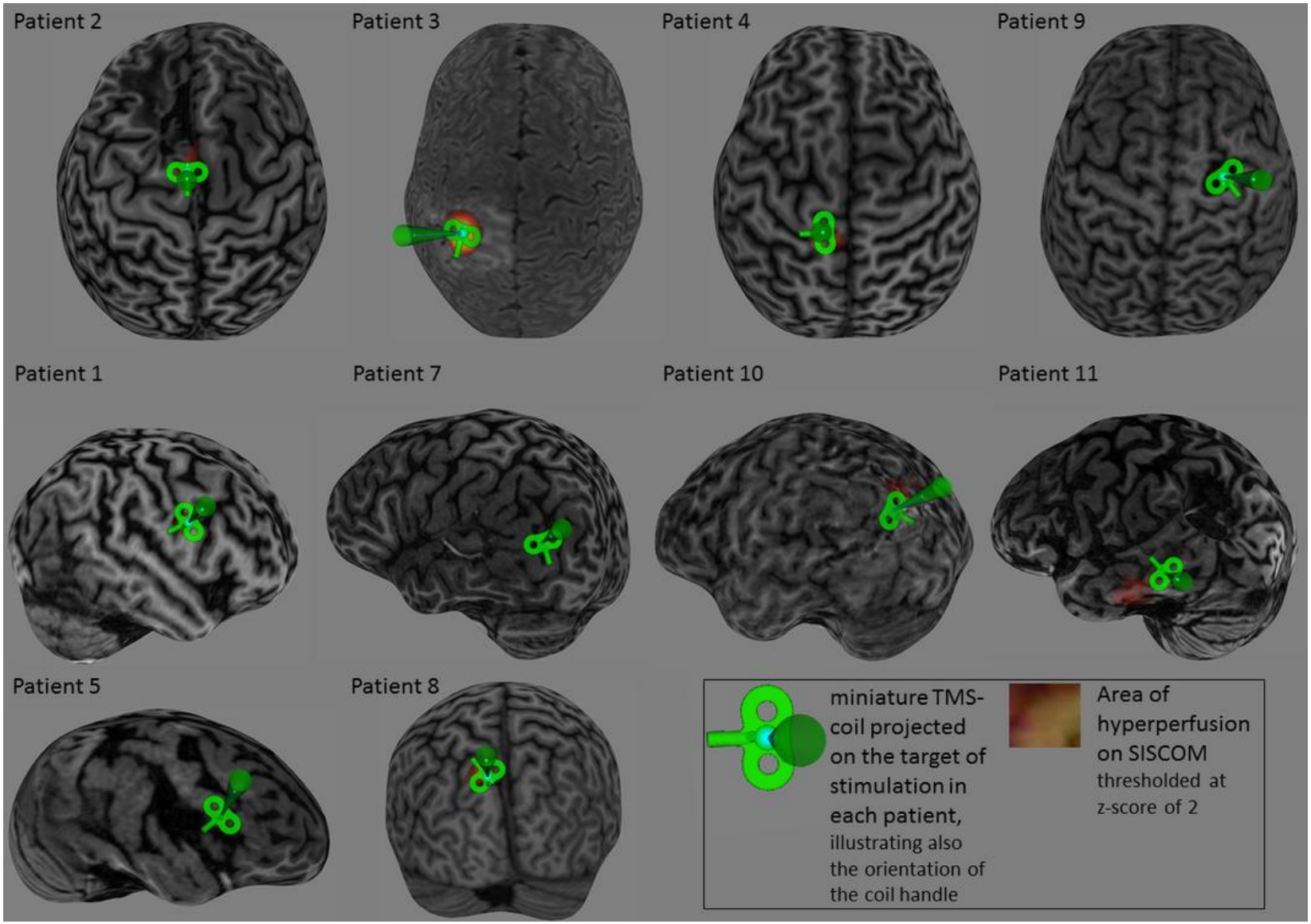

Figure 3.1
Target of stimulation in individual patients, based on all available data of a presurgical workup.
A miniature TMS coil is positioned over the target of stimulation on a 3D rendering of the brain. The orientation of the coil during rTMS is illustrated. SISCOM hyperperfusion is visualized in an orange color.

3.4 Results

3.4.1 Study population

Fifteen patients were screened for inclusion, of which 11 agreed to participate (patients 1–11) (Fig. 3.2). Demographics and clinical data of the randomized patients are given in Table 3.1. Patients included in our study had refractory epilepsy with a median of 24 seizures/month (range: 18/day to 2/month: one patient had lower seizure frequency than specified in inclusion criteria). They had failed on average 11 (±3) AEDs and were taking three AEDs (range 1–5) during the study. Four patients had undergone unsuccessful epilepsy surgery, with incomplete resections near eloquent cortex. Randomized patients were included from November 2012 until January 2014. The 11 randomized patients underwent at least one full session of rTMS with the allocated coil and kept a seizure diary during each 12-week treatment period. The data of one patient (patient 6) were not considered for further analysis since the seizure diary did not include the number of seizures per day on several occasions. Three patients did not finish the whole protocol. Patient 1 was excluded after the first session since the AED regimen was changed due to toxicity. Patient 10 discontinued the study after two treatment sessions, since she experienced the sessions as painful and not effective. Data of the observation period after the second (sham) treatment block were not available. Patient 11 discontinued because of a fourfold increase in seizure frequency during the second week of first treatment session with a figure-8 coil (Fig. 3.3).

Figure 3.2 CONSORT flowchart of recruitment and selection. AED: antiepileptic drug; pt: patient. Patients were numbered in order of randomization.

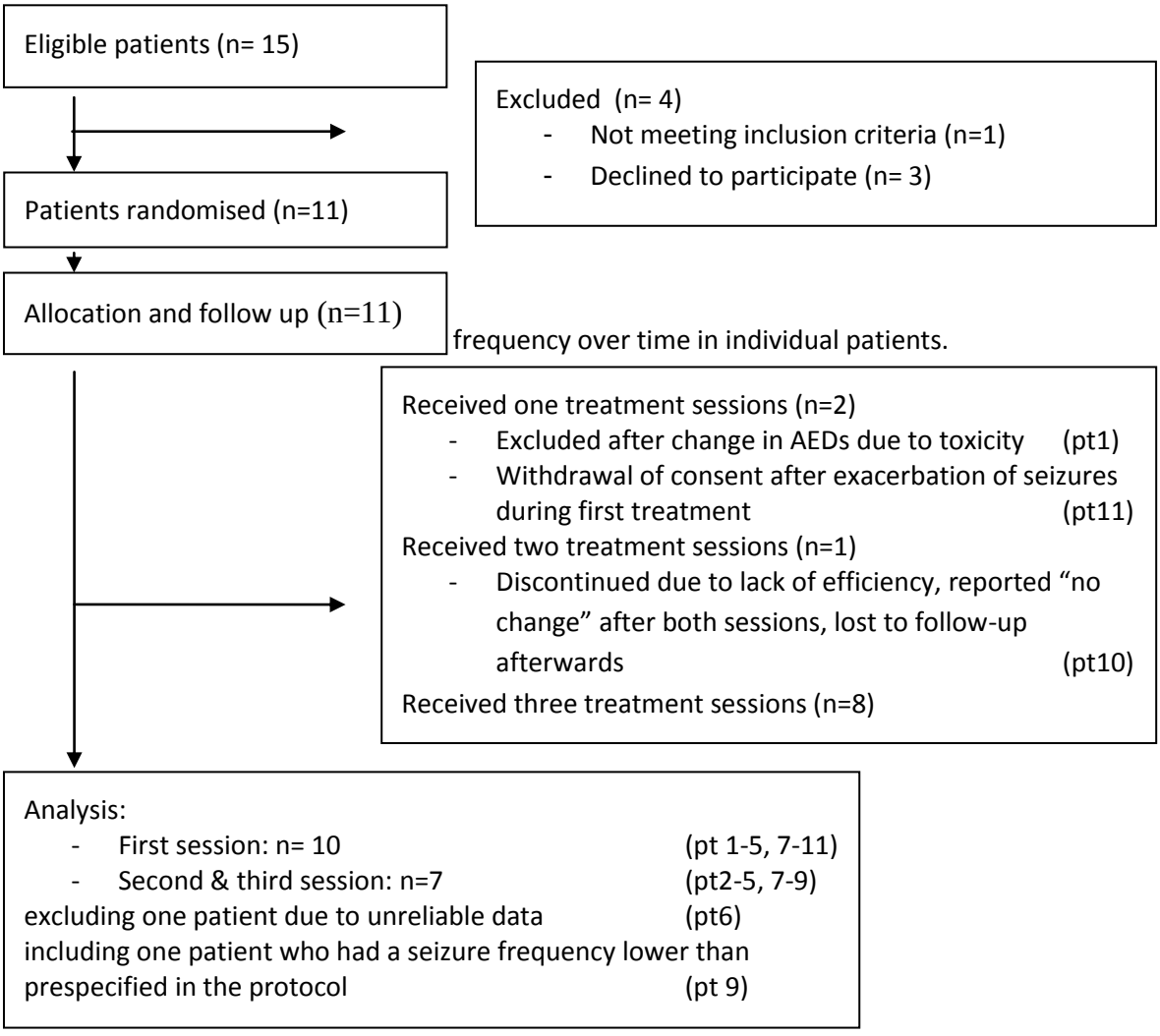

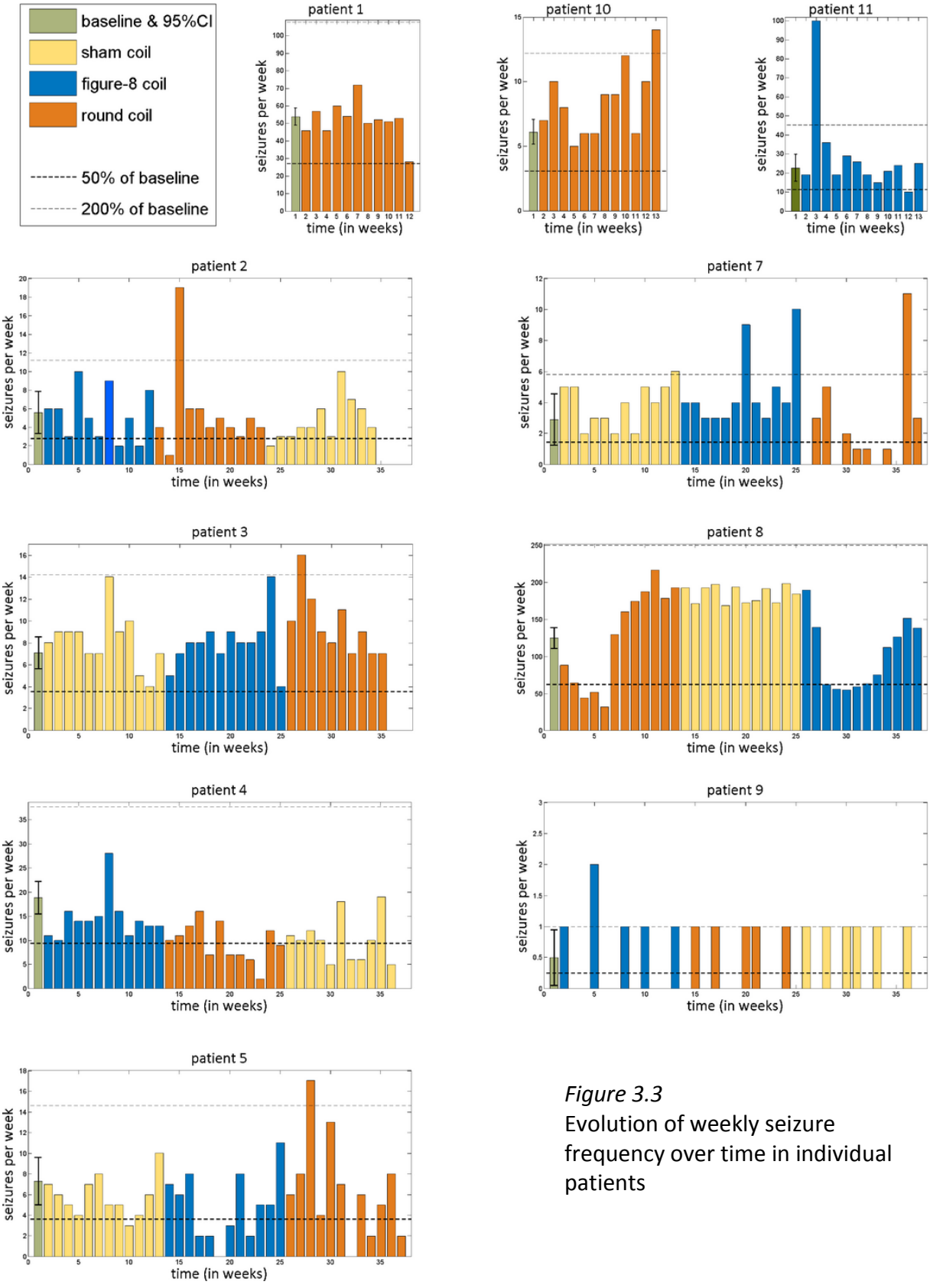

Figure 3.3
Evolution of weekly seizure frequency over time in individual patients

3.4.2 Efficacy

No difference in mean seizure rate could be detected in any of the conditions compared to baseline or between any of the conditions. After corrections for differences in baseline seizure count, results remained unchanged. Using a negative binomial regression model resulted in the same findings. To rule out an effect of shorter duration, a post hoc analysis restricted to the first month of each condition was performed. Again no change in average seizure frequency was detected. Statistically significant changes in the seizure frequency in individual patients between different treatment conditions were seen in patients 4 and 8 (Table 3.2 and Fig. 3.3). Patient 4 had an 18% seizure reduction after treatment with a figure-8 coil, 48% seizure reduction after round coil treatment, and a 44% reduction in the subsequent treatment condition using the sham coil. In patient 8, worsening in overall seizure frequency during the study period was significant, despite a clinically meaningful weekly seizure frequency reduction of >50% during the first month after each active treatment. After this initial seizure frequency reduction, seizure frequency increased above the 95% confidence interval (CI) of baseline seizure frequency during 18 weeks following the reduction after the treatment with a round coil (including the following period of sham treatment), and for >20 weeks after treatment with the figure-8 coil (data not shown in Fig. 3.3).

3.4.3 Secondary outcome measures

Seven patients were able to fill out questionnaires. The baseline average quality of life based on the QOLIE-31 was 50/100 (with higher scores meaning better quality of life). In three of six patients there was an improvement in QoL with medium effect size[107] after using the round coil, three of five reported improvement after treatment with the figure-8 coil, and one of five after sham treatment. The latter patient reported an improvement compared to baseline after each treatment, with the smallest effect size after sham treatment. One patient had worse scores after treatment with the round and the sham coil. No relation with the treated hemisphere was seen. No suicidal ideations were reported during the study. When rating the global impression of change, five of six patients reported no change after sham-treatment, four of seven after figure-8 treatment, and five of eight after treatment with the round coil. A moderate unfavorable evolution was reported by three different patients after one treatment session—sham, figure-8, and round coil treatment, respectively. Patient 8 reported first a very favorable response followed by an unfavorable one, as can be seen also in the seizure evolution over time (Fig. 3.3, Table 3.2). We checked allocation concealment by asking the patients to guess the coil used in each session. For the first treatment session, correct guessing of the allocated treatment was not higher than could be expected by chance (Binomial test, $p = 0.26$); for subsequent coils, patients could guess the allocated treatment better than could be expected by chance.

3.4.4 Adverse effects

The most important adverse effect noted in this study was a negative effect on seizure frequency. In patient 8, there was a clear increase in seizure frequency after an initial reduction, and this increase was maintained up to 20 weeks after the end of the study. This rebound in seizure frequency was not a gradual process but rather an abrupt change from one day to the next, and it was accompanied by severe headache during 1 week in this patient with occipital epilepsy. Patient 11 had a marked increase in seizure frequency during the days of rTMS. Electroclinically these seizures were comparable to the habitual seizures of the patient. The seizures were more frequent during the actual stimulation and in the hours following treatment. One patient experienced hearing problems after stimulation, which was helped by placing some pads between the ear and the coil. Four patients experienced headache. Two patients experienced fatigue with active treatment; two other patients experienced fatigue with sham treatment. One patient reported difficulties concentrating. Side effects were minor according to the patients, except in one patient in whom the headache started within minutes of active treatment and felt like “the operative scar was going to explode.”

3.5 Discussion

We report the data of a double-blind sham-controlled crossover trial of low frequency rTMS in patients with refractory neocortical epilepsy. We found no difference between targeted rTMS over the focus using a figure-8 or a round coil.

Surprisingly, our study demonstrated no overall effect on seizure frequency using 0.5 Hz rTMS. This negative finding for targeted rTMS using a figure-8 coil is in contrast with the effect size of 0.71 (with a 95% CI at 0.30–1.12) in the meta-analysis of Hsu et al.[103] and of 0.64 in the study of Sun et al.[94] Our protocol was designed to incorporate factors known to be associated with a positive outcome: a 2-week 0.5 Hz paradigm at an intensity 90% of rMT like the latter study combined with detailed delineation of the focus including ictal single-photon emission computed tomography (SPECT)[92] and neuronavigation to position the coil.

Our protocol was most similar to the one described in the study of Sun et al.,[94] which is the largest study reporting positive results to date. It is not described in their study how many patients experienced a 50% seizure reduction, but the number is probably high given that 11 of 31 patients in the active treatment group were seizure-free at the end of the 8-week observation period. They used a custom-made figure-8 coil with 87 mm loops, whereas we used the Magstim figure-8 coil with 70 mm loops. In their study, patients took on average two AEDs, which is lower than three AEDs taken in our patients' sample. This could explain variable responses to rTMS.[108,109] The effect of a combination of AEDs on the ability of rTMS to induce brain plasticity has not been studied, but we speculate that high doses of combined AEDs may limit the effect of rTMS to induce synaptic alterations. Of note, the patient in our study who experienced a transient improvement after both active coils took only one AED.

An important determining factor for rTMS response is the etiology of the epilepsy. Several other trials using rTMS have been negative,[90,92,95,97,98,100,102] but those trials often used nonfocal stimulation[90,92,98,100,102] and included patients with both focal and multifocal epilepsy[92,97,100,102] or neocortical and mesial temporal epilepsy.[90,92,95,98,100,102] Patients with mesial temporal lobe epilepsy or multifocal epilepsy were, therefore, excluded from our study. Encephalomalacia was present in 35% of the population of Sun et al.,[94] but not in our population. Fregni et al.[99,101] reported positive results in two trials in patients with polymicrogyria or nodular heterotopia. We included several patients with malformations of cortical development, but not these subtypes. In addition, procedural details can affect how the brain is stimulated in otherwise identical protocols. One example is the way the MT is defined. Using neuronavigation and EMG results in less chance to overestimate the rMT and thus can lead to a lower intensity used for stimulation compared to previous studies that relied on anatomic surface markers.

Variability in rTMS response has also been ascribed to age, gender, time of day, previous physical and mental activity, genetic factors,[110] brain states during stimulation,[49,50] short breaks in sessions,[51] and corticospinal excitability.[52] Moreover, the effect on individual neurons depends on their orientation relative to the induced electrical field, and in epileptogenic lesions the architecture of the neuronal elements can be different from that of other brain regions. Part of the difference in response to rTMS between our study and the study of Sun et al.[94] might reflect reported inherent neurophysiologic differences between Chinese and Caucasians.[111] This means that identical and seemingly identical rTMS protocols can have varying effects on an individual's brain.
Even for well-established stimulation protocols over the motor cortex, large variability is seen, with only 25–36% of healthy subjects showing the expected changes in MEP amplitudes in both directions.[48,52]

The variability in response in different studies using rTMS can be explained at least partially by the small sample sizes and variability in rTMS protocols in combination with a large interindividual variability in response to TMS-induced plasticity.

In our study, one patient experienced a >50% reduction in seizure frequency during the month following each active treatment, but afterwards a rebound phenomenon was observed with a clear increase in seizure frequency. This increased seizure frequency compared to baseline, was maintained up to 20 weeks after the end of the study. This is to our knowledge the first report of rebound seizures after successful treatment with rTMS. Moreover, our low-frequency protocol exacerbated seizure frequency acutely in one individual.

rTMS has been considered as a treatment that is well-tolerated when respecting the guidelines.[60] We agree that this is true in the majority of cases, but in patients with preexisting allodynia over a scar from previously failed epilepsy surgery, rTMS may be very painful. Half of our patients had some improvement in QoL scores, consistent with the observation that rTMS can influence psychological functioning irrespective of seizure reduction.[94] Improvement in QoL was not dependent on the stimulated hemisphere. It has to be noted that the QOLIE-31 questionnaire specifically asked about the 4 weeks before administration of the questionnaire and we thus recorded changes occurring 8–12 weeks after the first stimulation session. Our patient 8 had a significant improvement in QoL 1 month after treatment, but not at the time when we administered the QoL questionnaire.

3.6 Conclusion

We report the first pilot study of neuronavigated rTMS in the treatment of focal neocortical epilepsy comparing a figure-8 and a round coil, but found no difference in efficacy. To our surprise, we found no clear overall effect on seizure frequency. We did see one acute exacerbation during active treatment and one patient who responded during 1 month, with deterioration afterward. Because our study was small—as most rTMS studies in epilepsy—a large multicenter trial will be needed to determine the position of neuronavigated rTMS in the treatment of refractory focal neocortical epilepsy.

3.7 Acknowledgements

This work has been supported by a grant from the Institute of Innovation by Science and Technology Flanders (IWT), project number 090850. Our gratitude goes to Dr. R. Hauman, Dr. B. Legros, and Dr. S. Ferrao Santos, who referred patients to participate in the study, the New York State Psychiatric Institute for the use of the CSSRS, and the Epilepsy Therapy Group for the use of the QOLIE-31.

3.8 Postscript

After the publication of our study, a meta-analysis on the safety of rTMS for the treatment of epilepsy was published, that included trials published until Augustus 2015.[57] Since we encountered side effects that were not previously reported, we composed a letter to the editor to accompany the meta-analysis to disseminate our findings to the broadest extend, so future work on TMS in people with epilepsy would be based on all available information on safety.

This text has been published as Response to “Safety of repetitive transcranial magnetic stimulation in patients with epilepsy: A systematic review” by Luisa Santos Pereira and colleagues.

Laura Seynaeve, Wim Van Paesschen. Epilepsy & Behavior. 2016 Sep;62:308. doi: 10.1016/j.yebeh.2016.07.002. PMID: 27492628 [112]

“We have read with much interest the paper entitled “Safety of repetitive transcranial magnetic stimulation in patients with epilepsy: a systematic review”[57] by Luisa Santos Pereira et al. The main conclusion of the study was “that the risk of seizure induction in patients with epilepsy undergoing [repetitive transcranial magnetic stimulation] rTMS is small and that the risk of other adverse events

is similar to that of rTMS applied to other conditions and to healthy subjects". The study examined data of several trials reporting reduction in seizure frequency or epileptic discharges in patients with epilepsy. However, since TMS in epilepsy was first used as a way to activate the seizure focus in a preoperative setting, studying the safety of TMS in patients with epilepsy is important. Serendipitously, it was seen that TMS could also interrupt ongoing seizure activity. This observation, in conjunction with the demonstration of the induction of long-term inhibition using rTMS in other settings, led to the use of rTMS as an experimental treatment in refractory epilepsy. Pilot experiments showed that using rTMS in patients with epilepsy could be done with acceptable risk, and this led the way to larger trials. The systematic review includes papers published before August 7th, 2015. At that time, we were performing another trial with rTMS in patients with refractory focal epilepsy.[88] The informed consent of our study included a statement that worsening of seizures or provocation of seizures was not reported, when using the parameters that we were going to use. Unfortunately, this was not our experience. Of the eleven patients included, one experienced a rebound in seizure frequency using either active coil, and a second patient had a four-fold increase in seizure frequency after active stimulation. This is to our knowledge the first demonstration of a rebound phenomenon after rTMS treatment for seizure reduction and the most severe form of seizure worsening reported to date. We felt compelled to report our findings, so future studies with rTMS in patients with epilepsy can include a more balanced statement concerning the risks associated with the treatment."

3.9 Supplementary material

Table 3.1S: scores on quality of life in epilepsy questionnaire (QoLie-31) in the different conditions

QoLIE		coil			difference		
	baseline	figure-of-8	round	sham	figure-of-8	round	sham
patient 1	43.59		59.51			15.92	
patient 2	not able to fill in questionnaires						
patient 3	62.24	69.11	70.66	59.51	6.87	8.42	-2.73
patient 4	40.8	69.16	53.63	50.22	28.36	12.83	9.42
patient 5	not able to fill in questionnaires						
patient 7	62	57.23	28.46	51.51	-4.77	-33.54	-10.49
patient 8	37.1	47.69	40.47	38.32	10.59	3.37	1.22
patient 9	74.22	73.14	73.67	70.4	-1.08	-0.55	-3.82
patient 10	29.57		44.02	n/a		14.45	
patient 11	not able to fill in questionnaires						
mean (SD)	51.0 (16.3)	63.3 (10.6)	51.8 (16.4)	54.0 (11.9)	8.0 (12.9)	0.8 (17.1)	-1.3 (7.3)

4. The effect of rTMS therapy on brain metabolism as measured by FDG-PET

In this chapter the effects of rTMS on the brains' metabolism are explored. The data were acquired during the study described in the previous chapter.

4.1 Summary

Introduction
FDG-PET imaging is a uniquely suited to study metabolic changes in a number of neurological diseases, including epilepsy. Sequential scans can also demonstrate metabolic alterations as a result of an intervention. To study the effect of rTMS on the brain in patients with epilepsy, scanning was performed at baseline and following treatment in order to study ensuing differences.

Methods
A double-blind sham-controlled randomized controlled cross-over trial was performed on 10 patients with well-characterized refractory focal non-mesial epilepsy. The active conditions were using the figure-8 or the round coil, the sham condition used a sham coil. The order between the three conditions was randomized between subjects. Scanning was performed at baseline and following each of the conditions. Overall change in metabolism was studied on quantitative images and changes between conditions studied on subtraction images after proportional scaling.

Results
Different patterns emerged. No clear change was observed in patients after sham stimulation, if this was the first condition. A carry-over effect was observed if sham stimulation was following either of the active conditions. Decrease in metabolism of the stimulation target was seen in 3/8 after figure-8 stimulation (not all patients followed through the whole study) and 5/9 after round coil stimulation. Increase in metabolism was seen in 2 patients. No clear effect between pattern of metabolic change and clinical change was observed. There was no patient that had a lasting reduction in seizure frequency.

Conclusion
rTMS affects brain metabolism in patients with refractory epilepsy and induced changes can be observed 12 weeks after stimulation, implying that metabolic changes outlast clinically observed changes in brain function.

4.2 Introduction

For patients with refractory focal epilepsy who are not good candidates for surgery, alternative treatments are needed. Since seizures are caused by an excitation-inhibition imbalance in the brain, techniques that are able to change brain function using electrical current seem promising. Repetitive rTMS is a non-invasive brain stimulation technique that is able to alter the excitability of cortical networks by patterned application of a time-varying electromagnetic field over a pre-specified brain region, that could be used to treat epilepsy [89,113]. Changes in the brain induced by rTMS can be detected using functional imaging, including 2-deoxy-2-[^{18}F]-fluoro-D-glucose (FDG)-PET (FDG-PET) imaging [114].
Post-rTMS changes on FDG-PET imaging have been detected in monkeys [115] and humans [116] when stimulating over the motor cortex. Cynomologous monkeys (n=10) underwent one session of rTMS (20 trains of 5Hz monophasic pulses for 20 seconds with an inter-train interval of 40 seconds (total of 2000 pulses) at subthreshold intensity) during general anesthesia (ketamine + propofol + curare)

over the right motor cortex and were imaged at several time-points[115]. In order not to induce anemia as a result of repetitive blood sampling, the PET-scans were reconstructed as non-quantitative images. Since the acquisition was the same in all scans, this method of image reconstruction is suitable. The TMS protocol used in this study would- if applied in humans- result in increased excitability of the motor cortex[51]. Post-treatment PET scans at day 1 and 8 showed a decrease activity in the precentral gyrus (most prominent left) and an increase in cingulate and orbitofrontal gyri bilateral; these changes were no longer present by day 16. The protocol used in this study is one that in humans would increase cortical excitability. In this study however it decreased brain activity over the stimulated area, both during stimulation and up to more than one week after a single session. This implies that aftereffects at a metabolic level are much more long-lasting than conventional TMS excitability parameters, like MTs. In awake humans (n=8) a similar experiment was performed. The rTMS-protocol consisted of a single 5Hz rTMS-session with 1800 pulses over the left motor cortex[116]. Tracer injection was immediately after the rTMS stimulation and no scanning was performed at later time points. In this study, an increase in activity was seen in the primary and supplementary motor cortex bilaterally. This might be more as expected compared to the results in monkeys, since the rTMS protocol used is considered excitatory. The analysis was limited to motor and primary auditory cortices, other brain regions were not studied. Within the studied regions, intra-individual variability was paramount, with some subjects showing only ipsi- and others only contralateral motor cortex activation and the change varied between 0.7% and 9.8% difference.

In healthy controls, studies also have been performed on non-motor regions[117,118]. In one study the FDG-tracer was injected during a 30-minutes session of 1Hz over the left prefrontal cortex (active condition, n=7) or sham stimulation (control condition, n=7)[117]. The metabolic rate of tracer uptake was measured on the basis of PET-imaging and concurrent arterial blood sampling. In these quantitative PET-images complex changes ensued compared to baseline imaging: decrease in metabolism was seen compared to baseline in the anterior cingulate bilateral, cerebellum bilateral, hypothalamus, the left putamen/caudate, right superior frontal cortex and midbrain; increase in metabolism was seen in the left angular gyrus, bilateral inferior occipital gyrus, left cuneus and right posterior insula. When sham stimulation was compared to baseline, changes in metabolism were also apparent with a decrease in the left anterior cingulate and globus pallidus and an increase in the right inferior and superior temporal gyrus, the lingual gyrus bilateral, the middle occipital gyrus bilateral and the left parahippocampal gyrus. Comparing active to sham stimulation a decrease in the left superior frontal gyrus and an increase in the cuneus bilaterally was observed. This widespread observed difference in uptake between baseline and post-intervention scan (either active or sham) is likely due to the fact that for the post-intervention scan FDG-injection was performed during stimulation (either active or sham rTMS). Of course, being subjected to a treatment with rTMS is a different experience compared to idle waiting during injection. In this study they tried to correct for this difference it in part by having an auditory discrimination task performed by the subjects during tracer injection. Comparing active with sham stimulation, a decrease in metabolism in the region that was stimulated, seems to make sense. The low-frequency rTMS used in this study is considered an inhibitory protocol[119], whereas the studies on motor mapping described earlier used a excitatory rTMS protocol.

A study on the effects of 5 consecutive days of 1Hz rTMS during 30 minutes in healthy volunteers (active condition n=22, sham condition n=5 with coil rotated 90°) was performed with scans acquired just after the last rTMS session[118]. Stimulation was over the right temporal lobe (T4-location according to 10-20 international electroencephalography (EEG) system). Baseline and post-treatment non-quantitative scans were compared after proportional scaling. Less activity after rTMS was seen in the right temporal region whereas more activity was seen in the precentral region bilateral, the right superior and middle frontal, prefrontal and cingulate gyri. Again, there was a decrease in activation over the stimulated region. The individual variability of this effect was not provided in these two articles on non-motor cortex stimulation[117,118]; only group data were analyzed.

FDG-PET imaging is also ideally suited for studies in epilepsy, since it has long been proven to successfully detect relevant abnormalities in epilepsy [120]. The epileptic focus and surrounding areas frequently are hypometabolic in the interictal state; however if tracer is injected during a (subclinical) seizure, hypermetabolism of the epileptic brain region is seen[121].

Since FDG-PET is thus extensively used in epilepsy and changes induced by rTMS have been described in healthy controls, it seemed imperative to study the effect of rTMS on the brain of patients with epilepsy. We wanted to determine whether rTMS was able to alter the brain metabolism in epilepsy patients subjected to a treatment trial of rTMS in refractory focal epilepsy. Since an inhibitory 1Hz rTMS protocol was used, decrease in activity in the areas close to the target of stimulation with increase in metabolism in other brain regions might be expected. Since the effect on metabolism might outlasts electrophysiological changes (as effects in monkey study lasted more than a week [115]) it could be envisioned that metabolic changes can be seen even though no behavioral effect would be apparent- that is, reduction in seizure frequency in this case. With this in mind, the data of the study were analyzed, knowing that overall no significant difference in mean seizure rate could be detected in any of the conditions compared to baseline or between any of the conditions.

4.3 Methods

4.3.1 Study design

We conducted a prospective, double-blind cross-over trial using three different coils to compare a figure-8 and round coil active treatment to a sham treatment condition in each patient. The details of the clinical part of the study can be found in chapter 3[122]. In this study, we used the same numbering for the patients as in the clinical part of the study. Using the figure-8 coil, the maximal stimulation will occur underneath its geometric center whereas with the round coil, inhibition of brain tissue surrounding the center of the coil is expected (Figure 1). Both could be effective since epilepsy is not only a problem of hyperexcitability of the focus but also of failure to prevent spread to neighboring brain regions. The trial was approved by the ethical committee of the University Hospitals Leuven and registered (NCT01745952) on ClinicalTrials.gov. Written informed consent was obtained from all participants.

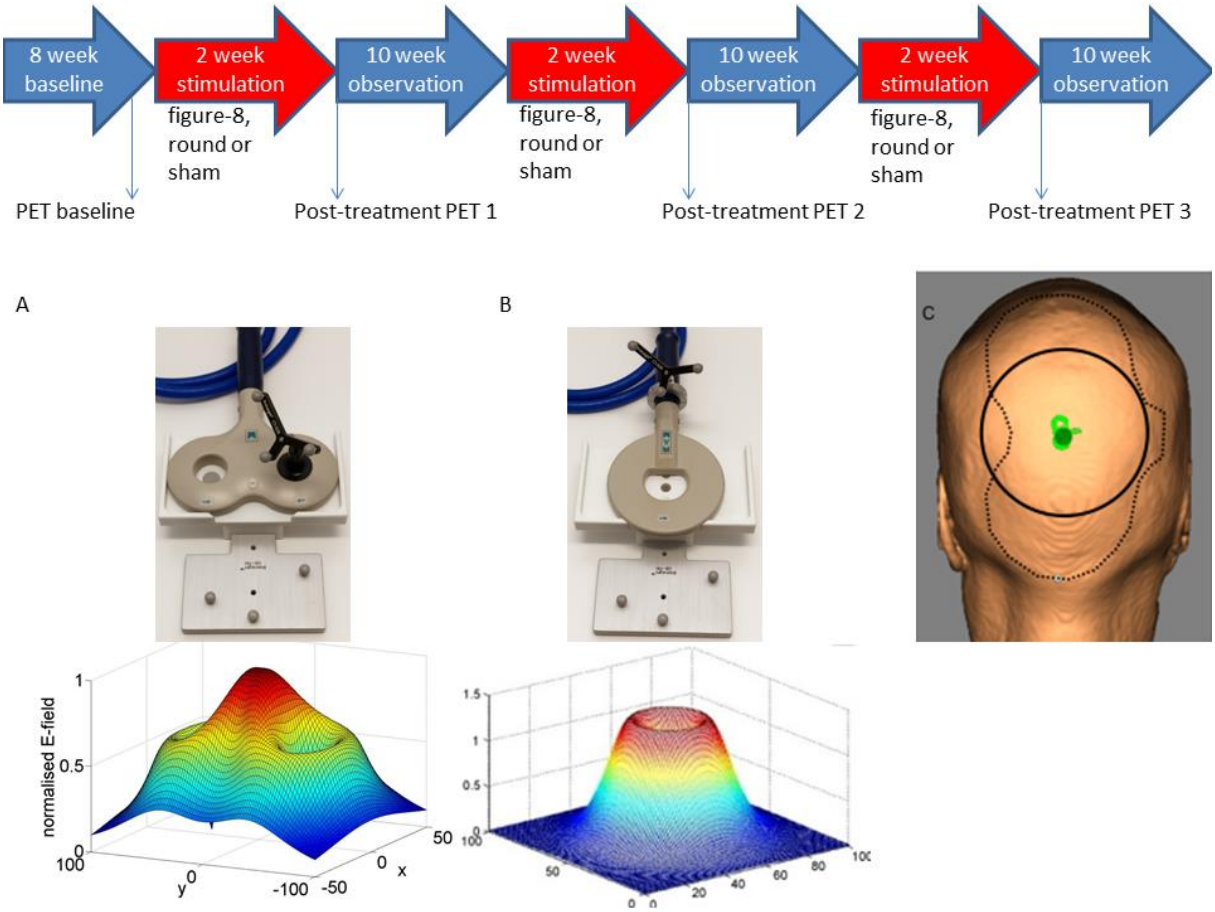

Figure 4.1 Study timeline and coil types used in the study:
above: study-timeline from the clinical study as described in chapter 3; below: coil types used in the study: panel A: figure-8 coil with representation of the size and extend of the field as studied by the developer (Magstim); panel B: round coil with representation of the size and extend of the field; panel C: size of the coil relative to the head, for the figure-8 coil (dashed line) and the round coil (full line)- for both coils the geometric center of the coil was positioned over the target: for the figure-8 coil the maximal field strength is above the target, for the round coil the area around the center gets the maximal field strength.

4.3.2 Image reconstruction

All patients received 4 FDG-PET scans: one at baseline and one in the week following each two-week treatment condition (figure 8, round, sham in a random order per patient). Patients were scanned dynamically for 60 minutes on a HiRez Biograph16 PET-CT camera (Siemens Healthcare, Knoxville, USA) immediately following an injection of 74 MBq FDG (± 4.7 MBq). This dose is a third of the habitual injected dose for FDG-PET scans and was chosen to limit the cumulative radiation exposure to 9 mSv for the whole trial. Patients fasted for 6 hours prior to FDG injection. During scanning, the head was fixed using a vacuum cushion to minimize movement. No EEG-monitoring during scanning was performed since wearing an EEG cap becomes uncomfortable and this in turn increases head movements. Patients were monitored clinically for seizure activity. Patients were instructed to stay awake during the 60-minute scanning session in a dimly lit room. During the 60 minutes of dynamic imaging, five frames of one minute followed by 11 frames of five minutes each were acquired.

Reconstruction was performed in two ways, resulting in non-quantitative and quantitative uptake FDG-PET images.
Non-quantitative images were created used maximum likelihood expectation maximization (MLEM) reconstruction with resolution recovery [123] and corrected for attenuation using a CT transmission scan. The summed image of the uptake between 30 and 60 minutes after injection was used for further analysis. Scans were inspected for movement before summation of the frames. Image analysis was performed using statistical parametric mapping (SPM) software (version SPM8; Wellcome Department of Cognitive Neurology, University College, London, United Kingdom) in Matlab R2012b (MathWorks, Natick, USA). Post-treatment PET scans were rigidly coregistred to the baseline PET-scan using mutual information.
Static subtraction images were created by subtracting the baseline scan from each of the post-treatment scans after correction for overall difference in activity using proportional scaling and smoothed using a FWHM of 10mm. Only voxels with information in both scans were retained. These subtraction images were transformed in maps showing the difference between the two images as percentage change and converted into z-score images.
Quantitative uptake images were reconstructed using the Hunter method[124]. The resulting images give a quantitative value for the metabolic rate of glucose using a population based arterial input function which was calibrated by a late venous blood sample. In the analysis, the first five minute frames were summed and all following frames were registered to this scan.

In order to discern the region that was stimulated using neuronavigated rTMS, the baseline PET scan was coregistered to the anatomical MRI using mutual information and the same transformation was applied to the coregistered post-treatment images.

4.4 Results

4.4.1 Participants

The interval between the end of the 10 days-rTMS stimulation period and the PET-scans ranged from 0 to 5 days (mean 2.8 ± 1.4 days). No seizures were reported or observed during any of the scans, except for patient 8. Note that patient 6 was excluded from the analysis, both for the clinical part of the trial (seizure diaries unavailable) as for the imaging part (did not respect fasting for six hours prior to the PET scan). Patient 1 and patient 11 took a low dose of a benzodiazepine prior to scanning to aid in preventing seizures during scanning. Patient 8 had very frequent seizures of short duration which occurred also during each of the scanning sessions. Patients 1, 10 and 11 did not participate in the whole study and thus only the scans from the treatment trials that did take place, could be analyzed. Patient 1 was scanned after rTMS using the round coil, patient 10 was scanned after treatment using the round coil and a second time after sham treatment and patient 11 was scanned after treatment using the figure-8 coil.

In two patients, venipuncture was difficult and not all blood samples to measure glucose and tracer concentration for calibration of the population based input function were obtained for the different time points. No dynamic uptake scans could thus be created in patient 4 for two out of four scans, namely the scans after both active treatments and the scan after sham-treatment in patient 7.
Movement was too pronounced for image reconstruction for the scan after treatment with the round coil in subject 3 (for a graphical overview, see Figure 2).

4.4.2 Changes in FDG-PET activity

Patterns of tracer uptake, reflecting metabolic activity, were visually inspected on the quantitative images (Figure 2). At baseline, abnormalities in FDG-PET activity were apparent, with hypometablism in the epileptic region: four patient had prior (unsuccessful) epilepsy surgery which can be seen as hypometabolism in the region that was resected: left frontal in patient 2, right central in patient 9, left parietal in patient 10 and 11 but also in the other patients hypometabolism was apparent, which was most pronounced in patient 3 and 5.

Global changes in metabolism after treatment were especially apparent in patient 3, who showed a diffuse increase in metabolism, and to a lesser extent in patient 7. Patient 8 on the other hand showed a global decrease in metabolic activity after active treatment.

	FDG-PET activity baseline	FDG-PET activity after stimulation with figure-of-8	FDG-PET activity after stimulation with round coil	FDG-PET activity after stimulation with sham coil
4.3 0 Patient 1	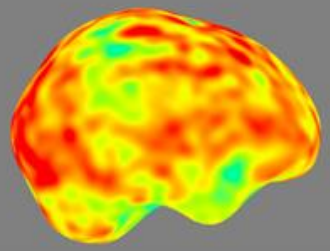	Not performed	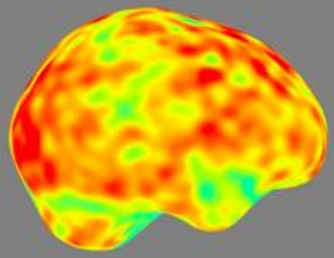	Not performed
6.9 0 Patient 2	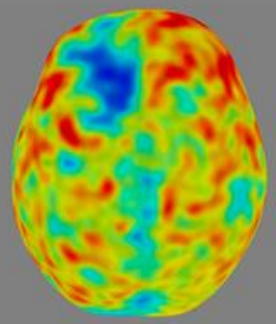	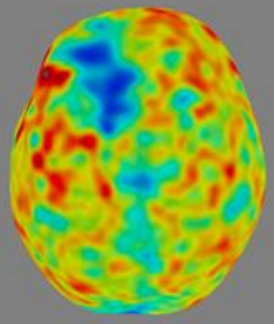 1	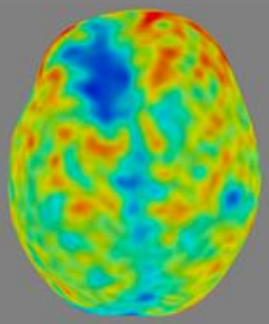 2	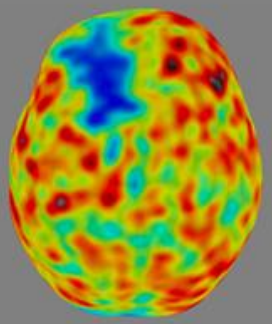 3
2.7 0 Patient 3	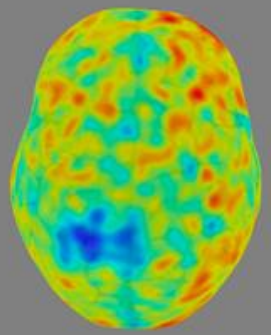	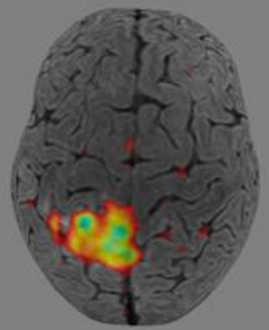 2	Reconstruction not available due to movement artefacts 3	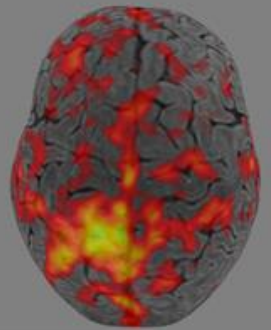 1

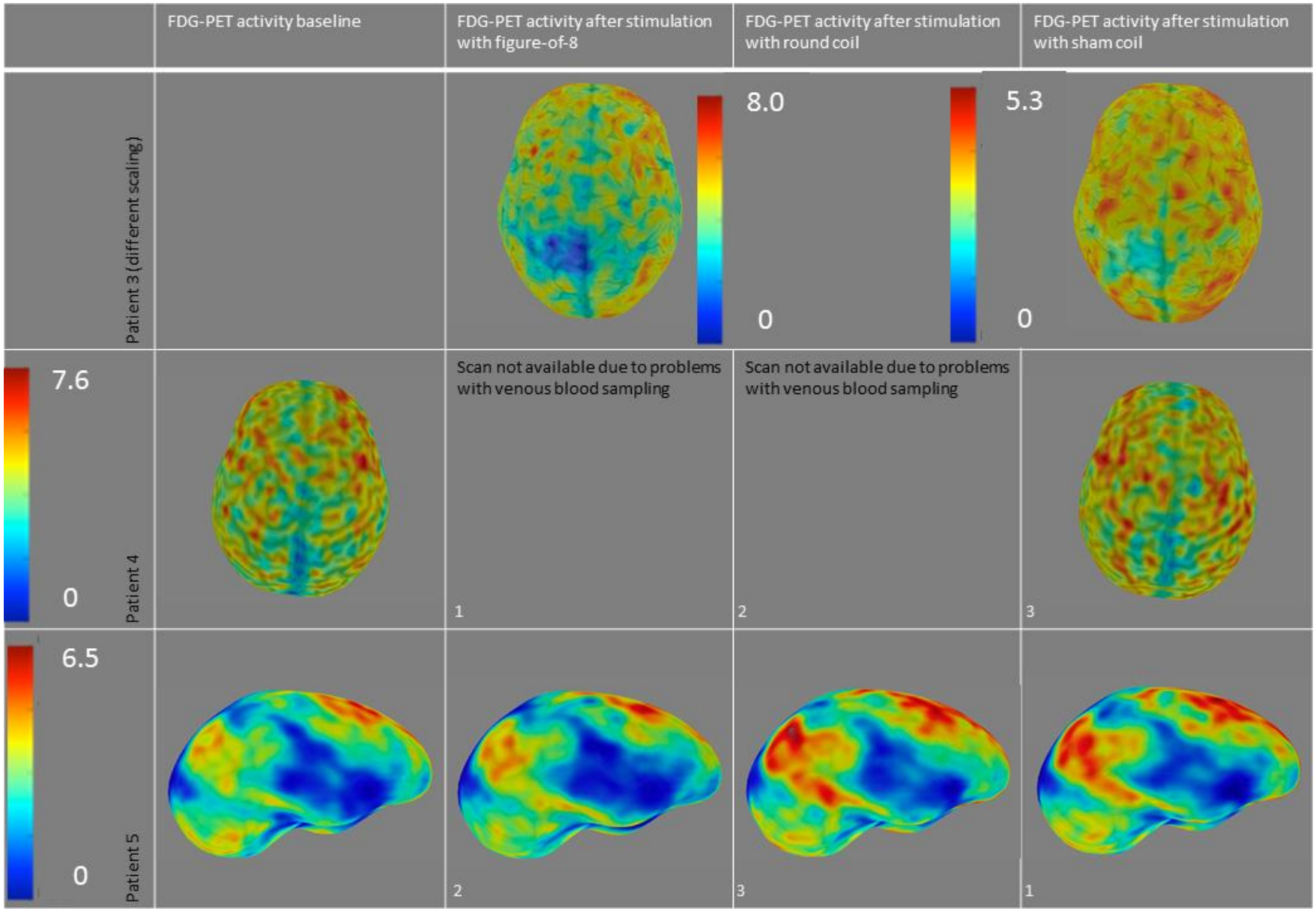
FDG-PET activity baseline
FDG-PET activity after stimulation with figure-of-8
FDG-PET activity after stimulation with round coil
FDG-PET activity after stimulation with sham coil
Patient 3 (different scaling)
8.0
0
5.3
0
7.6
0
Patient 4
Scan not available due to problems with venous blood sampling
Scan not available due to problems with venous blood sampling
1
2
3
6.5
0
Patient 5
2
3
1

	FDG-PET activity baseline	FDG-PET activity after stimulation with figure-of-8	FDG-PET activity after stimulation with round coil	FDG-PET activity after stimulation with sham coil
Patient 7	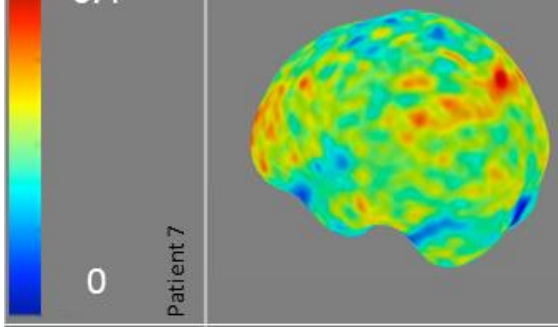	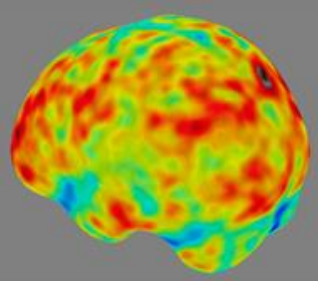 2	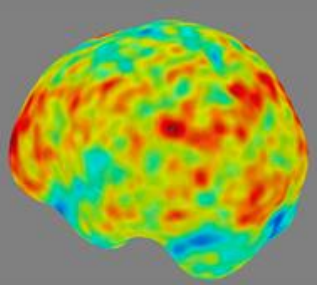 3	Scan not available due to problems with venous blood sampling 1
Patient 8	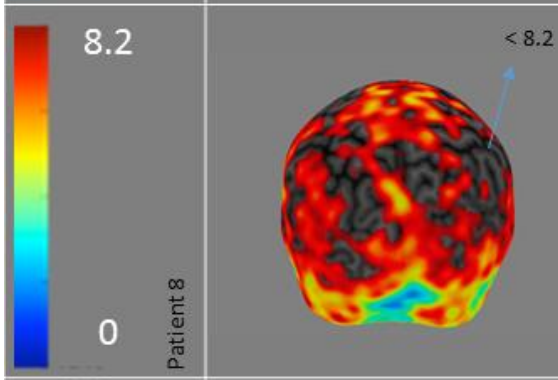	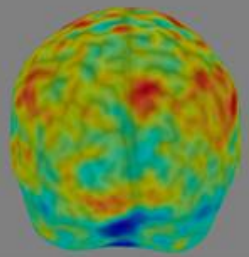 3	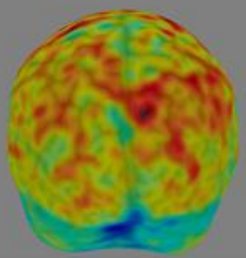 1	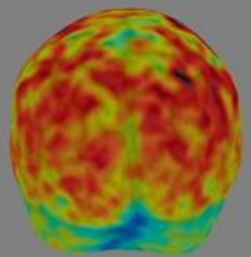 2
Patient 9	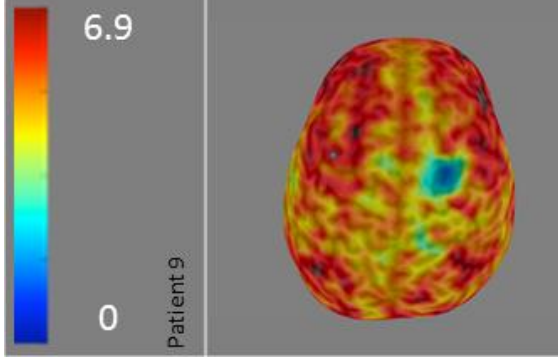	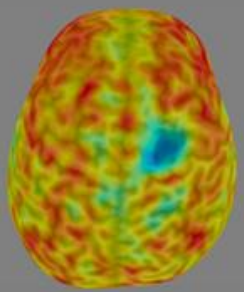 1	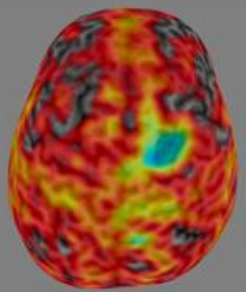 2	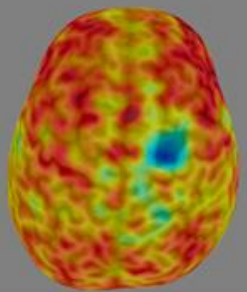 3

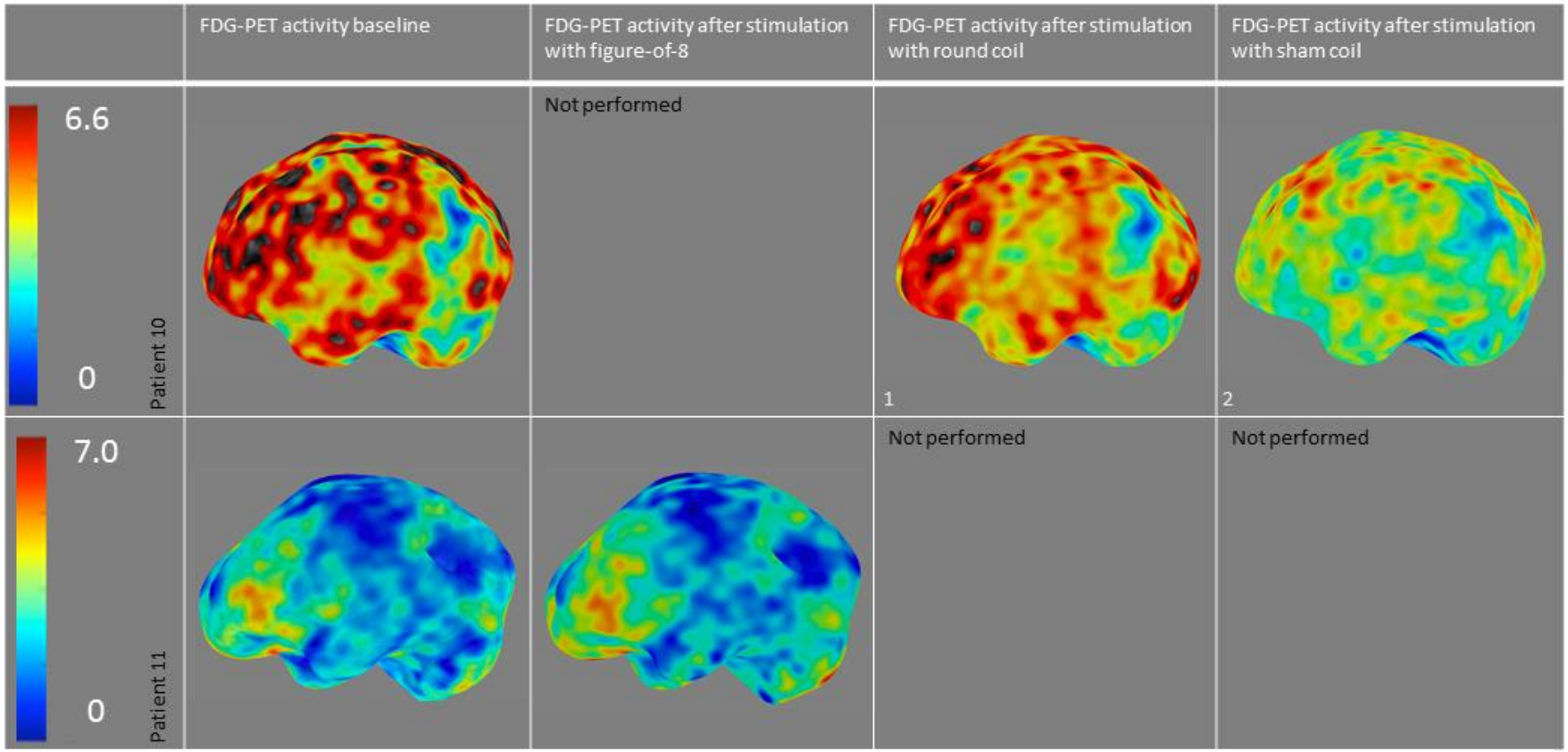

Figure 4.2

Quantitative images of FDG-PET uptake of the patients, for the different conditions.

Order of conditions in a patient is given by numbers (1-2-3). Scaling of the metabolic rate of glucose uptake is in (mg glucose)/(min * 100g tissue); scaling of the images is shown at the left of each row. Intensities higher than those on the color scale are in grey. Images are of the cortical surface (at 4mm peeling depth).

In order to study the local changes in metabolism surrounding the area of stimulation, the non-quantitative subtraction images were studied (Figure 3). In all patients, the TMS coil was positioned differently, based on the epileptic focus. The order in which the coils were used in the cross-over trial also differed.
In three patients, sham stimulation was the first condition (patients 3, 5 and 7): in none of these scans, a difference in the stimulated area was observed. All three do have an increase in the occipital lobe compared to baseline. This posterior increase compared to baseline is a consistent finding over all subjects, when the scan after sham stimulation is compared to baseline, irrespective of the order in which the coils were used.
In the patients were sham was used after active stimulation, the pattern of change was reminiscent of the changes seen in the scan acquired after the previous condition, with exceptions for subject 8 and 9.
After stimulation with the figure-8 coil, hypometabolism at the target of stimulation was seen in only three out of eight subjects (patient 2, 4, and 7). Hypometabolism within the probable area of stimulation with the round coil was seen in five out of nine (patients 2, 4, 8, 10 and a small decrease in patient 3 but within an area that was much more pronounced in the scan of the earlier condition). Stimulation with a round coil results in a similar induced field strength along the whole curvature-this pattern was not reflected in the images: changes were in the form of blobs, no (semi)circular patterns were apparent.
Increase in activity was also occasionally seen: after stimulation with the figure-8 coil in patient 9 and after stimulation with the round coil in patients 7, 8, 9 and 10 (in all but one, this increase in activity is over the occipital lobe). The pattern in subject 9 is thus increase in uptake at the target area after both active treatment conditions and a reversal of this pattern with ensuing decrease in activity compared to baseline after sham stimulation, which was the last condition in this patient.
Changes in different brain regions at a distance from the target of stimulation were seen in all subjects, resulting in both a decrease and an increase in activity.

Based on the seizure diaries, no overall effect of rTMS stimulation was observed. In individual patients, changes were seen in patient 4 and 8. Patient 4 had an 18% seizure reduction after treatment with a figure-8 coil, 48% seizure reduction after round coil treatment, and a 44% reduction in the subsequent treatment condition using the sham coil. No clear effect of this change is seizure frequency is apparent in the PET-images.

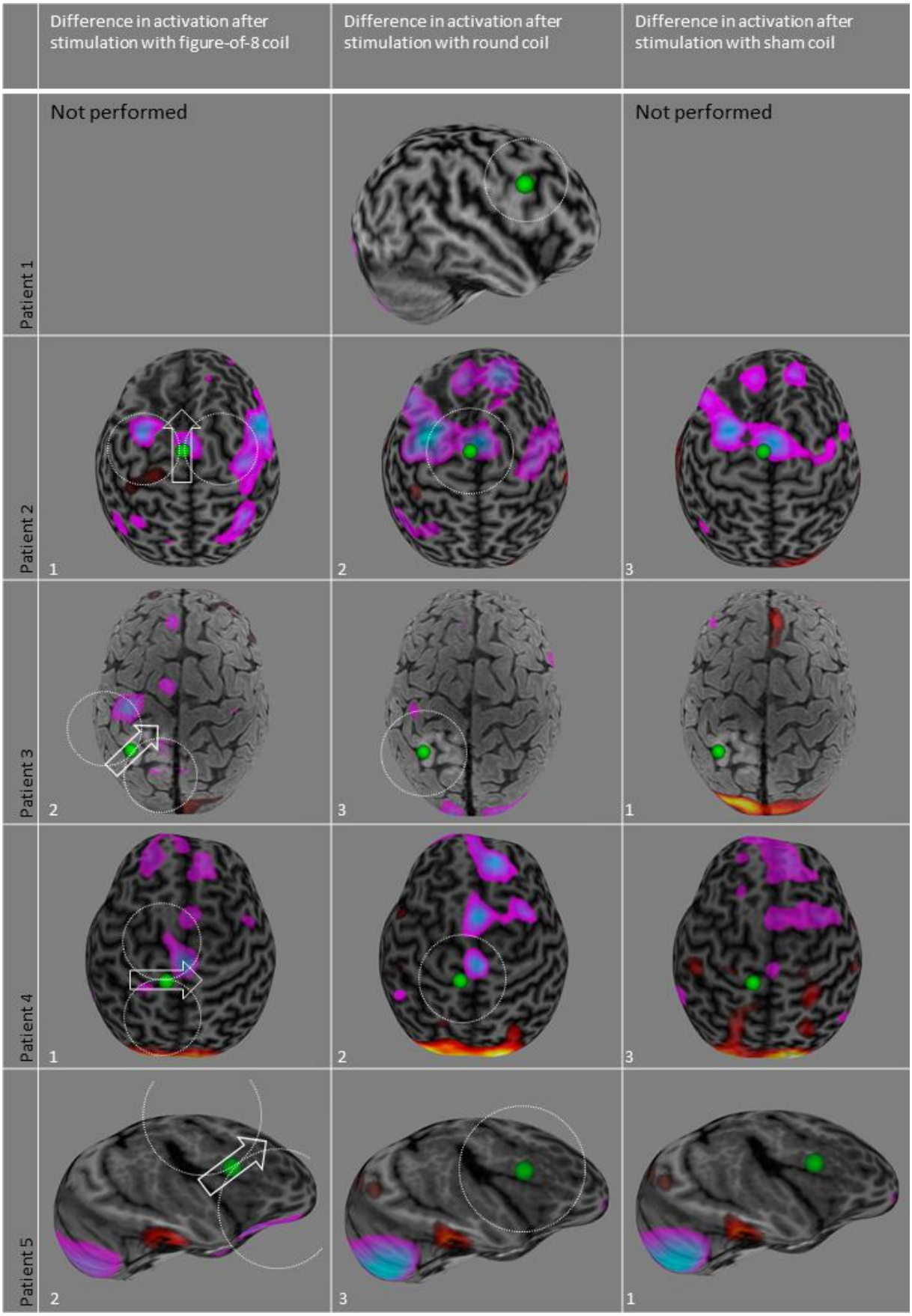
Difference in activation after stimulation with figure-of-8 coil
Difference in activation after stimulation with round coil
Difference in activation after stimulation with sham coil
Patient 1
Not performed
Not performed
Patient 2
1
2
3
Patient 3
2
3
1
Patient 4
1
2
3
Patient 5
2
3
1

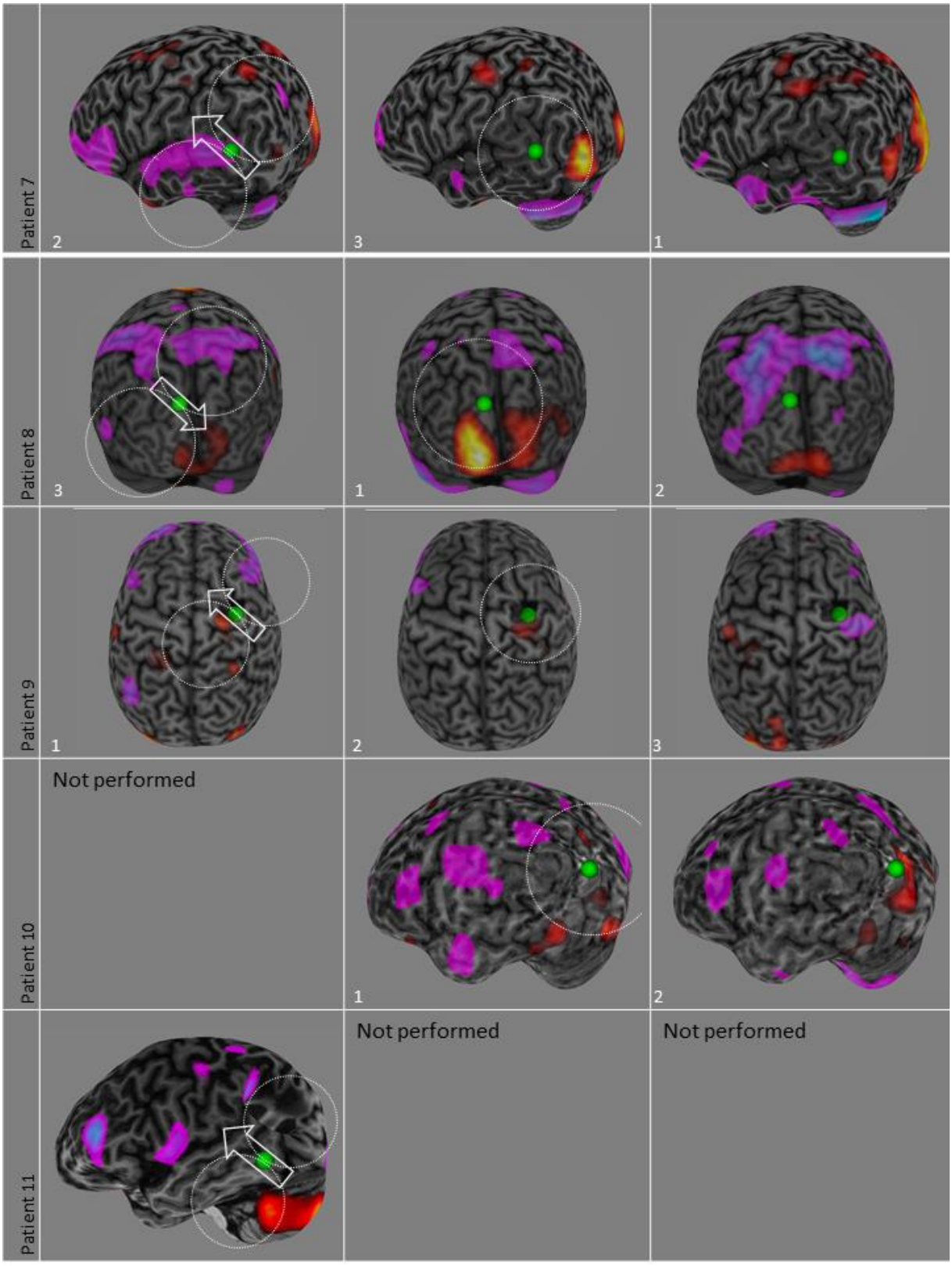

Figure 4.3 Differential activation after each of the conditions for the different patients, compared to baseline. Decreased activation in cool color scale (pink: z-score of -1.5; blue z-score >2,5), increased activation in hot color scale (red: z-score of >1.5, yellow: z-score >2,5). The location and approximate relative size of the figure-8 and round coils are represented by dotted circles. Orientation of the figure-8 coil is given by an arrow. The target of stimulation is given by the green dot. Changes are given for the cortical surface.

In patient 8, worsening in overall seizure frequency during the study period was significant, despite a clinically meaningful weekly seizure frequency reduction of >50% during the first month after each active treatment. After this initial seizure frequency reduction, seizure frequency increased above the 95% CI of baseline seizure frequency during 18 weeks following the reduction after the treatment with a round coil (including the following period of sham treatment), and for >20 weeks after treatment with the figure-8 coil. This clinical complex picture is reflected by complex changes in PET-images. After each of the conditions, the PET scan showed an extensive decrease in metabolic activity in the brain compared to baseline. The scans after active stimulation were acquired at a time when the number of seizures was reduced >50% compared to baseline, whereas there was a significant increase in seizure frequency at the time the scan after sham treatment was acquired. The patient had a stimulus-sensitive occipital lobe focal epilepsy (patterns like stairs, pedestrian crossings, train tracks… would provoke seizures, besides seizures in which no clear trigger was present) with habitually a very high seizure frequency (weekly average baseline seizure count: 125 seizures/week). Changes in occipital regions are therefor in the region of interest (ROI). Increases in the primary and secondary visual cortices were observed in each scan compared to baseline (after proportional scaling) and more pronounced after active compared to sham treatment. This change was more pronounced with stimulation with the round coil compared to the figure-8 coil; the seizure reduction was also more pronounced after treatment with the round coil compared to the figure-8 coil. Parietal cortices became less active, most pronounced after the sham condition. Since the patient had a very high seizure burden, she reported to have had a seizure during each of the three scans. Timing of the seizure relative to the time elapsed during scanning was not possible.

The seizure frequency in patient 7 also seems to be affected in the third condition, namely after stimulation with a round coil but this change was not statistically significant. Whereas decreased activity of the target was seen after the figure-8 condition, this was not present after stimulation with the round coil. There was hyperactivity in the occipital lobe after the round coil stimulation, which seemed to be within the area of stimulation of the round coil but a less pronounced increase activity was also present in the scans after stimulation with the sham and the figure-8 coil, that were used prior.
In patients 2 after stimulation with the round coil, in 5 after stimulation with the round coil and in patient 11 after stimulation with the figure-8 coil a short lasting increase in seizure frequency was observed, with seizure frequencies at least doubling in the week that the PET scan was performed. In none of these scans a specific pattern could be discerned.

4.5 Discussion

In patients with epilepsy, interictal PET imaging is known to show decreased tracer uptake not only in the epileptogenic zone but also in areas at a distance, i.e. the functional deficit zone. These regions are dysfunctional, due to effects of the epilepsy and possibly AEDs. An increase of the brain metabolism could thus be a sign of improved brain functioning. This can be seen after successful epilepsy surgery [125] and other successful treatments to abolish ongoing seizure activity [126]. In this study, however, no patient had a lasting decrease in seizure frequency.

In patients were the sham stimulation was the first condition no changes in the epileptic zone were observed. In all scans after sham stimulation, changes at regions at a distance of the epileptic zone were observed. A consistent finding was an increase in the occipital lobe. In a prior study [117] this was also one of the regions showing an increase after sham stimulation. In the prior study however, the injection of FGD was performed during the sham stimulation- since the environment was thus quite different from that at baseline, this could be linked to changes in brain metabolism. In our study however scans were acquired after all stimulation sessions were performed and in the same conditions as during baseline scanning. A difference in setup could thus not explain this change.

In six out of eight subjects were sham was used after active stimulation, the pattern of change was reminiscent of the changes seen in the scan acquired after the previous condition. This would fit with a carry-over effect in which the twelve weeks of wash-out were not long enough to abolish all metabolic alterations. In monkeys [115] a single session of rTMS induced metabolic changes that were still apparent at day 8 after stimulation, but were no longer present at day 16, even though neurophysiological and behavioral effect are known to dissipate much faster (in the range of minutes to hours). Since cumulative effects of rTMS ensue with repetitive days of stimulation and cumulating numbers of TMS pulses, an extended effect of longer rTMS protocols on brain metabolism could be envisioned. Our study is the first to hint that effects last at least 12 weeks in most subjects.

Since an inhibitory rTMS protocol was used- the idea was to decrease the hyperexcitability of the epileptic focus- a decrease in activity after active stimulation would have been envisioned, similar to trials using FDG-PET imaging in healthy controls [117,118]. This effect was only seen in three out of eight and five out of nine subjects after stimulation with the figure-8 and the round coil respectively. Patients that showed this decrease in activity could not be differenced from other patients in the trial on the basis of effect on seizure frequency or change in quality of life scores. The lack of change is likely at least in part due to large interindividual variability in response to TMS-induced plasticity and additionally the use of multiple AEDs that can block the effect of TMS.

In patient 9 an increase in tracer uptake after both active treatments was seen, whereas decrease in the same area was seen after sham stimulation. In this patient the focus was in the wall of the resection cavity of prior epilepsy-surgery that was incomplete due to extension into eloquent cortex. It is unlikely that the changes measured are due to a direct effect of epilepsy, since the seizure burden was low and no seizures were recorded in the time period around the scanning. It is also unlikely that the effect is due to AEDs since levetiracetam has only minimal effect on TMS-based physiological measurements in healthy controls[108].
Since the effect of rTMS depends on a network of interneurons with specific orientations relative to the induced current, it seems possible that the effect of stimulation in this patient was different due to the resection— and this is reflected in the PET-alterations. In patient 10 the target of stimulation was also just at the border of a prior incomplete resection- here the changes are less evident, but only stimulation with the round coil was performed.
The observed changes in the scans of subject 8 are intriguing: this patient had a bimodal effect on seizure frequency with a 50% decrease followed by a significant increase in seizure frequency. She had multiple short daily seizures and seizures were also present during PET scanning. The observed changes in this case could thus be an effect of seizures. It could also be an effect of the important reduction in seizure frequency around the time of scanning after treatment with either active coil. Alternatively the regions around the epileptic focus became more active as an improvement in the functional deficit zone, with better visual processing in this patient with occipital lobe seizures. At the same time global and especially parietal metabolism decreased. This decrease was most pronounced in the scan after sham stimulation, at a time that seizure frequency had increased. After sham stimulation this could be interpreted as an effect of the rise in seizure frequency and the functional deficit zone becoming more pronounced. The explanation of this effect after active treatment is more elusive. It would be very unlikely that this heralds an impeding worsening of seizures, since the decrease in metabolism in the interictal state is considered to be secondary to seizures.
No clear change in metabolism was seen in patients with short-term increases in seizure frequency, so in other subjects, the decrease in metabolism was not present.
The fact that no changes were observed due to increases in seizure frequency, which would mean that changes in metabolism induced by rTMS are quite robust and not easily changed by fluctuating seizure frequencies. The long-lasting changes as described above also hint to the robustness of the changes.

This is a promising avenue for future research and clinical practice since brain stimulation is increasingly used for a wide range of neurological diseases and fundamental questions on underlying mechanism, optimal parameters of stimulation and duration of the effect (including long-term side effects) remain unanswered. Having a functional imaging technique that can be performed acutely and is able to predict clinical effects on an individual basis, will be a huge advantage both from a scientific and clinical perspective. It will help doctors and patients to maximize benefits from brain stimulation and advance our knowledge on the complex interactions between stimulation and brain functioning.

4.6 Conclusion

We report on the FDG-PET-images obtained during a trial with rTMS for refractory focal epilepsy. rTMS causes measurable change in brain metabolism in patients with epilepsy. No single pattern of change emerged. However, induced changes in the area of stimulation were only apparent after active stimulation and a carry-over effect was observed, pointing to a lasting change in metabolism after rTMS of at least 12 weeks. Also short term (1-2 week) increases in seizure frequency did not seem to affect the induced metabolic changes, pointing to a rather robust effect on the changes in metabolism. However, the magnitude of change was often rather limited. This study can inform future trials on rTMS therapy and FDG-PET imaging could elucidate the response to rTMS.

Acknowledgments:

We would like to thank the nuclear medicine department and especially Dr. Bliede Van den Broeck for the creation of the MLEM static images used for the creating of the subtraction scans

5 Optimized preoperative motor cortex mapping in brain tumors using advanced processing of transcranial magnetic stimulation data.

Knowing that the electric properties of the brain are very complex and reinforced by the findings of our study with FDG-PET imaging in epilepsy- where we saw that changes in underlying brain anatomy seemed to influence the resulting effect of the TMS on the brain- it seemed prerogative to use the best available analysis techniques, with the aim to end up with a state-of-the-art model to help plan neurosurgery.
Getting from an analysis pipeline described in a paper to a working pipeline for our clinically acquired data, was very laborious. Without the in-depth knowledge on image processing, mathematical and computer skills of my colleagues in ESAT, this chapter would not have been possible in its current form.
This chapter has been published:
Optimized preoperative motor cortex mapping in brain tumors using advanced processing of transcranial magnetic stimulation data.

Laura Seynaeve, Tom Haeck, Markus Gramer, Frederik Maes, Steven De Vleeschouwer, Wim Van Paesschen. NeuroImage: Clinical. 2019 Jan;101657. doi: 10.1016/j.nicl.2019.101657. PMID: 30660662

5.1 Summary

Background and objective**:**
TMS is a useful technique to help localize motor function prior to neurosurgical procedures. Adequate modelling of the effect of TMS on the brain is a prerequisite to obtain reliable data.

Methods:
Twelve patients were included with perirolandic tumors to undergo TMS-based motor mapping. Several models were developed to analyze the mapping data, from a projection to the nearest brain surface to motor evoked potential (MEP) amplitude informed weighted average of the induced electric fields over a multilayer detailed individual head model. The probability maps were compared with DCS data in all patients for the hand and in three for the foot. The gold standard was defined as the results of the DCS sampling (with on average 8 DCS-points per surgery) extrapolated over the exposed cortex (of the tailored craniotomy), and the outcome parameters were based on the similarity of the probability maps with this gold standard.

Results**:**
All models accurately gauge the location of the motor cortex, with point-cloud based mapping algorithms having an accuracy of 83–86%, with similarly high specificity. To delineate the whole area of the motor cortex representation, the model based on the weighted average of the induced electric fields calculated with a realistic head model performs best. The optimal single threshold to visualize the field based maps is 40% of the maximal value for the anisotropic model and 50% for the isotropic model, but dynamic thresholding adds information for clinical practice.

Conclusions**:**
The method with which TMS mapping data are analyzed clearly affects the predicted area of the primary motor cortex representation. Realistic electric field based modelling is feasible in clinical practice and improves delineation of the motor cortex representation compared to more simple point-cloud based methods.

Key points

- Probability maps of the motor cortex representation were created from a TMS mapping.
- The MEP-weighted averaged tissue specific induced fields based map performed best.
- This map can gauge both motor cortex outline and hotspot, by varying the threshold.

5.2 Introduction

Neurosurgical procedures in or close to the motor cortex can be complicated by permanent motor deficits. To prevent damage while aiming to maximize resection, functional mapping is required, especially in tumor surgery, where anatomy can become distorted and functional reorganization can have occurred. In functional mapping, we aim to outline the cortical motor representation[127] i.e., the cortical area that is necessary and sufficient for the generation of movement, rather than only the hotspot of a specific muscle. The current gold-standard to delineate the motor cortex is DCS. DCS is time-consuming, allows for only limited sampling in case of tailored craniotomies and can't be used for preoperative planning or patient counselling. fMRI can help localize functions in the brain, but its use in pre-surgical planning is limited by the altered neuro-vascular coupling -especially near lesions with increased vascularization, and the fact that all regions involved in a task become active and not just the essential brain regions[128–132]. A non-invasive, well-tolerated brain stimulation technique able to electrically activate brain regions responsible for generating movement directly- TMS seems the most promising technique for reliable functional pre-operative mapping.

TMS over perirolandic brain regions can lead to MEPs. The resulting MEPs can be measured using electromyography (EMG). The first experiments using TMS for presurgical mapping date back to the nineties[133] but most studies were published after TMS-coils coupled to neuronavigation became commercially available. Even with neuronavigation, only the position of the coil on the scalp is defined and the accuracy of functional mapping depends on our ability to predict from the position of the coil with a diameter spanning over ten centimeters, the exact location and spread of activation in the brain. Previous studies testing TMS mapping prior to tumor surgery reduced the effect of a TMS stimulation to a single point projected onto the cortex, used a point-cloud to represent the TMS samples and derived the motor representation from it based on a fixed threshold. Operationalizing the similarity between TMS data and DCS data, has been done in a number of ways. For TMS this was done using either the location of the stimulus eliciting the largest MEPs (e.g. Forster et al., 2011[134]; Tarapore et al., 2012[135]), the location of the stimulus eliciting MEPs at the lowest stimulation intensity (e.g. Picht et al., 2009[136]) or by calculating the center of gravity (CoG, i.e. the geometrical midpoint) of the thresholded outline (e.g. Takahashi et al., 2013[137]; Zdunczyk et al., 2013[138]). Average distance measures varied between studies from 2.1 mm[135] to 10 mm[134,136] and more, depending on the muscle of interest, and with a large range. More detailed maps of the motor representation can be obtained from this point-cloud by spline interpolation[127]. The thresholding is based on measured MEP-amplitudes known to show considerable trial-to-trial variability[44] and to be dependent on the relative orientation of the induced electrical field with respect to the underlying brain anatomy and properties of tissues underneath the TMS coil[139,140]. To improve the localization of the motor cortex, modelling of the induced electrical field might be useful, taking into account the coil properties, its orientation and the properties of different tissue classes that make up the inside of the head[141]. Several algorithms have been published to calculate the induced electric field, e.g. the SimNibs workflow[39]. In this study, we tested several ways of calculating the motor representation, with increasing complexity, and compared the maps with intraoperative DCS data of patients with Rolandic brain tumors. Our aim was to determine what model is best suited to determine the motor representation and to make suggestions to optimize TMS mapping data analysis for clinical practice.

5.3 Methods

5.3.1 Participants

Patients with tumors close to or extending into the motor cortex were prospectively invited to undergo TMS mapping prior to neurosurgery, between February 2014 and September 2016. Active epilepsy and treatment with AEDs was not a contra-indication for participation since the safety of TMS in this patient group has been documented to be comparable to healthy subjects[57]. A tailored craniotomy based on neuronavigation and fMRI data and intraoperative DCS were performed in all cases. The study was approved by the local Ethics Committee of the University Hospitals Leuven. All patients gave written informed consent.

5.3.2 Ground truth data: DCS

The neurosurgical team was blinded for the pre-operatively acquired TMS data until after the surgery. During the surgical intervention, DCS data were obtained with the purpose of determining a safe corticotomy. The points of DCS were recorded in the neuronavigation system for off-line analysis (BrainLab, Germany). The locations of the points sampled on the navigation scan were extracted with a research tool provided by BrainLab. Since the craniotomy often caused some brain deformation, resulting in small shifts of the cortical surface compared to preoperative images, the DCS points were projected onto the nearest point of the cortical surface in the pre-operative MR imaging (see below) prior to further analysis. To serve as ground truth for comparison with the TMS maps, a binary map of the motor representation was necessary. Hence a DCS stimulation resulting in a motor response at any given intensity was thus considered a positive DCS point and the other points as negative; nearest neighbor interpolation was used in order to obtain the binary map from those DCS points. Since no data could be obtained from non-exposed cortex using DCS, the ground truth map was limited to the exposed cortex (Fig 5.1).

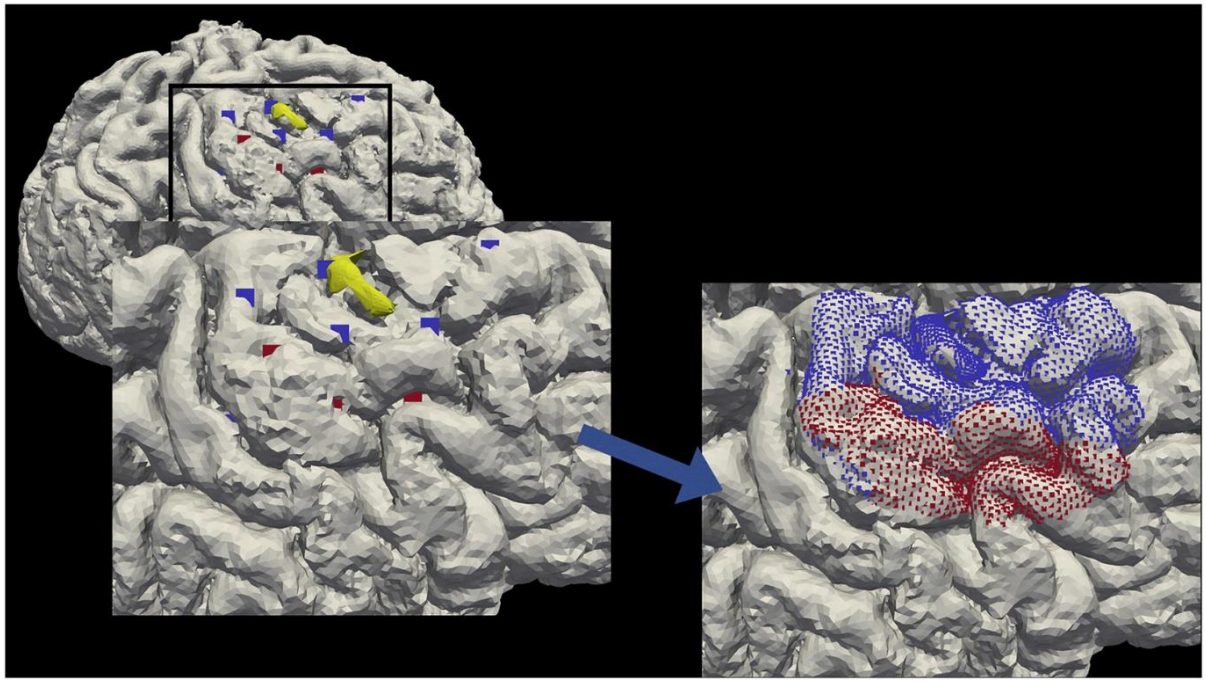

Figure 5.1
Ground truth binary map derived from direct electrical cortical stimulation (DCS) data- for upper limb in this example.
DCS points are represented as squares on the cortical (or tumor = yellow) surface; blue squares: no motor response evoked (in this example in hand muscles) in this location; red squares: motor response evoked in hand muscles in this location, at any stimulation intensity.
A binary map of the exposed cortex was derived from these DCS-points, assigning either a positive or negative value to each node of the cortical surface map, based on the value of the nearest DCS point.

5.3.3 TMS mapping procedure

TMS data were acquired in the days prior to the surgery. During TMS data acquisition, patients were seated comfortably in a chair with a tracker placed on their head for online, non-invasive registration/reference of the head to an anatomical MRI scan. Stimulation was performed with a Magstim Rapid2 (Magstim, United Kingdom), with standard 70-mm figure-8 coil; neuronavigation data and EMG measurements were recorded using BrainSight (Rogue Research, Canada). EMG was measured using pre-gelled Ag/AgCl electrodes affixed in a belly-tendon montage over the muscles of interest, namely APB for the upper limb and tibialis anterior muscle (TA) for the lower limb. Determination of the stimulation intensity was done in accordance to published guidelines[29,142] and set to 110% of the rMT of the muscle of interest and was kept constant during the procedure. Since MEPs have been shown to exhibit considerable trial-to-trial variability in amplitude[44] and the MEP amplitudes were used in further calculations, care was taken to obtain enough samples. This was done by sampling over a predetermined grid and taking 10 samples on each grid position. Mapping was continued in each direction until no MEP was seen in at least 5 consecutive measurements over the same grid position. Sampling was first performed over a 1x1cm grid and followed by sampling midway between those grid points. MEPs were measured as peak-to-peak amplitudes, of the maximal peak in the 10–90 ms time frame- trials with (voluntary) muscle activity prior to 10 ms were discarded.

5.3.4 Creation of the individual 3D head models

The anatomical T1- and T2-weighted images of the patients were used as input to generate a 3D volumetric mesh, consisting of different tissue classes, namely skin and subcutaneous tissue, skull, cerebrospinal fluid, grey matter, white matter, ventricles and brainstem with cerebellum, using surface and volume based meshing, as incorporated in the SimNibs workflow[141] (Fig 5.2).

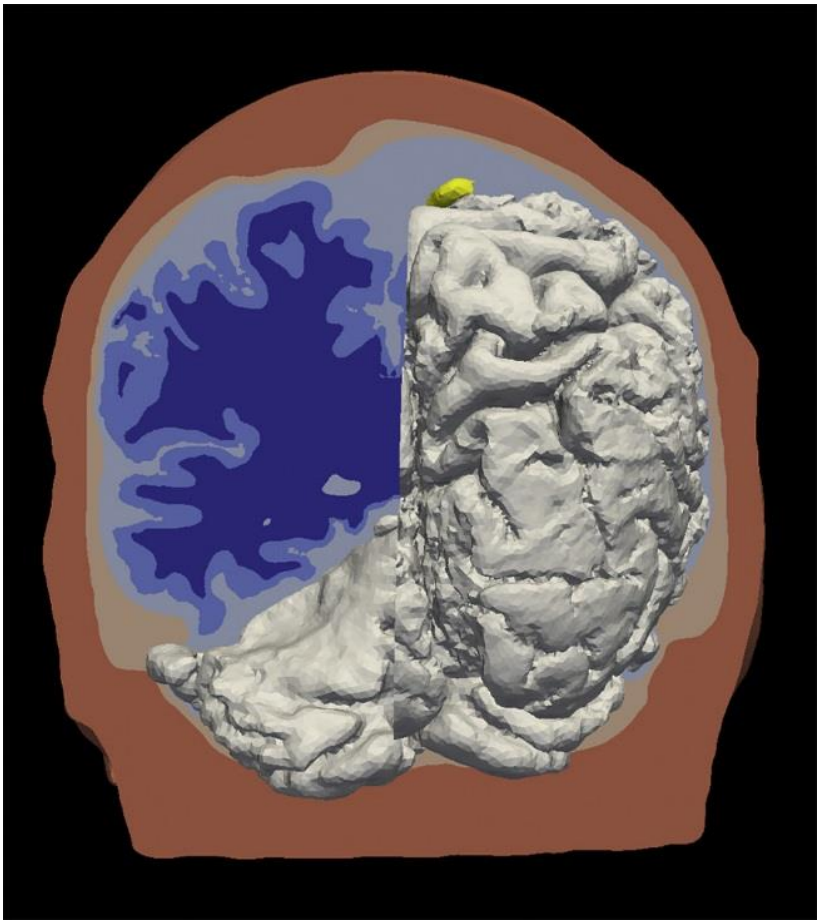

Figure 5.2
Individual 3D head model based on anatomical MRI. 3D volumetric mesh-model of an individual subject; left: cut thought the different tissue classes: skin and subcutaneous tissue (pale red), skull (pale pink), cerebrospinal fluid (light blue), grey matter (light blue), white matter (dark blue); right: 3D surface of cortex (grey) and tumor (yellow).

Tumor tissue was segmented manually and incorporated into the volumetric head model, taking care not to cause overlap with any of the other tissue classes. This was accomplished by manual segmentation in combination with meshing and mesh subtraction using VTK (ww.vtk.org) and correcting resulting meshes using meshfix[143].

5.3.5 Creation of the different probability maps

The workflow to create the different models from the TMS mapping data is illustrated in Fig. 5.3. The input data are the same for all models: the anatomical MRI and the coil positions and corresponding MEP amplitudes of all TMS-samples. Models can be divided into point-cloud based models (method 1&2), induced electric field based models (method 4) or a combination of both (method 3). Point-clouds were created by projecting the center of the TMS coil from the scalp to the cortical surface, for each sampled position, either to the nearest point (method 1) or along the plane perpendicular to the coil surface (method 2). From point-clouds a map was created using interpolation in order to

obtain a model of the motor representation[127]. The electric field induced in the head by the magnetic field of the TMS coil was calculated for each patient and each coil position, based on SimNibs algorithms. We adapted those in order to retain the actual 3D position and orientation of the coil throughout the process to account for the varying coil-scalp distance as the strength of the induced field falls off with the inverse power of the distance, and to include a tumor. In the calculation of the induced field, each tissue class had different conductive properties. In a simpler model, all tissue conductivities were set as equal, which we will called "isotropic"; in "anisotropic" modelling each tissue class was assigned conductive properties based on literature data. In order not to bias the results, we set the conductive properties of the tumor to the same value as the grey matter. Since tumor is also rich in cell bodies, we assumed the conductivity to be most similar to this tissue class, although accurate data are lacking. In order to combine all field calculations of all samples, either the point of maximal field strength on the cortical surface was taken and the maxima of all samples combined into a point-cloud (method 3) or a weighted average of all induced fields was calculated, using the MEP amplitudes as weighting factor (method 4).

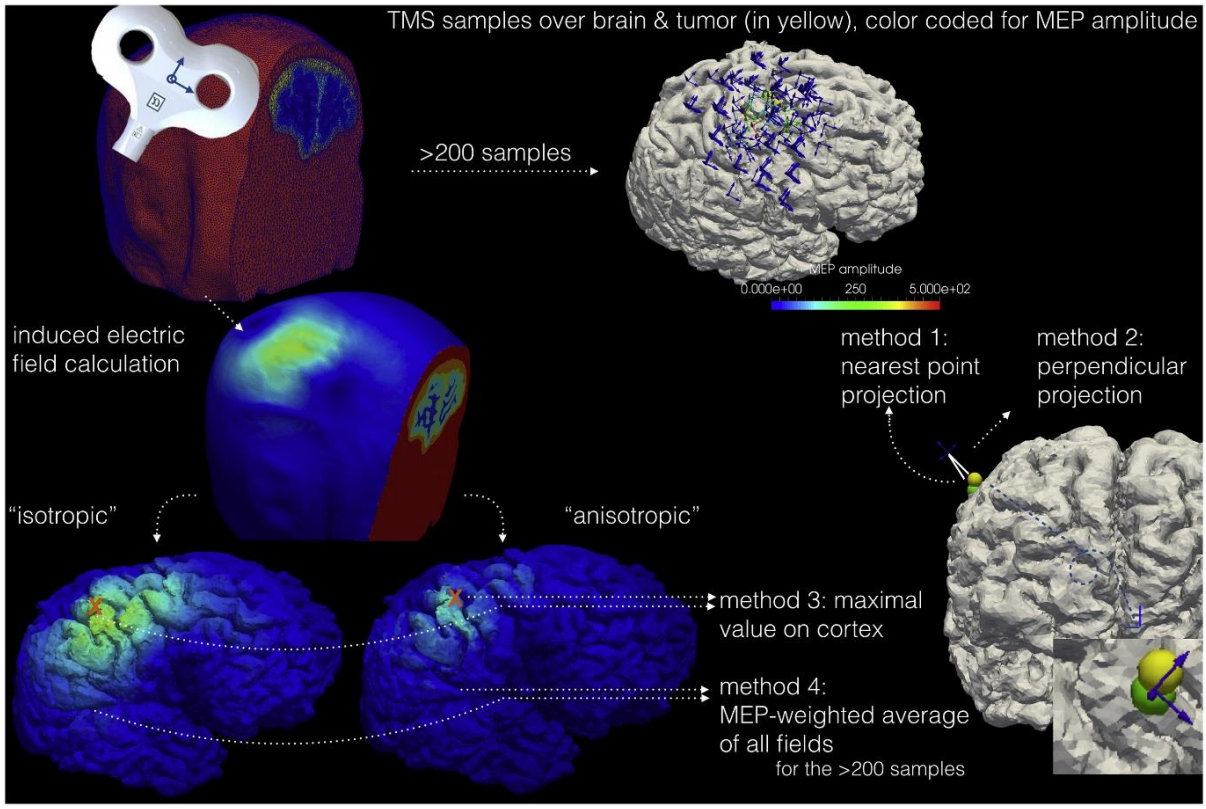

Figure 5.3
Creation of the different probability maps. The position of the TMS coil in space is represented as a 3D Cartesian axis. Its location is reported relative to the position of the head of the subject. This was done by referencing the head of the subject to the anatomical MRI in a previous step and by using neuronavigation to track the TMS coil and the subjects' head. The anatomical MRI of the subject is converted into a realistic 3D model, to obtain a finite element model of the head, with its different tissue classes. All TMS samples are taken into account to generate the different models, together with their respective MEP amplitudes.

For method 3 and 4, the induced electric field was calculated for each coil position. This was done by either setting the conductive value of the different tissue classes to the same value, in the "isotropic" modelling, or by assigning realistic conductive properties to each tissue class, in the "anisotropic" modelling. Only the fields obtained in the cortex (and tumour surface) were used for further calculations. Method 3 used the maximal value of the induced field as point of activation, to obtain a map. In method 4 the whole field over the cortex was used and these were combined for the different samples, by obtaining a weighted average, with the MEP value as weighting factor.

5.3.6 Outcome parameters

Maps created were visualized as 3D models. Our primary outcome parameter was how well the maps predicted the ground truth data, namely the binary DCS-based maps of the exposed cortex. The similarity of each probability map compared to the DCS-map was calculated for each individual patient, and plotted using receiver operating characteristic (ROC) curves in Matlab (Matworks, USA). ROC curves visualize sensitivity and specificity of the TMS-based map compared to the ground truth map, in a threshold-independent way, since all possible thresholds are analyzed. Paired t-tests were used to study differences in the sensitivity and specificity of the different models. Moreover, the maps were thresholded and the overall accuracy of the different models was compared. Accuracy was defined as TP + TN/TP + TN + FP + FN (with TP: true positive, TN: true negative, FP: false positive and FN: false negative). These maps were also used to calculate CoGs and compared to the location of the ground truth DCS points- CoG is the parameter used in most studies (the first study dating back to 1992[144]). For point-cloud based maps, the threshold was set to 50 µV MEP-amplitude. In method 4, a fixed percentage of the maximal value was used as threshold (as suggested in Pitkänen et al., 2017[127]) since the map is based on the strength of the induced field and not MEP-amplitudes.

5.4 Results

5.4.1 Participants and ground truth data: DCS

A flowchart of the patients screened and included can be found in Fig. 5.4. Patients' characteristics are given in Table 5.1. Twelve surgeries (one patient was operated twice) were included in our study. During neurosurgery, an average of eight (range: 5–11) locations were sampled with DCS. In eleven surgeries distal upper limb muscles were activated with an average of 2 (range: 1–3) positive responses per patient, and in three surgeries (including two that also mapped the upper limb) the distal lower limb was activated with DCS, with 1 positive response per patient.

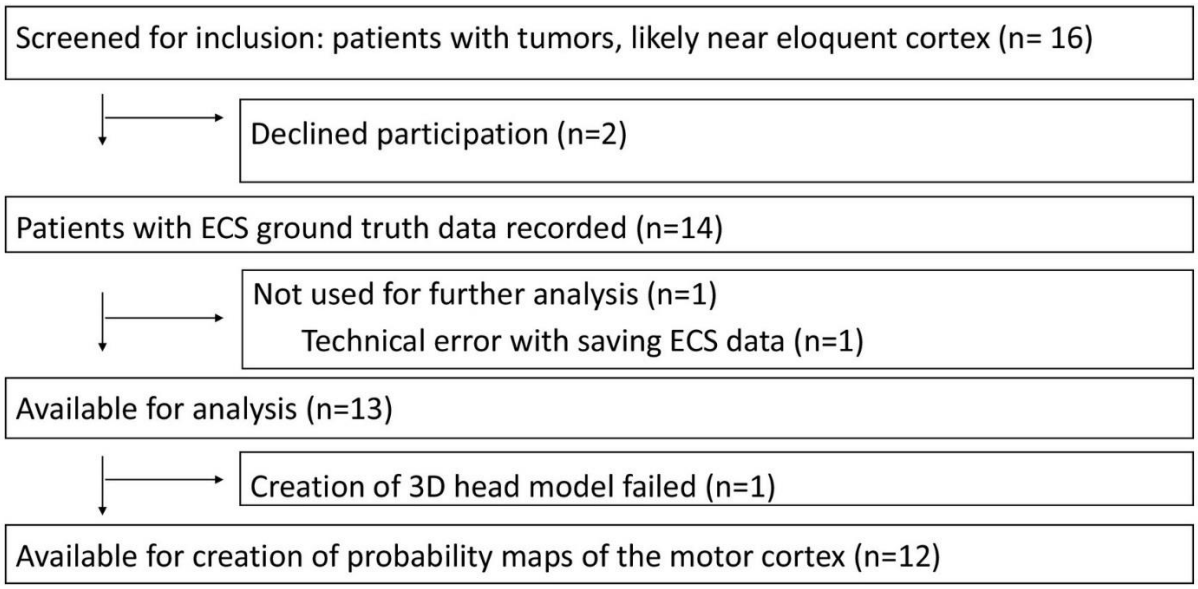

Figure 5.4 Flowchart of recruitment and selection.

Table 5.1: Patients' characteristics

	age	gender	pathology	relapse/ previous resection?	prior seizures	AED type	AED dose	ECS positive distal upper limb /total	Number of TMS pulses for upper limb mapping*	ECS positive distal lower limb /total	Number of TMS pulses for lower limb mapping*
1	52	M	HGG WHO IV	N	Y	LEV/ VPA	2000/ 1500mg	1/11	363	0/11	
2	19	F	LGG WHO II	N	N	-	-	2/8	100	0/8	
3	57	M	HGG WHO IV	Y	Y	LEV	1000mg	1/5	268	0/5	
4	30	M	LLG WHO II	Y	Y	CBZ/LEV/VPA	600/1500 /1750mg	3/7	237	0/7	
5	46	M	LGG WHO II	N	N	-	-	1/10	170	0/10	
6	73	M	HGG WHO IV	Y	Y	LEV	2000mg	3/7	119	0/7	
7	70	M	HGG WHO IV	Y	Y	LEV	1000mg	1/8	195	0/8	
8	49	M	LGG WHO II	N	Y	LEV	1000mg	1/8	280	0/8	
9	33	M	LCC, NOS	N	N	-	-	0/8		1/8	120
10**	56	M	HGG WHO IV	N	Y	LEV	2000mg	5/9	258	1/9	120
11**	56	M	HGG WHO IV	Y	Y	LEV	2000mg	3/8	175	1/8	185
12	71	F	metastatic RCC	N	N	-	-	2/7	180	0/7	

Abbreviations:
AED: anti-epileptic drugs; CBZ: carbamazepine; LEV: levetiracetam; VPA: valproate; ECS positive upper/total: number of intra-operative positions sampled with ECS during surgery compared to the total number of samples acquired; ECS positive lower /total: same for lower limb responses; HGG: high grade glioma; LCC, NOS: large cell carcinoma, not otherwise specified: metastasis without known primary tumor; LGG: low grade glioma; RCC: renal cell carcinoma; Y: yes, N: no; WHO: world health organization classification.
*data for mapping only reported if used in this study- that is, if intraoperatively the limb was also sampled
**data are from the same patient, having two surgeries, 7 months apart

5.4.2 TMS mapping procedure

For upper limb mapping, an average of 213 samples (±76) were recorded in 11 patients and 142 samples (range: 120–185) for lower limb mapping in three patients (Table 5.1). The anatomical MRI used for mapping and creation of the head models was recorded within a median of 17 days prior to surgery, with one outlier who underwent the fMRI 5 months prior to surgery (slow growing lesion).

5.4.3 Creation of the different probability maps

A representative example of one patient is shown in Fig. 5.5. Models 1–3 represent the location of motor areas, derived from the measured MEP amplitudes and scaled accordingly. Model 4, however, represents the areas where high induced electric fields are expected to generate MEPs. As supplementary material, all maps of all patients are included.

Figure 5.5 All models for one patient in the study, both for upper and lower limb panel a: DCS points sampled during surgery; panel b: ground truth map (similar to Figure 1) panel c: method 1: based on nearest-point projection, with interpolation over the surface, color coding refers to measured MEP amplitudes (in μV) panel d: method 2: based on projection along a plane perpendicular to the coil, with interpolation over the surface, color coding refers to measured MEP amplitudes (in μV) panel e: method 3 isotropic: based on the maximum of the induced field of each coil position sampled, color coding refers to measured MEP amplitudes (in μV) panel f: method 3 anisotropic: same as panel e but using tissue-specific conductivity values based on known tissue properties panel g: method 4 isotropic: based on MEP-amplitude informed weighted average of all fields, color coded for where high induced fields are likely to result in high MEP-amplitudes (red) and areas of low probability of motor responses (blue)panel h: method 4 anisotropic: same as panel g but using a tissue-specific conductivity value based on known tissue properties.

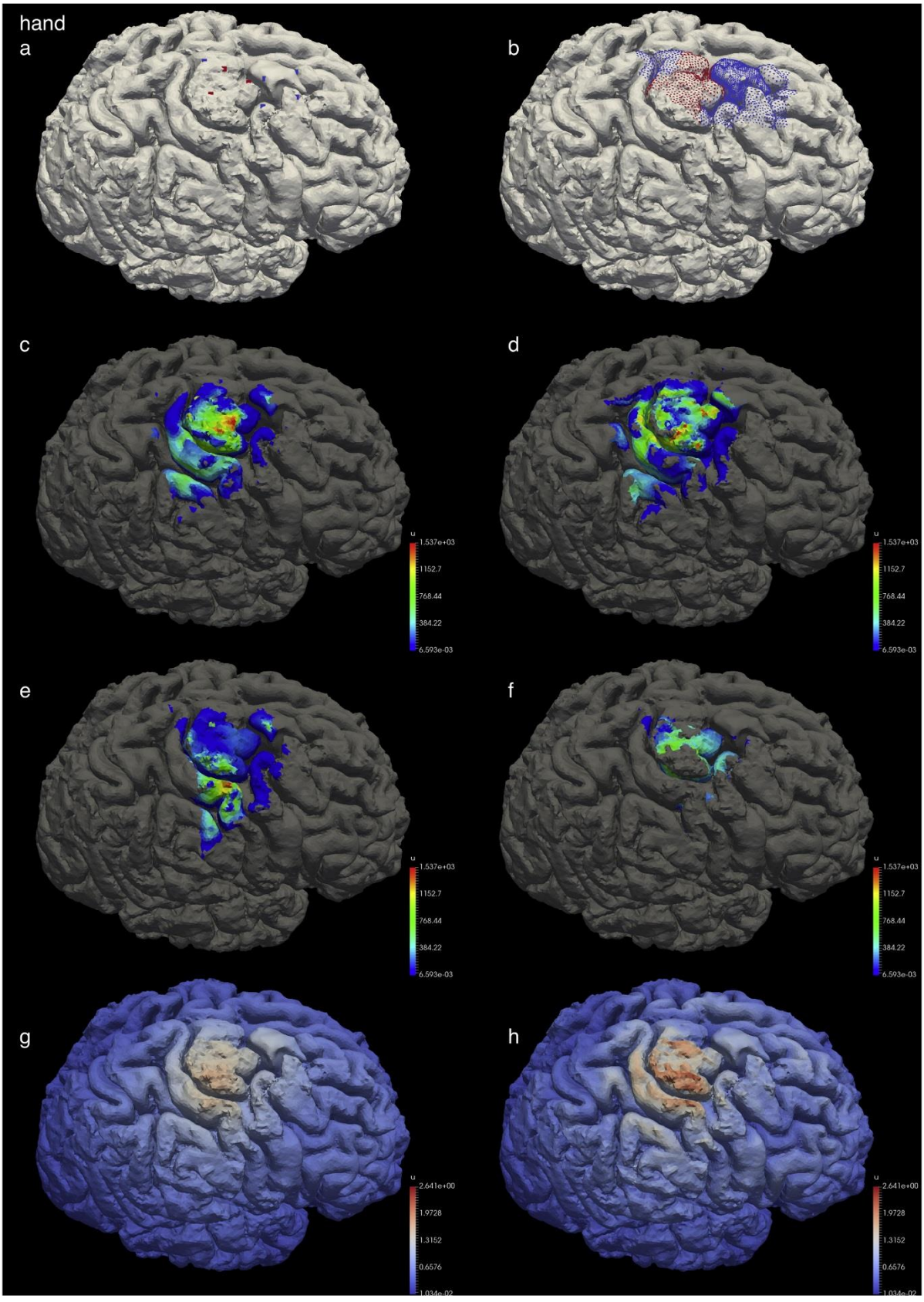
hand
a
b
c
d
e
f
g
h
u
1.537e+03
1152.7
768.44
384.22
6.593e-03
2.641e+00
1.9728
1.3152
0.6576
1.034e-02

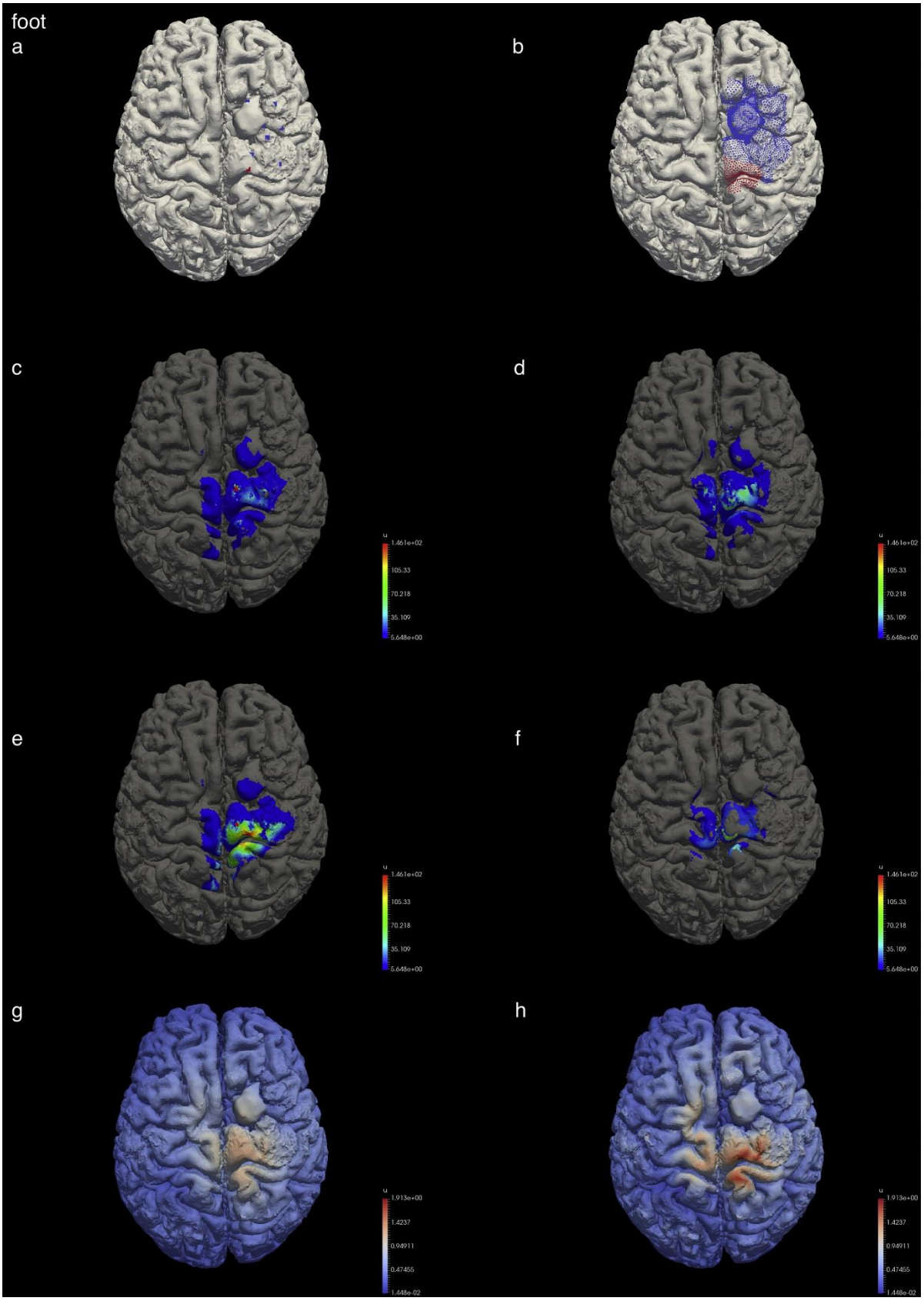
foot
a
b
c
d
e
f
g
h
1.461e+02
105.33
70.218
35.109
5.648e+00
1.913e+00
1.4237
0.94911
0.47455
1.448e-02

5.4.4 Outcome parameters

The ROC curves of the models can be seen in Fig. 5.6. Since all point-based interpolated maps never covered the whole exposed cortex, the ROC curves of those models are truncated; the area-under-the-curve (AUC) parameter in those instances is not so meaningful. The average AUC parameter of model 4 isotropic was 79% (±10%) and for the anisotropic model 75% (+/− 10%). The overall accuracy of model 1 was 86%, of model 2 85%, of model 3 isotropic 85%, of model 3 anisotropic 83%, of model 4 isotropic 64% and model 4 anisotropic 80%. Accuracies are driven primarily by the specificity due to the higher number of negative DCS points compared to positive points. Sensitivity and specificity of the different models, at optimal threshold, as based on the ROC curves, are found in Table 5.2. The best cut-off for model 4 isotropic was around 50% of the maximal value, as reported previously[127] whereas for the anisotropic model, a cut-off of around 40% of maximal (cut-offs were tested with 10% increments[127]), performed better - the maximal value obtained with the anisotropic models was on average also 14% higher compared to the isotropic model. 50% and 40% cut-offs respectively were thus used to threshold the map for CoG calculations. However, accuracies of the models at the fixed threshold were similar to the accuracy data obtained from the ROC curves (Table 5.3). The Euclidian distance between the CoG of a model and the DCS point is on average 11 mm (SD 1.5 mm) (Table 4a, Table 4b). For the six subjects in whom more than one positive DCS point was recorded, the distance measures decreased for the electric field based models when the DCS point was taken where a response could be evoked with the lowest amount of stimulating current instead of the center of the DCS points (table 5.5); however this difference was not significant in this low number of subjects.

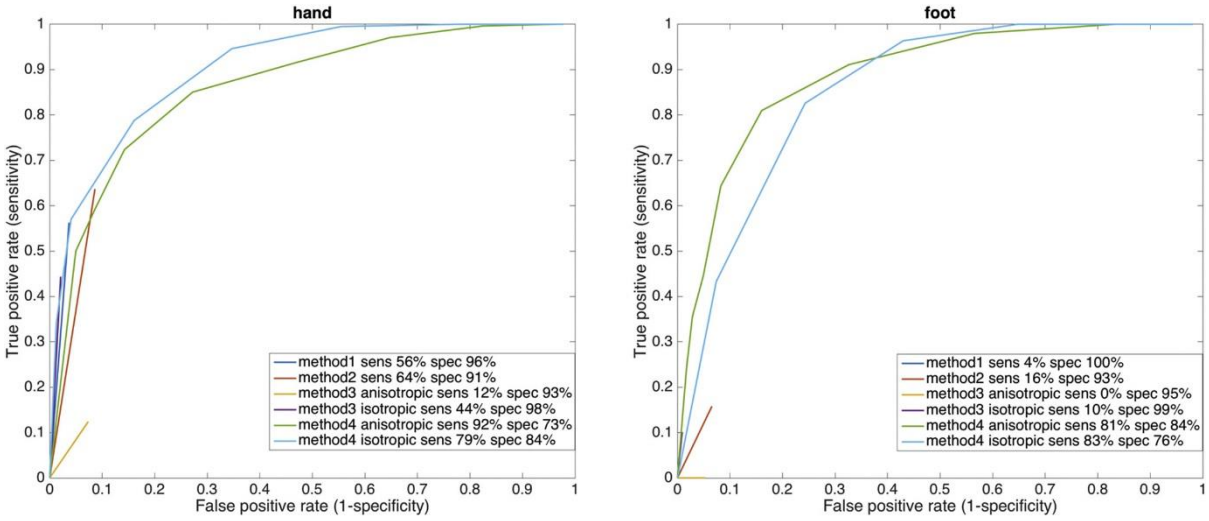

Figure 5.6 Receiver-operator characteristics (ROC) curves of the experimental maps of the subject who's maps are represented visually in Figure 5. Since the point-based methods do not have values for all points of the cortical (and tumour) surface, those graphs are truncated. Sensitivity and specific values are reported for the optimal cut-off. The area under the curse (AUC) for hand is 0.88 for the isotropic method and 0.83 for the anisotropic method; for the foot this is 0.84 and 0.86 respectively.

Table 5.2: Sensitivity and specificity of the different models (in %), for the different patients, compared to the DCS data, as calculated from the ROC curves. SD= standard deviation

	method 1		**method 2**		**method 3 isotropic**		**method 3 anisotropic**		**method 4 isotropic**		**method 4 anisotropic**	
	sens	**spec**	**sens**	**spec**	**sens**	**spec**	**sens**	**spec**	**sens**	**spec**	**sens**	**spec**
patient 1	31	94	37	91	20	95	37	93	87	86	81	80
patient 2	77	56	67	89	51	94	61	88	100	47	96	55
patient 3	33	70	68	68	7	75	3	90	85	48	76	58
patient 4	60	86	47	62	58	90	54	61	78	57	75	70
patient 5	28	98	33	97	39	96	53	91	80	81	65	74
patient 6	33	98	39	95	23	99	57	90	79	74	62	87
patient 7	32	87	48	87	19	78	10	100	71	72	67	60
patient 8	50	81	71	87	57	76	90	53	77	70	74	66
patient 9	68	87	82	83	36	92	79	77	94	72	74	79
patient 10 hand	56	96	64	91	44	98	12	93	79	84	92	73
patient 10 foot	4	100	16	93	10	99	1	99	83	76	81	84
patient 11 hand	28	90	73	77	28	88	15	96	60	55	45	57
patient 11 foot	97	85	94	85	97	86	47	93	96	84	93	96
patient 12	49	78	44	82	48	76	44	76	96	28	89	49
mean **SD**	46,1 27,9	86,1 7,3	55,9 24,7	84,8 5,1	38,3 23,9	88,7 9,4	40,2 33,5	85,7 16,2	83,2 13,0	66,7 18,4	76,4 16,0	70,6 15,5

Table 5.3: accuracy (in %) of the different thresholded maps, for the different patients, compared to the DCS based map ('ground truth')

accuracy thresholded		Model 1	Model 2	Model 3 isotropic	Model 3 anisotropic	Model 4 isotropic	Model 4 anisotropic
Patient 1	hand	89	90	85	90	90	86
Patient 2	hand	82	87	84	86	81	74
Patient 3	hand	95	83	81	85	84	68
Patient 4	hand	85	70	73	88	84	45
Patient 5	hand	94	94	89	94	93	80
Patient 6	hand	50	54	53	42	62	76
Patient 7	hand	88	89	88	88	45	53
Patient 8	hand	87	90	88	86	81	71
Patient 9	foot	87	85	78	86	82	63
Patient 10	hand	78	82	77	78	85	66
Patient 10	foot	93	93	93	93	92	41
Patient 11	hand	77	80	76	75	78	61
Patient 11	foot	95	95	95	98	96	62
Patient 12	hand	85	85	85	85	45	47
total	All: mean & SD	85 (12)	84 (11)	82 (11)	84 (14)	78 (16)	64 (14)
	Hand: mean & SD	83 (12)	67 (11)	65 (10)	66 (14)	60 (17)	53 (14)
	Foot: mean & SD	91 (4)	91 (5)	88 (10)	92 (6)	90 (7)	55 (12)

Table 5.4a: Distances (in mm) of the center of gravity (CoG), using pre-set thresholds, between each of the models and the positive DCS point (single positive DCS point (in 6/12) when only one positive DCS point was recorded or to the midpoint of all positive DCS points (marked with *)).

	Method 1	Method 2	Method 3 isotropic	Method 3 anisotropic	Method 4 isotropic	Method 4 anisotropic
1 hand	17.9	18.5	15.0	17.7	22.1	25.4
2* hand	12.9	12.1	10.0	10.6	18.0	18.7
3 hand	21.2	18.7	24.2	24.2	35.8	37.8
4* hand	9.2	8.4	11.1	5.4	12.3	11.8
5 hand	16.6	18.3	14.3	16.1	21.4	23.0
6* hand	8.3	10.6	16.4	14.6	18.6	18.9
7 hand	13.1	7.1	9.2	19.1	11.0	14.3
8 hand	11.9	13.7	13.2	9.0	13.0	12.6
9 foot	7.7	9.0	6.3	6.5	9.1	11.7
10* hand	10.4	6.9	10.1	10.3	9.9	12.0
10 foot	NaN	17.5	11.0	NaN	13.2	20.9
11* hand	17.0	11.4	12.8	12.0	19.1	20.5
11 foot	5.9	5.9	8.2	6.1	14.0	18.0
12* hand	4.9	4.0	NaN	NaN	11.3	14.4
all: mean (SD)	12.1 (5.0)	11.6 (5.1)	11.5 (4.5)	10.8 (5.8)	16.3 (7.0)	18.9 (7.1)
hand: mean (SD)	13.0 (4.8)	11.8 (5.1)	13.6 (4.4)	13.9 (5.5)	17.5 (7.5)	19.0 (7.7)
foot: mean (SD)	4.5 (1.3)	8.1 (6.0)	6.4 (2.4)	4.2 (0.3)	9.1 (2.6)	12.7 (4.7)

Table 5.4b: Distances (in mm) of the center of gravity (CoG), using pre-set thresholds, between each of the models and the single DCS point where a response was evoked using the lowest current, in patients with more than one DCS positive point recorded (in all for mapping of the hand).

	Method 1	Method 2	Method 3 isotropic	Method 3 anisotropic	Method 4 isotropic	Method 4 anisotropic
2	6.5	6.3	7.1	8.9	9.9	9.1
4	2.9	6.7	8.8	10.6	13.0	9.0
6	6.8	8.5	9.4	11.5	12.2	12.2
10h	6.5	6.5	6.5	10.2	14.6	9.0
11h	24.0	22.4	13.7	12.1	3.8	1.9
12	4.6	1.7	7.2	7.2	7.3	8.3
Mean (SD)	8.6 (7.7)	8.7 (7.1)	8.8 (2.6)	10.1 (1.8)	10.1 (4.0)	8.3 (3.4)

Table 5.5: Distances (in mm) for the ground truth maps: between DCS mean- that is the midpoint of all positive DCS points or a single positive DCS point (in 6/12) when only one positive DCS point was recorded DCS single- the single DCS point where the response was evoked at the lowest stimulation intensity (if available) and the CoG of the DCS positive maps created by nearest neighbor interpolation.

	DCS single-DCS mean	CoG- DCS mean	CoG- DCS single
Patient 1	-	8.6	-
Patient 2	8.6	5.5	12.9
Patient 3	-	8.8	-
Patient 4	11.4	6.0	10.0
Patient 5	-	9.4	-
Patient 6	12.8	17.9	12.6
Patient 7	-	3.7	-
Patient 8	-	5.4	-
Patient 9	-	6.5	-
Patient 10h	13.8	6.2	7.7
Patient 10f	-	2.7	-
Patient 11h	16.9	11.3	18.0
Patient 11f	-	4.5	-
Patient 12	12.8	10.2	5.1
Mean (SD)	12.7 (2.7)	7.6 (3.9)	11.1 (4.5)

5.5 Discussion

TMS is a useful and accepted method to locate the motor cortex prior to neurosurgical procedures. Its accuracy depends on the ability to predict from the position of the coil (with a coil diameter spanning over ten centimeters) placed on the head, the area of activation in the cortex. TMS does affect a whole area of the brain, rather than a single “activation point” as it has often been presented in previous studies. In this study, we created probability maps of the motor cortex that differed only in the way they were calculated, by adding progressively more information. The electric fields were calculated post-hoc from the scalp location- not during the recording- and thus more detailed and computationally complex methods could be used. The modelling could not only take scalp- brain distance and properties of the magnetic coil into account, but all anatomical details of the individual's head and the differential conductive properties of tissue classes. The aim was to determine the best way to analyze the TMS data in order to delineate the cortical motor representation, i.e. the cortical area that is necessary and sufficient for motor function. It was shown that simple projection models are accurate (accuracy ≥85%) and can be used to specifically point to a cortical area of the motor cortex (specificity >95%). However, the spread of activation is not captured. Clinically, these models can be used to pinpoint to a gyrus containing the motor cortex. Using the induced field to determine the point of maximal impact in the brain of the TMS pulse, did not improve the model compared to simple projections. The modelling did not only take scalp-brain distance and properties of the magnetic coil into account, but also all anatomical details of the subjects' head. In this modelling, the anisotropic model showed often only a very small area of activation; due the inherent local field increases at grey-white matter borders[139] the maxima of samples obtained over larger areas of the scalp coincided on the same focal point at a bend of a

sulcal surface. The reason for this lack of additional benefit is that the effect of TMS is more extensive than one focal point- a fact we wanted to capture in the electric field weighted average models. The interpretation of those maps is that regions with high values are those where high induced electric field strengths are likely to result in high MEP amplitudes. These maps can give an outline of the motor were 50% of the maximal value for the isotropic and 40% for the anisotropic model.

For clinical purposes, we suggest to use different thresholds, which is a unique benefit of these maps: a high threshold highlights the center of the motor area and a lower threshold is able to capture the whole motor representation (Fig. 5.7). The best accuracy for this type of probability map was obtained by the anisotropic version of this model, which the model that takes all known information of anatomy and conductivity into account.

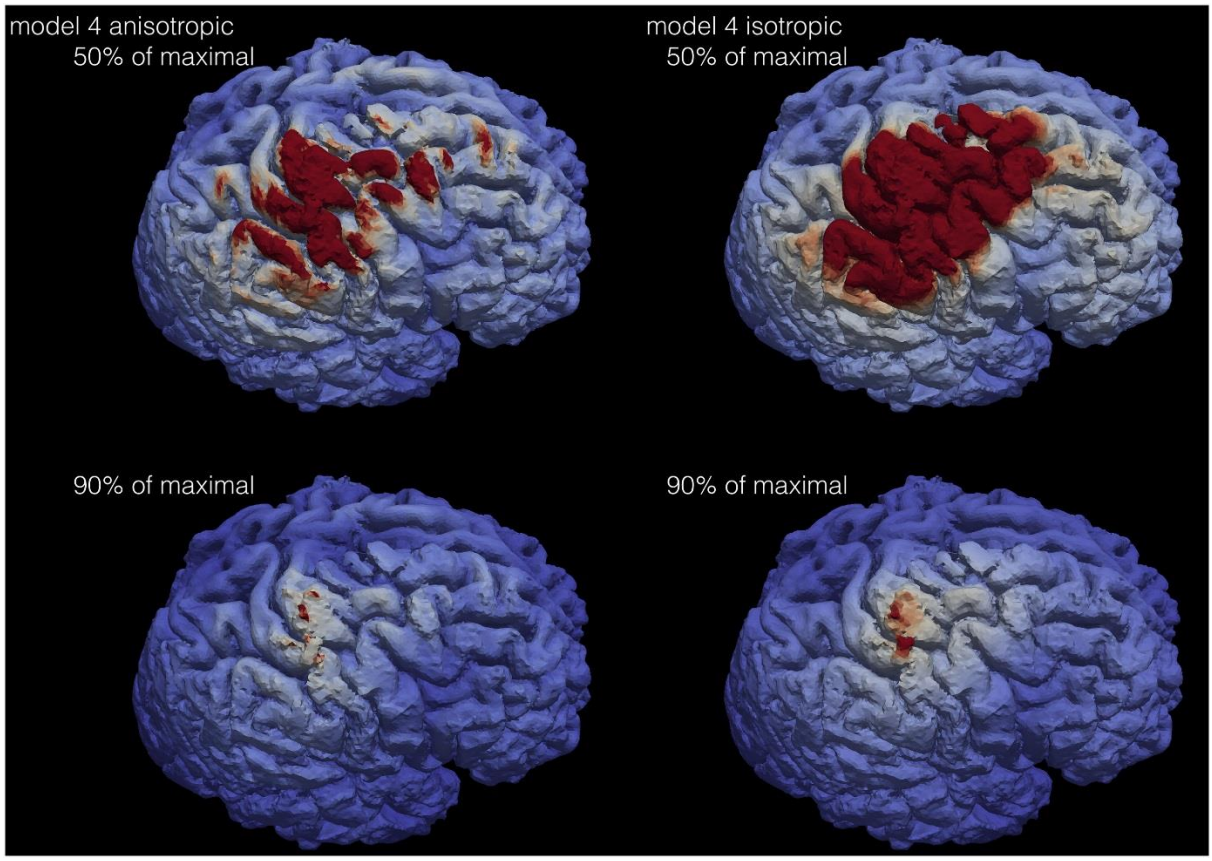

Figure 5.7 Illustration of the effect of the chosen threshold on the corresponding map. The upper and lower panels represent the same map, but at a different threshold, to demonstrate that with the same map both the area of the motor representation can be shown (although at the cost of some false-positive zones) and the motor "hotspot". This image also illustrates that the anisotropic map is often more suited to gauge the motor representation.

In order for these models to work, care needs to be taken to counter the inherent considerable trial-to-trial variability in MEP amplitudes, for instance by measuring several MEP amplitudes from a similar location and by using an interpolation over the surface, which should limit problems caused by outliers[127], as was done in our study. It should be noted that previous motor TMS studies in neurosurgical patients used a simple curvilinear representation of the cortical surface whereas we used the real cortical surface. This inherently leads to larger Euclidian differences between two points and distance measures. Our results, therefore, are not completely comparable with previous studies. Moreover, the CoG is dependent on the cut-off used and especially for field-based models; the CoG shifts considerably when changing the threshold and is thus not a robust outcome measure. The average distance in our study was 11 mm, depending on the modelling used. The rather low number of DCS points in our study also affected distance measures, but the resulting ground truth map was clinically relevant. It was left to the discretion of the neurosurgeon (who was blinded for the pre-operatively acquired TMS results) to determine the location and number of DCS points, which in this study were based mainly on sulcal anatomy. Previous studies have used a setup were the TMS-based locations of the motor cortex have been used to guide the DCS sampling[136,145–147] or have used a much higher number of DCS points[148], both of which can improve distance measures. The ground truth data in our study also did not have any information on contribution of different parts within one gyrus to the resulting motor output, since this was not the aim of the study. The anisotropic induced field based model predicts that different parts of one gyrus contributing unequally to the resulting motor output. Whether this can also be demonstrated using DCS mapping, will need further study. It should also be noted that the modelling in this study was based on priors derived from healthy volunteers. The model could benefit from more knowledge about the differential conductivity of (different parts of) the tumor, especially if it was combined with automated and reliable tumor segmentation. Moreover, TMS based mapping cannot sample selectively from subcortical structures and thus in order to preserve white matter tracts during surgery, another mapping technique will need to be added (like tractography or intraoperative direct subcortical stimulation).

Depending on the clinical question, a different way to analyze the motor TMS data can be chosen. We argue that calculating a realistic head model and obtaining a weighted average electric field based model, is preferable, since it captures more information compared to point-cloud based models is feasible since it is based on data available preoperatively and a workflow with freely available software. The input data can be acquired with a number of different TMS equipment (including coils from different vendors) and software. It is also more robust since the model takes the coil orientation into account and averages out the inherent MEP-amplitude variability. Since acquisition can be done separately from analysis, pooling of data from different centers becomes a possibility and could be exploited to explore the modelling's full potential. The output is an easy to manipulate, threshold-adjustable detailed 3D model of the patients' brain, which can be loaded in the intraoperative navigation software.

5.6 Acknowledgments

This work was supported by the Institute for innovation by science and technology Flanders (IWT) [TBM grant 09085]. The work has been awarded a Belgian Brain Tumor Support prize in 2016.
We would like to thank the patients and their caregivers for participation in the trial, the colleagues of the department of Neurology and Neurosurgery for their organizational support, special thanks goes to Mr. Van Driel for the intra-operative data collection, to the Medical Imaging Research Centre colleagues for technical support and to Dr. Duerinck for the critical revision of a previous version of this manuscript.

5.7 Supplementary figures

For each patient, the 3D head model of grey matter and tumor is shown. DCS points are added as cubes: blue cubes for negative DCS points and red cubes for positive DCS points. The different probability maps are represented onto the grey matter and tumor surface.

The first row: point model 1 (label a) and point model 2 (label b): both use a linear projection. (scaling unit= microV, yellow= no data)

The second row: point model 3: using the maximum of the induced field, to determine the area of the cortex that is activated: first for anisotropic modelling (label c), next for isotropic modelling (label d). (scaling unit = microV, yellow= no data)

The third row: region model: calculated as a weighted average of all induced electric fields and their respective MEPs: first for anisotropic modelling (label e), next for isotropic modelling (label f). (scaling unit =V/m)

The small inserts represent the same models, in a different scaling, to clarify differences.

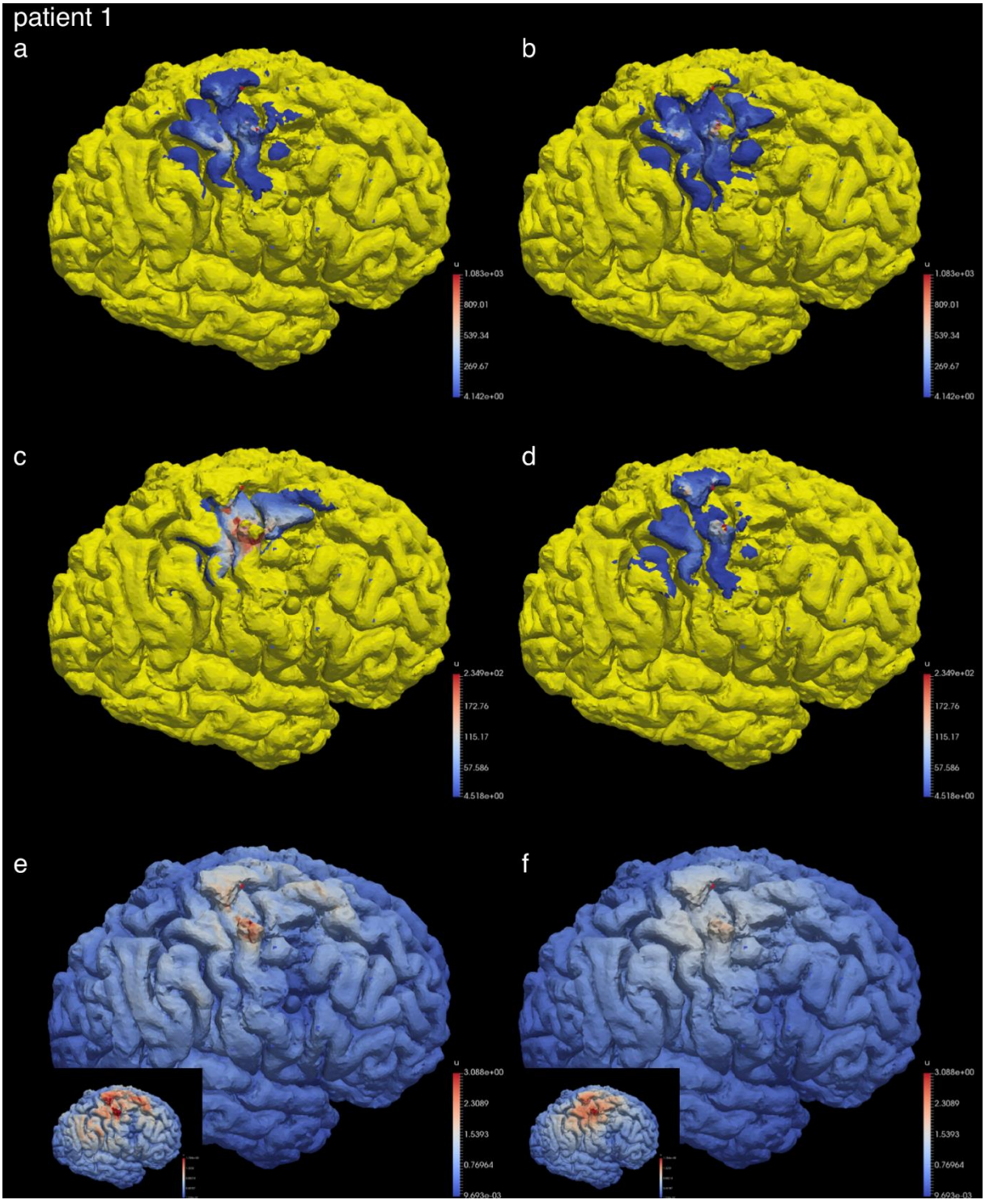
patient 1
a
b
c
d
e
f
u
1.083e+03
809.01
539.34
269.67
4.142e+00
2.349e+02
172.76
115.17
57.586
4.518e+00
3.088e+00
2.3089
1.5393
0.76964

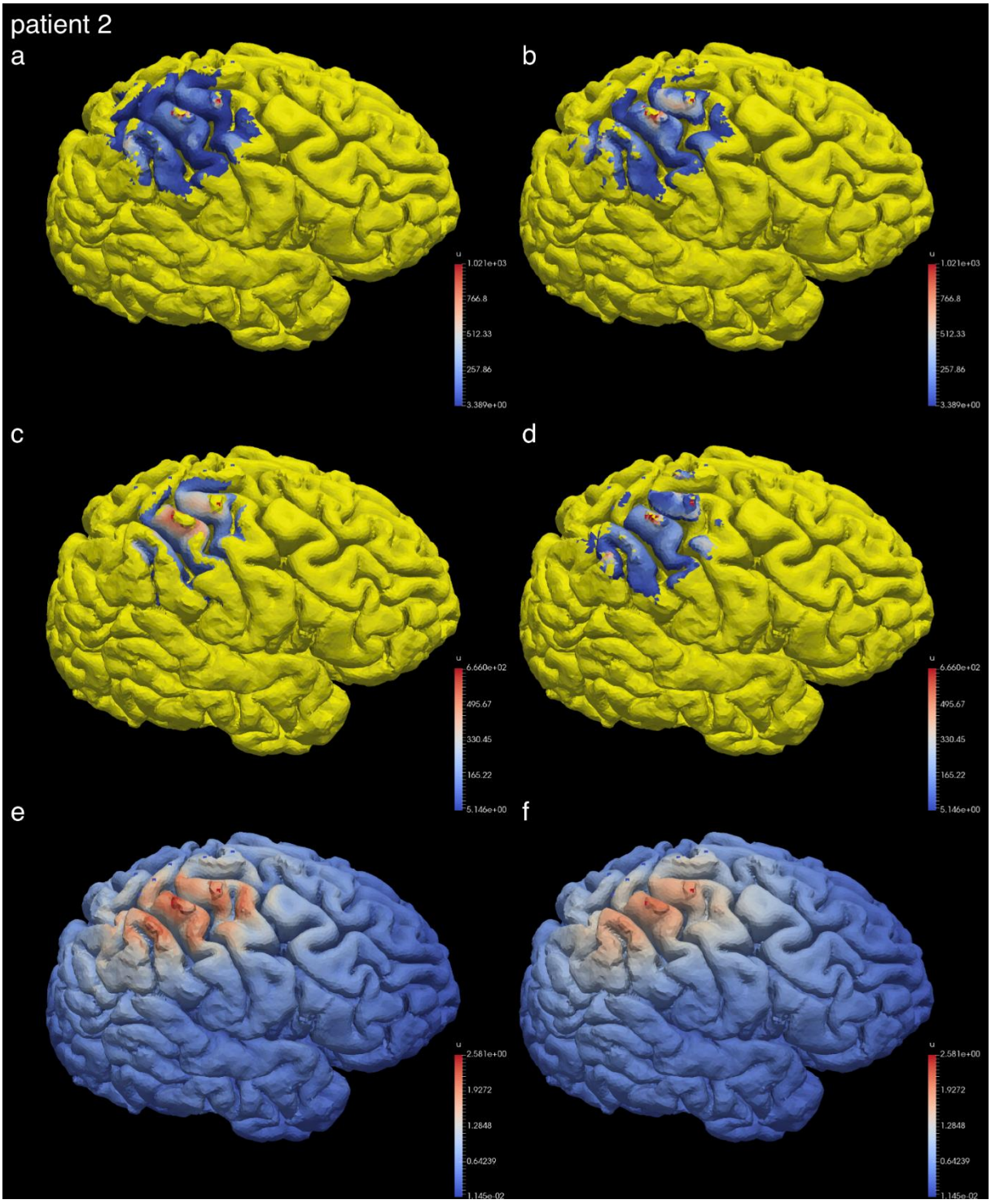
patient 2
a
b
c
d
e
f
u
1.021e+03
766.8
512.33
257.86
3.389e+00
6.660e+02
495.67
330.45
165.22
5.146e+00
2.581e+00
1.9272
1.2848
0.64239
1.145e-02

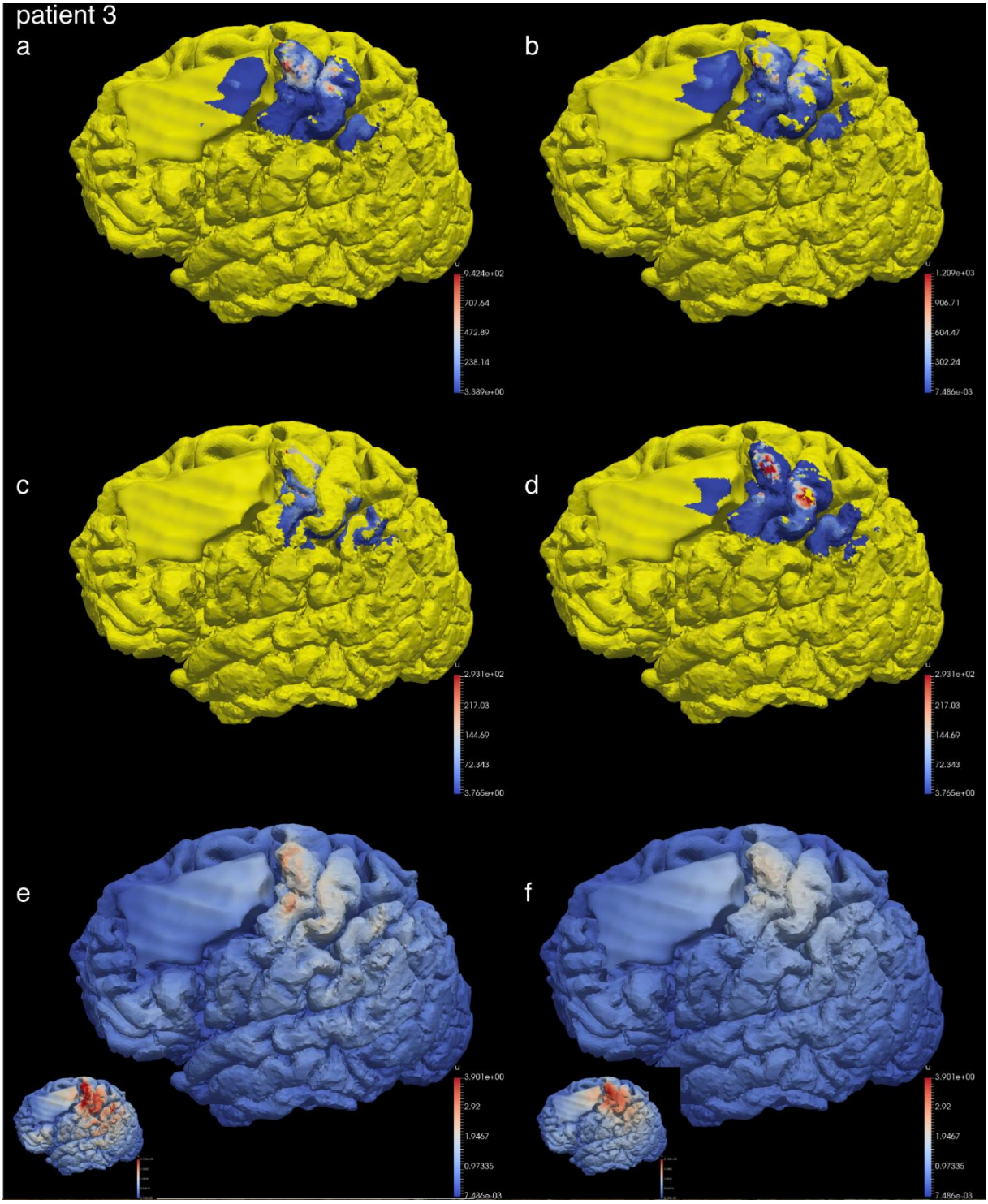
patient 3
a
9.424e+02
707.64
472.89
238.14
3.389e+00
b
1.209e+03
906.71
604.47
302.24
7.486e-03
c
2.931e+02
217.03
144.69
72.343
3.765e+00
d
2.931e+02
217.03
144.69
72.343
3.765e+00
e
3.901e+00
2.92
1.9467
0.97335
7.486e-03
f
3.901e+00
2.92
1.9467
0.97335
7.486e-03

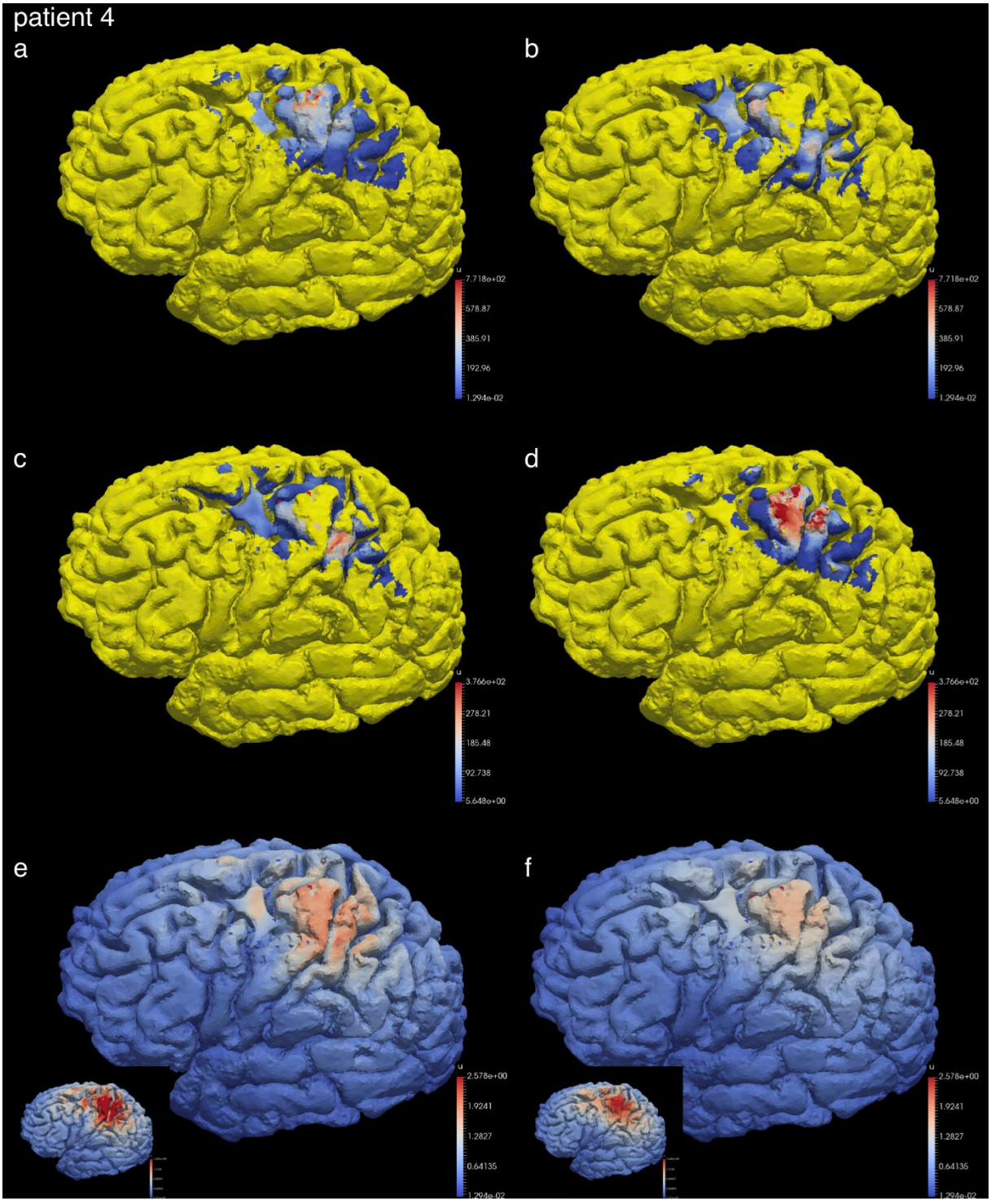
patient 4
a
7.718e+02
578.87
385.91
192.96
1.294e-02
b
7.718e+02
578.87
385.91
192.96
1.294e-02
c
3.766e+02
278.21
185.48
92.738
5.648e+00
d
3.766e+02
278.21
185.48
92.738
5.648e+00
e
2.578e+00
1.9241
1.2827
0.64135
1.294e-02
f
2.578e+00
1.9241
1.2827
0.64135
1.294e-02

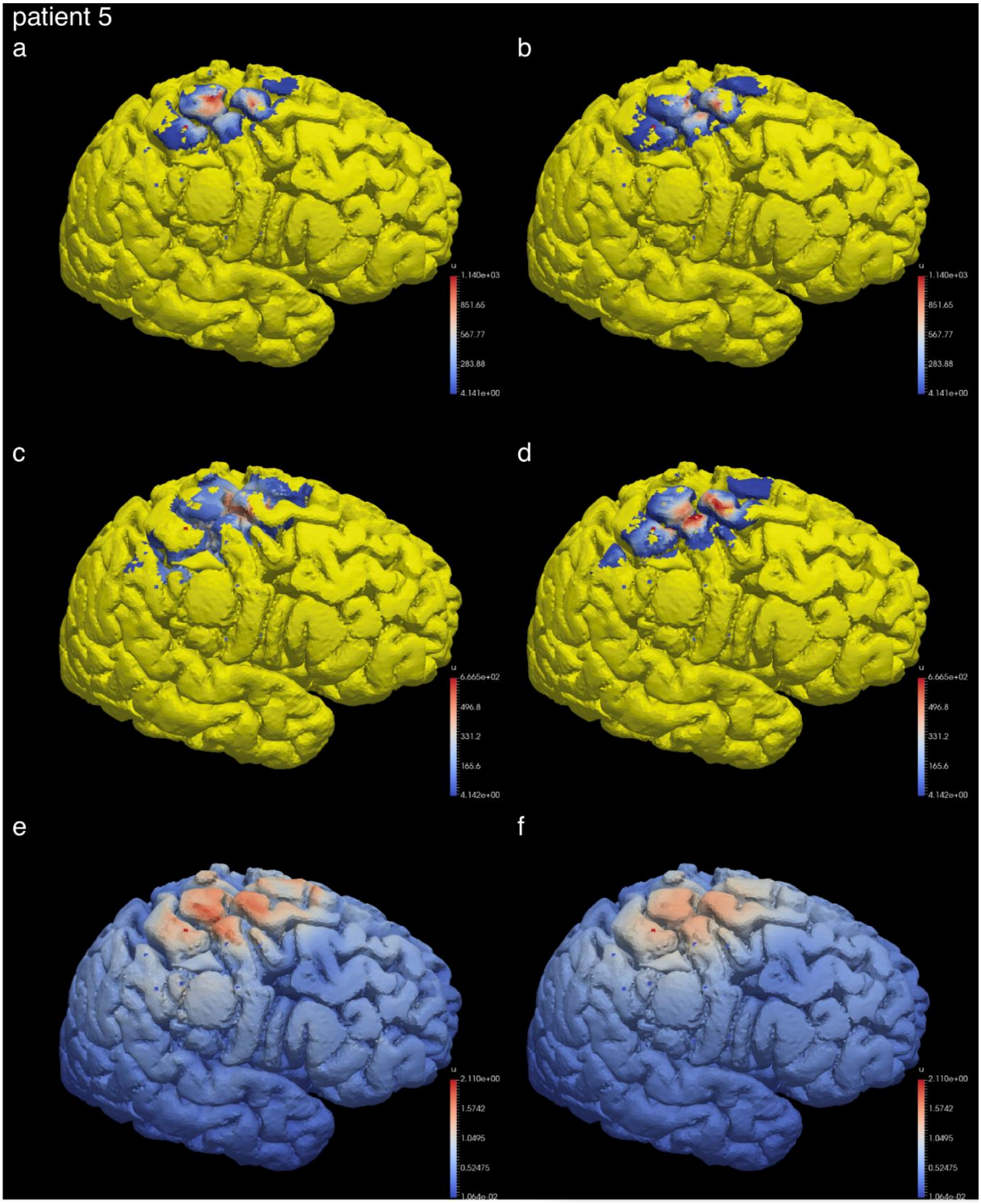
patient 5
a
1.140e+03
851.65
567.77
283.88
4.141e+00
b
1.140e+03
851.65
567.77
283.88
4.141e+00
c
6.665e+02
496.8
331.2
165.6
4.142e+00
d
6.665e+02
496.8
331.2
165.6
4.142e+00
e
2.110e+00
1.5742
1.0495
0.52475
f
2.110e+00
1.5742
1.0495
0.52475

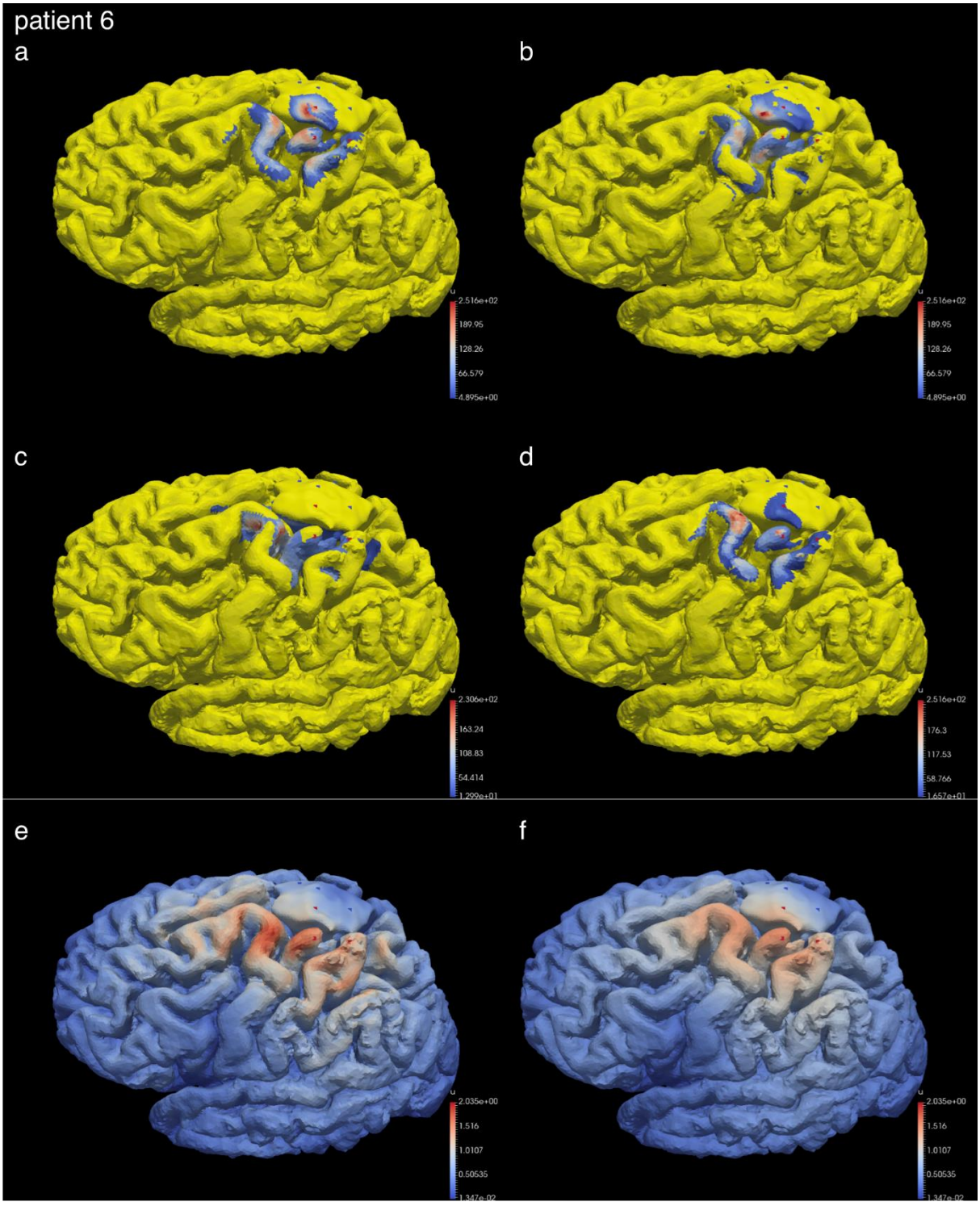
patient 6
a
2.516e+02
189.95
128.26
66.579
4.895e+00
b
2.516e+02
189.95
128.26
66.579
4.895e+00
c
2.306e+02
163.24
108.83
54.414
1.299e+01
d
2.516e+02
176.3
117.53
58.766
1.657e+01
e
2.035e+00
1.516
1.0107
0.50535
1.347e-02
f
2.035e+00
1.516
1.0107
0.50535
1.347e-02

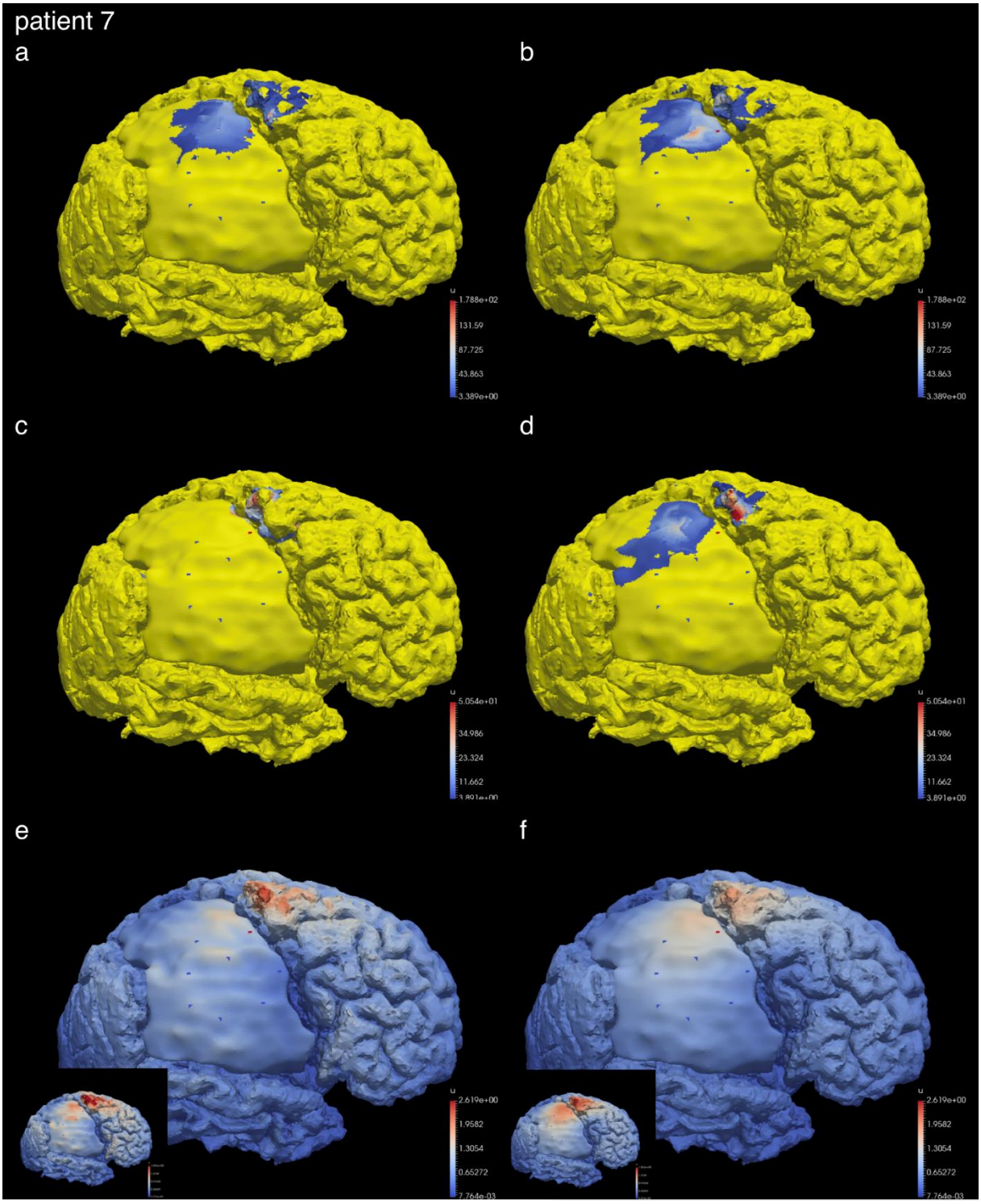
patient 7
a
1.788e+02
131.59
87.725
43.863
3.389e+00
b
1.788e+02
131.59
87.725
43.863
3.389e+00
c
5.054e+01
34.986
23.324
11.662
d
5.054e+01
34.986
23.324
11.662
3.891e+00
e
2.619e+00
1.9582
1.3054
0.65272
f
2.619e+00
1.9582
1.3054
0.65272

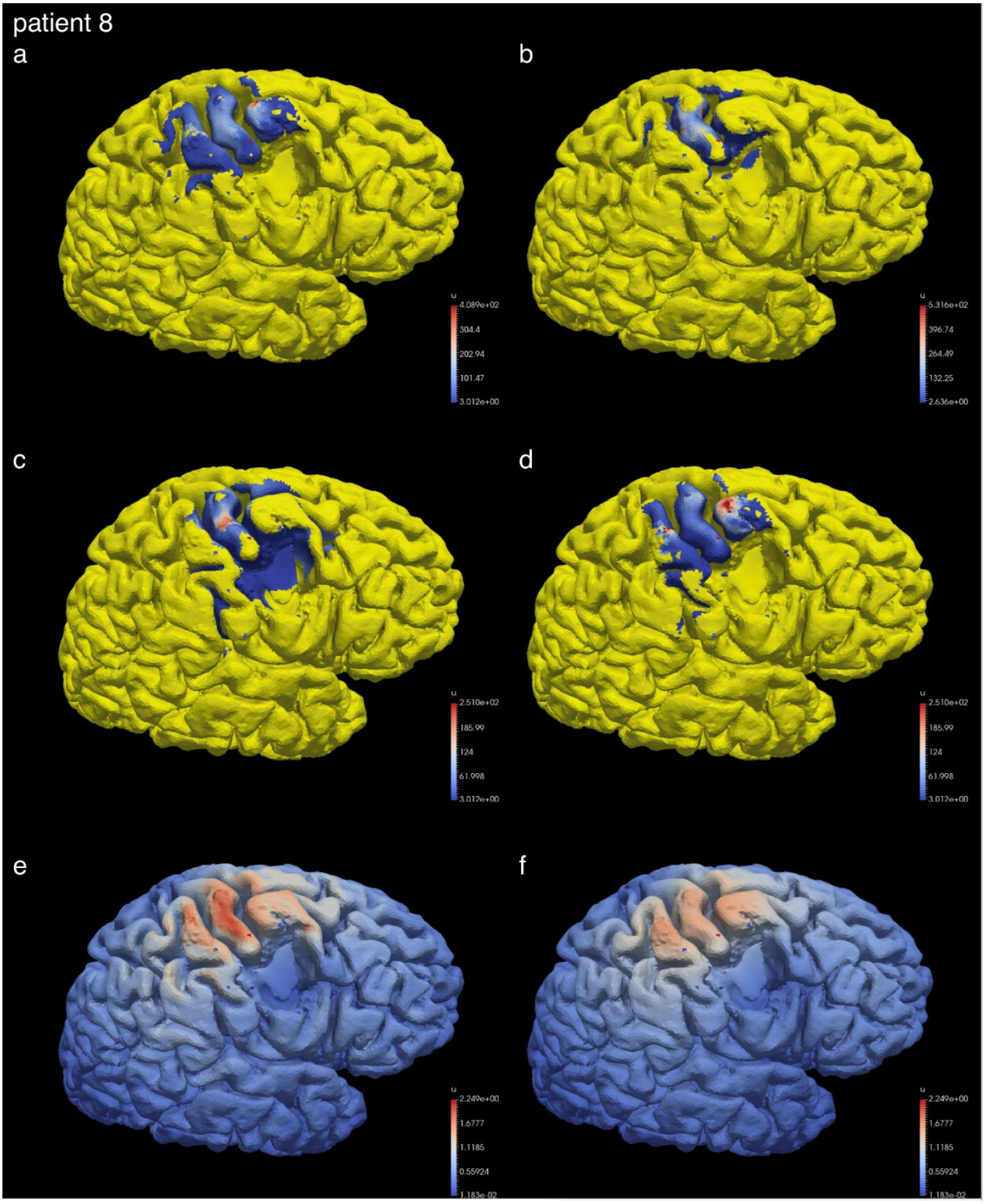
patient 8
a
4.089e+02
304.4
202.94
101.47
3.012e+00
b
5.316e+02
396.74
264.49
132.25
2.636e+00
c
2.510e+02
185.99
124
61.998
3.012e+00
d
2.510e+02
185.99
124
61.998
3.012e+00
e
2.249e+00
1.6777
1.1185
0.55924
1.183e-02
f
2.249e+00
1.6777
1.1185
0.55924
1.183e-02

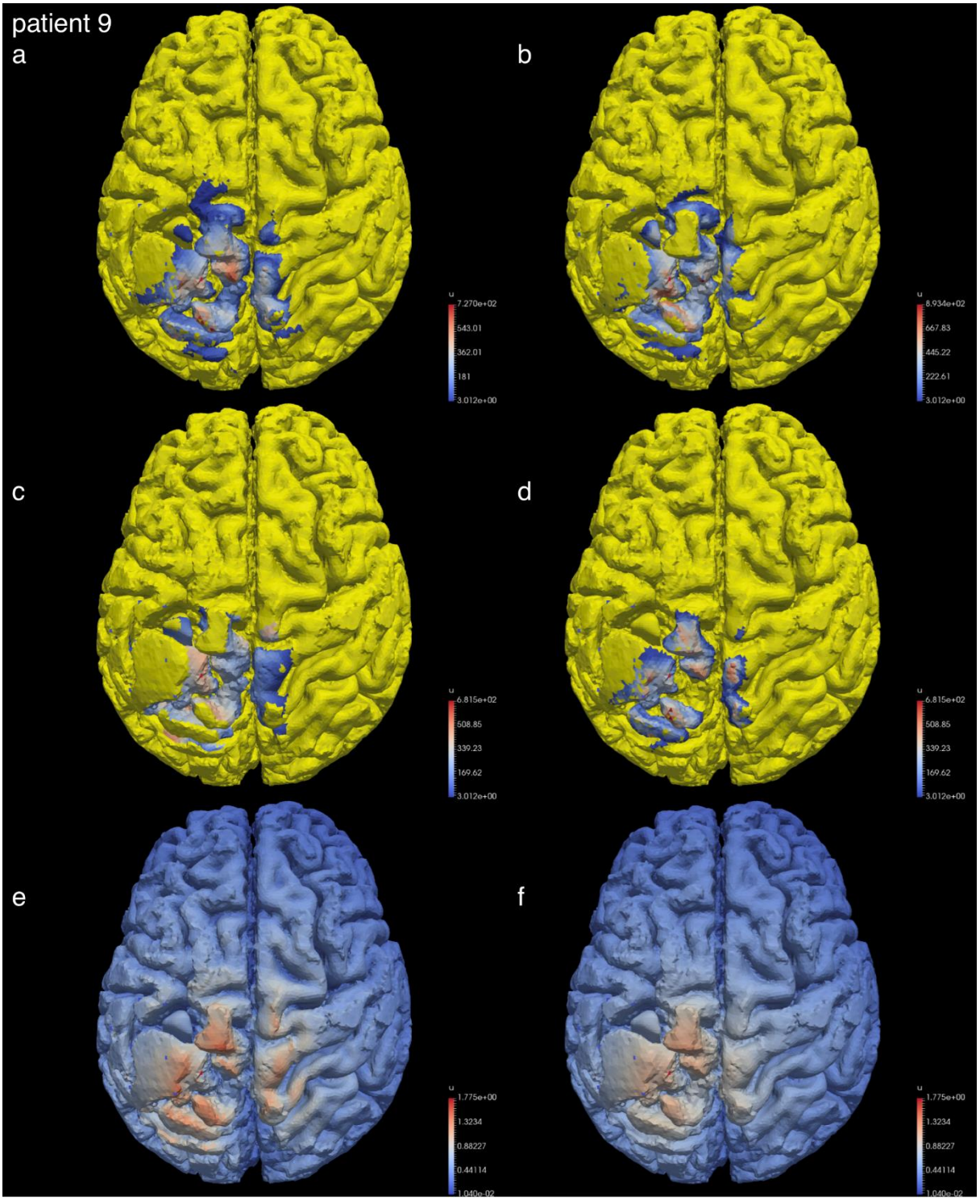
patient 9
a
b
c
d
e
f
7.270e+02
543.01
362.01
181
3.012e+00
8.934e+02
667.83
445.22
222.61
3.012e+00
6.815e+02
508.85
339.23
169.62
3.012e+00
6.815e+02
508.85
339.23
169.62
3.012e+00
1.775e+00
1.3234
0.88227
0.44114
1.040e-02
1.775e+00
1.3234
0.88227
0.44114
1.040e-02

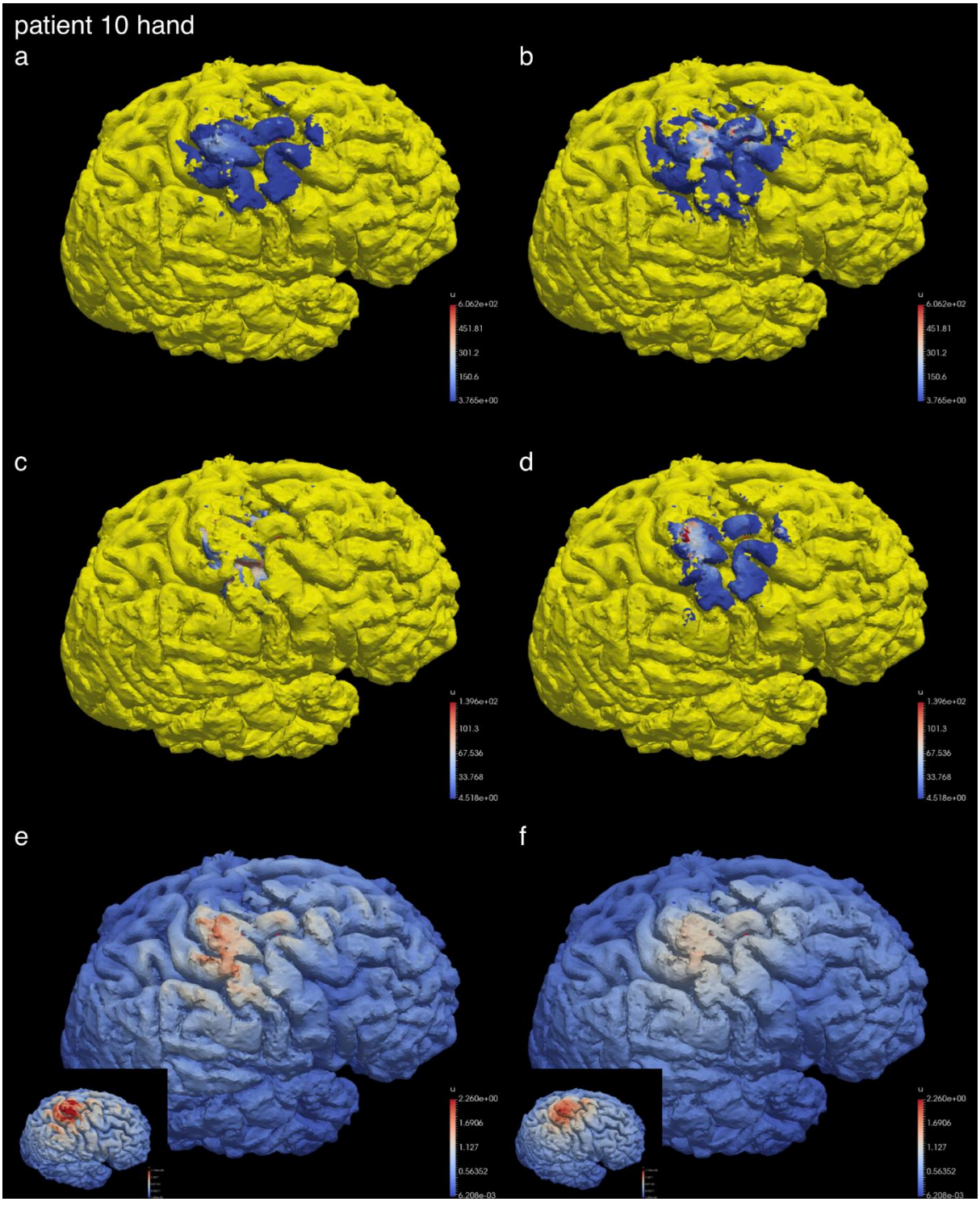
patient 10 hand
a
b
c
d
e
f
6.062e+02
451.81
301.2
150.6
3.765e+00
1.396e+02
101.3
67.536
33.768
4.518e+00
2.260e+00
1.6906
1.127
0.56352
6.208e-03

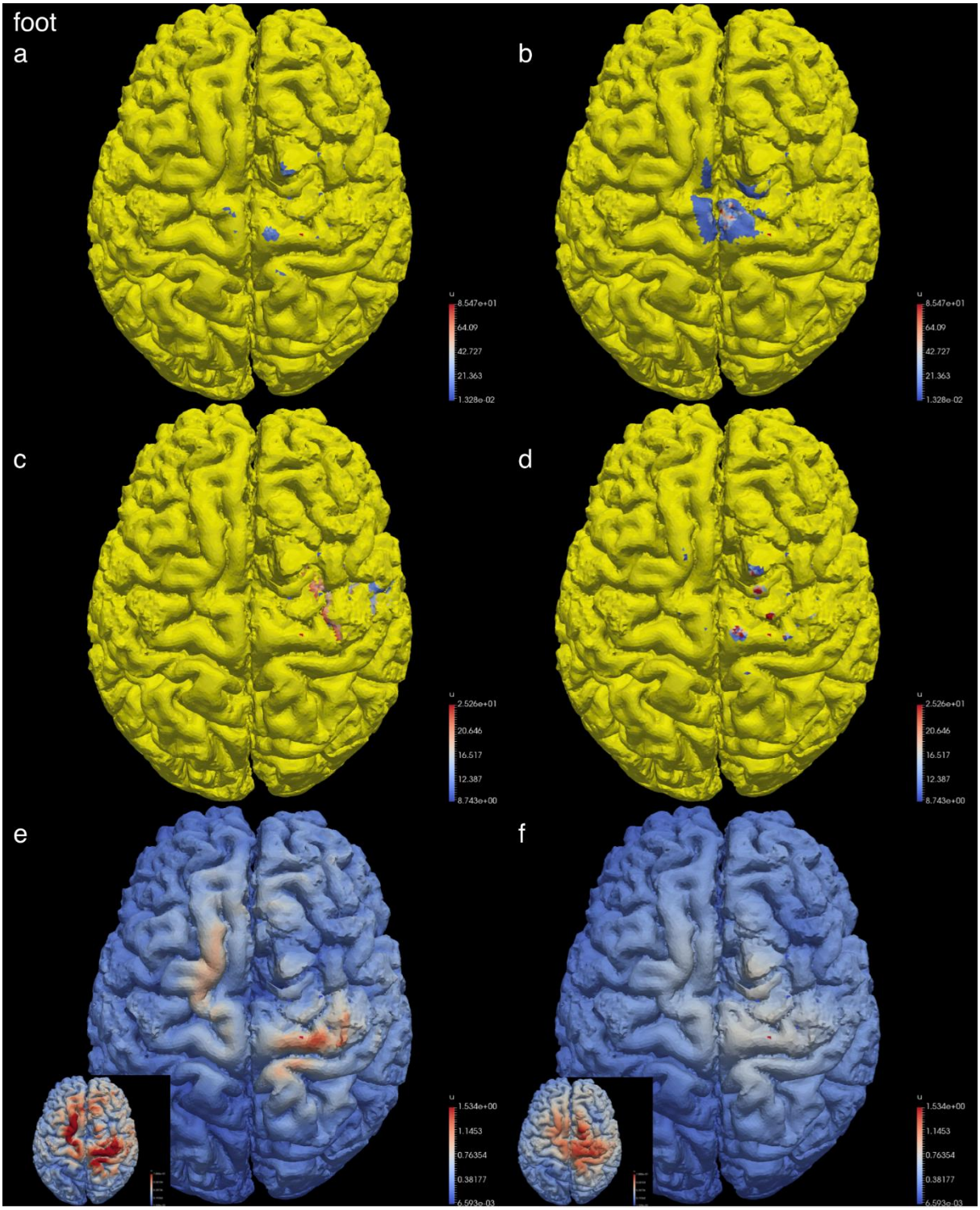
foot
a
b
c
d
e
f
8.547e+01
64.09
42.727
21.363
1.328e-02
2.526e+01
20.646
16.517
12.387
8.743e+00
1.534e+00
1.1453
0.76354
0.38177
6.593e-03

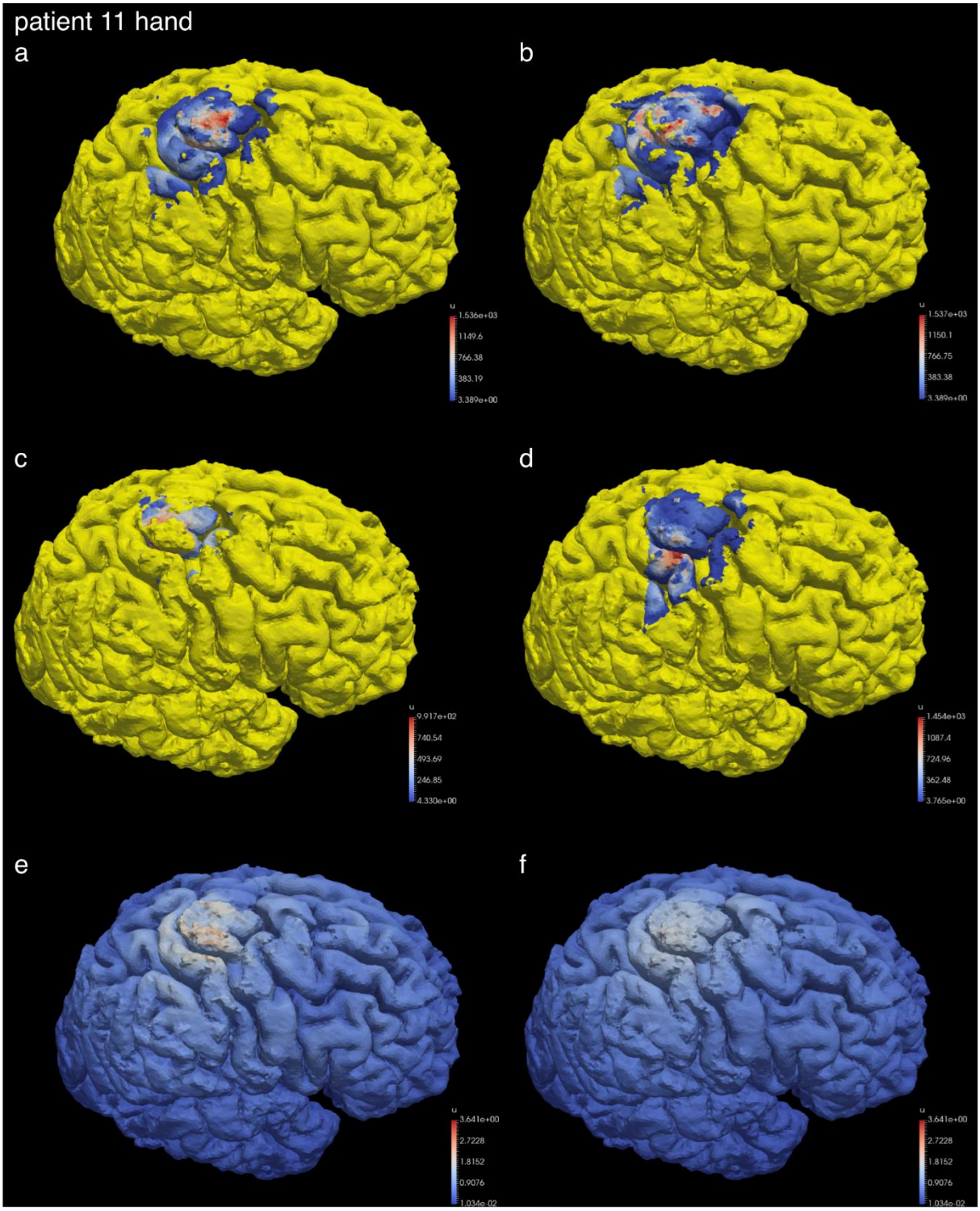
patient 11 hand
a
1.536e+03
1149.6
766.38
383.19
3.389e+00
b
1.537e+03
1150.1
766.75
383.38
3.389e+00
c
9.917e+02
740.54
493.69
246.85
4.330e+00
d
1.454e+03
1087.4
724.96
362.48
3.765e+00
e
3.641e+00
2.7228
1.8152
0.9076
1.034e-02
f
3.641e+00
2.7228
1.8152
0.9076
1.034e-02

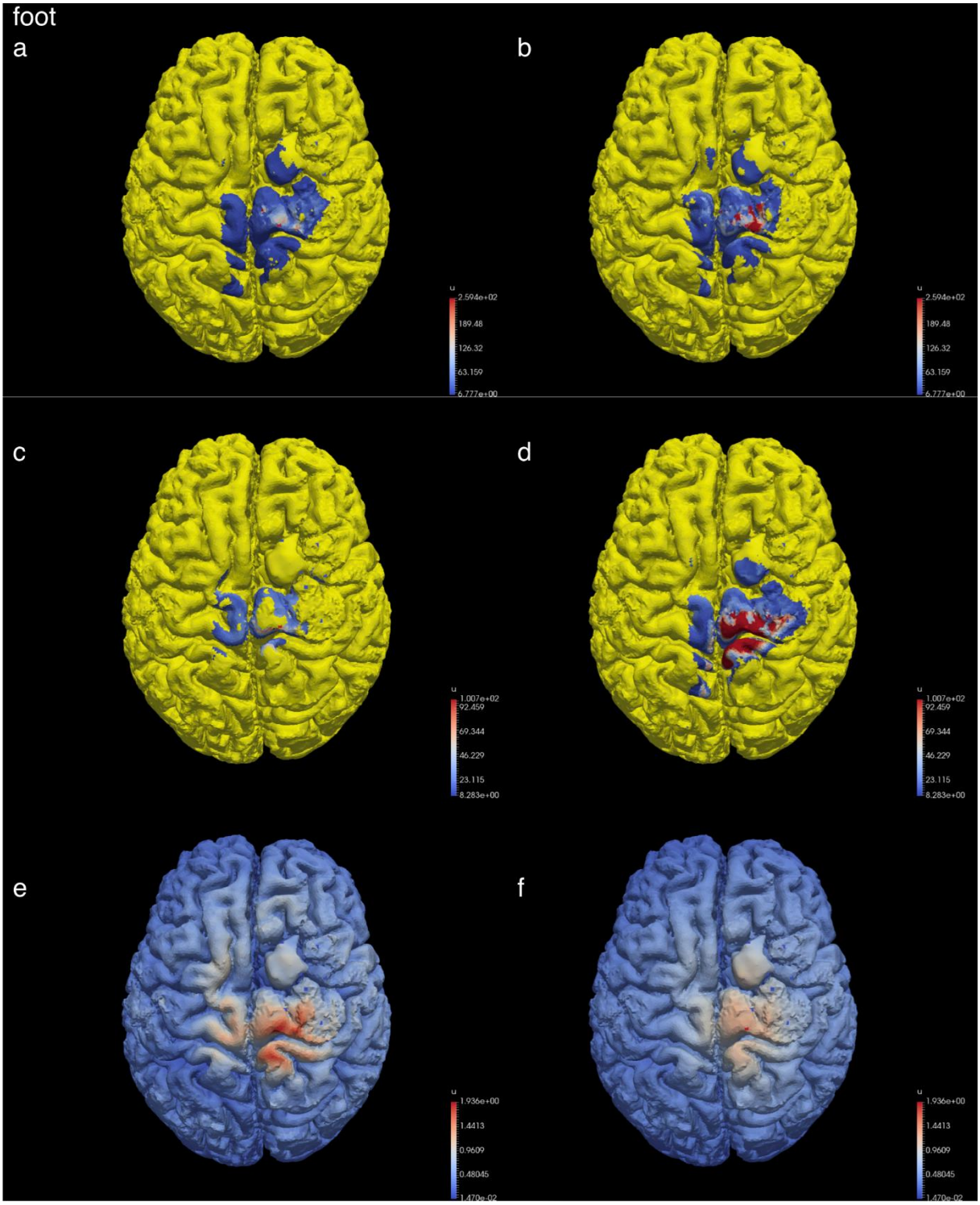
foot
a
b
c
d
e
f
u
2.594e+02
189.48
126.32
63.159
6.777e+00
u
1.007e+02
92.459
69.344
46.229
23.115
8.283e+00
u
1.936e+00
1.4413
0.9609
0.48045
1.470e-02

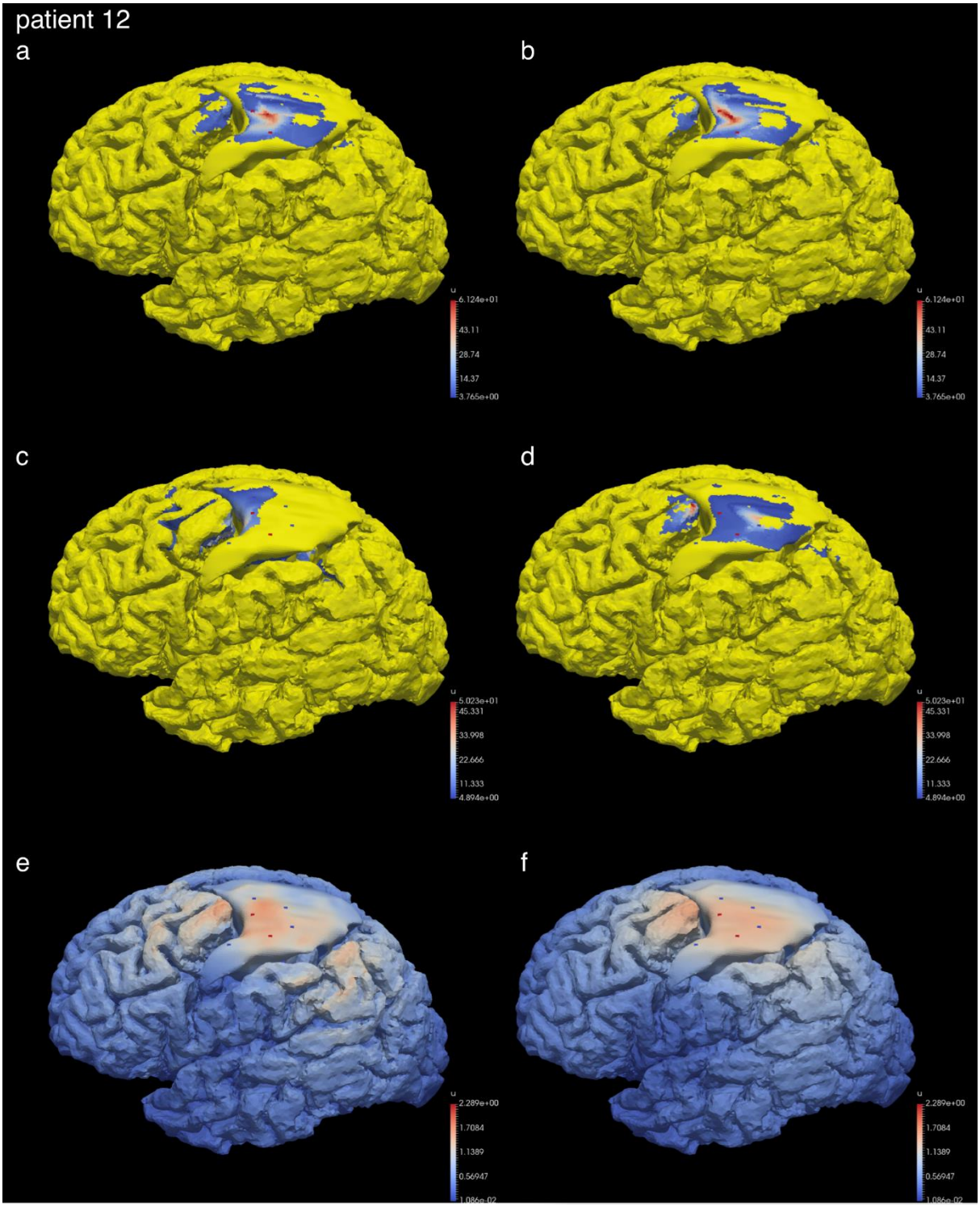
patient 12
a
6.124e+01
43.11
28.74
14.37
3.765e+00
b
6.124e+01
43.11
28.74
14.37
3.765e+00
c
5.023e+01
45.331
33.998
22.666
11.333
4.894e+00
d
5.023e+01
45.331
33.998
22.666
11.333
4.894e+00
e
2.289e+00
1.7084
1.1389
0.56947
f
2.289e+00
1.7084
1.1389
0.56947

6 Automated speech analysis to improve TMS-based language mapping: algorithm and proof of concept

As described in the previous chapter, mapping of the motor cortex with TMS is based on quantitative data, namely MEP amplitudes. No such measure existed for language based mapping. In this chapter a new automated speech algorithm is described. These analyzes would not have been possible without the in-depth knowledge of computer speech analysis of ESAT-PSI group.
This chapter has been submitted for publication:
Automated speech analysis to improve TMS-based language mapping: algorithm and proof of concept.

Laura Seynaeve, Deepak Baby, Hugo Van hamme, Steven De Vleeschouwer, Patrick Dupont, Wim Van Paesschen

6.1 Summary

Introduction:
TMS-induced disturbances in confrontational naming tasks are useful to delineate anterior language areas. This technique is labor-intensive and still considered largely experimental. Our aim was to develop a new and faster algorithm for language mapping using TMS.

Materials and methods:
Experiments were based on online TMS-mapping during a confrontational naming task. We developed a speech analysis algorithm that was able to cope with TMS noise, and displayed the subject's answers and reaction time (RT) automatically. The speech analysis algorithm was developed with front-end speech enhancement to suppress the TMS noise, while retaining speech sounds. We tested the algorithm in 8 healthy controls and three patients with tumors nearby language cortex prior to awake surgery. In these patients, TMS-RT-based probability maps of the language cortex were created and compared to intra-operative DCS.

Results:
The speech analysis algorithm performed with high accuracy (90%) and specificity (96%) on the data derived in healthy volunteers and with a lower accuracy (61%) in patients. A TMS-RT-based probability map of the language cortex in the three patients was consistent with anatomical knowledge, DCS data and was able to predict postsurgical transient language decline in one patient with negative DCS-mapping.

Conclusion:
Automated speech analysis during online TMS mapping is possible in the delineation of language cortex in clinical practice. TMS-induced increases in RT of correct responses during a confrontational naming task may be an important biomarker of language cortex.

6.2 Introduction

TMS is a non-invasive technique able to probe the cortical function, including language function both in healthy volunteers[149] and prior to neurosurgical procedures[142]. Confrontational naming tasks have been shown to be the best test to probe the anterior language areas with TMS [70,142]. Even though the clinical feasibility of using TMS in patients to probe the language network was first demonstrated in 1991 [150], its use in preoperative mapping is still considered experimental [142]. This is in contrast to motor cortex mapping that is routinely used in a wide variety of clinical settings and is used

extensively in research. The protocol used for motor cortex mapping is standardized and international consensus guidelines [29,151] are widely adopted. In language mapping, on the other hand, different strategies are being used. Variability is not only seen between research groups focusing on different aspects of language processing in healthy volunteers [152,153] but even centers performing preoperative language mapping, using the same hardware and software setup, have been using different stimulation protocols [142]. The difficulty in standardizing language protocols is largely due to the inherent complexity of language in all its aspects. Where motor functioning is often reduced to an easily measured motor evoked potential amplitude value, no such single, easily measured value is available for language mapping.
The current state-of-the-art analysis of language TMS data in patients involves evaluation by one or two skilled speech and language therapists who need to go over the entire video and audio files (usually > 1 hour of data per subject), which is time-consuming. In addition, reaction times (RTs) - which have been shown to give relevant information on language function in healthy volunteers [149,152]- are often not measured, due to its labor-intensive nature. When RT are measured, determination of speech onset is difficult to discern in TMS noise, which increases inter- and intra-rater variability, reducing the repeatability, reliability and its widespread use.
In this study, we have developed an automatic evaluation routine for a picture-naming task with TMS using machine speech recognition. The algorithm does not require video recordings, was developed to cope with TMS noise and gives both a transcript of words spoken and timing parameters, thus making at the same time qualitative assessment [154] and RT measurement possible. Our algorithm is also cheaper, requires far less storage and is advantageous in scenarios where the subject is not comfortable with a video recording, compared with the current state-of-the-art.
We tested the automated evaluation routine on partly simulated data from healthy volunteers and- as proof of principle- on brain tumor patients prior to intra-operative DCS mapping. We believe that automatic evaluation routines are indispensable to allow for further dissemination and standardization of TMS-based language mapping.

6.3 Material and methods

6.3.1 Data-collection

Healthy controls (Dutch-speaking, 3 males and 5 females) were asked to name black-and-white line drawings based on the Snodgrass and Vanderwart picture set (object naming task) [76]. The data were recorded in the same environment as the actual TMS setup, but without applying stimulation. 140 pictures were selected and presented in a randomized order, in four blocks of 35 pictures. Two runs to familiarize the subjects with the pictures and the setup were provided prior to recording. The stimuli were presented for 3 seconds and the corresponding responses were simultaneously recorded using Presentation version 14.8 (Neurobehavioral Systems, USA). The audio-recordings taken from the eight healthy subjects are denoted as S1 to S8 and the combination of all the recordings are denoted as S1-S8. The dataset thus generated contained 1120 recordings (140 images x 8 subjects).

Separately, multiple realistic recordings of rTMS noise were recorded, using a figure-8 coil (Magstim, United Kingdom), delivering 5 consecutive pulses of 5Hz over several positions of the head to simulate an actual mapping session- no naming was performed during this recording.

In a separate set of experiments, patients with brain tumors who were to undergo awake surgery for intra-operative language mapping, were asked to participate in a TMS-based mapping study, prior to surgery. The TMS protocol used was in accordance with published data [142] (schematic of experimental design Figure 6.1A). Patients were seated in front of a computer screen and using neuronavigation, the head was registered to the anatomical brain MRI. TMS-stimulation used a 5Hz-stimulation during 1s, at an intensity set at 120% of rMT. Stimulation onset was simultaneous with each new picture presentation. The picture-data set was the same as for the object naming task

described above. The whole picture-dataset was already provided in print before the recording, to allow for familiarization; a test run without rTMS was recorded first, followed by a run with rTMS. Three male patients were included (patient 1: 31 years old, grade II astrocytoma in left frontal lobe, on levetiracetam 2000mg/d; patient 2: 30 years old, grade II oligodendroglioma in left frontal lobe, on valproate 1750mg/d, levetiracetam 1500mg/d, carbamazepine 600mg/d; patient 3: 21 years old, grade III astrocytoma in left parietal lobe, on levetiracetam 1500mg/d). Stimulation targets were recorded with the system used for neuronavigation (Brainsight, Rogue Research, Canada) for offline analysis. The study was approved by the local Ethics Committee of the University Hospitals Leuven. All patients gave written informed consent.

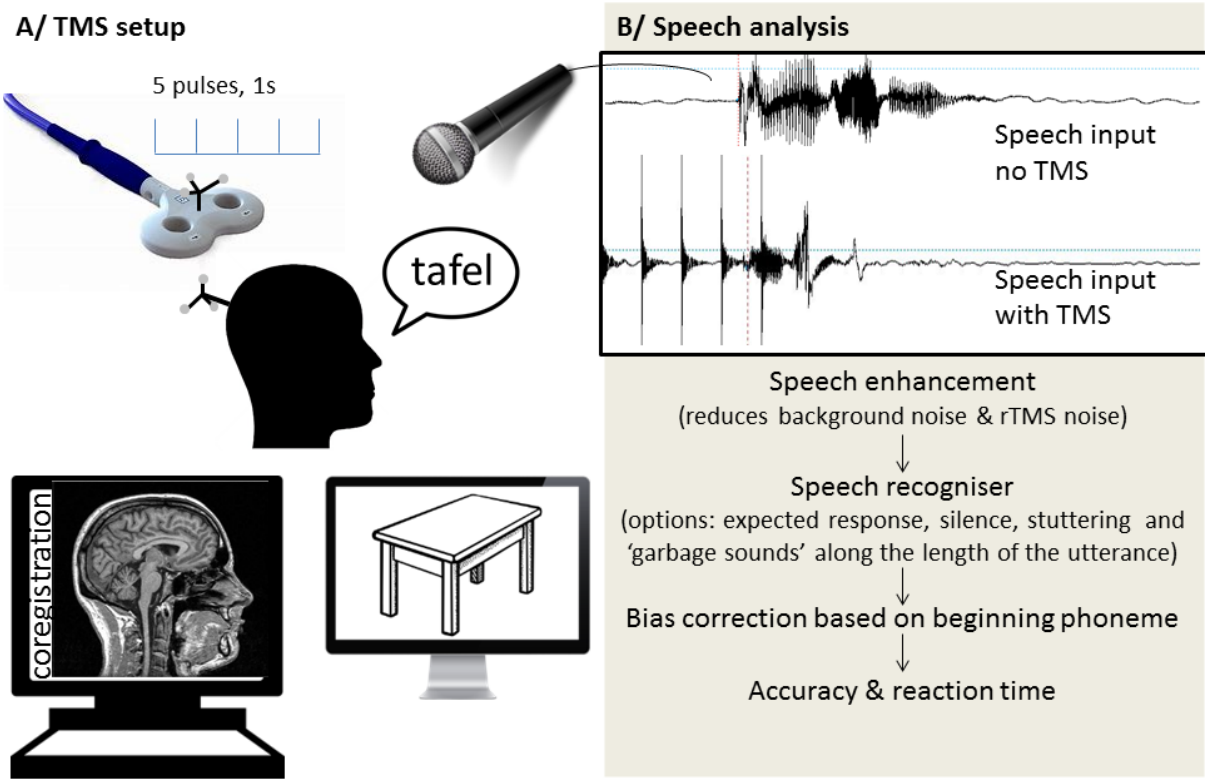

Figure 6.1 Setup of the experiment
A/ setup of typical TMS experiment: speech output is recorder during an object naming task while the patient is seated in front of a screen. Neuronavigation is used to reference the head of the patient to his anatomical MRI. rTMS (5 Hz, 5 pulses) is applied at the onset of presentation of an object.
B/ schematic of the speech recognition algorithm.

6.3.2 Creation of dataset

The RT of the naming in healthy volunteers were manually annotated by a speech technology expert together with a neurologist using Praat software [155], based on spectrograms, pitch contours and voice activity. This dataset was denoted as *rTMS-Noise-free*. Data for speech recognition containing rTMS noise were synthetically created from the recordings of the healthy volunteers and the rTMS-noises, with an rTMS noise at the onset (this corresponds to the presentation of a picture) and some (random) delay of the recording, including thus the speech onset. A delay for a random time period between 50 and 300 ms was added in order to have frequently an overlap between speech onset and the rTMS noise- the most challenging and clinically relevant scenario. For each recording, an rTMS-noise recording was chosen at random. This procedure generated 1120 noisy delayed recordings that

is denoted as *rTMS-Noise + Delay* set. In addition a test set where no delay was present was also created artificially. This set was created by adding rTMS noise to the beginning of the noise-free recordings and this set is denoted as *rTMS-Noisy* set. Since the sets were partly simulated, the accuracy of the RT measurements by the automatic routine could thus be reliably judged. These three sets (*rTMS-Noise-free* set, *rTMS-Noise+delay* set, *rTMS-Noisy* set) were used to test and tune the algorithm.

6.3.3 Creation of automated speech recognition algorithm

The aim of the algorithm was to recognize the spoken word as correct or incorrect and to give the corresponding RT for correct responses, both with and without rTMS noise (schematic representation in Figure 6.1B). Since the correct answer was known, the algorithm could make use of the expected response to model the word in the recording. For this, the speech recognizer contrasted the data likelihood for the model of the expected response, including synonyms, with the data likelihood for a generic model of words. An internal penalty parameter avoided the generic model from winning inappropriately. A response was marked as a correct response if the recognizer output matched the expected picture name or one of its synonyms. RT could be given with resolution of up to 10 ms [156]. The statistical speech model required for the speech recognizer was trained using the Flemish recordings contained in the CGN corpus [157]. A speech enhancement front-end that suppressed background noises such as fans or competing speech as well as rTMS noise was used [158]. This method was shown to significantly improve the performance of speech recognition algorithms when operated with noisy input, especially if noise snippets are available [159], as is the case with rTMS noise in this setup. The speech enhancement method operated on spectro-temporal representations of the input signal. A dictionary of thousands of spectro-temporal exemplars of speech and noise was first constructed. Incoming noisy speech is then decomposed in a weighted sum of these dictionary elements and the noise components are suppressed.

The recognizer yielded the timing information of the various outputs: expected response, silence (no response), stuttering (repeating parts of the stimulus name before uttering the complete name) and 'garbage' (mumbling and incomprehensible speech from the target speaker; phone sequences due to background speech or noises) along the length of the utterance. The recognizer alignments (from which the RTs are derived) contained some bias depending on the beginning sound (phoneme) of the response. These biases were not expected to be subject dependent since the recognition engine used was designed for speaker independent speech recognition. In this work, these biases were compensated by the post-processing stage to yield RT as close as possible to the manually obtained RT. The speech recognizer yielded temporal alignments with differing offsets (or biases) depending on the beginning phoneme of the response. In order to correct for these biases, the test set was divided into 7 subsets based on the starting phoneme: vowels (VOW), voiced stops (VSTP e.g. /b/, /d/), unvoiced stops (USTP e.g. /k/,/p/,/t/), nasals (NAS e.g. /n/,/m/), sibilant fricatives (SIB e.g. /s/,/z/), non-sibilant fricatives (NSIB e.g. /h/,/f/) and liquids (LIQ e.g. /y/,/l/). For bias correction, the difference between the estimated and manually found RT for two subjects was calculated and the average bias for each class of starting phoneme was subtracted from the RT obtained by the automatic speech analyzer. Notice that the biases were computed from the first two subjects only in order to avoid the risk of over-tuning on the test data.

The automated routine was flexible since it was designed to handle scenarios when the subject said a synonym of an expected response. The observer could read the output of the recording (in phonemes) or listen to those recordings that were marked as wrong responses by the automatic routine and if the subject used a synonym, a separate routine was used to add synonyms to the existing setting. In addition, new pictures could be added, since the word models were built by joining phoneme models automatically.

As output, we generated a text file that summarized both accuracy and RT estimates.

6.3.4 Evaluation metrics for the accuracy and RT

In the picture naming task, we considered as true positives (TP) the trials in which a correct response was given and detected as correct, true negatives (TN) as wrong or no response detected when this was the case, false positives (FP) as wrong/no response given but marked as correct by the automatic routine and false negatives (FN) as the correct response marked as wrong by the automatic routine. In this task, we adjusted the weight to recognize the correct response in order to maximize the true negatives correctly. Notice that such a setting reduces the recognition of true positives.

For the RT prediction performance, the difference in RT was computed for the dataset by subtracting the 'gold truth' manual RT times from those obtained by the algorithm (= $RT_{auto} - RT_{man}$, where RT_{auto} is the RT from the automatic routine and RT_{man} the RT as obtained by manual annotation of the data).

In patients, the difference in RT with and without rTMS was computed for the correctly recognized responses as measured with the automated speech recognition algorithm: $RT_{diff} = RT_{rTMS} - RT_{noTMS}$, where RT_{rTMS} is the RT of the picture named while applying rTMS and RT_{noTMS} the RT of the naming of the same picture without rTMS.

6.3.5 Proof of principle: analysis of patient data

The TMS recordings of the patients were analyzed using a conventional method (human observing errors and dividing those into different error categories) and using the new algorithm. In the conventional method the brain was divided in anatomical subregions, as previously described for patients undergoing mapping prior to epilepsy surgery [154] and glioma surgery [70,160–163]. This was done based on anatomical landmarks, which can be a challenging task when distortions caused by the tumor are present [163]. For each anatomical brain region, the fraction was given of trials resulting in naming errors to the total number of naming trial while stimulating over a spot in this brain area. The target of stimulation on the cortical surface was obtained by a simple projection trough the center of the stimulation coil.

Since the automated speech algorithm gave not only accuracy, but also RTs, this parameter was also studied. An average RT for each brain region was calculated for each subject. For this the RT while naming the object without stimulation was subtracted from the RT during TMS mapping (so positive values= slower RT with TMS, negative values= faster RT with TMS). In order to make the difference in RT more comparable, these were transformed into z-scores. In one analysis, the z-scores of the different trials within one anatomical brain region were averaged. In another analysis a color-coded map was created based on the rTMS induced change in RT during object naming in the different location that were sampled. This is comparable to the use of MEP-amplitudes for motor mapping. The amount of slowing of the RT with TMS compared to no-TMS was assigned to each TMS-sample and the numbers used as an input to calculate a map. Since the difference in RT were inherently numerically small, compared to the absolute numerical value of MEP amplitudes, a visualization method that captured the differences was needed. For this, the inbuilt spatial averaging algorithm of the BrainSight software was used. The visualization method involved for each measured TMS-coil position the corresponding RT_{diff} value, which was spread out over a spherical area. In areas of overlap between spheres, the average was taken and the result was a color-coded ‘map’ on the 3D surface of the brain (Figure 6. 2).

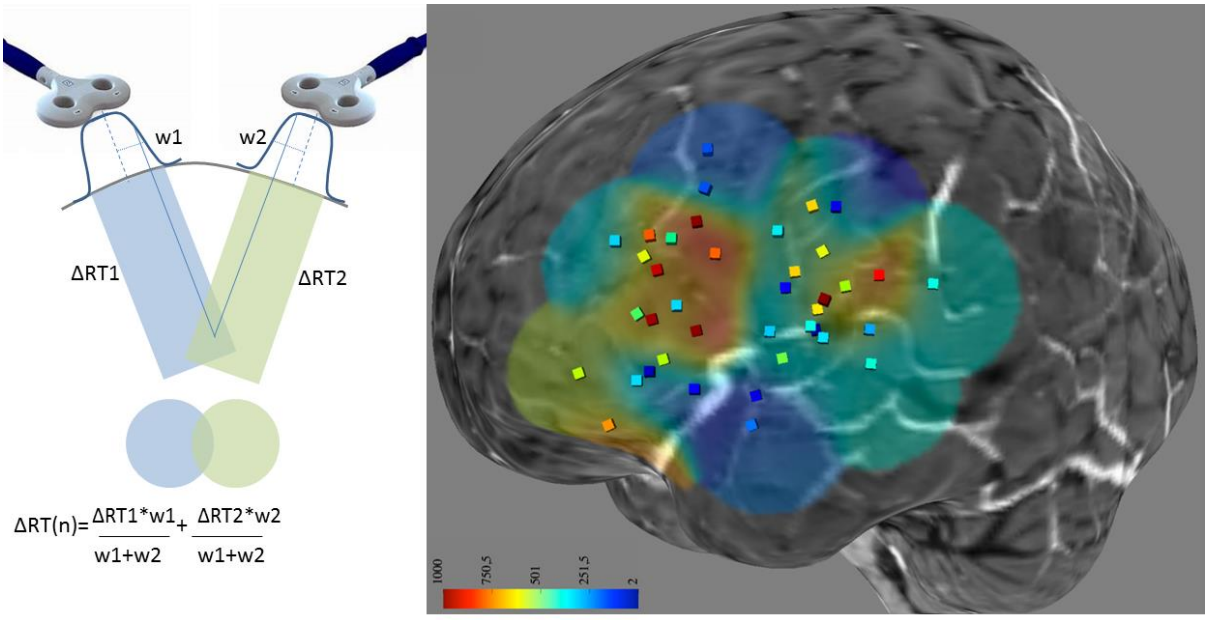

A/ algorithm to create map

B/ language-cortex probability map based on TMS-induced change in RT

Figure 6.2 Creation of the language-cortex probability map based on the TMS-induced change in RT during an object-naming task
A/ Each location was assigned the value of the difference in RT between naming of an object during rTMS stimulation at this location and no rTMS stimulation, for samples which were correctly named, and leading to no change or a slower RT, called ΔRT1 for location 1 and ΔRT2 for location 2. In order to interpolate the differences in RT observed at different locations, the RTs were smoothed out over neighboring location, using a weighting factor w, that was proportional to the distance to the center. A value was smoothed out using a Gaussian smooth, set to 17 mm FWHM which is the standard setting and this setting is based on the properties of the coil. B/ Actual coil positions of rTMS stimulation during object naming with color-coding based on the RTs. In addition, a smoothed map displaying regional differences in object naming RT induced by rTMS is shown, derived from the algorithm described in A with slowing between 2 ms (blue) and 1000 ms (red).

To gauge the relevance of this map, the data were compared to the results of intra-operative awake language mapping, the post-operative imaging and the post-operative language function in the days after surgery and three months later. TMS-based locations were compared with the location of DCS based on 3D cortical reconstructions and the intra-operative photographs.

6.4 Results

6.4.1 Accuracy and RT in healthy controls

The automatic routine yielded an overall accuracy of 90.4% (for the *rTMS-Noisy+Delay* set) with 96% specificity, i.e. correct detection of no-response events in the presence of TMS noise (Table 6.1).

Table 6.1: Performance of the automated speech recognizer: for each subject and each set (rTMS-Noise Free, rTMS Noisy and rTMS Noise+Delay Set) the number of trials correctly and incorrectly (no response/ wrong) named as determined by human rater ("occurring") was compared with the performance of the automated speech recognizer algorithm, both without and with using the speech enhancement algorithm ("SE") developed for this purpose.

Subject	Sex	Condition	correct responses			wrong/ no responses			overall	
			Occurring	detected (TP)		Occurring	detected (TN)		accuracy (%)	
				no SE	SE		no SE	SE	no SE	SE
S1	M	Noise-Free	135	125	126	5	5	5	92.9	93.6
		Noisy		132	132		5	5	97.9	97.9
		Noise+Delay		131	130		5	5	97.1	96.4
S2	F	Noise-Free	124	111	113	16	16	16	90.7	92.1
		Noisy		110	116		16	16	90.0	94.3
		Noise+Delay		111	114		16	16	90.7	92.9
S3	M	Noise-Free	134	109	112	6	4	4	80.7	82.9
		Noisy		114	114		4	4	84.3	84.3
		Noise+Delay		110	115		3	5	80.7	85.7
S4	F	Noise-Free	139	118	119	1	1	1	85.0	85.7
		Noisy		117	119		1	1	84.3	85.7
		Noise+Delay		121	123		1	1	87.1	88.6
S5	F	Noise-Free	133	125	126	7	7	7	94.3	95.0
		Noisy		123	123		7	7	92.9	92.9
		Noise+Delay		120	125		7	7	90.7	94.3
S6	M	Noise-Free	131	124	124	9	9	9	95.0	95.0
		Noisy		119	121		9	9	91.4	92.9
		Noise+Delay		115	120		9	9	88.6	92.1
S7	F	Noise-Free	136	99	106	4	4	4	73.6	78.6
		Noisy		105	105		4	4	77.9	77.9
		Noise+Delay		112	112		4	4	82.9	82.9
S8	F	Noise-Free	137	122	123	3	2	2	88.6	89.3
		Noisy		120	124		2	2	87.1	90.0
		Noise+Delay		122	122		2	2	88.6	88.6
all (S1-S8)		*Noise-Free*	*1069*	*933*	*949*	*51*	*48*	*48*	*87.7*	*89.0*
		Noisy		*940*	*954*		*48*	*48*	*88.3*	*89.6*
		Noise+Delay		*942*	*961*		*47*	*49*	*88.4*	*90.4*

Table 6.2: Percentage of cases where the manual and automated RT measurements are within 40 ms of each other (value of 40 ms chosen for illustrative purposes); depending on the beginning sound: vowels (VOW), voiced stops (VSTP), unvoiced stops (USTP), nasals (NAS), sibilant fricatives (SIB), non-sibilant fricatives (NSIB) and liquids (LIQ).

S1-S8	without speech enhancement						
	VOW	USTP	VSTP	SIB	NSIB	LIQ	NAS
Noise-free	97.7	96.9	96.3	95.2	95.1	98.5	100
Noisy	97.7	85.0	63.6	85.5	78.8	95.8	96.3
Noise+delay	96.9	86.7	68.5	83.1	75.6	95.5	90.3
with speech enhancement							
	VOW	USTP	VSTP	SIB	NSIB	LIQ	NAS
Noise-free	97.7	96.9	93.4	93.4	92.0	95.6	100
Noisy	97.7	91.3	72.0	88.0	80.9	94.3	93.1
Noise+delay	97.6	92.9	76.9	89.2	79.2	94.0	90.3

Trials where the beginning sound was a voiced stop or non-sibilant fricative, resulted in less accurate RT measures (Table 6.2), as were a few other words of the dataset (like “oog” (eye)). These trials were not removed from calculation for generalizability. In no-TMS conditions both RT measures were quite similar- keeping in mind that the resolution was limited to 10ms. With TMS noise the average difference between both measures increased, and a clear improvement using speech enhancement was observed (paired t-test ($p \leq 0.001$)) (Table 6.3).

Table 6.3: The mean (μ) and standard deviation (σ) of the absolute difference in RT (in ms) obtained in the different sets (Noise-free, Noisy, Noise+Delay), either not using ("no SE") or using the speech enhancement algorithm developed ("with SE")

Subject	Condition	No SE		With SE	
		μ	σ	μ	σ
S1	Noise-free	11.0	12.7	10.9	11.8
	Noisy	27.3	88.2	13.9	20.9
	Noise+Delay	30.1	92.2	15.2	24.3
S2	Noise-free	12.5	40.3	9.4	10.8
	Noisy	36.8	110.5	20.8	30.2
	Noise+Delay	26.5	65.7	22.2	44.4
S3	Noise-free	20.7	78.3	13.4	26.4
	Noisy	57.2	156.7	21.3	23.8
	Noise+Delay	44.8	124.2	20.9	32.3

S4	Noise-free	13.5	21.3	16.6	22.7
	Noisy	31.8	66.5	25.1	36.4
	Noise+Delay	30.8	53.4	27.1	44.8
S5	Noise-free	11.0	12.9	10.3	12.7
	Noisy	27.2	62.6	22.7	39.1
	Noise+Delay	27.8	44.1	21.2	30.2
S6	Noise-free	12.0	23.0	13.5	25.1
	Noisy	28.5	54.3	25.1	40.1
	Noise+Delay	32.6	55.7	24.7	42.9
S7	Noise-free	17.3	33.4	21.1	34.7
	Noisy	47.1	167.4	42.3	147.9
	Noise+Delay	37.8	91.2	21.3	32.5
S8	Noise-free	7.9	10.8	13.1	26.1
	Noisy	23.7	32.6	20.1	29.4
	Noise+Delay	34.4	61.4	22.4	38.7
Overall	*Noise-free*	*13.0*	*34.9*	*13.4*	*23.2*
	Noisy	*34.5*	*101.4*	*23.8*	*60.1*
	Noise+Delay	*33.0*	*77.1*	*21.8*	*36.8*

6.4.2 Patient data

The TMS data were analyzed both by a human rater as previously described, as with the new algorithm. Using the automated speech recognition in the 3 patients, an overall accuracy of 71% and 96% specificity was obtained (Table 6.4). Overall the RT with TMS was slightly (mean difference 13ms) longer than without TMS (paired-t test of 165 observations over 3 patients, p=0.0001). The number of TMS-induced errors as determined by a human rater was 4%, 11% and 15% of all trials in the respective patients (Table 6.5). No-response errors, semantic paraphasias and neologisms were observed in anatomical brain regions like the inferior frontal gyrus, known to be involved in language processing; performance errors like speech sound distortions and stuttering were observed over a larger area of the brain (figure 6.3). RT were also used for mapping purposes: the TMS-RT-based maps were created and the resulting maps were consistent with anatomical knowledge, with a region in the posterior operculum and the ventral premotor region being part of the network serving language.

These maps were compared to the data of the intra-operative DCS-findings and to the postoperative outcome (Figure 6.3A). During intra-operative language mapping, an average of 9 points was sampled (range 8-10) with DCS. Patients 1 and 2 had one DCS-point that when stimulated resulted in speech- and language problems and patient 3 had no language-positive points with DCS (Figure 6.3A). The cortical area that was resected was delineated on the post-operative MRI; this area was then plotted onto the preoperative images for comparison (schematically represented in Figure 6.3A).

Comparing DCS with TMS, all DCS-positive points were located in TMS-positive regions of the RT-derived maps. In patient 1 the positive DCS point was located in the zone that showed the largest slowing; in patient 2 the DCS-positive point was in a region that showed TMS-RT-slowing, but the largest slowing was seen more anteriorly and this region was not sampled with DCS. In patient 1 and 2, regions with TMS-RT-slowing were not resected, and no clear postoperative deficits were seen. In patient 3, a resection was performed of a DCS-negative region that did show clear slowing using TMS-RT-based mapping: this patient had a severe post-operative language deficit with perseverations, severe naming, reading and repeating problems and moderate comprehension deficits, that fortunately almost completely normalized by month three.
The TMS-RT-based maps used trials with correct naming as an input. No response trials or incorrectly named object were not used to calculate the RT-based maps, since only correctly named and recognized trials have the RT measured. Only trials with no change in RT or slowing of RT were color coded. In subject 1 the RT-based-map was based on 43 available samples (technical error in saving part of TMS-data), in subject 2 on 68 samples and in subject 3 on 39 samples. It was shown that the TMS-RT-based maps gave added information compared to a mapping based solely on the trials with naming errors (Figure 6.3C).

Table 6.4: accuracy of the automated speech recognizing algorithm, as compared to human rater, for tumor patients

	Patient 1		Patient 2		Patient 3		*overall*		
	no TMS	with TMS	no TMS	with TMS	no TMS	with TMS	*no TMS*	*with TMS*	*total*
sensitivity	0.86	0.43	0.93	0.77	0.63	0.51	*0.81*	*0.57*	*0.69*
specificity	0.90	0.93	1.00	1.00	1.00	0.91	*0.97*	*0.95*	*0.96*
PPV	0.99	0.98	1.00	1.00	1.00	0.97	*1.00*	*0.98*	*0.99*
NPV	0.33	0.17	0.40	0.27	0.06	0.26	*0.26*	*0.23*	*0.25*
accuracy	0.86	0.48	0.94	0.78	0.64	0.58	*0.81*	*0.61*	*0.71*

Table 6.5: Number of trails with errors, as determined by human assessor, on the total trials recorded for each patient. Errors are divided in semantic errors, circumlocution errors, phonological errors, phonologic errors, neologisms and performance errors.

	semantic	circumlocution	phonological	neologism	performance	no response	total trials
patient 1	2	1	0	0	0	2	135
patient 2	2	0	0	1	6	2	103
patient 3	7	0	0	0	9	4	140

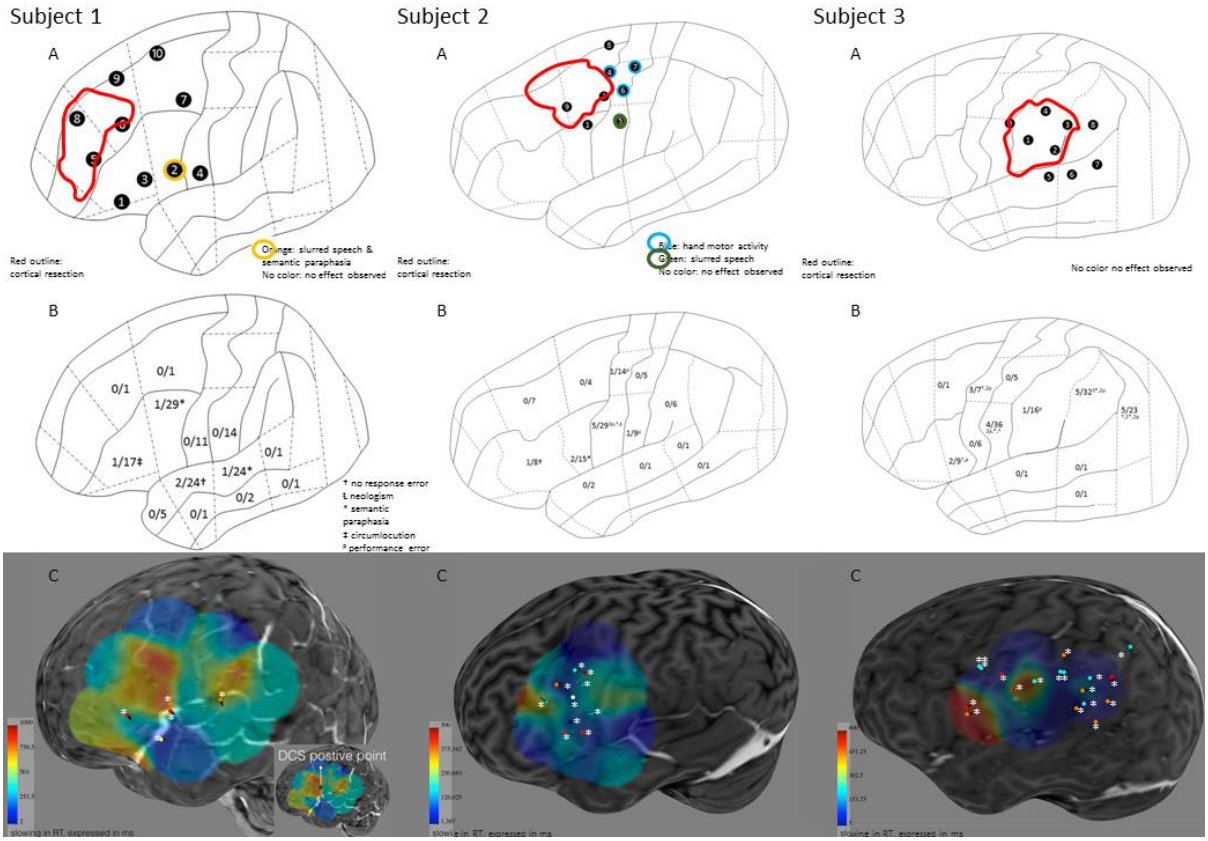

Figure 6.3 TMS-based mapping data of the three subjects, compared to intra-operative findings
A/ schematic representation of the patients' brain, with location of DCS points superimposed as numbered circles and the resection zone (as derived from post-operative MRI) as red outline. DCS points leading to an observable effect are circled, in blue for motor responses, in green for slurring and in orange for sematic paraphasias.
B/ number of trials that were marked as incorrect by a human rater, as a fraction of the total number of trials in different anatomical subregions. No response errors (†), neologisms (Ł), circumlocutions errors (‡), semantic paraphasies (*) and performance errors (p) were observed.
C/ TMS-RT-based color-coded map of the three patients in the study, with actual locations of incorrectly named trials- as determined by a human rater- superimposed as arrows (& marked with an extra white star for clarity): red arrow no response, white arrow neologism, yellow arrow circumlocution, blue arrow performance error and orange arrow semantic paraphasia. The maximal slowing in RT differed between patients and the absolute values of the color code (in ms) are given to the right of the respective images.

6.5 Discussion

TMS is a technique used for non-invasive probing of different cortical functions. The induced electric field interacts with the electrical activity of the neurons and this can lead to measurable behavioral effects. Mapping over the language cortex can induce anomia or speech arrest. Clinically determining the specific anatomical locations serving language functioning is critical for safe neurosurgery. For this purpose, mapping with TMS was performed over the regions of interest during an object naming task. These data were then analyzed by a human rater to detect naming errors. A high number of recorded trials compared to the number of positive trials in mapping studies over the language cortex, was observed in this way. In our study we observed a speech arrest in 8/378 trials (2.1%), compared to e.g. 16/457 trials (3.5%, 12 patients in the study, every trial was repeated 3 times, thus

1371 stimuli in total) in a previous study [70]. Other errors can also be induced, like semantic paraphasias, neologisms, circumlocution errors and performance errors/ hesitations, but also those occur rather infrequently: 28/378 trials (7.8%) in our study. In a previous study, infrequent occurrence was also observed: 5/457 (1.1%) [70]. A higher occurrence of errors was seen in a study that used several intensities and stimulation frequencies, with 3300/15296 trials (21.5%) in 35 patients [164].

The low number of positive trials compared to the total number of trials is especially troublesome since mapping over the lateral frontal and temporal areas is uncomfortable: patients rate it as uncomfortable (30%) to painful (70% of patients) [69] and healthy controls rate the procedure as 6/10 on a pain-scale when mapping over the lateral temporal regions [165]. This discomfort was present despite the lowering of the stimulation intensity if needed (e.g. in 7/12 patients [70]) and the choice to angle the coil to minimize discomfort rather that opting for a coil orientation that maximizes the effect on the underlying brain. Moreover, sites mapped positive do not necessary represent language-eloquent sites, as compared to DCS. In our study, the areas of the parcelated brain that were mapped with both DCS and TMS showed a positive response with TMS and not with DCS in ½ trials in patient 1, 5/8 in patient 2 and 0/10 in patient 3- the overall PPV was thus with 38% comparable to the positive predictive values described in the literature of 34-69% in inferior frontal and temporal regions [70,164,166].

One of the aims of our study was to determine if using RTs would improve TMS-based language mapping, since studies in healthy volunteers have shown that RT changed using TMS over the language cortex, in a location-specific pattern. However, automated methods of detecting RT that are able to cope with TMS noise, are scarce- even though being able to discern RT in an automated fashion would mean an important reduction in work load for studies that want to incorporate RT. One method that has been published, used an accelerometer over the laryngeal muscles. This method was able to handle TMS noise perfectly, since no acoustic data were used. However, all non-speech utterances were also recorded, so overall the specificity was 71% for voice onset and non-responses were correctly identified in 88% of events [167]. Our automatic routine yielded an overall accuracy of 90.4% (for the *rTMS-Noisy+Delay* set) with 100% specificity. Notice that sensitivity and specificity depend on the settings chosen. The automatic routine is flexible so that the observer can vary the parameters if higher detection accuracy on correct responses is required.

Our algorithm however was able to discern both speech onset and speech content, even in the presence of TMS noise. Our algorithm is easy-to-use, requires minimal adaptation of the system (only needs a microphone to record sounds), is fast, accurate and reliable.

RTs were obtained for all trials in which the correct response was recognized by the speech-recognizer algorithm. All TMS trials, where the RT was unchanged or slower compared to naming the same object without TMS, were used to create a TMS-RT-based color coded map. This method takes thus only trials were naming was correct into account- thus the trials that are considered "negative" by a human rater. It was based on the location of the coil at the time of the recording and used a simple spatial averaging over the brain, to create the map. This simple averaging did retain information on individual brain anatomy and the intricacies between the tumor and the surrounding brain- information that was often lost during postprocessing in previous studies that used a parceled anatomical model. To prevent losing this information, the parceled models used in our study for comparison, were based on the individual brain anatomy (these models are however similar enough to previous published analyzes, to allow for comparison [70,160–163]).

It was shown that the TMS-RT-derived maps were in accordance with anatomical knowledge, that all DCS-positive points were located in TMS-positive regions of the TMS-RT-derived maps, and that no postoperative deficits were seen after surgeries where no TMS-RT-derived positive regions were

resected whereas a severe but transient language deficit was seen after resection of a TMS-RT-derived positive but DCS negative region.

Of course, this is based on data of only three subjects and all conclusions need to be corroborated by studies on larger patient numbers. It is however interesting to speculate on the findings that were also seen in previous trials: that more positive regions are found using TMS compared to DCS. Based on TMS-RT-derived data of our patient 3, it might mean that TMS points to regions involved in language processing that are necessary but that some of these can be compensated for by other regions, whereas DCS relates more to long-term (3 months) outcome.

The maps were created with a median of 43 samples. This means mapping can be performed with a much smaller number of trials, shortening the procedure and thus making it better tolerable for the subject. One could envision adapting the algorithms to have it work online and giving real-time feedback on the number of samples recorded and a prediction on the number that is needed. Alternatively, it seems plausible that lower stimulation intensities can be used for mapping when RT is used as parameter of interest and not overt naming difficulties. This is in line with the reduction of the intensity needed over the motor cortex if response is measured using EMG compared to observing for muscle twitches. Lowering the stimulation intensity would also improve the patient-experience of the mapping procedure.

The performance of the algorithm can be improved further by taking a few points into account in the design of future experiments. It would be optimal if words beginning with voiced stop or non-sibilant fricative could be avoided, because the speech onset of such sounds are rather vague since the beginning of these can be elongated. For such cases, even manual annotation was difficult and an objective determination would be more desirable. Care needs to be taken to have a good quality of recording and to minimize unpredictable noises generated by manipulation of the equipment during the mapping procedure. Using a qualitative microphone on a stand with a pop filter and robot-guided navigation of the TMS-coil might prove useful in this regard. If available, the speech recognizer algorithm should use a database in the patient's own dialect. The accuracy of the automated speech recognition routine was lower in patients, compared to the performance in healthy controls, and this was at least partly due to the accent of some of the patients being more different from the standard pronunciations, whereas the healthy volunteers had less pronounced accents. The algorithm performed least well in the patient with the most pronounced accent. The speech enhancement setting is however flexible enough to incorporate knowledge of other noise sources, e.g. the specific sound of a cooled coil.

6.6 Conclusion

This study is the first to describe an automated speech recognizer able to work with data generated during TMS noise. The performance was tested and tuned on data of healthy volunteers: accuracies of 90% and higher were obtained. This study was also to our knowledge the first to study RT as a parameter to create a functional probability map of the brain, similar to using MEPs in the creation of a motor map. The information of the TMS-RT-based mapping was in line with anatomical knowledge, was not redundant compared to just scoring errors, was in line with DCS data and in one patient with a DCS-negative map, did point out a TMS-RT-based positive region that was resected and this patient had a severe post-operative language deficit that was improved at three months.

This study can thus be regarded as a proof of principle that RT measurements add relevant data for language mapping.

7. Concluding discussion

The objective of this project was to clinically validate motor and language functional mapping with TMS with the goal of ultimately replacing invasive DCS with non-invasive alternatives combining TMS, fMRI and MRI-based tractography and to prove that multimodal image-guided repetitive TMS (rTMS) is an effective treatment without side effects for refractory focal epilepsy with an epileptogenic zone in eloquent cortex.
In the experiments on mapping for motor and language functions, we have developed and tested ways to analyze the data, with the ultimate aim to use it as a first-line mapping technique before neurosurgery. In order to better understand how these contributions represent an advance, it is necessary to have a framework to evaluate progress.
Our study on rTMS in refractory focal epilepsy was unfortunately negative so it does not seem to be an effective treatment.

7.1 Evaluation of diagnostic tests

7.1.1 Framework for evaluation

Between the first conception of a new diagnostic technique and its ultimate wide-spread use in clinical practice is a long and winding road. This path of development has been studied and the different steps were laid out. Here we will use the framework of Fryback and Thornbury[168]. This framework was already used to assess diagnostic studies in the presurgical work-up of epilepsy patients[169] and thus this framework seems suited to evaluate also the diagnostic properties of eloquent cortex mapping prior to neurosurgery.
The framework divides the road from conception to implementation into six steps:

1. Technical efficacy: how accurately and precisely it measures what it is meant to measure
2. Diagnostic accuracy efficacy: how well the test predicts the condition (parameters like sensitivity, specificity, accuracy…)
3. Diagnostic thinking efficacy: impact of diagnostic test results on clinician's estimate of the probability that a patient has the condition (parameters like pre- and post-test probability)
4. Therapeutic efficacy: the effect of the test on subsequent treatment/care
5. Patient outcome efficacy: effect on outcome for patient
6. Societal efficacy: impact of the test on society (parameters like cost-benefit analysis)

The sequential steps to prove that a new test is of benefit are logical but do not take into account the many side-conditions that also need to be fulfilled: accessibility, financial hurdles, time constraints…
The fourth step of this framework receives often the most attention, with large-scale trials of drugs and interventions focusing primarily on this outcome parameter. The therapeutic efficacy of a diagnostic test can be trickier to study because of logistic and ethical barriers. Can a randomized trial be performed were part of the participants would not benefit from a new diagnostic test - especially if this new test would be non-invasive? To avoid such problems, diagnostic test studies often rely on retrospectively assessing the added benefit of a subsequent test on prospectively gathered data. This was also the way our studies on TMS-based mapping were designed. Alternatively two groups are compared: either a group that underwent the test compared to historical controls before the test was available or controls that were assessed in another center that does not have access to the new test. Both approaches carry a significant risk of inducing biases that are hard to control for. With historical controls, general improvement in health care outcomes over time is hard to control for and differences in outcome between two centers depend on much more than just having access to a specific test.

An individual patient is most interested to know how he or she is going to benefit from undergoing the test (step 5). The sixth step in the process is the hardest to decipher and depends not only on the merit of the test itself but also on the organization of healthcare. Choices made in these calculations have profound influences on the availability and accessibility of a new diagnostic test for the individual patient.

A diagnostic test's effect on subsequent care, treatment and outcome is very much dependent on the treating physicians' decision to act on the results of the test and his or her skillset. It is also known that abilities of surgeons may differ and that the same surgeon sometimes performs better than at other times, during similar surgeries. It can, therefore, be difficult to draw conclusions on the efficacy of a diagnostic test, if consequent treatments have a lot of variability. To compensate, sufficiently large numbers of subjects need to be included. This entails often a multi-center study and the execution of this type of trial is costly.

For trials of new drugs (e.g. AEDs), these costs are covered by pharmaceutical companies, who will benefit when those new drugs come to the market and/ or are reimbursed. For diagnostic trials this is much harder. In development of diagnostic tests, improvements are often made to an existing technique. In the case of our mapping studies, the input data that were used, can be generated with TMS-devices of different brands. The advances in our studies focused on the post-processing stages, this means on the software and not the hardware. The return-on-investment in software development is a topic that has raised considerable interest in the community, since it has been shown to be much more difficult to have a good return when investing in software, compared to companies devoted to selling pharmaceutical products or devices.
Moreover, even if new and efficacious software (or hardware) is marketed, getting reimbursement for the use of this new diagnostic test, is often very difficult.

Since measuring performance of a diagnostic test on subsequent therapeutic outcome can thus be complicated, more emphasis is placed on the diagnostic performance of a test. The best way to do this is by using ROC analysis[170] as we did in our study on motor cortex mapping.

7.1.2 Where is TMS-based motor mapping situated on the road to widespread clinical use?

In our study, the neurosurgeon was blinded to the TMS results until after the surgery. We were, therefore, not able to gauge the effect of this test on the diagnostic thinking efficacy (step 3) or therapeutic efficacy (step 4). Our study mainly focused on analysis techniques and thus an improvement of the diagnostic accuracy efficiency (step 2). There have been studies on motor mapping in neurosurgical patients, aimed at studying diagnostic thinking efficacy or therapeutic efficacy. These studies focused on the change in treatment plan based on the results of mapping studies or on the chance of obtaining a gross total resection compared to a group of patients that did not undergo mapping with TMS.
In a large monocentric study[171] with 250 patients, the neurosurgeons were asked to device a surgical plan based on clinical data and anatomical MRI. The results of motor TMS mapping were revealed afterwards and the surgeon had to state if the data would change the surgical plan, including access, size of craniotomy, planned extent of resection and whether to go for biopsy or resection. The decision for no surgery or only biopsy was changed in 69% to some form of resective surgery after the results of TMS mapping were revealed. The decision to perform resective surgeries was abandoned in 1% afterwards. Changes with an increase in planned extent of resection were seen in 35% and a decrease in 4%. Patients with open surgeries did undergo asleep DCS of the motor cortex (n=165). Outcome data were compared to 115 historical controls: macroscopic total resections were seen in 59% of the mapped group and 42% of the controls ($p<0.05$). There was no difference in overall survival. In the group that had low-grade gliomas progression-free survival was 22 months,

compared to historical controls that had a progression free survival of 15 months ($p<0.05$). Since this study used historical controls, it seems likely treatment in both groups differed in more than just surgery. Historical controls were more likely to undergo a "watchful waiting" approach in the past, in contrast to more aggressive radio- and chemotherapy schemes used at present in high-risk low grade glioma patients. Compared to historical controls, postoperative deficits increased to 9% (controls 6%; $p>0.05$).
Similarly, another single center trial studied a cohort of 100 patients harboring lesions in the peri-Rolandic area that underwent TMS mapping prior to surgery. This cohort was compared to a matched group of historical controls (n=100)[172]. All 200 studied subjects had asleep motor mapping with DCS performed. Outcome parameters were size of craniotomy, duration of surgery, changes in motor function after surgery-either transient or lasting- and extent of resection. Craniotomies were smaller, there was no difference in operating time, new postoperative paresis was seen in 16% of cases versus 15% in controls, on long term follow-up the motor function degraded more in the control group (75% stable and 13% new long-term paresis compared to 81% and 18% in controls) and the volume of tumor rest on post-operative imaging was smaller compared to controls.
A similar study was done on 70 subjects with high grade gliomas compared to 70 matched historical controls[173]. Again, craniotomy size was smaller and hospital stay was shorter, which might be a consequence of this. New motor deficits after surgery did not differ between groups. The rate of gross total resection was 66% in subjects who underwent mapping compared to 46% in controls. Probably because of more debulking in the intervention group, more patients underwent radiotherapy but also chemotherapy rates were higher - for unknown reasons - in the group that underwent mapping. Consequently, overall survival rates were higher in that group. The different rates of adjuvant treatment however suggests residual bias between both groups, inherent to using historical controls.

A comparison of a group that was treated in the same period with (n=93) and another group without (n=34) having access to TMS-based motor mapping was also published[174]. It was performed by comparing the patients that were evaluated in two campuses of the same hospital. As the authors also state, this should minimize biases since all else was the same, including the surgical team.
All patients underwent asleep motor mapping during surgery. More patients had a macroscopic complete resection in the group that underwent TMS-based mapping (61% versus 45%; $p<0.05$). Similar to other studies, no increase in motor deficits after surgery was seen compared to controls and no significant change in operating time. In the mapped group, the treatment plan was altered in 10%.

Based on the data presented in this thesis and prior studies on the topic, pre-operative mapping of the motor cortex has enough data to support its clinical use, and should be offered to all patients with lesions near or extending into motor areas. Barriers are of logistic and financial nature: solutions need to be devised for this. In all patients offered motor fMRI, TMS-based mapping should also be offered, preferentially to complement the data.
Expanding the use of a diagnostic technique will also spark the interest in the technique and will lead to sequential improvements in its performance.

Based on the data we obtained in our study, comparing different techniques of analysis, we recommend using advanced modelling. In this way, this thesis has contributed to the improvements in performance of this mapping technique.

7.1.3 Where is TMS-based language mapping situated on the road to widespread clinical use?

TMS-based language mapping is less advanced on the developmental path compared to motor mapping and the path has been winding. It is interesting to look at the history of the development in

a bit more detail. This complex history is due to a variety of factors, including the fact that the first clinical developments turned out to be unreliable when studied further. The idea was that TMS could be used to study in what hemisphere language was dominant in patients prior to epilepsy surgery. The idea was similar to the Wada-test as described above. High frequency stimulation trains were used to stimulate both hemispheres while the patient was counting and speech arrest was studied[150,175,176]. Later, lower frequency stimulation trains were used during a similar setup[177,178], but further development was not pursued since the Wada-test could not be replicated using this protocol. However, it was further developed in healthy volunteers and used to study the organization of the language cortex[179]. Devlin and colleagues recognized the importance of using neuronavigation to target the TMS-coil and to measure RTs. RTs were measured in a task requiring button presses and a single TMS-pulse applied over the anterior language area resulted in an 11% slowing in RT. TMS-based studies on language organization in healthy volunteers not only resulted in more detailed information of the organization of the brain[149], but also in improvement of the TMS-paradigms. This resulted in studies on technical efficacy (step 1), focusing e.g. on the number of pulses needed in a stimulation train[180] or the best timing between onset of stimulation and presentation of the image to be named[166].
From these developments and inspired by the advances in TMS-based motor mapping, studies on mapping the language cortex were conceived. One problem to be tackled was how to map the cortex. In healthy volunteers many stimuli over a limited number of targets was applied to obtain robust outcome data. This was not the way mapping the language cortex in a presurgical setup was possible. Inspiration came from a study in epilepsy patients that underwent cortical grid implantation for refractory focal epilepsy. This type of implanted EEG is placed over a region of interest to localize the epileptic focus. At the same time, electric current can be applied over neighboring electrodes of the grid to map the cortex, similarly to what is done with DCS. Due to the spacing of the electrodes on the grid and the brain shift caused by implantation, the spatial detail of the mapping is limited to a minimum of 1cm. In order to understand brain functioning better a parcellated brain model was used to pool the data of several patients. The results of the mapping were divided in different types of linguistic errors[154]. In studies on preoperative motor mapping, data were also analyzed by projecting the results of TMS-based mapping and DCS onto a parcellated brain model, as described in chapter 6 of this thesis[70,160,163,181]. The number of patients included in the trials on language mapping were smaller than those in recent motor cortex mapping (25[160], 12[70], 20[163] and 27[181] patients in the respective studies). These trials were used to calculate diagnostic accuracy efficiency (step 2). One trial also studied the effect on therapeutic efficiency[160] by comparing the outcome to an equal number of controls operated on before mapping became available. Outcome parameters studied were similar to those of the trials with motor cortex mapping: craniotomy size, duration of surgery, residual tumor, hospital stay and postoperative change in language function. Complications and performance score were also studied. All subjects underwent awake surgery with DCS mapping. In the intervention group, 84% had mild or no postoperative language deficits, whereas in the control group the numbers were 52% and 48%. The definition of language deficit, including cut-off on linguistic scores used to categorize patients into the two groups, were not given in the paper. The other outcome parameters showed no significant effect. There was a shorter anteroposterior diameter of the craniotomy but the overall craniotomy volume was not different. Part of the lack of benefit can be due to the much lower number of subjects studied compared to motor mapping studies.

When reviewing the literature on language mapping with TMS, insufficient performance of the test in early clinical trials has slowed the further development. We, therefore, focused on the first steps of the developmental pathway. Moreover, not only the performance but also the tolerability of the test can be problematic. Where motor cortex mapping is generally well tolerated, this is not the case for language mapping (see discussion in chapter 6). Our study on language mapping, therefore, fits largely into step 1 of the framework. We believe our trial was very useful since new ways to analyze

the data were developed. With our improvements, performing a TMS-based mapping study can become less labor-intensive and more detailed, due to our automated speech analysis method. Moreover, we conceived, developed and did preliminary testing of a new way to analyze, interpret and visualize the mapping data. Our method takes the full individual anatomy into account, which is of benefit when large tumors causing disruption of normal anatomy are present. In addition all correctly named items are considered in the mapping and not only the errors that could be induced. This can lead to faster and better tolerable TMS-based language mapping procedures.

7.2 rTMS in epilepsy: where do we come from and how to move on?

In this project, we were unable to prove that rTMS effectively reduced seizure frequency. It was also not completely free of side effects. The rTMS study we have conducted was a randomized sham-controlled crossover trial that included 11 patients with well-defined focal epilepsy. rTMS (0.5 Hz) was targeted to the focus during three treatment conditions consisting of 1,500 stimulations/day for 10 weekdays at 90% of rMT followed by a 10-week observation period. The active treatment condition consisted of stimulation with either a figure-8 or a round coil. Both were tested in a cross-over design, since a different effect on the epileptic focus seemed possible. Both coils were centered with their geometrical midpoint over the focus. The geometrical center of the figure-8 coil is where both wings intersect at the midline and the geometrical center of the round coil is in the center of the hole in the middle of the coil (Figure 2.5). Regarding the round coil, placing the geometric center over the target of stimulation, results in a weak E-field at this stimulation target since no coil windings are positioned directly over this point. The target of stimulation was chosen as to represent the multimodal imaging defined epileptic focus. Inhibition at the center of the coil (and by extension at the underlying epileptic focus) using the round coil might be anticipated because a weak E-field would result in weak current and *in vitro* weak electric currents are preferentially activating neurons with a low firing threshold, such as *gamma*-Aminobutyric acid (GABA)-ergic interneurons[182]. On the other hand, under the rim of the round coil, higher threshold neurons are expected to be activated, since higher currents will be induced. It is thus possible that rTMS was leading to an excitatory effect on the inhibitory restraint surrounding the epileptic focus[183], especially using the round coil. Using the figure-8 coil, higher currents will be induced in the targeted region, that is the epileptic focus.

The hypothesis was that using low-frequency rTMS, seizures would be reduced. However, since it is still not determined what components determine the inhibitory effect seen using low frequency rTMS, variable responses are paramount. It is unclear how the resulting effect of rTMS is composed: what type of neurons contribute, the relative contribution of different types of neurons, the relative change in excitability of different types of neurons, the strength and direction of synaptic changes over different synapses…[184]. So differential contributions of the involved processes, can lead to differences in overall effect. More measurable factors that also contribute to variability are age, gender, ethnicity, time of day, previous physical and mental activity, genetic factors, brain states during stimulation, short breaks in sessions, orientation of the neurons relative to the induced electrical field...[88]. Another important factor is the distance between coil and focus, since the induced field falls off quickly with the distance. Whereas only patients with neocortical focal epilepsy were included- so the focus was rather superficial- the distance between the coil and the cortex was variable. Since the individual motor threshold was used as a basis for setting stimulation intensity, part of the interindividual variability of skull thickness was compensated for but no correction for skin-cortex distance was applied to adapt the stimulation intensity. Also, as explained in part 2, the intensity of stimulation used was slightly lower than anticipated due to a technical error.

None of the patients achieved an overall 50% seizure reduction. Side effects in the study were a rebound in seizure frequency after initial reduction (one patient), increase in seizure frequency during and shortly following active stimulation (three patients, in one patient x4), hearing problems

after stimulation (one patient) and headache (four patients, one severe). Fatigue and concentration difficulties were reported both during active and sham treatment (two patients each, respectively). Even though this study had a negative primary outcome, interesting data were acquired, including sequential PET scans after each of the treatment conditions. The resulting changes in the PET scans *in vivo* evidence of the fact that complex changes are seen after rTMS stimulation.

A Cochrane review on rTMS in epilepsy has been published[185]. It did not include the study we performed but all prior studies and to our knowledge, no new controlled trials on the topic were published since our publication. Standard outcome parameters in epilepsy studies like responder rates and percentage seizure reduction were checked. The 50% responder rates were reported in three studies[92,101,102] and only one had a positive outcome: 10/12 patients in the intervention group could be classified as responders[101]. In two[92,101] of the trials[92,96,101,102,186,187] a significant reduction in seizure frequency was reported. Pooling these results in impossible due to large differences in stimulation protocol and time points at which the outcome data were analyzed. A more extensive description on the different studies and possible explanations for the observed differences can be found in the discussion of chapter 3.
The limitation of all studies on rTMS in epilepsy is the small sample size. Also in our study the sample size was low and the study was might have been unpowered. Based on the data reported in a previous study by Fregni and colleagues[10], 29 patients were needed to have at least 80% power to show a reduction of 50% between the active coil and the sham conditions[88]. The low number of patients in rTMS trials is in contrast to the number of patients included in phase 3 trials of drugs for epilepsy, where hundreds of patients are included in each treatment arm.

The last sentence of our paper in rTMS in epilepsy thus reads: because our study was small — as most rTMS studies in epilepsy — a large multicenter trial will be needed to determine the position of neuronavigated rTMS in the treatment of refractory focal neocortical epilepsy. In addition, the Cochrane review concluded that larger scale studies are necessary.

However, it might be easier in theory than to conceive let alone execute such a trial. First, the best paradigm has not yet been determined. This might be handled by allowing changing the parameters during the study in predefined ways. This will lead to a quite complex study outline. Alternatively, the vast number of possible protocols that need to be tested before an actual large-scale trial can be set up is overwhelming. Due to size and form differences of the brain between humans and animals, animal experiments are likely not going be very informative on what protocol parameters would be optimal. The trial - when agreed upon the protocol - will also need to include hundreds of patients, similar to phase III drug trials in epilepsy. Considering the adaptive protocol and the number of subjects needed, this will be a laborious trial. Since patients have to come to the hospital for repeated sessions of treatment over longer time periods, investment of both patients and investigators is larger than that of a drug trial. Funding needed to execute such a trial might thus be higher than in trials with drugs. It needs to be seen how such a trial could be organized.

7.3 Future perspectives

7.3.1 Will invasive DCS be replaced with non-invasive alternatives?

Minimal invasive procedures on the brain will likely become the standard of care in the future, for some indications. Currently, several minimal invasive treatment alternatives are available. Refractory mesial temporal lobe epilepsy can also be treated minimally invasive by laser ablation[188–190] or non-invasively by radiosurgery[191]. There is already evidence that cognitive outcomes are better after those less invasive treatments, compared to craniotomy[192]. These techniques have also successfully been used to treat other brain lesions leading to refractory epilepsy. Hospital stay is much shorter and there are none of the complications related to the craniotomy. Other non-invasive techniques, like MRI-guided focused ultrasound, are being developed and trials were already performed using it for thalamotomy in refractory essential tremor[193].
In minimal invasive or non-invasive treatments, no craniotomy is performed and thus DCS is no longer an option. Therefore, we will rely more on multimodal non-invasive functional mapping. It will be accurate and combined with an ever expanding knowledge on brain functioning and aided by the intelligence of well-designed computer algorithms a better prediction of individual outcome will could obtained.

Before multimodal non-invasive functional mapping will replace more invasive techniques, we are faced with barriers. One of those barriers has more to do with human psychology than scientific merits. DCS has high face validity[194], meaning that it seems to measure what it is intended to measure and thus the results are accepted as reliable, even though they come with uncertainties, and false positive and false negative findings, like all diagnostic tests. False positive findings can be a result of misinterpreting baseline language deficits or as a result of current spread to neighboring locations, or simply by fatigue of the patient. False negative findings can be seen especially if the task performed does not measure the ensuing deficit (e.g. a patient is still able to talk and count but develops a severe anomia) or when the parameters of stimulation are not sufficient to affect brain functioning. The use of DCS is limited by patient's cooperation, ensuing fatigue, interpretation problems with pre-existing language problems, time-constrains of the surgery, induction of seizures (sometimes only controllable with reinstitution of anesthesia)…
For now, DCS is still considered as a gold standard by most neurosurgeons. This will likely change in the future. To get an idea on how this transition process might unfold, we can look at the transition from the Wada-test to fMRI in prediction of language and memory outcome after temporal lobe surgerys[195]. The Wada-test was considered the gold standard and had high face validity: if language or memory was impaired during unilateral anesthesia of the studied hemisphere, surgery was not performed on this hemisphere as not to risk deficits after surgery. Again, this interpretation was complicated by factors like anesthesia going from one hemisphere to the other and a more general decrease in performance, patient cooperation, the test battery used during the testing and also the fact that the decision not to operate based on the Wada test was never validated. Currently, with the same scientific evidence and roughly the same results after temporal lobe surgery worldwide, a majority of epilepsy surgery centers rarely to never use the Wada-test anymore. Only by relying less on the Wada test, it became clear that fMRI could sometimes even be superior from a patient outcome efficacy perspective (step 5 of the diagnostic framework) to the Wada test for post-operative outcome prediction, e.g. being better able to predict post-operative verbal memory[196]. Moreover, the costs of the Wada test are larger (with a factor of 3.7[197]) compared to fMRI, so the societal efficacy of transitioning from Wada-testing to fMRI as diagnostic modality of choice, seems obvious. However, a transition process is as much a psychological and socially driven process as a reflection of the advances in science.

One should sometimes be reminded of the fact that the most important parameter to study is patient outcome, not concordance to another diagnostic test that was in use before.

If we envision that non-invasive multimodal mapping would replace DCS in the near future, another hurdle that needs to be tackled is the problem of brain shift during surgery and the decreased reliability at that moment of neuronavigation and preoperatively obtained data. Some methods that have been developed are able to recalculate the position of the brain based on intra-operatively obtained data, like sonography or intra-operative MRI. However, the brain shift is a non-linear deformation and the deformations are unequal over the brain. Advances in the field of biomechanics and non-linear image transformation that accurately reflect the brain shift during surgery is thus needed.
In any case, non-invasive motor cortex mapping will replace invasive mapping sooner than language mapping, since non-invasive motor mapping has already progressed further on the developmental path.

7.3.2 Will rTMS be used as a treatment for refractory epilepsy?

The effects observed in our study do not support the use of rTMS as a treatment for refractory focal epilepsy. Any effect of rTMS on seizure frequency will be temporary and the protocol with repeated pulses on several days, makes it a labor-intensive treatment. However, neuro-modulation- either invasive or non-invasive- may still be part of the armamentarium for treating epilepsy. Even though treatment with drugs is the mainstay, focusing solely on drug development may not lead to significant improvements in reducing the number of people suffering from refractory epilepsy. Proof of this is that although many new AEDs came to the market in the last three decennia, overall rates of seizure freedom did not increase.
The spot at the horizon for epilepsy is to prevent and cure all epilepsy. Before we get there, we should strive to have no seizures, good health (this includes no side effects) and no effects on reproduction (including no fetal toxicity). In this regard, neuromodulation could have a place in the treatment of refractory epilepsy.
Current neuromodulation treatments that are routinely used are vagal nerve stimulation (VNS), deep brain stimulation (DBS) implanted in the anterior nucleus of the thalamus and responsive brain neurostimulation (RNS). The expected results of VNS is reduction in seizure frequency (not seizure freedom) in the patients who respond to the treatment (e.g. 63% response rate[198]). It is unfortunately not possible to predict who will respond. Similarly, DBS offers seizure reduction in patients who respond to the treatment (e.g. 68% 5-year response rate[199]). The RNS system[200] offers similar benefits with a 66% response rate over 7 years follow-up. This system has not been approved in Europe. Non-invasive neuromodulation devices are also available, including external vagal nerve[201] and external trigeminal nerve stimulation devices[202–204]. Efficiency seems to be less than with implanted devices and the number of patients included in the studies is low. Since the systems are however completely non-invasive, it could be a promising avenue for further research. Since TMS-devices are bulky and expensive, home TMS-stimulation does seem more complex and will probably not be developed. Other neuromodulation devices will be developed and will need to find their place in our treatment armamentarium.

I found this topic of brain stimulation very stimulating to work on. I hope this thesis will contribute on the further dissemination of the techniques.

Bibliography

1. Pallud J, Blonski M, Mandonnet E, et al. Velocity of tumor spontaneous expansion predicts long-term outcomes for diffuse low-grade gliomas. Neuro Oncol. 2013;15:595–606.
2. Jakola AS, Myrmel KS, Kloster R, et al. Comparison of a strategy favoring early surgical resection vs a strategy favoring watchful waiting in low-grade gliomas. JAMA. 2012;308:1881–1888.
3. McGirt MJ, Chaichana KL, Attenello FJ, et al. Extent of surgical resection is independently associated with survival in patients with hemispheric infiltrating low-grade gliomas. Neurosurgery. 2008;63:700–708.
4. Sanai N, Berger MS. Glioma extent of resection and its impact on patient outcome. Neurosurgery. 2008;62:753–766.
5. Yang T, Temkin N, Barber J, et al. Gross total resection correlates with long-term survival in pediatric patients with glioblastoma. World Neurosurg. 2013;79:537–544.
6. McGirt MJ, Mukherjee D, Chaichana KL, Than KD, Weingart JD, Quinones-Hinojosa A. Association of surgically acquired motor and language deficits on overall survival after resection of glioblastoma multiforme. Neurosurgery. 2009;65:463–469.
7. Patchell RA, Tibbs PA, Walsh JW, et al. A randomized trial of surgery in the treatment of single metastases to the brain. N Engl J Med. 1990;322:494–500.
8. Maltoni M, Nanni O, Derni S, et al. Clinical prediction of survival is more accurate than the Karnofsky performance status in estimating life span of terminally ill cancer patients. Eur J Cancer. 1994;30A:764–766.
9. Sperling MR, Barshow S, Nei M, Asadi-Pooya AA. A reappraisal of mortality after epilepsy surgery. Neurology. 2016;86:1938–1944.
10. Trinka E, Bauer G, Oberaigner W, Ndayisaba J-P, Seppi K, Granbichler C a. Cause-specific mortality among patients with epilepsy: results from a 30-year cohort study. Epilepsia. 2013;54:495–501.
11. Sillanpää M, Shinnar S. Long-term mortality in childhood-onset epilepsy. N Engl J Med. 2010;363:2522–2529.
12. Scott Perry M, Duchowny M. Surgical versus medical treatment for refractory epilepsy: Outcomes beyond seizure control. Epilepsia. 2013;54:2060–2070.
13. Engel J, McDermott MP, Wiebe S, et al. Early Surgical Therapy for Drug-Resistant Temporal Lobe Epilepsy. JAMA. 2012;307:922.
14. Bonelli SB, Thompson PJ, Yogarajah M, et al. Imaging language networks before and after anterior temporal lobe resection: results of a longitudinal fMRI study. Epilepsia. 2012;53:639–650.
15. Jehi L, Friedman D, Carlson C, et al. The evolution of epilepsy surgery between 1991 and 2011 in nine major epilepsy centers across the United States, Germany, and Australia. Epilepsia. 2015;56:1526–1533.
16. Cloppenborg T, May TW, Blümcke I, et al. Trends in epilepsy surgery: stable surgical numbers despite increasing presurgical volumes. J Neurol Neurosurg Psychiatry. 2016;87:1322–1329.
17. Rapport F, Shih P, Mitchell R, et al. Better evidence for earlier assessment and surgical intervention for refractory epilepsy (The BEST study): a mixed methods study protocol. BMJ Open. 2017;7:e017148.
18. Mills SJ, Thompson G, Jackson A. Advanced magnetic resonance imaging biomarkers of cerebral metastases. Cancer Imaging. 2012;12:245–252.
19. GBD 2015 Neurological Disorders Collaborator Group VL, Abajobir AA, Abate KH, et al. Global, regional, and national burden of neurological disorders during 1990-2015: a systematic analysis for the Global Burden of Disease Study 2015. Lancet Neurol. 2017;16:877–897.

20. Due-tonnessen P, Rasmussen I, Berntsen EM, Bjornerud A, Emblem KE. Identifying the Central Sulcus in Patients With Intra-axial Lesions : A Multicenter Study Comparing Conventional Presurgical MRI to Topographical Analysis and BOLD-fMRI. J Comput Assist Tomogr. 2014;38:1–8.
21. Jung NH, Delvendahl I, Kuhnke NG, Hauschke D, Stolle S, Mall V. Navigated transcranial magnetic stimulation does not decrease the variability of motor-evoked potentials. Brain Stimul. 2010;3:87–94.
22. Opitz a, Legon W, Rowlands a, Bickel WK, Paulus W, Tyler WJ. Physiological observations validate finite element models for estimating subject-specific electric field distributions induced by transcranial magnetic stimulation of the human motor cortex. Neuroimage. 2013;81:253–364.
23. Julkunen P. Methods for estimating cortical motor representation size and location in navigated transcranial magnetic stimulation. J Neurosci Methods. 2014;232:125–133.
24. Vitikainen AM, Salli E, Lioumis P, Mäkelä JP, Metsähonkala L. Applicability of nTMS in locating the motor cortical representation areas in patients with epilepsy. Acta Neurochir (Wien). 2013;155:507–518.
25. Julkunen P, Säisänen L, Danner N, et al. Comparison of navigated and non-navigated transcranial magnetic stimulation for motor cortex mapping, motor threshold and motor evoked potentials. Neuroimage. 2009;44:790–795.
26. Westin GG, Bassi BD, Lisanby SH, Luber B. Determination of motor threshold using visual observation overestimates transcranial magnetic stimulation dosage: Safety implications. Clin Neurophysiol. 2014;125:142–147.
27. Rossini PM, Barker a T, Berardelli a, et al. Non-invasive electrical and magnetic stimulation of the brain, spinal cord and roots: basic principles and procedures for routine clinical application. Report of an IFCN committee. Electroencephalogr Cinical Neurophysiol. 1994;91:79–92.
28. Rossini PM, Burke D, Chen R, et al. Non-invasive electrical and magnetic stimulation of the brain, spinal cord, roots and peripheral nerves: Basic principles and procedures for routine clinical and research application. An updated report from an I.F.C.N. Committee. Clin Neurophysiol. 2015;126:1071–1107.
29. Groppa S, Oliviero a., Eisen a., et al. A practical guide to diagnostic transcranial magnetic stimulation: Report of an IFCN committee. Clin Neurophysiol. 2012;123:858–882.
30. Kimiskidis VK, Papagiannopoulos S, Sotirakoglou K, et al. The repeatability of corticomotor threshold measurements. Neurophysiol Clin. 2004;34:259–266.
31. Mills KR, Nithi KA. Corticomotor threshold to magnetic stimulation: normal values and repeatability. Muscle Nerve. 1997;20:570–576.
32. Awiszus F. Fast estimation of transcranial magnetic stimulation motor threshold: Is it safe? Brain Stimul. 2011;4:50–57.
33. Boroojerdi B, Meister IG, Foltys H, Sparing R, Cohen LG, Töpper R. Visual and motor cortex excitability: a transcranial magnetic stimulation study. Clin Neurophysiol. 2002;113:1501–1504.
34. Badawy R, MacDonell R, Jackson G, Berkovic S. The peri-ictal state: Cortical excitability changes within 24 h of a seizure. Brain. 2009;132:1013–1021.
35. Amassian VE, Eberle L, Maccabee PJ, Cracco RQ. Modelling magnetic coil excitation of human cerebral cortex with a peripheral nerve immersed in a brain-shaped volume conductor: the significance of fiber bending in excitation. Electroencephalogr Clin Neurophysiol. 1992;85:291–301.
36. Maccabee PJ, Amassian VE, Eberle LP, Cracco RQ. Magnetic coil stimulation of straight and bent amphibian and mammalian peripheral nerve in vitro: locus of excitation. J Physiol. 1993;460:201–219.
37. Maccabee PJ, Nagarajan SS, Amassian VE, et al. Influence of pulse sequence, polarity and

amplitude on magnetic stimulation of human and porcine peripheral nerve. J Physiol. 1998;513.
38. Roth Y, Pell GS, Zangen A. Realistic shape head model and spherical model as methods for TMS coil characterization. Clin Neurophysiol. 2015;126:1455–1456.
39. Thielscher A, Antunes A, Saturnino GB. Field modeling for transcranial magnetic stimulation: A useful tool to understand the physiological effects of TMS? Conf Proc. Annu Int Conf IEEE Eng Med Biol Soc IEEE Eng Med Biol Soc Annu Conf. IEEE; 2015;2015:222–225.
40. Krieg TD, Salinas FS, Narayana S, Fox PT, Mogul DJ. Computational and experimental analysis of TMS-induced electric field vectors critical to neuronal activation. J Neural Eng. 2015;12:046014.
41. Johnson KA, Baig M, Ramsey D, et al. Prefrontal rTMS for treating depression: location and intensity results from the OPT-TMS multi-site clinical trial. Brain Stimul. 2013;6:108–117.
42. Bashir S, Edwards D, Pascual-Leone A. Neuronavigation increases the physiologic and behavioral effects of low-frequency rTMS of primary motor cortex in healthy subjects. Brain Topogr. 2011;24:54–64.
43. Rossini PM, Rossi S. Transcranial magnetic stimulation: Diagnostic, therapeutic, and research potential. Neurology. 2007;68:484–488.
44. Bastani A, Jaberzadeh S. A Higher Number of TMS-Elicited MEP from a Combined Hotspot Improves Intra- and Inter-Session Reliability of the Upper Limb Muscles in Healthy Individuals. PLoS One. 2012;7.
45. Kimiskidis VK, Koutlis C, Tsimpiris A, Kälviäinen R, Ryvlin P, Kugiumtzis D. Transcranial Magnetic Stimulation Combined with EEG Reveals Covert States of Elevated Excitability in the Human Epileptic Brain. Int J Neural Syst. 2015;25:1550018.
46. Hoogendam JM, Ramakers GMJ, Di Lazzaro V. Physiology of repetitive transcranial magnetic stimulation of the human brain. Brain Stimul. 2010;3:95–118.
47. Karabanov A, Ziemann U, Hamada M, et al. Consensus Paper: Probing Homeostatic Plasticity of Human Cortex With Non-invasive Transcranial Brain Stimulation. Brain Stimul. 8:442–454.
48. Maeda F, Keenan JP, Tormos JM, Topka H, Pascual-Leone A. Interindividual variability of the modulatory effects of repetitive transcranial magnetic stimulation on cortical excitability. Exp Brain Res. 2000;133:425–430.
49. Silvanto J. State-dependency of transcranial magnetic stimulation. Brain Topogr. 2008;21:1–10.
50. Weisz N, Steidle L, Lorenz I. Formerly known as inhibitory: effects of 1-Hz rTMS on auditory cortex are state-dependent. Eur J Neurosci. 2012;36:2077–2087.
51. Rothkegel H, Sommer M, Paulus W. Breaks during 5 Hz rTMS are essential for facilitatory after effects. Clin Neurophysiol. 2010;121:426–430.
52. Hamada M, Murase N, Hasan A, Balaratnam M, Rothwell JC. The role of interneuron networks in driving human motor cortical plasticity. Cereb Cortex. 2013;23:1593–1605.
53. Schmidt S, Fleischmann R, Picht T. Recovery of motor function after intensive navigated transcranial magnetic stimulation: A case report of unexpected therapeutic effects. Clin Neurol Neurosurg. 2013;115:215–217.
54. Lefaucheur J-P, André-Obadia N, Antal A, et al. Evidence-based guidelines on the therapeutic use of repetitive transcranial magnetic stimulation (rTMS). Clin Neurophysiol. 2014;125:1–57.
55. Rotenberg a, Bae E, Muller P, et al. In-session seizures during low-frequency repetitive transcranial magnetic stimulation in patients with epilepsy. Epilepsy Behav. 2009;16:353–355.
56. Bae EH, Schrader LM, Machii K, et al. Safety and tolerability of repetitive transcranial magnetic stimulation in patients with epilepsy: a review of the literature. Epilepsy Behav. 2007;10:521–528.
57. Pereira LS, Müller VT, da Mota Gomes M, Rotenberg A, Fregni F. Safety of repetitive transcranial magnetic stimulation in patients with epilepsy: A systematic review. Epilepsy Behav. 2016;57:167–176.

58. Rossi S, Hallett M, Rossini PM, et al. Safety, ethical considerations, and application guidelines for the use of transcranial magnetic stimulation in clinical practice and research. Clin Neurophysiol. 2009;120:2008–2039.
59. Wassermann EM, Wassermann EM. Risk and safety of repetitive transcranial magnetic stimulation. Electroencephalogr Clin Neurophysiol. 1998;108:1–16.
60. Rossi S, Hallett M, Rossini PM, Pascual-Leone A. Safety, ethical considerations, and application guidelines for the use of transcranial magnetic stimulation in clinical practice and research. Clin Neurophysiol. 2012;120:323–330.
61. Schrader LM, Stern JM, Fields TA, Nuwer MR, Wilson CL. A lack of effect from transcranial magnetic stimulation (TMS) on the vagus nerve stimulator (VNS). Clin Neurophysiol. 2005;116:2501–2504.
62. Bajbouj M, Gallinat J, Lang UE, et al. Motor cortex excitability after vagus nerve stimulation in major depression. J Clin Psychopharmacol. 2007;27:156–159.
63. Di Lazzaro V, Oliviero A, Pilato F, et al. Effects of vagus nerve stimulation on cortical excitability in epileptic patients. Neurology. 2004;62:2310–2312.
64. Philip NS, Carpenter SL, Carpenter LL. Safe Use of Repetitive Transcranial Magnetic Stimulation in Patients With Implanted Vagus Nerve Stimulators. Brain Stimul. 2014;7:608–612.
65. Liu A, Pang T, Herman S, Pascual-Leone A, Rotenberg A. Transcranial magnetic stimulation for refractory focal status epilepticus in the intensive care unit. Seizure. 2013;22:893–896.
66. Chervyakov A V, Chernyavsky AY, Sinitsyn DO, Piradov MA. Possible Mechanisms Underlying the Therapeutic Effects of Transcranial Magnetic Stimulation. Front Hum Neurosci. 2015;9:303.
67. Pereira LCM, Oliveira KM, L'Abbate GL, Sugai R, Ferreira J a., Da Motta L a. Outcome of fully awake craniotomy for lesions near the eloquent cortex: Analysis of a prospective surgical series of 79 supratentorial primary brain tumors with long follow-up. Acta Neurochir (Wien). 2009;151:1215–1230.
68. Maizey L, Allen CPG, Dervinis M, et al. Comparative incidence rates of mild adverse effects to transcranial magnetic stimulation. Clin Neurophysiol. 2013;124:536–544.
69. Tarapore PE, Picht T, Bulubas L, et al. Safety and tolerability of navigated TMS for preoperative mapping in neurosurgical patients. Clin Neurophysiol. 2016;127:1895–1900.
70. Tarapore PE, Findlay AM, Honma SM, et al. Language mapping with navigated repetitive TMS: Proof of technique and validation. Neuroimage. 2013;82:260–272.
71. Rogić M, Deletis V, Fernández-Conejero I. Inducing transient language disruptions by mapping of Broca's area with modified patterned repetitive transcranial magnetic stimulation protocol. J Neurosurg. 2014;120(5):1033-41.
72. Rösler J, Niraula B, Strack V, et al. Language mapping in healthy volunteers and brain tumor patients with a novel navigated TMS system: Evidence of tumor-induced plasticity. Clin Neurophysiol. 2014;125:526–536.
73. Duffau H, Lopes M, Arthuis F, et al. Contribution of intraoperative electrical stimulations in surgery of low grade gliomas: a comparative study between two series without (1985-96) and with (1996-2003) functional mapping in the same institution. J Neurol Neurosurg Psychiatry. 2005;76:845–851.
74. Talacchi A, Turazzi S, Locatelli F, et al. Surgical treatment of high-grade gliomas in motor areas. The impact of different supportive technologies: a 171-patient series. J Neurooncol. 2010;100:417–426.
75. De Witt Hamer PC, Robles SG, Zwinderman AH, Duffau H, Berger MS. Impact of intraoperative stimulation brain mapping on glioma surgery outcome: A meta-analysis. J Clin Oncol. 2012;30:2559–2565.
76. Snodgrass JG, Vanderwart M. A standardized set of 260 pictures: norms for name agreement, image agreement, familiarity, and visual complexity. J Exp Psychol Hum Learn. 1980;6:174–

215.
77. Hervey-Jumper SL, Li J, Lau D, et al. Awake craniotomy to maximize glioma resection: methods and technical nuances over a 27-year period. J Neurosurg. 2015;123:325–339.
78. Szelényi A, Bello L, Duffau H, et al. Intraoperative electrical stimulation in awake craniotomy: methodological aspects of current practice. Neurosurg Focus. 2010;28:E7.
79. Schucht P, Seidel K, Beck J, et al. Intraoperative monopolar mapping during 5-ALA-guided resections of glioblastomas adjacent to motor eloquent areas: evaluation of resection rates and neurological outcome. Neurosurg Focus. 2014;37:E16.
80. Raabe A, Beck J, Schucht P, Seidel K. Continuous dynamic mapping of the corticospinal tract during surgery of motor eloquent brain tumors: evaluation of a new method. J Neurosurg. 2014;120:1015–1024.
81. Riva M, Fava E, Gallucci M, et al. Monopolar high-frequency language mapping: can it help in the surgical management of gliomas? A comparative clinical study. 2016;124(5):1479-89.
82. Rosenow F, Lüders H. Presurgical evaluation of epilepsy. Brain. 2001;124:1683–1700.
83. Cook MJ, O'Brien TJ, Berkovic SF, et al. Prediction of seizure likelihood with a long-term, implanted seizure advisory system in patients with drug-resistant epilepsy: A first-in-man study. Lancet Neurol. 2013;12:563–571.
84. Eggleston KS, Olin BD, Fisher RS. Ictal tachycardia: the head-heart connection. Seizure. 2014;23:496–505.
85. Osorio I, Schachter S. Extracerebral detection of seizures: a new era in epileptology? Epilepsy Behav. 2011;22 Suppl 1:S82-7.
86. van Elmpt WJC, Nijsen TME, Griep PAM, Arends JBAM. A model of heart rate changes to detect seizures in severe epilepsy. Seizure. 2006;15:366–375.
87. Hampel KG, Vatter H, Elger CE, Surges R. Cardiac-based vagus nerve stimulation reduced seizure duration in a patient with refractory epilepsy. Seizure. 2015;26:81–85.
88. Seynaeve L, Devroye A, Dupont P, Van Paesschen W. Randomized crossover sham-controlled clinical trial of targeted low-frequency transcranial magnetic stimulation comparing a figure-8 and a round coil to treat refractory neocortical epilepsy. Epilepsia. 2016;57.
89. Ridding MC, Rothwell JC. Is there a future for therapeutic use of transcranial magnetic stimulation? Nat Rev Neurosci. 2007;8:559–567.
90. Tergau F, Naumann U, Paulus W, Steinhoff BJ. Low-frequency repetitive transcranial magnetic stimulation improves intractable epilepsy. Lancet. 1999;353:2209.
91. Menkes DL, Gruenthal M. Slow-frequency repetitive transcranial magnetic stimulation in a patient with focal cortical dysplasia. Epilepsia. 2000;41:240–242.
92. Joo EY, Han SJ, Chung SH, Cho JW, Seo DW, Hong SB. Antiepileptic effects of low-frequency repetitive transcranial magnetic stimulation by different stimulation durations and locations. Clin Neurophysiol. 2007;118:702–708.
93. Santiago-Rodríguez E, Cárdenas-Morales L, Harmony T, Fernández-Bouzas A, Porras-Kattz E, Hernández A. Repetitive transcranial magnetic stimulation decreases the number of seizures in patients with focal neocortical epilepsy. Seizure. 2008;17:677–683.
94. Sun W, Mao W, Meng X, et al. Low-frequency repetitive transcranial magnetic stimulation for the treatment of refractory partial epilepsy: A controlled clinical study. Epilepsia. 2012;53:1782–1789.
95. Theodore WH, Hunter K, Chen R, et al. Transcranial magnetic stimulation for the treatment of seizures: a controlled study. Neurology. 2002;59:560–562.
96. Tergau F, Neumann D, Rosenow F, Nitsche MA, Paulus W, Steinhoff B. Can epilepsies be improved by repetitive transcranial magnetic stimulation?--interim analysis of a controlled study. Suppl Clin Neurophysiol. 2003;56:400–405.
97. Daniele O, Brighina F, Piazza A, Giglia G, Scalia S, Fierro B. Low-frequency transcranial magnetic stimulation in patients with cortical dysplasia. J Neurol. 2003;250:761–762.
98. Brasil-Neto JP, De Araújo DP, Teixeira W a., Araújo VP, Boechat-Barros R. Experimental

therapy of epilepsy with transcranial magnetic stimulation: Lack of additional benefit with prolonged treatment. Arq Neuropsiquiatr. 2004;62:21–25.
99. Fregni F, Thome-Souza S, Bermpohl F, et al. Antiepileptic effects of repetitive transcranial magnetic stimulation in patients with cortical malformations: an EEG and clinical study. Stereotact Funct Neurosurg. 2005;83:57–62.
100. Kinoshita M, Ikeda A, Begum T, Yamamoto J, Hitomi T, Shibasaki H. Low-frequency repetitive transcranial magnetic stimulation for seizure suppression in patients with extratemporal lobe epilepsy - A pilot study. Seizure. 2005;14:387–392.
101. Fregni F, Otachi PTM, Do Valle A, et al. A randomized clinical trial of repetitive transcranial magnetic stimulation in patients with refractory epilepsy. Ann Neurol. 2006;60:447–455.
102. Cantello R, Rossi S, Varrasi C, et al. Slow repetitive TMS for drug-resistant epilepsy: Clinical and EEG findings of a placebo-controlled trial. Epilepsia. 2007;48:366–374.
103. Hsu W-Y, Cheng C-H, Lin M-W, Shih Y-H, Liao K-K, Lin Y-Y. Antiepileptic effects of low frequency repetitive transcranial magnetic stimulation: A meta-analysis. Epilepsy Res. 2011;96:231–240.
104. Kimiskidis VK, Kugiumtzis D, Papagiannopoulos S, Vlaikidis N. Transcranial magnetic stimulation (TMS) modulates epileptiform discharges in patients with frontal lobe epilepsy: a preliminary EEG-TMS study. Int J Neural Syst. 2013;23:1250035.
105. Cramer JA, Perrine K, Devinsky O, Bryant-Comstock L, Meador K, Hermann B. Development and cross-cultural translations of a 31-item quality of life in epilepsy inventory. Epilepsia. 1998;39:81–88.
106. Wassermann E, Epstein C, Ziemann U. Oxford Handbook of Transcranial Stimulation. 2008.
107. Fiest KM, Sajobi TT, Wiebe S. Epilepsy surgery and meaningful improvements in quality of life: Results from a randomized controlled trial. Epilepsia. 2014;55:886–892.
108. Ziemann U. TMS and drugs. Clin Neurophysiol. 2004;115:1717–1729.
109. Fregni F, Boggio PS, Valle AC, et al. Homeostatic effects of plasma valproate levels on corticospinal excitability changes induced by 1 Hz rTMS in patients with juvenile myoclonic epilepsy. Clin Neurophysiol. 2006;117:1217–1227.
110. Ridding MC, Ziemann U. Determinants of the induction of cortical plasticity by non-invasive brain stimulation in healthy subjects. J Physiol. 2010;588:2291–2304.
111. Yi X, Fisher KM, Lai M, Mansoor K, Bicker R, Baker SN. Differences between Han Chinese and Caucasians in transcranial magnetic stimulation parameters. Exp Brain Res. 2014;232:545–553.
112. Seynaeve L, Van Paesschen W. Response to “Safety of repetitive transcranial magnetic stimulation in patients with epilepsy: A systematic review” by Luisa Santos Pereira and colleagues. Epilepsy Behav. 2016;62:308.
113. Carrette S, Boon P, Dekeyser C, et al. Repetitive transcranial magnetic stimulation for the treatment of refractory epilepsy. Expert Rev Neurother. 2016;16:1093–1110.
114. Siebner HR, Bergmann TO, Bestmann S, et al. Consensus paper: Combining transcranial stimulation with neuroimaging. Brain Stimul. 2009;2:58–80.
115. Hayashi T, Ohnishi T, Okabe S, et al. Long-term effect of motor cortical repetitive transcranial magnetic stimulation [correction]. Ann Neurol. 2004;56:77–85.
116. Siebner HR, Peller M, Willoch F, et al. Lasting cortical activation after repetitive TMS of the motor cortex: a glucose metabolic study. Neurology. 2000;54:956–963.
117. Kimbrell T a, Dunn RT, George MS, et al. Left prefrontal-repetitive transcranial magnetic stimulation (rTMS) and regional cerebral glucose metabolism in normal volunteers. Psychiatry Res. 2002;115:101–113.
118. Lee M, Kim SE, Kim WS, et al. Cortico-cortical modulation induced by 1-Hz repetitive transcranial magnetic stimulation of the temporal cortex. J Clin Neurol. 2013;9:75–82.
119. C. Caparelli E. Is 1 Hz rTMS Always Inhibitory in Healthy Individuals? Open Neuroimag J. 2012;6:69–74.

120. Duncan JS. Imaging in the surgical treatment of epilepsy. Nat Rev Neurol. Nature Publishing Group; 2010;6:537–550.
121. Schur S, Allen V, White A, et al. Significance of FDG-PET Hypermetabolism in Children with Intractable Focal Epilepsy. Pediatr Neurosurg. 2018;53:153–162.
122. Seynaeve L, Devroye A, Dupont P, Van Paesschen W. Randomized crossover sham-controlled clinical trial of targeted low-frequency transcranial magnetic stimulation comparing a figure-8 and a round coil to treat refractory neocortical epilepsy. Epilepsia. 2016;57.
123. Vunckx K, Dupont P, Goffin K, Van Paesschen W, Van Laere K, Nuyts J. Voxel-based comparison of state-of-the-art reconstruction algorithms for 18F-FDG PET brain imaging using simulated and clinical data. Neuroimage. 2014;102 Pt 2:875–884.
124. Hunter GJ, Hamberg LM, Alpert NM, Choi NC, Fischman AJ. Simplified measurement of deoxyglucose utilization rate. J Nucl Med. 1996;37:950–955.
125. Güvenç C, Dupont P, Van den Stock J, et al. Correlation of neuropsychological and metabolic changes after epilepsy surgery in patients with left mesial temporal lobe epilepsy with hippocampal sclerosis. EJNMMI Res. 2018;8:31.
126. Nelissen N, Van Paesschen W, Baete K, et al. Correlations of interictal FDG-PET metabolism and ictal SPECT perfusion changes in human temporal lobe epilepsy with hippocampal sclerosis. Neuroimage. 2006;32:684–695.
127. Pitkänen M, Kallioniemi E, Julkunen P, Nazarova M, Nieminen JO, Ilmoniemi RJ. Minimum-Norm Estimation of Motor Representations in Navigated TMS Mappings. Brain Topogr. 2017;30:711–722.
128. Hill DL, Smith a D, Simmons a, et al. Sources of error in comparing functional magnetic resonance imaging and invasive electrophysiological recordings. J Neurosurg. 2000;93:214–223.
129. Hou BL, Bradbury M, Peck KK, Petrovich NM, Gutin PH, Holodny AI. Effect of brain tumor neovasculature defined by rCBV on BOLD fMRI activation volume in the primary motor cortex. Neuroimage. 2006;32:489–497.
130. Sunaert S. Presurgical planning for tumor resectioning. J Magn Reson Imaging. 2006;23:887–905.
131. Wang L, Chen D, Olson J, Ali S, Fan T, Mao H. Re-examine tumor-induced alterations in hemodynamic responses of BOLD fMRI: implications in presurgical brain mapping. Acta radiol. 2012;53:802–811.
132. Zacà D, Jovicich J, Nadar SR, Voyvodic JT, Pillai JJ. Cerebrovascular reactivity mapping in patients with low grade gliomas undergoing presurgical sensorimotor mapping with BOLD fMRI. J Magn Reson Imaging. 2014;40:383–390.
133. Krings T, Buchbinder BR, Butler WE, et al. Functional magnetic resonance imaging and transcranial magnetic stimulation: complementary approaches in the evaluation of cortical motor function. Neurology. 1997;48:1406–1416.
134. Forster MT, Hattingen E, Senft C, Gasser T, Seifert V, Szelényi A. Navigated transcranial magnetic stimulation and functional magnetic resonance imaging: Advanced adjuncts in preoperative planning for central region tumors. Neurosurgery. 2011;68:1317–1324.
135. Tarapore PE, Tate MC, Findlay AM, et al. Preoperative multimodal motor mapping: a comparison of magnetoencephalography imaging, navigated transcranial magnetic stimulation, and direct cortical stimulation. J Neurosurg. 2012;117:354–362.
136. Picht T, Mularski S, Kuehn B, Vajkoczy P, Kombos T, Suess O. Navigated transcranial magnetic stimulation for preoperative functional diagnostics in brain tumor surgery. Neurosurgery. 2009;65:93–99.
137. Takahashi S, Vajkoczy P, Picht T. Navigated transcranial magnetic stimulation for mapping the motor cortex in patients with rolandic brain tumors. Neurosurg Focus. 2013;34:E3.
138. Zdunczyk A, Fleischmann R, Schulz J, Vajkoczy P, Picht T. The reliability of topographic measurements from navigated transcranial magnetic stimulation in healthy volunteers and

tumor patients. Acta Neurochir (Wien). 2013;155:1309–1317.
139. Thielscher A, Opitz A, Windhoff M. Impact of the gyral geometry on the electric field induced by transcranial magnetic stimulation. Neuroimage. 2011;54:234–243.
140. Laakso I, Hirata A, Ugawa Y. Effects of coil orientation on the electric field induced by TMS over the hand motor area. Phys Med Biol. 2014;59:203–218.
141. Windhoff M, Opitz A, Thielscher A. Electric field calculations in brain stimulation based on finite elements: An optimized processing pipeline for the generation and usage of accurate individual head models. Hum Brain Mapp. 2013;34:923–935.
142. Krieg SM, Lioumis P, Mäkelä JP, et al. Protocol for motor and language mapping by navigated TMS in patients and healthy volunteers; workshop report. Acta Neurochir (Wien). 2017;159:1187–1195.
143. Attene M. A lightweight approach to repairing digitized polygon meshes. Vis Comput. 2010;26:1393–1406.
144. Wassermann EM, McShane LM, Hallett M, Cohen LG. Noninvasive mapping of muscle representations in human motor cortex. Electroencephalogr Clin Neurophysiol. 1992;85:1–8.
145. Finke M, Fadini T, Kantelhardt S, Giese a, Matthaus L, Schweikard a. Brain-mapping using robotized TMS. Conf Proc IEEE Eng Med Biol Soc. 2008;2008:3929–3932.
146. Kantelhardt SR, Fadini T, Finke M, et al. Robot-assisted image-guided transcranial magnetic stimulation for somatotopic mapping of the motor cortex: a clinical pilot study. Acta Neurochir (Wien). 2010;152:333–343.
147. Mangraviti A, Casali C, Cordella R, et al. Practical assessment of preoperative functional mapping techniques: navigated transcranial magnetic stimulation and functional magnetic resonance imaging. Neurol Sci. 2013;34:1551–1557.
148. Picht T, Schmidt S, Woitzik J, Suess O. Navigated brain stimulation for preoperative cortical mapping in paretic patients: Case report of a hemiplegic patient. Neurosurgery. 2011;68:1475–1480.
149. Schuhmann T, Schiller NO, Goebel R, Sack AT. The temporal characteristics of functional activation in Broca's area during overt picture naming. Cortex. 2009;45:1111–1116.
150. Pascual-Leone a, Gates JR, Dhuna a. Induction of speech arrest and counting errors with rapid-rate transcranial magnetic stimulation. Neurology. 1991;41:697–702.
151. Chen R, Cros D, Curra A, et al. The clinical diagnostic utility of transcranial magnetic stimulation: Report of an IFCN committee. Clin Neurophysiol. 2008;119:504–532.
152. Sakreida K, Lange I, Willmes K, et al. High-resolution language mapping of Broca's region with transcranial magnetic stimulation. Brain Struct Funct. 2017;223:1297–1312.
153. Hämäläinen S, Mäkelä N, Sairanen V, Lehtonen M, Kujala T, Leminen A. TMS uncovers details about sub-regional language-specific processing networks in early bilinguals. Neuroimage. 2018;171:209–221.
154. Corina DP, Loudermilk BC, Detwiler L, Martin RF, Brinkley JF, Ojemann G. Analysis of naming errors during cortical stimulation mapping: implications for models of language representation. Brain Lang. 2010;115:101–112.
155. Boersma P, van Heuven V. Speak and unSpeak with Praat. Glot Int. 2001;5:341–347.
156. Duchateau J, Kong YO, Cleuren L, et al. Developing a reading tutor: Design and evaluation of dedicated speech recognition and synthesis modules. Speech Commun. 2009;51:985–994.
157. Schuurman I, Schouppe M. CGN, an annotated corpus of spoken Dutch. Proc 4th Int Work Linguist Interpret Corpora (LINC-03) Budapest. Epub 2003.
158. Baby D, Virtanen T, Gemmeke JF, van Hamme H. Exemplar-based noise robust automatic speech recognition using modulation spectrogram features. Epub 2014:519–524.
159. Baby D, Virtanen T, Gemmeke JF, Van hamme H. Coupled dictionaries for exemplar-based speech enhancement and automatic speech recognition. IEEE/ACM Trans Audio Speech Lang Process. 2015;23:1788–1799.
160. Sollmann N, Ille S, Hauck T, et al. The impact of preoperative language mapping by repetitive

navigated transcranial magnetic stimulation on the clinical course of brain tumor patients. BMC Cancer. 2015;15:261.
161. Sollmann N, Kubitscheck A, Maurer S, et al. Preoperative language mapping by repetitive navigated transcranial magnetic stimulation and diffusion tensor imaging fiber tracking and their comparison to intraoperative stimulation. Neuroradiology. 2016;58(8):807-18.
162. Ille S, Kulchytska N, Sollmann N, et al. Hemispheric language dominance measured by repetitive navigated transcranial magnetic stimulation and postoperative course of language function in brain tumor patients. Neuropsychologia. 2016;91:50-60.
163. Picht T, Krieg SM, Sollmann N, et al. A Comparison of Language Mapping by Preoperative Navigated Transcranial Magnetic Stimulation and Direct Cortical Stimulation During Awake Surgery. Neurosurgery. 2013;72:808–819.
164. Ille S, Sollmann N, Hauck T, et al. Combined noninvasive language mapping by navigated transcranial magnetic stimulation and functional MRI and Its Comparison With Direct Cortical Stimulation. 2015;123:1–14.
165. Meteyard L, Holmes NP. TMS SMART – Scalp mapping of annoyance ratings and twitches caused by Transcranial Magnetic Stimulation. J Neurosci Methods. 2018;299:34–44.
166. Krieg SM, Tarapore PE, Picht T, et al. Optimal timing of pulse onset for language mapping with navigated repetitive transcranial magnetic stimulation. Neuroimage. 2014;100:219–236.
167. Vitikainen A-M, Mäkelä E, Lioumis P, Jousmäki V, Mäkelä JP. Accelerometer-based automatic voice onset detection in speech mapping with navigated repetitive transcranial magnetic stimulation. J Neurosci Methods. 2015;253:70-7.
168. Fryback DG, Thornbury JR. The efficacy of diagnostic imaging. Med Decis Mak. 1991;11:88–94.
169. Burch J, Marson A, Beyer F, et al. Dilemmas in the interpretation of diagnostic accuracy studies on presurgical workup for epilepsy surgery. Epilepsia. 2012;53:1294–1302.
170. Krupinski EA, Jiang Y. Anniversary Paper: Evaluation of medical imaging systems. Med Phys. 2008;35:645–659.
171. Frey D, Schilt S, Strack V, et al. Navigated transcranial magnetic stimulation improves the treatment outcome in patients with brain tumors in motor eloquent locations. Neuro Oncol. 2014;16:1365–1372.
172. Krieg SM, Sabih J, Bulubasova L, et al. Preoperative motor mapping by navigated transcranial magnetic brain stimulation improves outcome for motor eloquent lesions. Neuro Oncol. 2014;16:1274–1282.
173. Krieg SM, Sollmann N, Obermueller T, et al. Changing the clinical course of glioma patients by preoperative motor mapping with navigated transcranial magnetic brain stimulation. BMC Cancer. 2015;15.
174. Picht T, Frey D, Thieme S, Kliesch S, Vajkoczy P. Presurgical navigated TMS motor cortex mapping improves outcome in glioblastoma surgery: a controlled observational study. J Neurooncol. 2016;126:535–543.
175. Michelucci R, Valzania F, Passarelli D, et al. Rapid-rate transcranial magnetic stimulation and hemispheric language dominance: usefulness and safety in epilepsy. Neurology. 1994;44:1697–1700.
176. Jennum P, Friberg L, Fuglsang-Frederiksen a, Dam M. Speech localization using repetitive transcranial magnetic stimulation. Neurology. 1994;44:269–273.
177. Wassermann EM, Blaxton T a., Hoffman E a., et al. Repetitive transcranial magnetic stimulation of the dominant hemisphere can disrupt visual naming in temporal lobe epilepsy patients. Neuropsychologia. 1999;37:537–544.
178. Epstein CM, Woodard JL, Stringer a Y, et al. Repetitive transcranial magnetic stimulation does not replicate the Wada test. Neurology. 2000;55:1025–1027.
179. Devlin JT, Matthews PM, Rushworth MFS. Semantic processing in the left inferior prefrontal cortex: a combined functional magnetic resonance imaging and transcranial magnetic stimulation study. J Cogn Neurosci. 2003;15:71–84.

180. Hauck T, Tanigawa N, Probst M, et al. Stimulation frequency determines the distribution of language positive cortical regions during navigated transcranial magnetic brain stimulation. BMC Neurosci. 2015;16:5.
181. Ille S, Sollmann N, Hauck T, et al. Impairment of preoperative language mapping by lesion location: a functional magnetic resonance imaging, navigated transcranial magnetic stimulation, and direct cortical stimulation study. 2015;123:314–324.
182. Kawaguchi Y, Kubota Y. GABAergic cell subtypes and their synaptic connections in rat frontal cortex. Cereb Cortex. 1997;7:476–486.
183. Schevon CA, Weiss SA, McKhann G, et al. Evidence of an inhibitory restraint of seizure activity in humans. Nat Commun. 2012;3:1011–1060.
184. Matheson NA, Shemmell JBH, De Ridder D, Reynolds JNJ. Understanding the Effects of Repetitive Transcranial Magnetic Stimulation on Neuronal Circuits. Front Neural Circuits. 2016;10:1–4.
185. Chen R, Spencer DC, Pulman J. Transcranial magnetic stimulation for the treatment of epilepsy. Cochrane Database of Systematic Reviews 2016, Issue 8. Art. No.: CD011025.
186. Theodore WH, Hunter K, Chen R, et al. Transcranial magnetic stimulation for the treatment of seizures: a controlled study. Neurology. 2002;59:560–562.
187. Wang Y, Wang X, Ke S, et al. Low-frequency repetitive transcranial magnetic simulation prevents chronic epileptic seizure. Neural Regen Res. 2013;8:2566–2572.
188. Donos C, Breier J, Friedman E, et al. Laser ablation for mesial temporal lobe epilepsy: Surgical and cognitive outcomes with and without mesial temporal sclerosis. Epilepsia. 2018;59:1421–1432.
189. Youngerman BE, Oh JY, Anbarasan D, et al. Laser ablation is effective for temporal lobe epilepsy with and without mesial temporal sclerosis if hippocampal seizure onsets are localized by stereoelectroencephalography. Epilepsia. 2018;59:595–606.
190. Kang JY, Wu C, Tracy J, et al. Laser interstitial thermal therapy for medically intractable mesial temporal lobe epilepsy. Epilepsia. 2016;57:325–334.
191. Barbaro NM, Quigg M, Cole AJ, et al. Radiosurgery versus open surgery for mesial temporal lobe epilepsy : The randomized , controlled ROSE trial. Epub 2018.:1–10.
192. Drane DL. MRI-Guided stereotactic laser ablation for epilepsy surgery: Promising preliminary results for cognitive outcome. Epilepsy Res. 2018;142:170–175.
193. Park Y-S, Jung NY, Na YC, Chang JW. Four-year follow-up results of magnetic resonance-guided focused ultrasound thalamotomy for essential tremor. Mov Disord. 2019;34:727-34.
194. Junck L, Hervey-jumper SL. Resection of gliomas around language areas: can fMRI contribute? 2015;84(6):550–1.
195. Mathern GW, Beninsig L, Nehlig A. From the Editors: Epilepsia's survey on the necessity of the Wada test and intracranial electrodes for cortical mapping. Epilepsia. 2014;55:1887–1889.
196. Dupont S, Duron E, Samson S, et al. Functional MR Imaging or Wada Test: Which Is the Better Predictor of Individual Postoperative Memory Outcome? Radiology. 2010;255:128–134.
197. Medina LS, Aguirre E, Bernal B, Altman NR. Functional MR Imaging versus Wada Test for Evaluation of Language Lateralization: Cost Analysis. Radiology. 2004;230:49–54.
198. García-Navarrete E, Torres C V., Gallego I, Navas M, Pastor J, Sola RG. Long-term results of vagal nerve stimulation for adults with medication-resistant epilepsy who have been on unchanged antiepileptic medication. Seizure. 2013;22:9–13.
199. Salanova V, Witt T, Worth R, et al. Long-term efficacy and safety of thalamic stimulation for drug-resistant partial epilepsy. Neurology. 2015;84:1017–1025.
200. Morrell MJ. Responsive cortical stimulation for the treatment of medically intractable partial epilepsy. Neurology. 2011;77:1295–1304.
201. Bauer S, Baier H, Baumgartner C, et al. Transcutaneous Vagus Nerve Stimulation (tVNS) for Treatment of Drug-Resistant Epilepsy: A Randomized, Double-Blind Clinical Trial (cMPsE02). Brain Stimul. 2016;9:356–363.

202. Slaght SJ, Nashef L. An audit of external trigeminal nerve stimulation (eTNS) in epilepsy. Seizure. 2017;52:60–62.
203. Soss J, Heck C, Murray D, et al. A prospective long-term study of external trigeminal nerve stimulation for drug-resistant epilepsy. Epilepsy Behav. 2015;42:44–47.
204. DeGiorgio CM, Soss J, Cook IA, et al. Randomized controlled trial of trigeminal nerve stimulation for drug-resistant epilepsy. Neurology. 2013;80:786–791.

Summary

Introduction
The goal of this project was to clinically validate motor and language functional mapping with TMS and to treat refractory focal epilepsy with multimodal image-guided repetitive TMS (rTMS).

Each year, more than 65,000 people are diagnosed with cancer in Belgium. Of those, 10-25% will experience brain metastasis at some point in the disease course. Part of these brain lesions need surgery, especially if only one brain metastasis is present, as is the case in half of the patients[18]. Primary brain tumors are rarer with an age-adjusted incidence rate of 21.42 per 100,000[19]. In addition, some forms of epilepsy are amendable to surgery and up to 1600 new patients each year in Belgium could in theory be evaluated for this option. With surgery, the aim is not only to render the patient seizure free by removal of the epileptogenic zone, but equally important, to preserve normal functioning, like movement and speech. Anatomical knowledge and fMRI are used to gauge risk of inducing deficits with surgery. However, due to the tumor changing both the anatomy and the response of the brain that is measured with fMRI, those methods are far from perfect. Therefore, if surgery is deemed possible, direct mapping of the brain with DCS can be performed. Especially for language, DCS is done during awake surgery. This is not possible in all patients, can complicate surgery and has false positive and false negative findings. Moreover, the information is only available during the surgery. TMS-based mapping is an attractive, non-invasive alternative method to map brain function. This has been developed further for motor and language function.
In epilepsy, if surgery is not an option and seizures continue despite adequate anti-epileptic drug treatments, alternatives are needed. Since rTMS can change the excitation-inhibition balance in the brain by pattern application of repeated TMS-pulses, it could prove to be a valuable treatment option. Conflicting evidence was available on this prior to our experiments. To advance the knowledge on rTMS in epilepsy further, FDG-PET scans were performed at baseline and after each treatment condition.

rTMS in epilepsy
We have conducted a randomized sham-controlled crossover trial that included 11 patients with well-defined focal epilepsy. rTMS (0.5 Hz) was targeted to the focus during three treatment conditions consisting of 1,500 stimulations/day for 10 weekdays at 90% of resting motor threshold (rMT) followed by a 10-week observation period. None of the patients achieved an overall 50% seizure reduction. Side effects in the study were a rebound in seizure frequency after initial reduction in seizure frequency (one patient) and increase in seizure frequency during and shortly following active stimulation (overall change in seizure frequency over 1 month and 12 weeks observation period not significant).
FDG-PET scans showed that rTMS caused measurable change in brain metabolism in patients with epilepsy. No single pattern of change emerged. Only three out of eight subjects showed a relative decrease in brain metabolism around the stimulation target after stimulation with the figure-8 coil, and five out of nine after the round coil. Increased metabolism around the stimulation target was seen in few patients. FDG-PET metabolic changes in the area of stimulation were only apparent after active stimulation, not sham treatment, and a carry-over effect after active treatment was observed, pointing to a lasting change in metabolism after rTMS of at least 12 weeks. Widespread changes at a distance of the stimulation target were also observed in all patients. These observations indicate that rTMS induces plastic changes in the brain, but a clear and predictable pattern was not present. This could in part explain the lack of efficacy of rTMS as a treatment of refractory focal epilepsy in the study.

TMS-based motor and language mapping

In our study on TMS-based motor cortex mapping, we created and analyzed different models. To delineate the whole area of the motor cortex representation, the model based on the weighted average of the induced electric fields calculated with a realistic head model performed best. The optimal single threshold to visualize the field-based maps was 40% of the maximal value for the anisotropic model and 50% for the isotropic model. For clinical purposes, we suggest to use different thresholds, which is a unique benefit of these maps: a high threshold highlights the center of the motor area and a lower threshold is able to capture the motor representation completely. The interpretation of those maps is that regions with high values are those where high induced electric field strengths are likely to result in high MEP amplitudes.

For language mapping, we have developed and tested new ways to setup the mapping and analyze the data. Our automated speech analysis algorithm was able to discern both speech onset and speech content, even in the presence of TMS noise. Our algorithm was easy-to-use, fast, and reliable and had high accuracy (90%) and specificity (96%) on the data derived in healthy volunteers and with a lower accuracy (61%) in patients. A TMS-RT-based probability map of the language cortex in the three patients was consistent with anatomical knowledge, DCS data and was able to predict postsurgical transient language decline in one patient with negative DCS-mapping. TMS-induced increases in RT of correct responses during a confrontational naming task may be an important biomarker of language cortex. Further studies might want to focus on TMS-RT-based mapping of the language cortex with lower stimulation intensities, which would make the procedure less painful. Patient's comfort should be maximized for the technique to become a first-line test in the preoperative delineation of language cortex.

Conclusion

Contributions have been made in TMS-based motor mapping and current performance is in the range that inducing it to clinical care seems reasonable. Our contributions in TMS-based language mapping should make future trials on the topic easier due to the development of an automated speech analysis algorithm and a new direction for future research has been explored, namely the use of TMS-induced increases in RT of correct responses during a confrontational naming task as a relevant marker to map the language cortex.

In the development of rTMS as treatment for epilepsy, we have published a negative trial. Future directions of research based on these findings were discussed, especially since the clinical data were corrugated by changes in brain metabolism as measured with FDG-PET.

Samenvatting

Inleiding
De doelstellingen van deze thesis waren het klinisch valideren van het aflijnen van de motorische en taalfuncties met transcraniële magnetische stimulatie (TMS) en het behandelen van medicatie-resistente focale epilepsie door middel van multimodaal beeldvorming-gestuurde repetitieve TMS. Elk jaar worden in België meer dan 65 000 mensen gediagnosticeerd met kanker, waarvan ongeveer 10-25% uitzaaiingen naar de hersenen zullen krijgen in de loop van het ziekteverloop. Een deel van deze letsels zal moeten geopereerd worden, vooral als het slechts om een enkele uitzaaiing gaat, wat het geval is in ongeveer de helft van de patiënten[18]. Hersentumoren die ontstaan in de hersenen zijn zeldzamer, met een leeftijd-aangepaste incidentie van 21.42 per 100 000[19]. Ook bij bepaalde vormen van epilepsie kan een operatie een goede optie zijn, en ongeveer 1600 nieuwe patiënten per jaar zouden in België eigenlijk moeten geëvalueerd worden om na te gaan of voor hen een operatie een optie is.
Bij een operatie is het doel niet alleen om het letsel te verwijderen maar even belangrijk om te zorgen dat mensen normaal kunnen blijven functioneren, met een normale motoriek en spraak. Kennis van de anatomie en functionele magnetische resonantie beeldvorming (fMRI) worden gebruikt om een inschatting te maken van het risico op functionele uitval door een operatie. Door de veranderde anatomie bij een tumor en door veranderde reacties zoals die gemeten worden met fMRI bij een tumor, zijn deze inschatting alles behalve perfect. Daarom zal vaak als er wordt ingeschat dat een operatie mogelijk is, gekozen worden om een rechtstreekse stimulatie van de hersenen uit te voeren d.m.v. directe elektrische stimulatie van de hersenen. In het bijzonder voor operaties in de buurt van de taalzones, zal dit gebeuren tijdens wakkere chirurgie. Dit is echter niet mogelijk bij elke patiënt en bovendien maakt dit de operatie gecompliceerder en zijn er ook bij deze test vals-positieve en vals-negatieve bevindingen. Deze informatie is ook alleen beschikbaar tijdens de operatie zelf, niet vooraf. Aflijnen van belangrijke hersenengebieden op basis van TMS is dan ook een aantrekkelijk, niet-invasief alternatief. Dit werd in deze thesis verder onderzocht, zowel voor motoriek als voor taal.
Bij patiënten met epilepsie, als er aanvallen blijven ondanks goede behandeling met medicatie en opereren geen optie is, zijn alternatieve behandelingsmogelijkheden noodzakelijk. Als met TMS herhaald en met een bepaald patroon de hersenen worden gestimuleerd kan dit de balans tussen prikkelbaarheid en onderdrukking door impulsen in de hersenen veranderen; op die manier zou dit een zinvolle optie kunnen zijn voor de behandeling van epilepsie. Er was tegenstrijdige informatie over de effectiviteit van deze behandeling voor we aan de experimenten in deze thesis begonnen. Om nog meer te leren over rTMS en het onderzoek in de toekomst verder vooruit te helpen, gebeurden er ook FDG-PET scans voor de start en na elke behandeling om meer informatie te krijgen over veranderingen in hersenmetabolisme.

rTMS in epilepsie
We hebben een gerandomiseerde studie uitgevoerd met drie behandelingsarmen: actieve behandeling met achtvormige TMS-spoel, actieve behandeling met ronde TMS spoel en een namaak TMS-spoel als controle-conditie. Elke patiënt was gepland elke behandeling te ondergaan in willekeurige volgorde. Patiënten en studiemedewerkers die het effect opvolgden, waren geblindeerd voor welke spoel er gebruikt werd in welke volgorde. 11 patiënten met goed omlijnde focale epilepsie werden geïncludeerd. rTMS (0.5 Hz) werd gericht naar de focus tijdens elk van de drie condities. Stimulatie was onder vorm van 1500 stimulaties per dag gedurende 10 weekdagen aan 90% van de motorische drempel in rust, gevolgd door een observatieperiode van 10 weken.

Geen van de deelnemers had een 50% verminderding in aanvalsfrequentie. Nevenwerkingen gezien in de studie was een toename in aanvallen, na een initiële vermindering in aanvallen (bij een patiënt)

en een toename van de aanvalsfrequentie tijdens en kort na de behandeling (hoewel deze toename over 1 maand en 12 weken beschouwd niet statistisch verhoogd was).

De FDG-PET scans toonden dat rTMS een meetbare verandering in hersenmetabolisme veroorzaakt in patiënten met epilepsie. De veranderingen waren echter niet eenduidig. In drie van de acht en vijf van de negen behandelingen met achtvormige en ronde spoel respectievelijk, werd er een verminderde activiteit gezien rond de plaats die gestimuleerd werd. Vermeerdering van de activiteit in de stimulatie-regio werd gezien in enkele patiënten. Deze veranderingen waren er alleen na actieve stimulatie en konden nog steeds –maar in mindere mate- gezien worden als de volgende scan na nep-stimulatie gebeurde, wat er op lijkt te wijzen dat de effecten van rTMS op metabolisme minstens 12 weken aanhouden. Verspreide veranderingen op afstand van de stimulatieplaats werden ook gezien.

TMS-gebaseerde motorische en taalfunctie aflijning
In onze studie naar TMS-gebaseerde aflijning van de motorische cortex, hebben we verschillende modellen gecreëerd en geanalyseerd. Om de hele oppervlakte van de motorische cortex representatie af te lijnen, leek het model gebaseerd op het gewogen gemiddelde van de berekende geïnduceerde elektrische velden in een realistisch hoofdmodel het beste. De optimale drempel om deze te tonen was 40% van de maximale waarde voor het anisotroop model en 50% voor het isotroop model. Voor klinische toepassingen raden we echter aan om verschillende drempels te gebruiken, wat een voordeel is van deze map: een hoge drempel zal het centrum tonen en een lage drempel de uitgebreidheid van de motorische cortex representatie. Regio's met hoge waardes hebben een grote kans om een hoog-amplitude motorische geëvoceerde potentialen op te wekken.

Voor het aflijnen van de taalfunctie hebben we vernieuwde opstellingen en analysemethodes ontwikkeld en getest. Het automatische spraakherkenningsalgoritme kon zowel wanneer er gesproken werd als wat er gezegd werden onderscheiden, ook al waren er de luide storing van de TMS-ontladingen. Het algoritme was gebruiksvriendelijk, betrouwbaar en had een hoge accuraatheid (90%) en specificiteit bij gezonde vrijwilligers. Bij de drie patiënten in de studie was de accuraatheid 61%.
Een TMS-reactietijd-gebaseerd waarschijnlijkheidsmodel van de locatie van de taalcortex werd gecreëerd voor elk van de patiënten en deze waren in overeenstemming met anatomische kennis, DCS gegevens en bij een patiënt leek deze tijdelijke ernstige achteruitgang van de spraak te voorspellen. In deze patiënt toonde de DCS niets aan. Vertraging in reactietijd door TMS bij verder correct benoemde voorwerpen lijkt dus een belangrijk teken om te onderzoeken bij het aflijnen van de taalfuncties.

Conclusie
We hebben een bijdrage geleverd aan de kennis over TMS-gebaseerde aflijning van de motorische cortex. De betrouwbaarheid van deze test lijkt momenteel voldoende om deze deel te laten uitmaken van de klinische praktijk.
De bijdragen aan het verder verfijnen van het aflijnen van de taalgebieden zouden toekomstige studies over het onderwerp moeten vereenvoudigen, door de beschikbaarheid van een automatisch spraakherkenningsalgoritme. Ook hebben we een nieuwe richting uitgestippeld voor verder onderzoek: het gebruik van TMS-geïnduceerde toename van de reactietijden bij correct benoemde voorwerpen zou een relevante parameter kunnen zijn om taalgebieden af te lijnen.

In de ontwikkeling van rTMS als een behandeling voor epilepsie hebben we een negatieve studie gepubliceerd. Hoe het in de toekomst nu verder moet, werd geanalyseerd, te meer omdat er ook interessante gegevens werden verzameld over veranderingen in metabolisme door deze therapie.

Scientific acknowledgement, personal contribution and conflict of interest statements

This thesis was written by Laura Seynaeve. The thesis was revised by my promoter and co-promoter. A first draft of the introduction and conclusion was also checked by my partner, Olivier Stevens. The photographic materials in this thesis were created by my brother, Vincent Seynaeve and the cover was designed by sister-in-law Cristal.
The experiments conducted were performed by Laura Seynaeve, under supervision of Prof. Dr. Van Paesschen.
Experimental setup for the rTMS in epilepsy experiments was discussed between Laura Seynaeve, Annemie Devroye and Prof. Dr. Wim Van Paesschen, with input from Prof. Dupont. Annemie Devroye collected the seizure outcome data of this experiment, under supervision of Prof. Dr. Van Paesschen. Laura Seynaeve analyzed the seizure outcome data only after the experiments in order to maintain the double-blind study setup. Steffen Fieuws gave advice on the statistical analysis of the data. The aforementioned contributors revised the manuscript.
Kwinten Porters and Mieke Steukers performed PET scans in the study, under supervision of Prof. Dr. Karolien Goffin. Prof. Patrick Dupont and Prof. Dr. Karolien Goffin gave advice on image acquisition and analysis. Dr. Bliede van de Broeck (MLEM) and Prof. Patrick Dupont (Hunter method) performed image reconstruction. Laura Seynaeve performed image analysis under guidance and using scripts provided by Prof. Patrick Dupont. Part of this material has been discussed during the thesis defense of the Postgraduate Studies on Advanced Medical Imaging, under supervision of Prof. Dr. Karolien Goffin, Prof. Patrick Dupont and Prof. Dr. Wim Van Paesschen.
Guido Van Driel, acquired the intra-operative data for the experiments on motor cortex mapping, under supervision of Prof. Dr. Steven De Vleeschouwer and Prof. Dr. Tom Theys. Tom Haeck created the scripts to do the modelling. Prior to the use of these scripts, Tom Haeck, Laura Seynaeve and Pieter Slagmolen supervised the master thesis of Karen De Leener, for her master in Civil Engineering, under supervision of Prof. Paul Suetens. Afterwards Tom Haeck and Laura Seynaeve supervised the thesis of Jesu Kiran Spurgen, for his thesis in Postgraduate Studies in Advanced Medical Imaging, under supervision of Prof. Frederik Maes. The data of neither were used in this thesis. This work did enable Tom Haeck to get in depth knowledge on the scripts. Tom Haeck created the pipeline to go from the raw data to the final models, in collaboration with Laura Seynaeve. Laura Seynaeve analyzed these data. Markus Gramer created the scripts to bring all the imaging data into the same space. The manuscript in the current form, as it is published has been improved upon by advice of many people, after discussions on the topic during presentations (see CV).
Deepak Baby created the automated speech analysis method under supervision of Prof. Hugo Van hamme. The data acquisition was performed by Laura Seynaeve. Deepak Baby performed the analysis of the healthy control data and Laura Seynaeve the patient's data. The manuscript on language TMS has been written by Laura Seynaeve and Deepak Baby, and critically revised by Prof. Patrick Dupont, Prof. Hugo Van hamme and Prof. Dr. Wim Van Paesschen.

This work has been supported by a TBM-grant from the Institute of Innovation by Science and Technology Flanders (IWT), project number 090850.

None of the authors declare to have any conflict of interest pertaining to this thesis.

Dankwoord

"*Het dankwoord is het enige dat iedereen leest*"
Citaat van meerdere collega's die voor me hun doctoraat hebben afgelegd

Laat me dan ook beginnen met u, die dit nu aan het lezen bent, te bedanken voor uw aanwezigheid op deze verdediging en uw interesse in mijn thesis. Graag nodig ik u uit om ook de rest van dit manuscript te doorbladeren.
Als u dit doet, zal u zien dat er veel mensen zijn die ik mijn dank verschuldigd ben. In de eerste plaats zou ik de patiënten willen bedanken voor hun deelname aan de studies. Helaas zijn een deel van de deelnemers in tussentijd aan hun ziekte overleden. We wensen hun naastbestaanden veel sterkte bij dit verlies. Het feit dat neurologische aandoeningen –in het bijzonder hersentumoren- nog zo vaak en snel fataal aflopen, moet een stimulans zijn voor ons allen om verder onderzoek te ondersteunen.

De belangrijkste ondersteuning van de onderzoeken in deze thesis, staat op naam van Professor Wim Van Paesschen. Zonder hem zou deze thesis nooit tot stand gekomen zijn: van het initiële idee en aanvraag voor het project tot de finale versie. Hij was en is echt een fantastische promotor! Professor, u heeft me begeleid van mijn eerste kennismaking met de neurologische kliniek tot het afleggen van deze thesis en u zal steeds een voorbeeld blijven. U heeft me de weg gewezen in het onderzoek, van onze eerste meeting over TMS in Oxford tot het afgewerkt manuscript dat nu voorligt. Toen het minder goed ging tijdens de eerste zwangerschap, was u er met ondersteunende woorden- en hier sta ik terug met een bolle buik…
Zonder mijn copromotoren, Professor Steven De Vleeschouwer en Professor Stefan Sunaert, zou deze thesis ook nooit tot stand gekomen zijn. Professor De Vleeschouwer, u heeft me ingeleid in de wereld van de wakkere chirurgie en de TMS-gebaseerde mapping. Uw gewaardeerde kritische beschouwingen hebben deze thesis tot een hoger niveau getild en uw zorg en gedrevenheid voor de patiënten sterkt tot voorbeeld. Professor Sunaert, uw enthousiasme om nieuwe technieken te proberen en steeds nog betere resultaten na te streven, werkte aanstekelijk.

Graag wil ik mijn interne juryleden, Professor Johan van Loon en Professor Stephan Claes bedanken voor hun adviezen over deze thesis. Daarnaast wil ik Professor Van Loon ook bedanken om me te laten kennis maken van binnenuit met de neurochirurgie en epilepsie-chirurgie in het bijzonder en Professor Claes voor de interessante gesprekken over het gebruik van TMS in de psychiatrie. Graag wens ik ook de leden van het thesis advies comité te bedanken voor hun inzichten en in het bijzonder Professor Dymarkowski.

I would like to thank Professor Krieg, Professor Maertens de Noordhout and Professor Kimiskidis for accepting to be part of the jury and for their valued advice on the thesis. I'm honoured and humbled that you found the time in your busy schedule to review my thesis.
Professor Krieg, your enlightening papers on mapping with TMS have been an inspiration and stepping stone for this thesis. Professor Kimiskidis, your insights in TMS in epilepsy are unparalleled- I really valued your input during your visit to Leuven and during the IFCN in Berlin. Professor Maertens, thank you for your unrelenting effort to put clinical neurophysiology –and especially TMS- on the map in Belgium.

Deze thesis was niet mogelijk zonder de financiële steun van het IWT.
Ik wens ook de Belgian Association for NeuroOncology (BANO) te bedanken voor hun ondersteuning, met de uitreiking van de Belgian brain tumor support price in 2016.

Mijn doctoraatsjaren zouden er heel anders uitgezien hebben zonder mijn fantastische collega Dr. Simon Tousseyn. Simon, als ouderejaars doctoraatsstudent nam je me onder je vleugels, zodat ik zelf mijn vleugels heb kunnen uitslaan. We hebben veel gelachen en iets minder gezaagd, je was er altijd, mijn steun en toeverlaat, mijn klankbord, zonder wie mijn PhD-ervaring nooit hetzelfde zou geweest zijn… Het is wel een beetje spijtig dat je er vandaag niet kon bijzijn omdat je in Cleveland bent, maar dat is omwille van je onstilbare gedrevenheid om de zorg voor epilepsiepatiënten en het wetenschappelijk onderzoek steeds te verbeteren! Ook Gwendolyn en Arthur moeten bedankt worden, omdat ze je delen met de wetenschap.

Graag had ik Annemie Devroye bedankt voor de studie met rTMS in epilepsie- zonder haar was het nooit gelukt.
Guido Van Driel, ik heb zo veel van je geleerd, over EEGs, over wakkere chirurgie, over mensen geruststellen en over hoe mooi het leven kan zijn: het was altijd leuk om een excuus te hebben om je op te zoeken.

Professor Patrick Dupont, wat hadden we zonder u moeten beginnen: u leerde me alles wat ik weet over data analyseren, over multimodale en geavanceerde beeldvorming en over zo veel andere dingen die belangrijk zijn in het leven.

Professor Karolien Goffin, dank voor uw betrokkenheid, zonder u was de PET-studie nooit gelukt. Dank ook voor uw inlevende adviezen over het combineren van onderzoek en gezin met jonge kinderen.

Dr. Maarten Schrooten, ik wou dat de omstandigheden anders waren…
Onze gesprekken waren altijd stimulerend. Geen idee was te moeilijk om te verwerpen, als een idee wetenschappelijke of klinische meerwaarde had, dan kon het worden uitgevoerd- tijd noch moeite werden gespaard. We konden altijd bij u terecht- meestal met technische problemen (wat moet u hebben afgezien met die overmaat aan X-chromosomen) maar evengoed voor een lekker recept of advies over de aankoop van een buggy.

Special thanks to Kate (Katarzyna Adamczuk): I have no idea what I should have done without you. You taught me how to handle a TMS machine, to analyse data, to do cognitive tests… You are really a genius centipede, able to juggle many different and challenging scientific deadlines, while always smiling and being attentive to the need of people around you. Tomasz is also to be thanked, since he needs to share you with your projects- we also have very fond memories of your wedding (at least I do, the copious amount of food and especially drinks have induced amnesia in some).
Ik wens ook Kate's collega's van het labo voor cognitieve neurologie, onder leiding van Professor Rik Vandenberghe, te bedanken, in het bijzonder Natalie Nelissen die me begeleid heeft tijdens mijn co-assistentenwerk en zo mijn interesse in dit soort onderzoek heeft aangewakkerd, Natalie Caspari die me heeft geholpen met TMS-procedures in het begin, Veerle Neyens van wie het wetenschappelijk traject parallel met het mijne liep en waarbij we elkaar dan ook konden steunen en Rose Bruffaerts- die ook een collega ASO neurologie was en me dus wegwijs kon maken, niet alleen in cognitieve testen maar ook in de praktische aspecten van het leven als PhD student + ASO.

Professor Stefan Swinnen en collega's van het FABER labo wens ik ook te bedanken, voor hun demonstraties met TMS en ook het mogen lenen van hun toestel.

De motor mapping data zouden er niet zijn zonder Tom Haeck. Tom, zonder jou had ik mijn tanden stukgebeten op dit project. Het was boeiend om met jou de mogelijke pistes uit te testen en nadien ook resultaten te hebben. En kijk, ook mijn PhD is ein-de-lijk af geraakt.

Without Markus Gramer I would have been most in the transformational forest… Moreover, he provided me with the best home-made cookies in the world- so even if I would have gotten lost, I would have been able to use the crumbs to find my way back.
Ook de cijfers-ridders Jeroen Hermans, Brecht Heyde en David Robben wil ik bedanken omdat ze met één blik een fout uit mijn MatLab pogingen haalden, waar ik zelf gefrustreerd uren naar kon staren.
Anke Wouters, wetenschappelijke sneltrein en altijd hyper-enthousiast: zonder jou zou het niet hetzelfde geweest zijn.

Ook zonder de andere "Louvre" collega's (aka. Medical Image Research Center) zou mijn leven en onderzoek er anders hebben uitgezien. Hoe zou ik anders geleerd hebben hoe belangrijk het is tot op de letter en het punt correct te lezen wat er staat- of het nu in mijn poging tot coderen was of om te weten dat als er een papier ophangt "gelieve gebruikte tassen en glazen in de afwasmachine te plaatsen" dat dit wil zeggen dat bestek er niet in hoort… Of dat er geen betere manier bestaat om tot nieuwe wetenschappelijke inzichten te komen en plannen om de wereld te verbeteren, dan op vaste momenten te lunchen, koffie te drinken of een stuk fruit te eten. Jongens en meisjes uit Simons' smurfenwereld: An, Annemie, Catarina, Charlotte, Daan, Daniel, Dorothee, Dorothy, Dzemilla, Hans, Ine (x2), Jaap, Janaki, Jasmien, Jonatan, Leonardo, Pieter, Philip, Stijn, Thibault, Thijs, Wouter: jullie waren onovertroffen en geweldig!
Ik wens dan ook Professor Paul Suetens te bedanken door wie zo'n vruchtbare omgeving kon ontstaan en Professor Frederik Maes, om me uit te leggen hoe beeldanalyse werkt en voor zijn gewaardeerde input. Beide Professoren wens ik ook te bedanken omdat hun PhD studenten ook aan dit thesis-project mochten meewerken.
Ook wens ik Bart De Dobbelaer en Dominique Delaere te bedanken voor hun ondersteuning.

Ik wil ook Silvia Kovaks en Sofie Van Cauter bedanken om me zo veel te leren over fMRI, voor hun flexibiliteit, hun mogelijkheden om scans van onder het stof te duiken en de altijd fijne gesprekken. Zonder Ron Peeters zou ik de MRI zelfs niet binnen hebben mogen gaan en zonder hem zouden er nooit zo'n technisch mooie scans kunnen zijn gebeurd- en hoe anders zou ik een fantoom hebben kunnen onderzoeken (zie figuur p. 14).

Het project rond taalmapping, dit zou nooit gelukt zijn zonder Deepak Baby en Professor Hugo van Hamme.

Onze labmeetings waren altijd boeiend, met dank aan Bori (Borbàla Hunyadi) en Canan Güvenç. Bori, you introduced me in the wonderful world of machine learning. Canan, je was een fantastische collega en je motivatie een voorbeeld- alsook je kookkunsten.

Ik zou ook graag de stafleden van de dienst neurologie van het UZ Leuven bedanken voor de goede opleiding tot neuroloog en de mogelijkheden die ik heb gekregen om onderzoek en opleiding te combineren. Ik wil ook mijn collega's (toen) ASOs bedanken voor de superfijne sfeer tijdens de opleiding, die zo veel verder rijkt dan de deuren van het ziekenhuis!
Ook wil ik iedereen die ondersteuning bood bedanken, in het bijzonder het secretariaat neurologie en dat van de faculteit. Stefanie Geysels, zonder jou was vandaag niet mogelijk geweest!
Ik wil ook graag iedereen bedanken die werkzaam is op de afdelingen neurologie en neurochirurgie van het UZ Leuven en het operatiekwartier. Graag wil ik ook de stafleden en de ASOs neurochirurgie bedanken voor de vlotte samenwerking voor het verzamelen van data voor de mapping in neurochirurgische patiënten. In het bijzonder wil ik Professor Tom Theys vermelden. Ook de medewerkers van BrainLab wens ik te bedanken, voor hun hulp met het exporteren van de data.

Mijn huidige collega's, en in het bijzonder Professor Jacques De Keyser, zou ik willen bedanken voor hun interesse in mijn werk en de tijd die ik ervoor gekregen heb. Ik wil ook Professor Johnny Duerinck

bedanken voor zijn adviezen maar vooral voor zijn niet-aflatend enthousiasme voor wetenschappelijke innovatie.

Vanzelfsprekend zou ik hier nooit hebben kunnen staan zonder de steun van mijn familie: dank je mama en papa, dank je Xavier, Vincent en Anne-Charlotte, dank je lieve schoonouders en schoonbroers en -zussen: zonder jullie zou het nooit gelukt zijn!
Olivier, bijna 14 jaar zij we samen- de helft ervan tijdens mijn opleiding ASO + PhD- hoe kan ik dat nu samenvatten in een paar regels… jouw steun en liefde waren onontbeerlijk. Lieve Tobias, je herkende modellen van hersenen voor je de letters van je naam herkende: ik hoop toch dat je later zal terugkijken op deze periode en je zal herinneren dat wat we kleurden niet alleen hersenmodellen waren.

Zeker ook bedankt aan hen die ik ten onrechte in het dankwoord vergeten ben…

Curriculum vitae

Personal data

Date of birth	October 16, 1984
Current work address	Department of Neurology, UZ Brussel, Laarbeeklaan 101, 1090 Brussel (Jette)
Current work email	laura.seynaeve@uzbrussel.be

Education

2002-2005	Medicine (bachelor)	KU Leuven, KULAK, Belgium	magna cum laude
2005-2009	Medicine (master)	KU Leuven, Belgium	summa cum laude
2014	EFMG certification	USMLE step 1 231, step 2 CK 257	
2013-2015	Postgraduate studies in advanced medical imaging	KU Leuven, Belgium	summa cum laude
2009-2016	Neurology residency	UZ Leuven, OLV Aalst, Belgium	
2016	Fellow of the European board of neurology	European board exam	
2016-now	PhD project: Multimodal image-guided transcranial magnetic stimulation in the delineation of eloquent cerebral cortex in the neurosurgical patient and the treatment of refractory partial epilepsy Laboratory for Epilepsy Research, KU Leuven, Belgium		

Publication list

- Optimized preoperative motor cortex mapping in brain tumours using advanced processing of transcranial magnetic stimulation data.
  Seynaeve L, Haeck T, Gramer M, Maes F, De Vleeschouwer S, Van Paesschen W. Neuroimage Clin. 2019 Jan 9:101657.
- Early-Onset Creutzfeldt - Jakob disease Mimicking Immune-Mediated Encephalitis.
  Wiels WA, Du Four S, **Seynaeve L**, Flamez A, Tousseyn T, Thal D, D'Haeseleer M. Front Neurol. 2018 Apr 10;9:242.
- Correlation of neuropsychological and metabolic changes after epilepsy surgery in patients with left mesial temporal lobe epilepsy with hippocampal sclerosis.
  Güvenç C, Dupont P, Van den Stock J, **Seynaeve L**, Porke K, Dries E, Van Bouwel K, van Loon J, Theys T, Goffin KE, Van Paesschen W. EJNMMI Res. 2018 Apr 12;8(1):31.
- Using high-amplitude and focused transcranial alternating current stimulation to entrain physiological tremor.
  Khatoun A, Breukers J, Op de Beeck S, Nica IG, Aerts J, **Seynaeve L**, Haeck T, Asamoah B, Mc Laughlin M. Scientific reports. 2018 8:4927
- Electrocorticography of Spatial Shifting and Attentional Selection in Human Superior Parietal Cortex.
  Schrooten M, Ghumare EG, **Seynaeve L**, Theys T, Dupont P, Van Paesschen W, Vandenberghe R. Front Hum Neurosci. 2017 May 11;11:240.
- Rapidly Progressive Cerebellar Hemiataxia with High Levels of GAD65 Reactive Antibodies: Case Report.
  Wiels W, Guisset F, Vandervorst F, Peeters I, **Seynaeve L**, Costa O, Flamez A, De Keyser J. Movement Disorder Clinical Practice. 2017.
- Response to "Safety of repetitive transcranial magnetic stimulation in patients with epilepsy: A systematic review" by Luisa Santos Pereira and colleagues.
  Seynaeve L, Van Paesschen W. Epilepsy Behav. 2016 Sep;62:308
- Randomized crossover sham-controlled clinical trial of targeted low-frequency transcranial magnetic stimulation comparing a figure-8 and a round coil.

Seynaeve L, Devroye A, Dupont P, Van Paesschen W. Epilepsia. 2016 Jan;57:141-50

- A fatal case of Epstein Barr encephalitis presenting as fever of unknown origin.
  Seynaeve L, Caekebeke J, Cypers G. Acta Neurol Belg. 2013 Mar;113:91-4.
- Treatment, by insertion of multiple uncovered metallic stents, of intraductal papillary mucinous neoplasm of the pancreas with biliary obstruction by mucus impaction.
  Seynaeve L, Van Steenbergen W. Pancreatology. 2007;7:540-3.

Conferences:

- Belgian Association for Neuro-Oncology, 2017: short presentation: Advanced image processing to improve motor cortex mapping with TMS

* 2016 Belgian brain tumor support price

- Brain plasticity in epilepsy, Leuven, 2017: invited talk: Neuronavigated, repetitive Transcranial Magnetic Stimulation for the treatment of epilepsy.

- ASCO Annual meeting 2019: GLIAVAX - A stratified phase II clinical trial of avelumab and axitinib in patients with recurrent glioblastoma.
  Neyns B, Ben Salama L, Awada G, De Cremer J, Schwarze JK, Seynaeve L, Du Four S, Fischbuch L, Van Binst AM, Everaert H, Michotte A, Rogiers A, Theuns P, Duerinck J
- American Academy of Neurology, Boston, 2017: poster: Advanced head models to improve TMS-based motor cortex localisation.
  Seynaeve L, Haeck T, Gramer M, De Vleeschouwer S, Van Paesschen W
- American Academy of Neurology, Vancouver, 2016: e-poster: rTMS Induces Changes in FDG Brain Metabolism in Patients with Epilepsy
  Seynaeve L, Van den Broeck B, Dupont P, Goffin K, Van Paesschen W
- Belgian Society of Neurosurgery Annual Meeting, Brussels, 2016: short presentation: Pre-operative delineation of the motor cortex in tumour patients by transcranial magnetic stimulation and advanced head modelling
  Seynaeve L, Haeck T, Kiran Spurgen J, Kovacs S, Maes F, De Vleesschouwer S, Van Paesschen W
- International Conference on Basic and Clinical Multimodal Imaging, Utrecht, 2015: poster: Localization of the motor cortex on magnetic resonance images by transcranial magnetic stimulation
  De Leener K, Seynaeve L, Haeck T, Slagmolen P, De Vleeschouwer S, Maes F, Theys T, Van Loon J, Sunaert S, Kovacs S, Van Cauter S, Suetens P, Van Paesschen W
- American Academy of Neurology, San Diego, 2015: poster: Double-blind sham-controlled, crossover-randomized trial with repetitive transcranial magnetic stimulation for the treatment of refractory focal epilepsy.
  Seynaeve L, Devroye A, Dupont P, Goffin K, Van Paesschen W
- Belgian Society of Neurosurgery Annual Meeting, Brussels, 2015: poster:
  Pre-operative functional mapping of the motor cortex
  Seynaeve L, De Vleeschouwer S, Dupont P, Sunaert S, Van Cauter S, Kovacs S, Van Paesschen W
- 11th European Congress on Epileptology, Stockholm, 2014: poster:
  Comparison of language fMRI during two tests of association and language in temporal lobe epilepsy patients
  Seynaeve L, Adamczuk K, Kovacs S, Vandenberghe R, Sunaert S, Dupont P, Van Paesschen W
- Organization of Human Brain Mapping annual meeting, Hamburg, 2014: poster:
  Comparison of language fMRI during two paradigms of language in temporal lobe epilepsy

Seynaeve L, Adamczuk K, Kovacs S, Vandenberghe R, Sunaert S, Dupont P, Van Paesschen W

Other publications and talks

- Epilepsiedag, Gent, 2019: invited talk: een update over epilepsie en veelgestelde vragen.
- Epilepsiedag, Leuven, 2016: session: epilepsie bij ouderen
- Breinwijzer festival deelname: 2014: Leuven & Gent, 2015: Gent: wetenschapsfestival over de hersenen voor het grote publiek
- Book chapter:
  Hoofdstuk 7: Transcraniële Magnetische Stimulatie & taaltherapie.
  Laura Seynaeve, Eline Verwilligen.
  In: Het (voor)beeldig brein. Taal en interventionele geneeskunde. Ed. Robert E. *et al*. Garant Publisher, Antwerp, 2013.